Politechnika Wrocławska

DZIEDZINA: Nauki inżynieryjno-techniczne

DYSCYPLINA: Inżynieria Chemiczna

ROZPRAWA DOKTORSKA

Molekularnie wdrukowywane polimery jako sensory selektywne wobec S–metolachloru

mgr Dominika Rapacz–Kinas

Promotor:
dr hab. inż. Joanna Wolska, prof. uczelni

Promotor pomocniczy:
dr hab. inż. Katarzyna Smolińska–Kempisty, prof. uczelni

Słowa kluczowe: polimery wdrukowane molekularnie, proces sorpcji, proces desorpcji, selektywność, S–metolachlor, monitoring mikrozanieczyszczeń

WROCŁAW 2026

Składam serdeczne podziękowania

Paniom Promotor dr hab. inż. Joannie Wolskiej oraz dr hab. inż. Katarzynie Smolińskiej–Kempisty za poświęcony czas, nieocenioną pomoc, merytoryczne rady oraz cierpliwość. Dziękuję za stworzenie wyjątkowych możliwości do rozwoju, a także przekazaną wiedzę na każdym etapie przygotowywania niniejszej pracy.

Zespołowi Katedry Inżynierii Procesowej i Technologii Materiałów Polimerowych i Węglowych za współpracę w miłej i przyjaznej atmosferze.

Mężowi, Mamie oraz Dziadkom za motywację, która doprowadziła mnie do tego momentu oraz wsparcie w realizacji założonych celów.

Spis treści

1. Streszczenie w języku polskim

Niniejsza rozprawa doktorska *Molekularnie wdrukowywane polimery jako sensory selektywne wobec S–metolachloru* stanowi cykl siedmiu powiązanych tematycznie publikacji naukowych i wypełnia lukę w tematyce polimerów wdrukowywanych molekularnie z powinowactwem do S–metolachloru. Przeprowadzony przegląd literatury wskazał, że w obszarze obejmującym syntezę polimerów z odciskami molekularnymi selektywnymi wobec herbicydów w znikomym stopniu skupiono się na projektowaniu tzw. „*inteligentnych*" (ang. „*smart*") sorbentów zgodnie z koncepcją „*zielonego wdrukowania molekularnego*".

Ciągły rozwój cywilizacyjny oraz technologiczny stale przyczynia się do zwiększania stopnia zanieczyszczenia środowiska oraz pogorszania stanu jakości wód. W wodach mogą być obecne szkodliwe substancje, takie jak leki, metale ciężkie, herbicydy, czy detergenty. Związki te bardzo często występują w śladowych ilościach, nawet w stężeniach rzędu ng × L^{-1}, co sprawia, że tradycyjne metody analityczne mogą okazać się niewystarczająco czułe, a w konsekwencji tego – badana próbka wody może wydawać się pozornie czysta. Dlatego kluczowy jest etap przygotowania próbki do analizy. W ostatnich latach polimery wdrukowywane molekularnie są szeroko wykorzystywane w chemii analitycznej, ze względu na wysoce selektywną możliwość wiązania cząsteczki wybranego analitu. Te syntetyczne sorbenty naśladują naturalnie występujące enzymy, a mechanizm ich działania można opisać za pomocą znanego modelu zamka i klucza. Podczas syntezy na powierzchni matrycy polimeru tworzone są specyficzne miejsca wiążące, które są komplementarne kształtem, rozmiarem oraz obecnością grup funkcyjnych do cząsteczki docelowego analitu, podobnie jak konkretny klucz pasuje do właściwego zamka.

Mając na uwadze duże koszty analizy, związane z koniecznością posiadania drogiej aparatury pomiarowej oraz zatrudnienia wysoce wykwalifikowanego personelu, a także trudności w oznaczeniach rzeczywistego stężenia danego związku, celem rozprawy doktorskiej była synteza „*inteligentnych*" molekularnie wdrukowywanych polimerów, selektywnych wobec S–metolachloru, otrzymanych zgodnie z koncepcją tak zwanej „*zielonej chemii*". W ramach realizacji niniejszej pracy otrzymano cztery rodzaje materiałów: blokowe polimery z odciskiem molekularnym reagujące na zmiany temperatury lub pH oraz sorbenty typu rdzeń–otoczka z warstwą molekularnie wdrukowanego polimeru, wykazującego odpowiedź na zmianę temperatury lub pH. Najistotniejszym zadaniem było opracowanie składu mieszaniny reakcyjnej. Dobór odpowiednich monomerów funkcyjnych, mających powinowactwo do cząsteczki wzorca, umożliwiający utworzenie stabilnych kompleksów prepolimeryzacyjnych, a także wyselekcjonowanie środka sieciującego i inicjatora reakcji oraz ustalenie wzajemnego stosunku molowego reagentów stanowiły kluczowe zadanie. Wybór był o tyle trudny, iż ograniczał się do związków chemicznych rozpuszczalnych w wodzie, która została wykorzystana jako porofor. Dodatkowo, mimo szerokiego zastosowania S–metolachloru w opryskach przeznaczonych do zwalczania chwastów, jego ograniczona rozpuszczalność w wodzie stanowiła duże wyzwanie w przygotowaniu odpowiedniego stężenia wzorca.

W celu charakterystyki zsyntetyzowanych materiałów przeprowadzono badania kinetyki oraz izoterm sorpcji, a otrzymane dane dopasowano do odpowiednich modeli.

Zoptymalizowano warunki sorpcji oraz desorpcji, zarówno w trybie statycznym, jak i dynamicznym – na kolumnach do ekstrakcji do fazy stałej. W celu weryfikacji skuteczności działania polimerów, proces sorpcji z powodzeniem przeprowadzono na próbkach rzeczywistych, pochodzących z rzeki oraz ze stawu, znajdujących się w pobliżu upraw kukurydzy. Sorbenty analizowano różnymi technikami badawczymi, wykorzystano, m.in.: spektroskopię w podczerwieni, skaningową mikroskopię elektronową, analizę termograwimetryczną oraz technikę dynamicznego rozpraszania światła, a także porozymetrię i chłonność wody.

Wyniki otrzymane w ramach realizacji rozprawy doktorskiej stanowią istotny wkład w rozwój badań nad syntezą i charakterystyką „*inteligentnych*" polimerów z odciskiem molekularnym selektywnych wobec S–metolachloru. Zaprojektowanie warunków reakcji zgodnie z koncepcją „*zielonej chemii*" – bez strat energii oraz w medium wodnym, a także stworzenie samoregenerujących się materiałów, zdolnych do kilkukrotnego wykorzystania, wpisuje się w zasady „*greenification*" dotyczące „*zielonego*" wdrukowywania molekularnego oraz przyczynia się do promowania ekologicznych i zrównoważonych technologii. Dalsze plany badawcze zostaną rozszerzone o nowe sorbenty o specyficznej selektywności w stosunku do określonych herbicydów w celu opracowania multifunkcyjnej kolumny SPE.

2. Streszczenie w języku angielskim

The present doctoral dissertation *Molecularly imprinted polymers as sensors selective to S–metolachlor* comprises a series of seven thematically related scientific publications, thereby filling a gap in the field of molecularly imprinted polymers with affinity for S–metolachlor. A review of the literature revealed a lack of attention devoted to the design of "*smart*" sorbents in the field of synthesising molecularly imprinted polymers selective to herbicides, in accordance with the concept of "*green molecular imprinting*".

Continuous civilisational and technological development constantly contributes to increasing environmental pollution and deteriorating water quality. Harmful substances such as medicines, heavy metals, herbicides and detergents may be present in water. These compounds are very often found in trace amounts, even in ng × L^{-1}, which means that traditional analytical methods may not be sensitive enough and, as a result, the water sample tested may appear to be clean. Therefore, the stage of preparing the sample for analysis is crucial. In recent years, molecularly imprinted polymers have been widely used in analytical chemistry due to their highly selective ability to bind molecules of a selected analyte. These synthetic sorbents mimic naturally occurring enzymes, and their mechanism of action can be described using the well–known lock and key model. During synthesis, specific binding sites are created on the surface of the polymer matrix, which are complementary in shape, size and functional groups to the target analyte molecule, just as a specific key fits into the right lock.

Considering the high costs of analysis, associated with the need for expensive measuring equipment and highly qualified personnel, as well as the difficulties in determining the actual concentration of a given compound, the aim of the doctoral dissertation was to synthesise molecularly imprinted polymers that are selective for S–metolachlor, obtained in accordance with the concept of so–called "*green chemistry*". As part of this work, four types of materials were obtained: block molecularly imprinted polymers that react to changes in temperature or pH, and core–shell sorbents with a layer of molecularly imprinted polymer that respond to changes in temperature or pH. The most important task was to develop the composition of the reaction mixture. The selection of appropriate functional monomers with affinity for the template molecule, enabling the formation of stable pre–polymerisation complexes, as well as the selection of a cross–linking agent and reaction initiator and the determination of the molar ratio of the reagents were key tasks. The choice was difficult because it was limited to chemical compounds soluble in water, which was used as a porophore. In addition, despite the widespread use of S–metolachlor in weed control sprays, its limited solubility in water posed a major challenge in preparing the appropriate concentration of the template.

In order to characterise the synthesised materials, sorption kinetics and isotherms were studied, and the data obtained were fitted to appropriate models. Sorption and desorption conditions were optimised, both in static and dynamic modes, on solid phase extraction columns. In order to verify the effectiveness of the polymers, the sorption process was successfully carried out on real samples, also taken from a river and a pond located near corn fields. The sorbents were analysed using various research techniques, including infrared

spectroscopy, scanning electron microscopy, thermogravimetric analysis, dynamic light scattering, porosimetry and water absorption.

The results obtained in the doctoral thesis constitute a significant contribution to the development of research on the synthesis and characterisation of "*smart*" polymers with a molecular imprint selective for S–metolachlor. The design of reaction conditions in accordance with the concept of "*green chemistry*" – without energy loss and in an aqueous medium – as well as the creation of self–cleaning materials capable of repeated use, is in line with the principles of "*greenification*" concerning "*green*" molecular imprinting and contributes to the promotion of environmentally friendly and sustainable technologies. Further research plans will be expanded to include new sorbents with specific selectivity towards specific herbicides to create multifunctional SPE columns.

3. Wykaz publikacji wchodzących w skład rozprawy doktorskiej

Rozprawa doktorska zatytułowana *Molekularnie wdrukowywane polimery jako sensory selektywne wobec S–metolachloru* stanowi cykl 7 zaprezentowanych publikacji opublikowanych w czasopismach wyszczególnionych na liście czasopism punktowanych Ministerstwa Nauki i Szkolnictwa Wyższego (MNiSW). Sumaryczny współczynnik Impact Factor zgodny z rokiem opublikowania wynosi 38.4, natomiast punktacja MNiSW jest równa 820.

P1: Rapacz D*, Smolińska–Kempisty K, Wolska J. Progress in development and the current state of the art depending on the polymerization environment – Short review. *Journal of Environmental Chemical Engineering*. 2024, vol. 12, nr 2, art. 112159, s. 1-12. https://doi.org/10.1016/j.jece.2024.112159.
Impact Factor: 7.2.
Punktacja MNiSW: 100 pkt.

P2: Rapacz D*, Smolińska–Kempisty K, Wolska J. A novel green molecularly imprinted polymers synthesized in an aqueous medium as S–metolachlor sensitive materials. *Talanta*. 2024, vol. 280, art. 126674, s. 1-9. https://doi.org/10.1016/j.talanta.2024.126674.
Impact Factor: 6.1.
Punktacja MNiSW: 100 pkt.

P3: Rapacz D*, Smolińska–Kempisty K, Wolska J. Preparation and characterization of SPE column with smart green molecularly imprinted polymers materials for selective determination of S–metolachlor herbicide. *Scientific Reports*. 2025, vol. 15, art. 3153, s. 1-10. https://doi.org/10.1038/s41598-025-87685-2.
Impact Factor: 3.9.
Punktacja MNiSW: 140 pkt.

P4: Rapacz D*, Smolińska–Kempisty K, Wolska J. Detection of S–metolachlor herbicide in water samples using new molecularly imprinted polymer for solid–phase extraction. *Journal of Water Process Engineering*. 2025, vol. 75, art. 107980, s. 1-10. https://doi.org/10.1016/j.jwpe.2025.107980.
Impact Factor: 6.7.
Punktacja MNiSW: 100 pkt.

P5: Rapacz D*, Smolińska–Kempisty K, Wolska J. Eco friendly core–shell particles coated with molecularly imprinted polymers for S–metolachlor recognition and separation. *Analytica Chimica Acta*. 2025, vol. 1367, art. 344310, s. 1-10. https://doi.org/10.1016/j.aca.2025.344310.
Impact Factor: 6.0.
Punktacja MNiSW: 100 pkt.

P6: Rapacz–Kinas D*, Smolińska–Kempisty K, Wolska J. Core–shell molecularly imprinted polymer for selective recognition and detection of S–metolachlor in aqueous samples. *Scientific Reports*. 2026, vol. 16, art. 14750, s. 1-11. https://doi.org/10.1038/s41598-026-44780-2.
Impact Factor: 3.9.

Punktacja MNiSW: 140 pkt.

P7: Rapacz–Kinas D*, Smolińska–Kempisty K, Urbanowska A, Wolska J. Detection of S–metolachlor in Surface Water Near Cornfields Using pH-Sensitive *Green* Molecularly Imprinted Polymers. *Molecules.* 2026, vol. 31, art. 932, s. 1-17. https://doi.org/10.3390/molecules31060932.
Impact Factor: 4.6.
Punktacja MNiSW: 140 pkt.

* autor korespondencyjny

4. Wykaz stosowanych skrótów

2,4–D	kwas 2,4–dichlorofenoksyoctowy (ang. 2,4–dichlorophenoxyacetic acid)
2,4–DCP	2,4–dichlorofenol (ang. 2,4–dichlorophenol)
AA	akrylamid (ang. acrylamide)
AAc	kwas akrylowy (ang. acrylic acid)
APS	nadsiarczan amonu (ang. ammonium persulfate)
ATR	atrazyna (ang. atrazine)
COD	chemiczne zapotrzebowanie na tlen (ang. chemical oxygen demand)
CS	rdzień–otoczka (ang. core–shell)
CS–MIP	polimery wdrukowane molekularnie typu rdzeń–otoczka (ang. core–shell molecularly imprinted polymers)
CS–NIP	polimery bez odcisku molekularnego typu rdzeń–otoczka (ang. core–shell molecularly non–imprinted polymers)
DAD	detektor z matrycą diodową (ang. diode array detector)
DLS	dynamiczne rozpraszanie światła (ang. dynamic light scattering)
GLY	glifosat (ang. glyphosate)
HPLC	wysokosprawna chromatografia cieczowa (ang. high–performance liquid chromatography)
IF	współczynnik wdrukowania (ang. imprinting factor)
IR	spektroskopia w podczerwieni (ang. infrared spectroscopy)
LCST	dolna krytyczna temperatura rozpuszczania (ang. lower critical solution temperature)
MBAA	N,N'–metylenobis(akrylamid) (ang. N,N′–Methylenebis(acrylamide))
MIP	polimery wdrukowane molekularnie (ang. molecularly imprinted polymers)
MF	mikrofiltracja (ang. microfiltration)
NIP	polimery bez odcisku molekularnego (ang. non–imprinted polymers)
NIPAM	N–izopropyloakryloamid (ang. N–isopropylacrylamide)
PAAc	poli(kwas akrylowy) (ang. poly(acrylic acid))
PE	polietylen (ang. polyethylene)
PNIPAM	poli(N–izopropyloakryloamid) (ang. poly(N–isopropylacrylamide))
PVC	poli(chlorek winylu) (ang. poly(vinyl chloride))

RAM	materiały o ograniczonym dostępie (ang. restricted access media)
R_f	współczynnik regeneracji (ang. regeneration factor)
RT	temperatura pokojowa (ang. room temperature)
SEM	skaningowa mikroskopia elektronowa (ang. scanning electron microscopy)
SMCh	S–metolachlor (ang. S–metolachlor)
SPE	ekstrakcja do fazy stałej (ang. solid phase extraction)
TEMED	N,N,N',N'–tetrametyloetylenodiamina (ang. N,N,N′,N′–tetramethylethylenediamine)
TGA	analiza termograwimetryczna (ang. thermogravimetric analysis)
TOC	całkowity węgiel organiczny (ang. total organic carbon)
UF	ultrafiltracja (ang. ultrafiltration)

5. Wprowadzenie

5.1. Problem mikrozanieczyszczeń

Pierwsze badania dotyczące zanieczyszczenia wody przeprowadzono już na początku XIX wieku i były one spowodowane pojawieniem się różnych chorób śmiertelnych przenoszonych przez te medium. Zaobserwowano, że spożywanie wody o dużym poziomie zanieczyszczenia, powoduje wzrost liczby zgonów wywołanych chorobami rozprzestrzenianymi przez wodę. Początkowe próby uzdatniania wody, obejmujące wprowadzenie chloru w połączeniu z filtracją, miały na celu wyeliminowanie patogenów bakteryjnych [1-2]. Z kolei postęp technologiczny oraz rozwój cywilizacyjny doprowadziły do produkcji ogromnych ilości substancji organicznych, które zanieczyszczały zasoby wodne i przyczyniły się do obniżenia jakości wód [3-4]. Migracja tych niebezpiecznych związków chemicznych, przez różne media, w tym wodę, może stanowić zagrożenia dla zdrowia i życia ludzi oraz innych gatunków, a także powoduje zanieczyszczenie środowiska [5]. W wodach identyfikowane są różnorodne substancje, takie jak leki, narkotyki, surfaktanty, kosmetyki, metale ciężkie, czy środki ochrony roślin (herbicydy, pestycydy i fungicydy) [6-7]. Związki te tworzą tak zwane „*koktajle chemiczne*", w których stężenia substancji często znajdują się w zakresie od ng × L^{-1} do µg × L^{-1}, co niejednokrotnie jest poniżej ich granic wykrywalności [8-9]. Analiza próbek środowiskowych często jest skomplikowaną procedurą, wymagającą wykonania wielu kroków. Natomiast dokładność tych badań nie zależy jedynie od użytego aparatu pomiarowego, ale również od wszystkich etapów wykonanych wcześniej [10]. Najczęściej do oznaczeń wykorzystywane są tradycyjne techniki analityczne, takie jak chromatografia gazowa, chromatografia cieczowa czy spektrometria mas oraz techniki sprzężone będące ich połączeniem [11]. Metody te charakteryzują się dużą czułością, niskim limitem detekcji oraz dobrą powtarzalnością. Jednakże poza wieloma zaletami, posiadają również ograniczenia. Wymagają obsługi przez wysoko wykwalifikowany personel, a analiza oraz obróbka danych są czasochłonne [11-12]. Ponadto podczas analizy złożonych próbek środowiskowych mogą pojawiać się interferencje od pozostałych związków obecnych w matrycy, co może znacząco utrudnić badanie [13]. Dlatego tak ważny jest etap wstępnego przygotowania próbki do analizy. Pośród metod przygotowania oraz wzbogacania próbek wyróżnia się między innymi: ekstrakcję ciecz–ciecz, ekstrakcję do fazy stałej, mikroekstrakcję do fazy stałej i liofilizację [14].

5.2 Technika ekstrakcji do fazy stałej

Technika ekstrakcji do fazy stałej jest skuteczną, szeroko stosowaną, metodą przygotowania próbki, umożliwiającą zarówno usunięcie związków zakłócających, jak i zatężenie pożądanego analitu oraz oznaczenie mikrozanieczyszczeń w złożonych matrycach [15]. W technice SPE anality są rozdzielane pomiędzy fazę stałą (sorbent) a fazę ciekłą, i powinny wykazywać większe powinowactwo do sorbentu niż do matrycy próbki. Odpowiednio dobrane złoże pozwala kontrolować selektywność poprzez interakcje między tym sorbentem, a grupami funkcyjnymi analitów. Wśród tradycyjnych złóż w metodzie SPE wyróżnia się chemicznie związane krzemionki, materiały na bazie węgla oraz materiały jonowymienne. Najpopularniejszymi wypełnieniami do SPE są te na bazie krzemionki

z organiczną grupą C18 lub C8, używane do adsorpcji związków niepolarnych lub słabo polarnych. Jednakże ich ograniczeniem jest możliwa obecność resztkowych grup silanowych i niestabilność w ekstremalnych wartościach pH [16-17]. Z kolei złoża na bazie węgla posiadają zdolność adsorpcji zarówno związków niepolarnych, jak i polarnych. Ponadto cechują się one odpornością na wysokie temperatury oraz są odporne na ekstremalne wartości pH. Jednakże czasami problematyczna może okazać się elucja analitu ze złoża, spowodowana nieodwracalnym związaniem cząsteczki związku przez sorbent [18-19]. W chromatografii jonowymiennej, mechanizm rozdzielania opiera się o sorpcję i desorpcję obdarzonych ładunkiem elektrycznym fragmentów fazy stacjonarnej oraz przeciwnie naładowanych cząsteczek analitu. Jednakże wymiana jonów odbywa się na podstawie ich ładunku oraz wielkości, co sprawia, że separacja nie jest selektywna [20-21]. Mimo, że początek historii techniki SPE sięga lat 40. XX wieku, metoda ta w dalszym ciągu stanowi fundamentalny element przygotowania próbek [22]. Jednak, aby zapewnić selektywne wiązanie docelowych związków chemicznych ze złożonych matryc, technika SPE została ulepszona poprzez wprowadzenie sorbentów o dużym powinowactwie do analitu, takich jak materiały o ograniczonym dostępie (RAM), immunosorbenty, oraz polimery molekularnie wdrukowane (MIP) [17].

5.3. Molekularnie wdrukowywane polimery

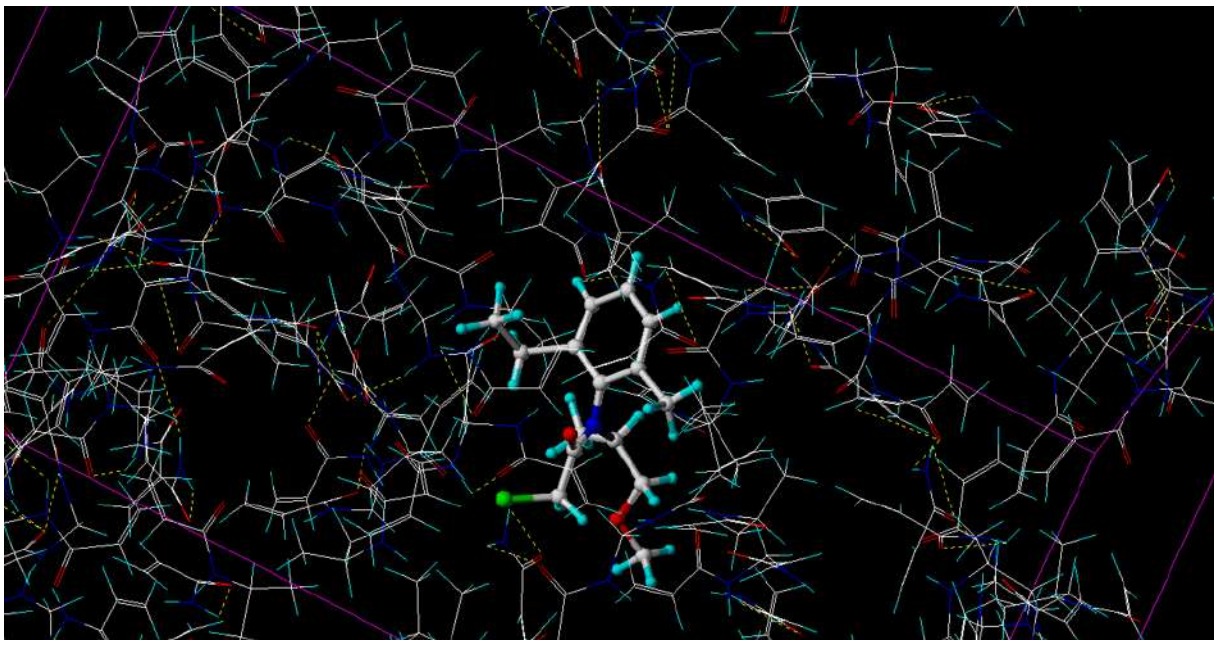

Rysunek 1. Modelowe oddziaływanie cząsteczki S-metolachloru z monomerami funkcyjnymi oraz środkiem sieciującym na podstawie algorytmu Leapfrog dostępnym na oprogramowaniu SYBYL 7.3.

Polimery wdrukowane molekularnie stanowią klasę materiałów syntetycznych, szeroko wykorzystywanych w chemii analitycznej, posiadających bardzo wysoko selektywne możliwości rozpoznawania, które naśladują naturalne interakcje przeciwciało–antygen [23-24]. Polimery te są syntezowane w wyniku reakcji polimeryzacji monomerów funkcyjnych, środka sieciującego oraz cząsteczki szablonu. W kolejnym kroku wdrukowane cząsteczki analitu są

usuwane z matrycy polimeru za pomocą odpowiednich metod. W ten sposób tworzone są swoiste wnęki „*rozpoznawcze*”, które są w pełni komplementarne kształtem, rozmiarem oraz obecnością grup funkcyjnych do analitu docelowego. Proces „*odciskania*” molekularnego nadaje tym polimerom wyjątkową selektywność oraz powinowactwo do cząsteczek docelowych, co czyni je niezwykle skutecznymi narzędziami w różnorodnych zastosowaniach analitycznych [25-26]. W procesach sorpcyjnych z wykorzystaniem MIPów wyróżnia się trzy główne rodzaje oddziaływań: kowalencyjne, niekowalencyjne i półkowalencyjne. Wszystkie opierają się na rozpoznawaniu molekularnym, zachodzącym między cząsteczkami docelowymi a monomerami funkcyjnymi. W latach 70. XX wieku opisano strategie odciskania kowalencyjnego, natomiast techniki wiązania niekowalencyjnego zostały wprowadzone w latach 90. XX wieku przez Klausa Mosbacha *et al*. [23]. Jednakże spośród wszystkich tych opcji, podejście niekowalencyjne jest wykorzystywane najczęściej, ze względu na odwracalność oraz „*elastyczne*” właściwości ponownego wiązania [27].

Z uwagi na wzrastającą globalną świadomość i odpowiedzialność, promowane jest programowanie nowoczesnych technologii w kierunku bardziej ekologicznych rozwiązań. Dlatego w ostatnich latach ogromną uwagę skupia się na tzw. „*zielonych*” polimerach molekularnie wdrukowanych, syntezowanych zgodnie z założeniami „*zielonej chemii*”. Ekologiczne zasady projektowania technologii MIPów określane są za pomocą akronimu „*greenification*”. Koncepcja ta opiera się między innymi o generowanie minimalnych ilości odpadów, kontrolowaną polimeryzację prowadzoną bez strat energii oraz zastąpienie organicznych porogenów i rozpuszczalników medium wodnym. Ponadto do wytycznych należą również: wielokrotne wykorzystanie tych samych sorbentów, projektowanie samooczyszczających się MIPów, optymalizacja syntezy poprzez modelowanie obliczeniowe, a także stosowanie nieszkodliwych reagentów oraz zwiększone bezpieczeństwo operatora. Jednakże, mimo wielu trendów wspierających „*zieloną chemię*” w celu poprawy ludzkiego zdrowia, ochrony środowiska i zwiększenia zrównoważonego rozwoju, w dalszym ciągu jest ona stosowana niezbyt powszechnie [13, 28-29].

Naukowcy od lat inspirują się naturą i starają się stworzyć materiały, które mogą zmieniać swoją strukturę w zależności od sytuacji, podobnie jak zachowują się organizmy żywe, aby przetrwać w środowisku [30]. Polimery wykazujące odpowiedź na bodźce, ulegające odwracalnym, fizycznym lub chemicznym zmianom swoich właściwości, w wyniku niewielkich zmian środowiskowych, określane są mianem „*inteligentnych*” polimerów. Materiały te mogą reagować na jeden lub wiele bodźców jednocześnie. Wśród czynników stymulujących polimery wyróżnia się między innymi: temperaturę, pH, natężenie światła, czy pole elektryczne lub magnetyczne [31-32]. Ze względu na ogromny potencjał, ten rodzaj polimerów wykorzystywany jest również do syntezy MIPów [33].

N-izopropyloakryloamid jest najczęściej stosowanym monomerem do syntezy „*termoczułych*” polimerów. Odpowiedź poli(N–izopropyloakryloamidu) (PNIPAM) na zmianę temperatury, przypisuje się właściwościom związanym z dolną krytyczną temperaturą rozpuszczania (LCST) [34]. W cząsteczce poli(N–izopropyloakryloamidu) obecne są hydrofilowe grupy amidowe oraz hydrofobowe grupy izopropylowe. Poniżej LCST, która dla PNIPAMu jest równa 32°C, grupy amidowe tworzą wiązania wodorowe z cząsteczkami wody,

w wyniku czego polimer pęcznieje i jest rozpuszczalny w wodzie. Natomiast, gdy temperatura jest wyższa niż LCST, następuje zwiększenie oddziaływań hydrofobowych i zerwanie wiązań wodorowych. Wówczas zachodzi przemiana fazowa, w wyniku której PNIPAM wypada z roztworu, a klarowny roztwór zmienia się w mleczną zawiesinę [33, 35-36].

Szeroko opisywanym przykładem materiału wrażliwego na zmianę pH jest poli(kwas akrylowy). Przy niskim pH grupy karboksylowe są protonowane, dominują oddziaływania hydrofobowe, co prowadzi do zmniejszenia objętości polimeru. Przejście konformacyjne kwasu poli(akrylowego), ze skondensowanego kształtu kulistego do rozluźnionej formy, rozpoczyna się w pH około 4,5–5. Wówczas grupy karboksylowe zaczynają dysocjować na jony karboksylanowe, co powoduje większą gęstość ładunku w polimerze i jego pęcznienie [37-39]. Warto zauważyć, że mechanizm działania „*inteligentnych*" polimerów może jednocześnie stanowić metodę odzysku analitów zaadsorbowanych przez polimery z odciskiem molekularnym. Mechanizm samoregeneracji materiałów, odbywa się bez użycia szkodliwych dla środowiska rozpuszczalników organicznych, wpisując się również w założenia „*zielonej*" chemii, czyniąc te polimery, materiałami przyjaznymi dla środowiska [8, P3-P5, P7].

Polimery molekularnie wdrukowane, syntezowane za pomocą tradycyjnej metody polimeryzacji w masie, pomimo dużej stabilności fizycznej oraz chemicznej, wytrzymałości mechanicznej, prostoty przygotowania, a także małych kosztów syntezy, wykazują również pewne wady. Ich ograniczeniami jest nieregularna morfologia powierzchni, głęboko osadzone wnęki, nierównomierny rozkład miejsc wiążących oraz wolniejsza kinetyka ponownego wiązania. Zwiększenie wydajności MIPów można osiągnąć za pomocą struktury rdzeń–otoczka, gdzie materiałowy rdzeń jest pokryty warstwą polimeru molekularnie wdrukowanego. Strategia ta zapewnia równomierny rozkład miejsc wiążących oraz ich zwiększoną dostępność, a także szybsze i wydajniejsze usuwanie oraz ponowne wiązanie cząsteczek analitu, co skraca czas analizy [27, 40-42].

5.4. S-metolachlor

S–metolachlor jest jednym z herbicydów powszechnie wykorzystywanych do zwalczania chwastów trawiastych i szerokolistnych, między innymi w uprawie kukurydzy, soi, słonecznika, ziemniaków i pomidorów [43-44]. Substancja czynna S–metolachloru jest stosunkowo dobrze rozpuszczalna w wodzie (488 mg × L^{-1}) [45] oraz absorbowana przez cząstki gleby. Następnie cząsteczki S–metolachloru mogą być wypłukiwane do wód powierzchniowych i podziemnych, a ze względu na stosunkowo długi okres półtrwania w wodzie (ponad 200 dni) oraz w glebie (nawet do 70 dni), mogą stanowić zagrożenie dla zdrowia ludzi i zwierząt oraz dla środowiska [46-47]. Metolachlor jest cząsteczką chiralną i występuje w postaci dwóch izomerów: R i S. Jednakże izomer S jest prawie zawsze stosowany w środkach ochrony roślin, ponieważ ma większą aktywność herbicydową [43]. Zbadano, że S–metolachlor jest sześciokrotnie bardziej skuteczny w zwalczaniu chwastów niż R–metolachlor [48]. To sprawiło, że pierwotnie wprowadzony na rynek w 1976 roku produkt racemiczny, jest zastępowany S-metolachlorem [49-50].

6. Cel pracy

W niniejszej rozprawie doktorskiej tak zwane „*inteligentne*" polimery wdrukowane molekularnie z powinowactwem do S–metolachloru, syntetyzowane zgodnie z koncepcją „*zielonej chemii*" stanowiły główny cel prowadzonych badań. Podjęcie tej tematyki badawczej było umotywowane między innymi faktem, że do 2024 roku nie istniała publikacja naukowa opisująca tzw. „*zielone*" polimery molekularnie wdrukowane selektywne wobec S–metolachloru. **Otrzymano cztery rodzaje sorbentów: molekularnie wdrukowane polimery blokowe wykazujące odpowiedź na zmianę temperatury lub pH, oraz sorbenty typu rdzeń–otoczka z naniesioną warstwą molekularnie wdrukowanego polimeru wrażliwego na temperaturę lub pH, selektywne wobec S–metolachloru.** Zarys rozprawy doktorskiej został przedstawiony w formie graficznej na Rysunku 2.

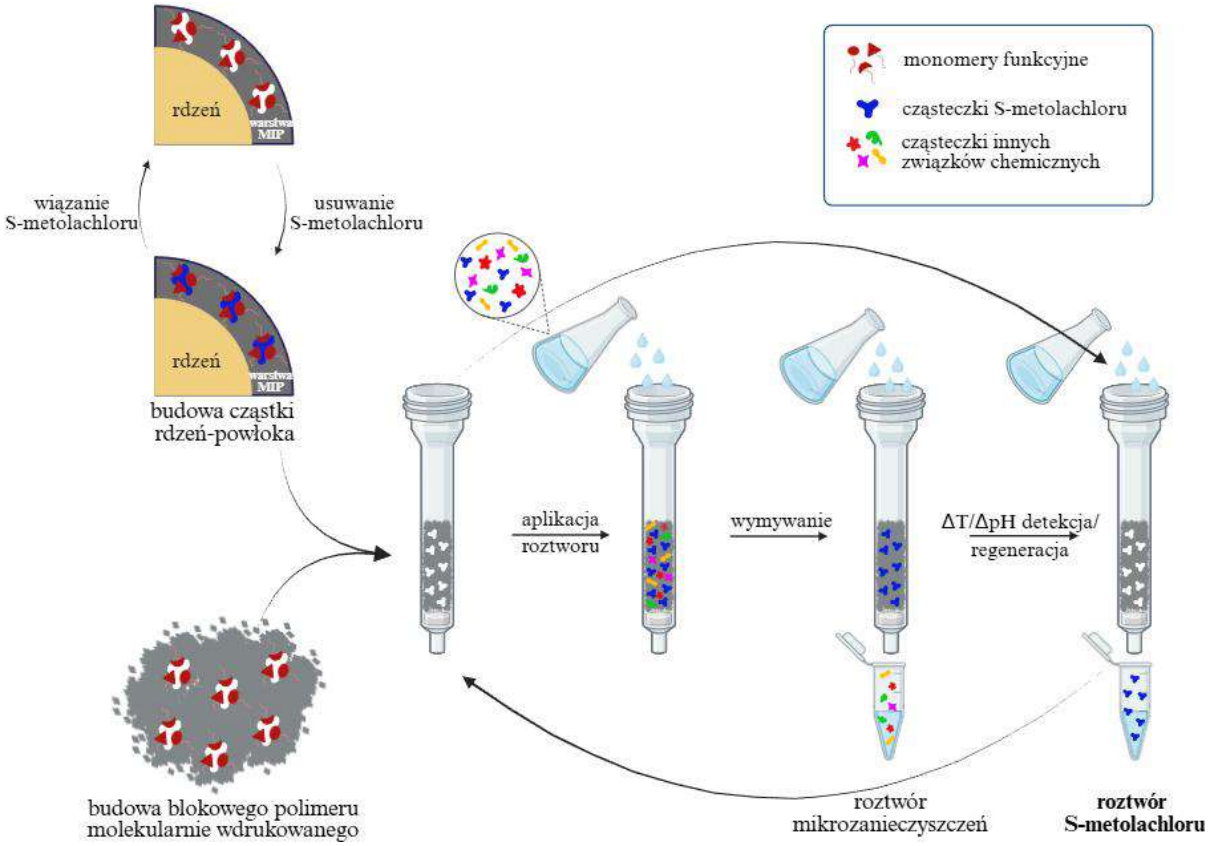

Rysunek 2. Schematyczne przedstawienie zakresu rozprawy doktorskiej.

Główne cele badawcze obejmowały:

1) Otrzymanie molekularnie wdrukowanych polimerów blokowych, reagujących na zmianę temperatury lub pH, selektywnych wobec S–metolachloru; w tym dobór odpowiednich reagentów: monomerów funkcyjnych, środka sieciującego oraz poroforu, mających powinowactwo do S–metolachloru i spełniających założenia „*zielonej chemii*" oraz optymalizacja warunków reakcji.

2) Opracowanie „*zielonych*” sorbentów typu rdzeń–otoczka, wykazujących odpowiedź na zmianę temperatury lub pH. Wyselekcjonowanie składu mieszaniny reakcyjnej oraz warunków syntezy.
3) Zbadanie procesu adsorpcji S–metolachloru na polimerach blokowych oraz materiałach typu rdzeń–otoczka pod względem selektywności, kinetyki oraz izoterm sorpcji.
4) Zaprojektowanie warunków sorpcji herbicydu na wszystkich rodzajach sorbentów w trybie statycznym, a także procesu sorpcji i desorpcji w trybie dynamicznym z wykorzystaniem kolumn typu SPE.
5) Przetestowanie skuteczności otrzymanych materiałów w zakresie wykrywania i oznaczania stężenia S–metolachloru w próbkach rzeczywistych.
6) Charakterystyka właściwości fizyko–chemicznych sorbentów m.in. poprzez wykorzystanie metody spektroskopii w podczerwieni, obrazowania skaningowym mikroskopem elektronowym, analizy termograwimetrycznej, czy techniki dynamicznego rozpraszania światła.

7. Zakres badawczy rozprawy

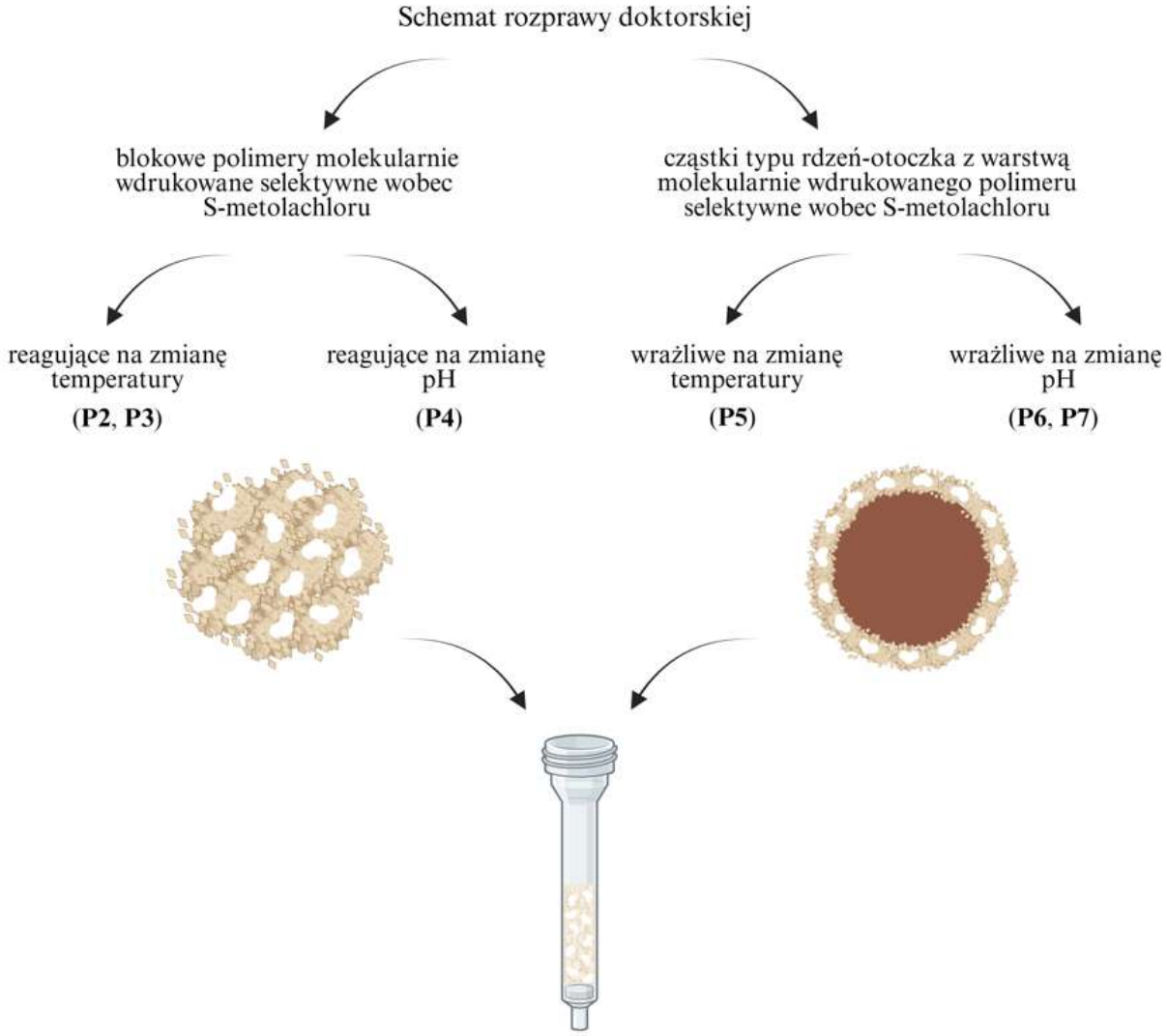

Rysunek 3. Schemat rozprawy doktorskiej.

Na rozprawę doktorską składa się siedem publikacji, w tym jedna praca przeglądowa oraz sześć prac badawczych, opublikowanych w recenzowanych czasopismach naukowych.

Artykuł przeglądowy **P1** opisuje problem mikrozanieczyszczeń wód oraz trudności, które pojawiają się podczas oznaczeń analitów ze złożonych próbek środowiskowych. Ponadto w pracy przedstawiona została luka w literaturze naukowej dotycząca syntezy polimerów wdrukowanych molekularnie selektywnych wobec herbicydów zgodnie z koncepcją tak zwanej „*zielonej chemii*". Szczególnie istotny był fakt, iż, do 2024 roku nie istniała ani jedna publikacja opisująca polimery z odciskiem molekularnym selektywne wobec S–metolachloru, syntezowane w środowisku wodnym, co podkreśla innowacyjność prowadzonych badań.

Drugi artykuł **P2** przedstawia blokowy polimer wdrukowany molekularnie, selektywny wobec S–metolachloru, wrażliwy na temperaturę, otrzymany zgodnie z założeniami tak zwanej „*zielonej chemii*". Ponadto opisuje dopasowanie procesu sorpcji do odpowiednich modeli izoterm, a także charakterystykę IR oraz SEM otrzymanych sorbentów.

Trzecia publikacja **P3** skupia się na zastosowaniu otrzymanego polimeru blokowego wrażliwego na temperaturę jako złoża w kolumnach typu SPE oraz charakteryzuje kinetykę sorpcji. W pracy opisana została optymalizacja warunków sorpcji oraz regeneracji złoża w trybie dynamicznym, na kolumnach SPE.

Czwarty manuskrypt **P4** przedstawia tak zwane „*zielone*" blokowe molekularnie wdrukowane polimery selektywne wobec S–metolachloru, reagujące na zmianę pH. W publikacji przedstawione zostało dopasowanie do modeli kinetyki oraz izoterm sorpcji, charakterystyka IR i SEM zsyntezowanych polimerów, oraz ich zastosowanie jako złoże w kolumnach typu SPE.

Piąty artykuł **P5** opisuje tak zwane „*zielone*" sorbenty typu rdzeń–otoczka selektywne wobec S–metolachloru, wykazujące odpowiedź na zmianę temperatury. W publikacji przedstawione zostało dopasowanie kinetyki oraz izoterm sorpcji do odpowiednich modeli, optymalizacja warunków sorpcji i desorpcji na kolumnach typu SPE, oraz charakterystyka IR i SEM otrzymanych sorbentów.

Szósta publikacja **P6** skupia się na polimerach typu rdzeń–otoczka wdrukowanych molekularnie, selektywnych wobec S–metolachloru, wrażliwych na zmianę pH, otrzymanych zgodnie z koncepcją tak zwanej „*zielonej chemii*". W pracy przedstawiono skład mieszaniny reakcyjnej oraz optymalizację warunków syntezy, a także zastosowanie sorbentów jako złoża w kolumnach typu SPE i opracowanie warunków sorpcji. Ponadto opisano charakterystykę SEM, TGA, IR polimerów, a także badania porowatości oraz średni rozmiar cząstek sorbentów.

W ostatnim, siódmym artykule **P7** scharakteryzowano proces sorpcji oraz desorpcji cząstek typy rdzeń–otoczka wdrukowanych molekularnie, reagujących na zmianę pH oraz dopasowano otrzymane wyniki do odpowiednich modeli izoterm oraz kinetyki sorpcji. Dodatkowo w pracy przetestowano skuteczność działania kolumn SPE wykorzystując wodę pobraną bezpośrednio z akwenów wodnych w pobliżu upraw kukurydzy. Zastosowano również filtrację membranową w celu weryfikacji możliwości stosowania otrzymanych kolumn bezpośrednio na pobranej wodzie. Kolejność przedstawionych prac w logiczny sposób wprowadza w tematykę rozprawy doktorskiej.

7.1. Aktualny stan wiedzy na temat polimerów wdrukowywanych molekularnie w kierunku S-metolachloru (Publikacja P1)

Rapacz D, Smolińska–Kempisty K, Wolska J. Progress in development and the current state of the art depending on the polymerization environment – Short review. *Journal of Environmental Chemical Engineering*. 2024, vol. 12, nr 2, art. 112159, s. 1-12. https://doi.org/10.1016/j.jece.2024.112159.

Pierwszy artykuł zatytułowany "**Progress in development and the current state of the art depending on the polymerization environment – Short review**" opublikowany w Journal of Environmental Chemical Engineering stanowi przegląd literaturowy wprowadzający w zagadnienia polimerów wdrukowanych molekularnie selektywnych wobec herbicydów. Praca opisuje aktualne problemy środowiskowe. W wodach wykrywane są różnorodne substancje, w tym leki, narkotyki, surfaktanty, metale ciężkie, czy środki ochrony roślin, takie jak herbicydy, pestycydy i fungicydy. Związki te, bardzo często występują w śladowych ilościach, tworząc tak zwane „*koktajle chemiczne*". Charakteryzują się one podobieństwem w zakresie budowy chemicznej i masy cząsteczkowej, co może prowadzić do występowania interferencji znacząco utrudniających proces analizy. Z tego powodu kluczowe znaczenie ma etap wstępnego przygotowania próbki. Jedną z powszechnie wykorzystywanych metod jest zatężanie próbek, wykonywane z zastosowaniem techniki ekstrakcji do fazy stałej. Jako złoże w kolumnach typu SPE często stosowane są polimery wdrukowane molekularnie. Sorbenty te posiadają specyficzne wnęki w matrycy polimeru, które są perfekcyjnie dopasowane pod względem kształtu, rozmiaru oraz obecności grup funkcyjnych do cząsteczki analitu, służącej jako szablon. W rezultacie tego w kolumnach zachodzi proces selektywnej sorpcji – cząsteczki analitu są wiązane w tych wnękach, podczas gdy pozostałe mikrozanieczyszczenia przechodzą przez kolumnę. Następnie przeprowadzany jest proces desorpcji analitu, co pozwala uzyskać jednoskładnikowy roztwór.

Na szczególną uwagę zasługują tak zwane „*zielone*" polimery wdrukowane molekularnie. Określenie to wynika ze sposobu ich syntezy opartej właśnie na zasadach „*zielonej chemii*" oraz trosce o środowisko. Takie podejście zakłada, że proces polimeryzacji prowadzony jest w sposób kontrolowany, minimalizując straty energii, a tradycyjne, szkodliwe organiczne środki porotwórcze zastępuje się ekologicznymi rozpuszczalnikami, na przykład medium wodnym. Ponadto, projektowanie samooczyszczających się materiałów, możliwych do wielokrotnego wykorzystania, przy jednoczesnym ograniczeniu strat energii, wpisuje się w koncepcję „*greenification*".

Niniejsza publikacja podkreśla również, jak ważny jest etap wstępnego przygotowania próbek do analizy, omawia metody syntezy oraz wykorzystanie polimerów wdrukowanych molekularnie jako sensorów selektywnych wobec herbicydów, stosowanych w analizach złożonych próbek środowiskowych. Szczegółowo przedstawia także właściwości i zastosowanie S–metolachloru, będącego kluczowym elementem niniejszej rozprawy doktorskiej. Ponadto wskazuje istniejącą lukę w literaturze naukowej, dotyczącą otrzymywania polimerów z odciskiem molekularnym wrażliwych na herbicydy, w szczególności S–metolachlor, zgodnie z ideologią zrównoważonego rozwoju i zasadami tak zwanej „*zielonej*

chemii”. Istotne jest to, że w roku 2024, kiedy praca została opublikowana, istniały jedynie cztery publikacje opisujące syntezę MIPów, wyłącznie w środowisku wodnym, selektywnych wobec herbicydów takich jak 2,4–D, 2,4–DCP, chlorotoluron i parakwat. Przegląd literatury wskazuje brak doniesień dotyczących polimerów wrażliwych na S–metolachlor, otrzymanych zarówno w medium wodnym, jak i w mieszaninie woda–rozpuszczalnik organiczny. To podkreśla, że badania stanowiące podstawę niniejszej rozprawy, mogą mieć istotny wkład w rozwój innowacyjnych rozwiązań dotyczących „*zielonych*” polimerów z odciskiem molekularnym.

Journal of Environmental Chemical Engineering 12 (2024) 112159

Contents lists available at ScienceDirect

Journal of Environmental Chemical Engineering

journal homepage: www.elsevier.com/locate/jece

Molecularly imprinted polymers toward herbicides – Progress in development and the current state of the art depending on the polymerization environment – Short review

Dominika Rapacz *, Katarzyna Smolinska-Kempisty *, Joanna Wolska *

Wroclaw University of Science and Technology, Department of Process Engineering and Technology of Polymer and Carbon Materials, Wybrzeże Wyspiańskiego 27, 50-370 Wroclaw, Poland

ARTICLE INFO

Editor: Rosario Rodil

Keywords:
Molecular imprinting
Herbicides
Polymerization in an organic environment
Polymerization in an aqueous environment

ABSTRACT

Molecularly imprinted polymers (MIPs) are types of specific materials capable of recognizing and selecting compounds toward which they have been imprinted. This ability has made these materials increasingly popular in different areas e.g. for monitoring the content of harmful substances in various products, including water. In addition, many chemicals of various structures and applications are used as templates. The presented paper is a review that demonstrates knowledge and understanding of the molecularly imprinted polymers toward herbicides, with particular emphasis on the impact and needs to control their content, e.g. in plant parts, soils, or groundwater. This work focused especially on one of the newest herbicides used in large amounts, S-metolachlor, which is used in maize cultivation. It reviews the latest publications describing polymerizations in organic solvents and in water. Due to the much better solubility of pesticides in organic solvents, this type of polymerization is much more often described. However, due to the growing concern for the environment and the principles introduced in the so-called green chemistry, increasing emphasis should be placed on polymerization in an aqueous environment.

Abbreviations: 2,4-D, 2,4-dichlorophenoxyacetic acid herbicide; 2,4-DCP, 2,4-Dichlorophenol; 2-VP, 2-vinylpyridine; 4-ATP, 4-aminothiophenol; 4-VP, 4-vinylpyridine; AA, Acrylic acid; ABDV, 2,2'-azobis(2,4-dimethylvaleronitrile); ACN, Acetonitrile; AIBN, Azobisisobutyronitrile; AM, Acrylamide; AME, Ametryn; AMMB, 2-acrylamide-6-methoxybenzothiazole; APTES, Aminopropyltriethoxysilane; ATR, Atrazine; ATU, N-allylthiourea; AuNPS, Gold nanoparticles; BPM, Bipolar membrane; BPO, Benzoyl peroxide; CDB, Cumyl dithiobenzoate; CL, Chemiluminescent; CMMC, 7-carboxymethoxy-4-methylcoumarin; DCM, Dichloromethane; DEA, Deethyltrazine; DEAMA, 2-(diethylamino)ethyl methacrylate; DEDA, Diethylene glycol diacrylate; DIA, Deisopropylatrazine; DMAEM, 2-dimethyl aminoethyl methacrylate; DMF, Dimethylformamide; DMSO, Dimethyl sulfoxide; DVTD, 1,3-divinyltetramethyldisiloxane; EDCs, Endocrine-disrupting chemicals; EGDMA, Ethylene glycol dimethacrylate; ERHD, Electrochemical reductive hydrodechlorination; ESPR, Electrochemical surface plasmon resonance; EtOH, Ethanol; FIM, N-[2-(6–4-methylpiperazin-1-yl)– 1,3-dioxo-1 H-benzo[de]isoquinolin-2(3 H)-ylethyl)acrylamide; FRP, Free radical polymerization; GC, Gas chromatography; GCE, Glassy carbon electrode; GLY, Glyphosate; GO, Graphene oxide; HPLC, High-performance liquid chromatography; HRP, Horseradish peroxidase; LLSME, Liquid-liquid-solid microextraction; MAA, Methacrylic acid; Macro-CTAs, Macromolecular chain-transfer agents; MBAM, N, N '-methylenebisacrylamide; MeOH, Methanol; Me_6TREN, Tris[2-(dimethylamino)ethyl]amine; MH, Maleic hydrazide; MIM, Molecularly imprinted membrane; MIPs, Molecularly imprinted polymers; MIP-Ppy, Molecularly imprinted polypyrrole; MIR, Molecularly imprinted resin; MISPE, Molecularly imprinted solid-phase extraction; MPTS, 3-methacryloxypropyl trimethoxysilane; MRL, Maximum residue limit; MWNTs, Multi-walled carbon nanotubes; NBD, Nitrobenzoxadiazole; NiHCF, Nickel hexacyanoferrate; OUA, Oligourethane acrylate; PANI, Polyaniline; PDA, 1,4-bis(acryloyl)piperazine; PEG, Polyethylene glycol; PGMMA, Poly(glyceryl monomethacrylate); $PhCH_3$,, Toluene; PHEMA, Poly(2-hydroxyethyl methacrylate); PMMA, Poly(methyl methacrylate); PNIPAM, Poly(N-isopropylacrylamide); POCIS-MIP, Polar Organic Chemical Integrative Sampler with Molecular Imprinted Polymer; QD, Quantum dots; RAFT, Reversible addition fragmentation chain transfer; RT, Room temperature; SDS, Sodium dodecyl sulfate; SERS, Surface-enhanced Raman spectroscopy; SI-ATRP, Surface-initiated atom transfer radical polymerization; SPE, Solid phase extraction; SPME, Solid-phase microextraction; TCM, Chloroform; TeCA, Tetrachloroethane; TEDMA, Tri(ethylene glycol) dimethacrylate; TEOS, Tetraethyl orthosilicate; TER, Terbuthylazine; TFM, Thifensulfuron-methyl; TRI, 2-amino-4-methoxy-6-methyl-1,3,5-triazine; TRIM, Trimethylolpropane trimethacrylate; VLCFA, Very long-chain fatty acid synthesis; WCMM, Water-compatible magnetic imprinted microsphere; ZnPP, zinc(II) protoporphyrin.

* Corresponding authors.
E-mail addresses: dominika.rapacz@pwr.edu.pl (D. Rapacz), katarzyna.smolinska@pwr.edu.pl (K. Smolinska-Kempisty), joanna.wolska@pwr.edu.pl (J. Wolska).

https://doi.org/10.1016/j.jece.2024.112159
Received 7 November 2023; Received in revised form 31 January 2024; Accepted 4 February 2024
Available online 6 February 2024

1. Introduction

The development of agriculture about 12 thousand years ago changed the way humans lived. They went from nomadic lifestyles to permanent settlements and agriculture. Although they were young growers, they noted that some types of plants are different and undesirable. Farmers did not want to pull them by hand and needed something to control these plants, referred to as *weeds*. By the mid-nineteenth century, clover and livestock manure were a source of fertility, and weeds were controlled by cleaning crops. In the early twentieth century, chemical weed control was invented, significantly improving agriculture quality. [1] Initially, fertilizers accounted for a few inorganic compounds such as sulfuric acid, copper salts, or sodium chlorate. [2] These compounds were referred to as herbicides, commonly used enzyme inhibitors. The origin of the word herbicide is a combination of the Latin words *herba* (noun, herbaceous plant) and *caedere* (verb, to kill). [1] The herbicides must conduct two contradictory objectives: to control the weed plants, but not to damage the crop plants. Detailed research on herbicides began in the 1950 s [3] According to the classification of the Herbicide Resistance Action Committee, herbicides are divided into groups based on the mode of action. One of them concentrates the herbicides causing inhibition of very long-chain fatty acid synthesis (VLCFA). [4] The largest family of this group is the chloroacetanilides, which includes S-metolachlor (2-chloro-N-(2-ethyl-6-methylphenyl)-N-(2-methoxy-1-methylethyl)acetamide), one of the three most commonly used herbicides in this category. [5] S-metolachlor is a herbicide with pre- and post-emergence action, commonly used as an inhibitor of growth shoots and roots in different cultivation, such as maize, soybean, cotton, sunflower, beans, or sugar cane to control a wide range of annual grasses and broadleaf weeds. [6] The cultivation of maize is gaining more and more popularity every year. As recently as the late 1990 s, the area planted in fields with this grain in Poland was about 100 thousand ha, [7] while in 2022 maize production ranked second among all cereal crops at about 1.9 million ha. [8] Due to favorable arometeorological conditions, it is estimated that there will be an even greater increase in the cultivation of maize, and thus the application of larger amounts of S-metolachlor for weed control. [7] S-metolachlor is highly poisonous and can be leached into groundwater. The active principle of S-metolachlor is soluble in water and is absorbed by soil particles. [9] Exactly metolachlor is the herbicide, which has the highest absorption in the soil of any chloroacetanilide. [10] The half-life ($T_{1/2}$) of metolachlor has been reported to decrease with increasing temperatures and to rise with soil depth. The relatively long half-life of metolachlor translates into more difficult metabolized by soil microorganisms. [11] Metolachlor comprises two R-isomers and two S-isomers (Fig. 1), but the S-isomers have more herbicidal activity. [12].

Given the above, there is a need to acquire new methods for detecting and monitoring S-metolachlor concentrations in waters.

The presented review aimed to show a gap in the field of synthesis of herbicide-sensitive MIPs in aquatic medium, according to green chemistry, with particular emphasis on S-metolachlor. Since only a small amount of molecularly imprinted polymers were synthesized in an aqueous medium, in this paper a comparison of these MIPs with those obtained in an organic medium was presented to show the overall.

2. Molecularly imprinted polymers

Even though most herbicides do not have carcinogenic properties, it is particularly important to use them consciously because, in larger amounts, they can be harmful to human health and the agroecosystem. Nonetheless, some herbicides can be carcinogenic even at low doses, therefore a tolerance range has been developed, known as the maximum residue limit (MRL). For the MRL value to be determined reliably and accurately, analytical methods and nanosensors are used. The analytical methods include, among others, high-performance liquid

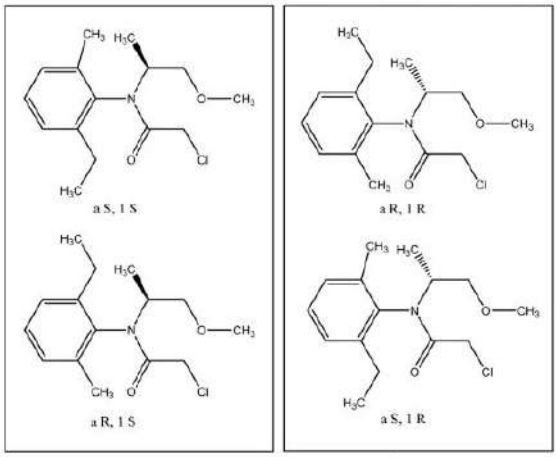

Fig. 1. Isomeric forms of metolachlor.

chromatography, gas chromatography, mass spectroscopy, spectrophotometric, and electrophoresis. These methods have high precision, low detection limits, and good repeatability. However, research by these methods also has a long analysis time and requires expensive research devices and qualified lab technicians. Moreover, these methods consume substantial amounts of organic solvents, which is contrary to the assumptions of *green chemistry*. Electrochemical methods are more popular because of their low cost, accuracy, fast test time, and environmental friendliness. The development of nanotechnology and the production of three-dimensional materials resulted in an increased interest in materials for the determination of herbicides. [13].

One type of detection materials are those based on molecularly imprinted polymers, which are characterized by portable and easy-to-use technology with a short analysis time. MIPs are powerful tools for the separation and enrichment of analytes. The binding capacity of MIP is due to the presence of cavities that have been formed by self-assembling polymerizable monomers around the template. The high selectivity of the materials is ensured by cavities in the polymer coating. [14] Most MIPs are obtained in three main steps. In the first step, the functional monomer is polymerized in the presence of an analyte template, cross-linker, solvent, and initiator. The second step is to remove the template from the polymer, resulting in cavities that are perfectly matched in shape, size, and functional groups to the target analyte will be created. In the third step, the synthesized MIP is evaluated on real samples containing the template. [15]· [16] Due to the way of interaction between the functional monomer and the template, there are several ways to receive MIP: a) covalent imprinting; b) non–covalent imprinting; c) semi–covalent imprinting; d) ion imprinting. [16] Non–covalent imprinting is more popular owing to lower constraints and more flexibility resulting from the choice of monomers. It is based on weak intermolecular interactions, e.g. hydrogen or van der Waals. This type of imprinting therefore appears to be more flexible in the range of chemical functionalities than covalent imprinting, whose flexibility is limited by reversible covalent interactions for templates and monomers. [17,18] MIPs are generically prepared by bulk polymerization, but also with the use of in-situ polymerization, emulsion polymerization, suspension polymerization, or precipitation polymerization. [16] At the same time, these simple and advanced separation tools show the high properties of selective recognition and separation of a specific chemical compound. [19] One of the most crucial factors in molecular imprinting is selecting an appropriate monomer, possessed of functional groups that can interact with the template molecules but do not reactively polymerize with the template. Additionally, the polymer must be sufficiently

cross-linked to ensure that the binding sites are unchanged after the removal of the template particles (Fig. 2). Moreover, the easy modification of the polymer viscosity influences the optimization of the reaction conditions for different templates. [20].

However, developing a procedure for obtaining effective materials requires a lot of research [21,22]. For this reason, scientists are increasingly reaching for the tool of computer molecular modeling [23–28]. The use of modeling is possible in the case of various types of templates, including herbicides [29]. The selection of functional or cross-linking monomers is based on those in the software database. This significantly reduces the work needed to select the best monomer. However, the limited number of monomers in the database can also be a problem. On the other hand, the limitation of the number of syntheses, and thus the reduction of the number of reactants thanks to computational modeling seems to be a green approach to developing novel analytical sorbents.

3. MIPs synthesized in an organic medium

3.1. 2,4-dichlorophenoxyacetic acid herbicide (2,4-D)

Almost all molecularly imprinted polymers reported in the literature are synthesized using organic solvents. Most of these works described in the literature focus on MIP-imprinted toward 2,4-dichlorophenoxyacetic acid herbicide (2,4-D). Some of the papers are featured in this review. In 2013 Wang and co-workers developed a novel paper-based MIP-grafted multi-disk micro-disk plate (P-MIP-MMP) for sensitive and specific chemiluminescent (CL) detection of 2,4-D. The MIP synthesis via in situ polymerization was carried out using the following: acrylamide (AM) as a functional monomer, ethylene glycol dimethacrylate (EGDMA) as a cross-linker, azobisisobutyronitrile (AIBN) as an initiator, 2,4-D as a template, ethanol and water as a solvent. The limit of detection of the received sensor was 1.0 pM and with the increasing concentration of 2,4-D, the CL intensity decreased logarithmically within the concentration range of 5.0 pM–10.0 μM. [30] In another work, Xu et al. demonstrated for the first time the preparation of MIP-based optosensing materials capable of selective detection of 2,4-D herbicide in pure undiluted milk with a detection limit of 0.13 μM. Initially, the grafted dual fluorescent 2,4-D-imprinted polymer was synthesized via successive surface-initiated atom transfer radical polymerization (SI-ATRP). Red CdTe quantum dots (QD) are indifferent to 2,4-D, while green nitrobenzoxadiazole (NBD) exhibits fluorescence enhancement after binding of this herbicide. The 2,4-D-MIP particles were received differently than before [30], 4- vinylpyridine (4-VP) and NBD were used as a functional monomers, EGDMA was used as a cross-linking agent, and tris [2-(dimethylamino)ethyl]amine (Me_6TREN), CuCl, ethyl 2-chloropropionate, and dried acetonitrile were applied as a ligand, metal salt, initiator and solvent, respectively. In the following step, the obtained MIPs were grafted onto the poly(glyceryl monomethacrylate) (PGMMA) brushes. [31] To date, the poor spectral reproducibility and lack of selectivity in the surface-enhanced Raman spectroscopy (SERS) method have resulted in its extremely constrained use. In the latest research, Feng et al. enabled target molecules to be detected by MIP traced on the surface of gold nanoparticles (AuNPS) as functional SERS substrate for the determination of 2,4-D in milk samples with a detection limit of 0.011 $\mu g \times mL^{-1}$. The determination of samples with various concentrations of 2,4-D was performed based on the SERS intensity in the Raman shift range of 1020 cm^{-1} to 1800 cm^{-1}. The MIP was synthesized using (3-aminopropyl)trimethoxysilane (APTES) as the functional monomer, tetraethyl orthosilicate (TEOS) as the cross-linker, 2,4-D as template particles, and 4-aminothiophenol (4-ATP) was used as an internal standard for SERS spectral normalization. [32] In recent work (2023), El-Beshlawy et al. present a potentiometric sensor covered with 2,4-D sensitive MIPs. Methacrylic acid (MAA) was employed as a functional monomer, EGDMA as a cross-linker, 2,4-D as a template analyte, benzoyl peroxide (BPO) as an initiator, and acetonitrile as a porous. The sensor showed LOD calculated as 3.6×10^{-7} M and a dynamic concentration range of 10^{-2} to 10^{-7} M of 2,4-D. [33].

3.2. Azines

An equally common group of herbicides is triazines. A study conducted by Chen et al. presents a novel strategy for the preparation of molecularly imprinted polymer monolithic fibers using microwave radiation, solving the problem of water compatibility of the prepared MIP fiber by liquid–liquid–solidmicroextraction (LLSME). The resulting fibers coupled by high-performance liquid chromatography (HPLC) were capable of recognizing and determining the S-triazine herbicides: atrazine (ATR); ametryn (AME); terbuthylazine (TER); 2-amino-4-methoxy-6-methyl-1,3,5-triazine (TRI), in water samples with the detection limits

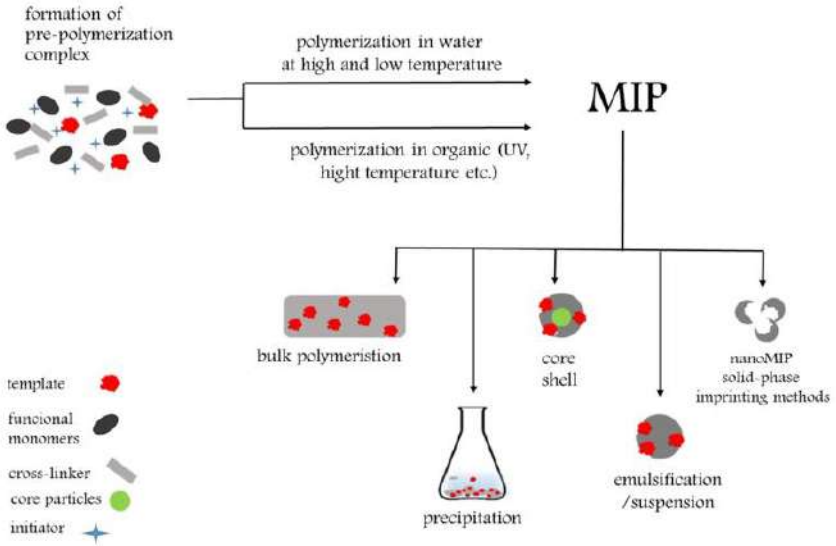

Fig. 2. Schematic receiving of MIPs.

of 0.8 μg × L^{-1}, 1.2 μg × L^{-1}, 1.5 μg × L^{-1}, 1.7 μg × L^{-1}, respectively, and good linearity in the concentration range of 2.5–80 μg × L^{-1}. The MIP was prepared by in situ polymerization method with the use of MAA (functional monomer), EGDMA (cross-linker), atrazine (template), AIBN (initiator), toluene, and dodecanol (porous agents). [34] Roland et al. described a MIP sensitive to ametryn synthesized via precipitation polymerization with the use of three different functional monomers MAA, AM, and 2-VP with various acidity/basicity. The reaction also used EGDMA as a cross-linker, AIBN as an initiator, ametryn as a template molecule, and toluene as a porogen. MIP-MAA was selected as the best matrix-monomer combination, allowing for the highest rebinding efficiency, while MIP-2-VP had the lowest efficiency. [35] Atrazine is one of the most described triazine herbicides. In 1999 Sergeyeva et al. were the first to develop a selective and sensitive photopolymerized imprinted membrane for this herbicide. MAA as a functional monomer, tri(ethylene glycol) dimethacrylate (TEDMA) as a cross-linker, and atrazine as a template was used. The reaction was conducted in the presence of oligourethane acrylate (OUA) and AIBN. The MIP membrane was capable of determining atrazine at a pH of 7.5 with a detection limit of 5 nM. [36] The MIP fluorescent chemosensor for selective detection of atrazine was synthesized by Liu and co-workers. Compared to previous studies [36], the cross-linking agent was changed to EGDMA, and vinyl-substituted zinc(II) protoporphyrin (ZnPP) was used as a fluorescent reporter and simultaneously as a functional monomer along with MAA. The molecular imprint was carried out on the surface of the MPS-silica and the sensor obtained had a detection limit of 1.8 μM. [37] Some of the more recent research, conducted by Salahshoor et al., involved photonic MIP colloidal crystal for the detection of atrazine and its metabolites deethyltrazine (DEA) and deisopropylatrazine (DIA) in water samples with a limit of detection of 0.1, 0.2, and 0.3 ppb and limit of quantification of 0.33, 0.66, and 1 ppb, respectively. Firstly, were formed organized structures composed of glass slides and SiO_2 particles. In the following step, acrylic acid (AA), EGDMA, AIBN, and atrazine were used to produce the MIPs. Finally, the colloidal crystals were formed by placing the poly(methyl methacrylate) (PMMA) slide on a glass slide. [38] In one of the more recent works by Roland et al. describe the synthesis of MIP by the precipitation polymerization method capable of trapping cyanazine from aqueous samples. In this article, MIP was prepared using three different functional monomers: MAA, AM, and 4-VP, while the remaining reagents used were the same for all syntheses. EGDMA was used as a cross-linker, cyanazine as a template, toluene as a porous agent, and AIBN as an initiator. Among the three synthesized MIPs, the one using AM as the functional monomer was the most effective because it showed the highest rebinding efficiency. [39] Bentazon is categorized under the thiadiazine group and MIP sensitive to this herbicide has been described by Geramizadegan et al. with the linear range as good as 0.05–1.0 μg × L^{-1} and the limit of detection of 0.05 μg × L^{-1}. For the synthesis of MIP, MAA was employed as a functional monomer, EGDMA as a cross-linker, bentazon as a template molecule, AIBN as an initiator, and chloroform as a porogen. In the next step, the obtained sorbent was packed in solid phase extraction (SPE) columns, and the herbicide concentration after the process was determined using the HPLC technique. [40].

3.3. Glyphosate

Quite a few publications concern MIP with high sensitivity to glyphosate (GLY). Zhao et al. synthesized an innovational chemiluminescence sensor with special selectivity of that herbicide by molecularly imprinted microspheres modified glass sheets. The imprinted microspheres were prepared by bulk polymerization, mixing AM, EGDMA, AIBN, glyphosate, chloroform, and methanol. A sensor showed a low limit of detection of 0.046 μg × L^{-1} and good selectivity. [41] In other research, Coble et al. described a Polar Organic Chemical Integrative Sampler with Molecular Imprinted Polymer (POCIS-MIP) capable of selectively recognizing glyphosate from both pulses- and continuous-delivery ways of this herbicide. Pulse delivery turned out to have a lower limit of detection (0.115 μg × L^{-1}) than continuous delivery (0.23 μg × L^{-1}). [42] Balciunas et al. introduced an electrochemical surface plasmon resonance (ESPR) sensor based on the molecularly imprinted polypyrrole (MIP-Ppy) deposited on a gold electrode with high selectivity for glyphosate and a sensitivity of 1.1 nM × L^{-1}. [43] Whereas Sawetwong et al. made up a Mn-ZnS quantum dot–MIP which has a detection limit of 0.002 μg × mL^{-1} and an operating range of 0.005–50 μg × mL^{-1}. The Mn-ZnS QD was coated with MIP as follows: poly(N-isopropylacrylamide) (PNIPAM) functional monomer, N, N′-methylenebisacrylamide (MBAM) cross-linker, AIBN initiator, glyphosate template, and ethanol were mixed with Mn-ZnS QD. [44].

3.4. Urea derivatives

Another herbicide used quite frequently is phenylurea, although there is no shortage of literature reports on molecularly imprinted polymers with high sensitivity and selectivity for this compound. Already in 2013 Kamel and Romian prepared MIPs via thermal polymerization with unique molecular recognition properties of phenylurea herbicides: diuron, fenuron, linuron, isoproturon, and methiuron. In a typical experiment, MAA was used as a functional monomer, EGDMA was used as the cross-linker, BPO was used as the radical initiator, phenylureas was used as the template, and acetonitrile was used as a solvent. Sensors with a good linear range of 2.5 × 10^{-5}, 1.0 × 10^{-5}, 3.1 × 10^{-5}, 5.3 × 10^{-5}, and 5.3 × 10^{-5} mol × L^{-1} and with a low detection limit of 1.0 × 10^{-5}, 7.1 × 10^{-6}, 1.3 × 10^{-5}, 1.8 × 10^{-5} and 1.6 × 10^{-5} mol × L^{-1} for linuron, isoproturon, diuron, fenuron, and methiuron, appropriately, were successfully obtained. [45] In other research, Wong et al. synthesized an electrochemical sensor modified with MIP and carboxyl-functionalized multi-walled carbon nanotubes, sensitive to diuron herbicides. A molecularly imprinted polymer was achieved by bulk polymerization in the solution method, using MAA or 2-vinylpyridine (2-VP) as the functional monomer, trimethylolpropane trimethacrylate (TRIM) as a cross-linker monomer, diuron template, AIBN as an initiator, and acetonitrile. Synthesized sensor, characterized by the linear range of between 5.2 × 10^{-8} and 1.25 × 10^{-6} mol × L^{-1} and a detection limit of 9 × 10^{-9} mol × L^{-1}. [46] The latest research, presented by Lu et al., describes a core-shell magnetic MIP selective to diuron particles, capable of determining DU in the range of 0.02 to 10.0 mg × L^{-1} and a limit of detection of 0.012 mg × L^{-1}. MIPs were also prepared by bulk polymerization, using the same reactants as in the synthesis described earlier by Wong, but a magnetic core was acted SiO_2-coated Fe_3O_4. This resulted in a wider range of linearity, but a slightly higher detection limit. [47].

3.5. Sulfonylureas

Monosulfuron belongs to the class of chemical compounds called sulfonylureas. In the study conducted by Xiangchao Dong et al., the synthesis of the molecularly imprinted polymer sensor with special selectivity for monosulfuron in the concentration range of 5–30 μg × mL^{-1} and a low detection limit of 0.08 μg × g^{-1} for a soil sample was demonstrated. In the bulk polymerization synthesis, MAA as a functional monomer, EGDMA as a cross-linker, AIBN as an initiator, and monosulfuron as a template were dissolved in the dimethylformamide (DMF). [48] A few years later, Guo and co-workers obtained a molecularly imprinted vinylimidazolium ionic liquid polymer sorbent. The imprinted materials were highly selective for chlorsulfuron, which is also one of the sulfonylurea herbicides and reached the adsorption equilibrium within 5 min. The MIP synthesis via bulk polymerization was carried out using vinylimidazolium ionic liquid as a functional monomer, EGDMA as a cross-linker, AIBN as an initiator, chlorsulfuron as a template, and a solvents mixture: toluene, methanol, and DMF. The MIP achieved showed a good linear range of 0.005–30 μg × L^{-1} and a detection limit of 0.001 μg × L^{-1} in water samples. [49] She et al. reported a molecularly

imprinted solid-phase extraction (MISPE) method capable of recognizing sulfonylurea herbicides: chlorsulfuron, monosulfuron, and thifensulfuron methyl. MIPs were obtained by precipitation polymerization involving functional monomer 2-(diethylamino)ethyl methacrylate) (DEAMA), cross-linker trimethylolpropane trimethacrylate (TRIM), chlorsulfuron template, initiator AIBN, dissolved in acetonitrile. The new sensor turned out to have better selectivity compared to the one obtained earlier. The average LODs were calculated as low as 0.1, 2.5, and 5.0 $\mu g \times kg^{-1}$ for chlorosulfuron, monosulfuron, and thifensulfuron, respectively. [50] In one of the latest works describing sulfonylureas, Andrade et al. present a MIP sorbent for microextraction of four herbicides: bensulfuron, chlorsulfuron, thifensulfuron, and tribenuron from corn samples, in the linearity range 2.5–40 $\mu g \times kg^{-1}$. The reaction was carried out similarly to Dong et al. [48] using MAA as the functional monomer and AIBN as the initiator. Still, the cross-liner was changed to EGDMA and porous to acetonitrile, which allowed to obtain a wider range of linearity, but not as low as in Guo's publication. The LOD for all herbicides was 0.25 $\mu g \times kg^{-1}$, however, She et al. received a lower LOD value for chlorsulfuron (0.1 $\mu g \times kg^{-1}$). [51] A MIP capable of detecting nicosulfuron, also belonging to the sulfonylurea group, is described by Piryaei et al. In this work, a MIP layer was deposited on the Fe_3O_4 modified surface of graphene oxide (GO) nanosheets, which resulted in linearity in the range of 0.01–100 1 $\mu g \times mL^{-1}$ and the LOD calculated as 2.9 ng $\times L^{-1}$. To synthesize molecularly imprinted polymers, the Fe_3O_4/GO nanocomposite was immersed in an acetonitrile solution of MAA (functional monomer) and nicosulfuron (template). As a cross-linker EGDMA was used, and AIBN was used as a initiator. [52].

Several publications focus on the MIP sensitivity to previously mentioned thifensulfuron-methyl (TFM), which also belongs to the sulfonylurea herbicide family. Xie and co-workers made up a chemiluminescence MIP sensor for the determination of TFM in the concentration range of 1.0×10^{-9} to 5.0×10^{-5} mol $\times L^{-1}$ and with a limit of detection of 8.3×10^{-10} mol $\times L^{-1}$. MIP was prepared via precipitation polymerization acting with AM as a functional monomer, EGDMA as a cross-linker, AIBN as the initiator, and acetonitrile as the solvent. [53] In another research, Li et al. described an electrochemiluminescence sensor sensitive to TFM, with wide linear ranges from 5.0×10^{-10} to 1.0×10^{-7} M and with a low detection limit of 0.32 nM. The scientist was the first to use the method of core-shell imprinted nanoparticles by a monomer-directing strategy for imprinting TFM at the surface of 3-methacryloxypropyl trimethoxysilane (MPTS) modified silica particles. In the first step, silica particles and MPTS were reacted in dry toluene, and after the experiment, the physically adsorbed MPTS was leached. The second step involved the synthesis of SiO_2 @MIP by undergoing the reaction generated by MPTS-SiO_2 and the remaining reagents used for the MIP synthesis described by Xie. [54].

3.6. Metolachlor

To date, less work on MIPs with selectivity to metolachlor has been described in the scientific literature. The first paper appeared in 2010, in which Hu et al. synthesized a MIP with a high selectivity sensor for chloroacetanilide herbicides: metolachlor, propisochlor, and butachlor. Obtained MIPs exhibit detection limits of 3.0, 9.6, and 38.0 $\mu g \times L^{-1}$ and good linearity in the range of 10–1000, 50–1000, and 100–1000 $\mu g \times L^{-1}$ respectively for metolachlor, propisochlor, and butachlor. The problem of embrittlement of the silica fiber solid-phase microextraction (SPME) substrate was solved by applying MIP on the surface of the stainless steel fiber by chemical bonding. The scientist performed bulk polymerization, using MAA as a functional monomer, TRIM as a cross-linker, AIBN as an initiator, metolachlor as a template analyte, and toluene as a porofor. [55] Similar research has been done by Wang et al. but used a molecularly imprinted solid phase extraction combined with gas chromatography (GC) as a tool for the concurrent distribution and determination of chloroacetamide herbicides: alachlor, acetochlor, pretilachlor, and metolachlor. The suspension polymerization method was used to synthesize the MIPs, relative to [55], using EGDMA as a cross-linker and acetonitrile as a porogen. For alachlor, acetochlor, pretilachlor, and metolachlor the limit of detection was calculated as low as 1.0×10^{-12}, 3.0×10^{-12}, 5.0×10^{-11}, 1.0×10^{-11} g $\times kg^{-1}$ and the quantification limit of 0.0005, 0.0015, 0.025 and 0.005 mg $\times kg^{-1}$, appropriately. [56] The water-compatibility problem of MIPs was also taken by Hu et al. applying a liquid-liquid-solid microextraction and the previously developed synthesis of metolachlor MIP-coated steel fiber. The linear ranges of 1–100, 5–100, and 5–100 $\mu g \times L^{-1}$ and LOD of 0.2, 1.4, and 2.8 $\mu g \times L^{-1}$ for metolachlor, propisochlor, and butachlor, respectively. [57] Alachlor, like metolachlor, belongs to the chloroacetanilide family. Li et al. developed a fluorescent MIP sensor that demonstrated linear fluorescence intensity in the alachlor concentration range of 1 to 150 μM and with a detection limit of 0.5 μM. MIP synthesis was carried out using fluorescent functional monomer 2-acrylamide-6-methoxybenzothiazole (AMMB), cross-linker N, N′-methylenebisacrylamide, alachlor template particles, initiator AIBN, and acetonitrile and DMF porous agents mixture. [58].

3.7. Others

Less frequently reported are MIPs sensitive to maleic hydrazide herbicide (MH). Fang et al. reported a chemiluminescence MIP sensor that can determine MH in the range 3.5×10^{-4} to 5.0×10^{-2} mg $\times mL^{-1}$ and with a limit of detection of 6.0×10^{-5} mg $\times mL^{-1}$. To obtain an MH-MIP, MAA – functional monomer, EGDMA – cross-linker, maleic hydrazine – template, AIBN – initiator, and methanol – porous agent, were mixed in a flask. [59] In another research, Elfadil and co-workers described an electrochemical MIP-SPE sensor combined with the carbon black-based electrode for the determination of maleic hydrazide (MH) with a limit of detection of 40 ppb. This strategy significantly reduced the synthesis time from a few hours to 5 min by using a high-power ultrasound probe. The MIP synthesis procedure was similar to Fang preparation but modified methanol to dimethyl sulfoxide (DMSO). The sonification time was established at 5 min, as complete polymerization then occurred, and the best polymer yield was obtained with an amplitude of 50%. [60].

There are the fewest publications on propanil and hexazinone herbicides. Liu et al. synthesized a fluorescence-based sensor combination of molecularly imprinted polymers with CdSe/ZnS core-shell quantum dots (QDs) for the determination of propanil in fish and samples of seawater with LODs of 0.42 $\mu g \times kg^{-1}$ and 0.38 $\mu g \times L^{-1}$ respectively. On the strength of fluorescence quenching of CdSe/ZnS QD-MIP, linearity in the range of 1.0 to 20.0 $\times 10^3$ $\mu g \times L^{-1}$ was calculated. The MIP-QDs were obtained using a modified reverse microemulsion method, involving the following reagents: aminopropyltriethoxysilane (APTES) as a functional monomer, tetraethoxysilane (TEOS) as a cross-linker in the presence of triton X-100, QDs, ammonia solution, propanil, and solvents: cyclohexane and acetone. [61] Toro's group through bulk polymerization synthesized a biomimetic selective MIP sensor with high sensitivity to hexazinone. For this purpose, three functional monomers: 2-vinylpyridine, methacrylic acid, and acrylamide with the cross-linker - EDGMA, the initiator - AIBN, the template - hexazinone, and the porous agent – dichloromethane (DCM) were mixed. In HCl at pH 2.5, the sensor showed a linear response range of 1.9×10^{-11} to 1.1×10^{-10} mol $\times L^{-1}$ and a detection limit of 2.6×10^{-12} mol $\times L^{-1}$. [62].

Only one paper deals with MIPs sensitive to bispyribac herbicide. In 2019 Nashwa S. Abdalla et al. were the first to introduce a novel screen-printed potentiometric sensor integrated with MIPs for the detection of that herbicide. Sensors were prepared to deposit polyaniline (PANI) film on a carbon screen printed platform and then coated with an ion-selective membrane with molecularly imprinted nanoparticles. The MIP was synthesized by dissolving functional monomer MAA, cross-linker EGDMA, free radical initiator BPO, and template bispyribac in acetonitrile. The sensor obtained can determine bispyribac with an operating range of 1.0×10^{-2} to 8.6×10^{-6} M and with detection limits

of 1.33 μg × mL^{-1}. [63].

In one of the latest works, Noor et al. described modified silica nanoparticles based on MIPs for the selective detection of pendimethalin, which belongs to the dinitroaniline group. For the MIPs synthesis, 4-vinylpyridine and 1-(but-3-en-1-yl)-[4,4'-pyridin] – 1-ium were used as a functional monomers, EGDMA was a cross-linker, AIBN was an initiator, pendimethalin was a template, and acetonitrile was used a porous. The tests examined the maximum capacity of the column, which was calculated as 532.69 mg × g^{-1}. [64] Fatah et al. reported a novel electrochemical MIP sensor sensitive to metribuzin, capable of its determination in the linearity range of 0.2 ng × mL^{-1} to 21,429 μg × mL^{-1}, and with LOD of 0.1 pg × mL^{-1}. MIP was synthesized via bulk polymerization with the use of itaconic acid as a functional monomer, EGDMA as a cross-linker, metribuzin as a template molecule, AIBN as an initiator, and acetone as a porogen. [65] Kamel et al. presented an imprinted polymer/reduced graphene oxide-modified glassy carbon electrode (GCE)-based module for the detection of imidacloprid with a linear range of 0.5 μM – 1.0 mM, and with a detection limit measured as 0.2 μM. MIPs were synthesized via the emulsion polymerization method with the use of MAA as a functional monomer, EGDMA as a cross-linker, imidacloprid as a template, BPO as an initiator, and acetonitrile as a porous. [66] Table 1 summarizes the results for molecularly imprinted polymers synthesized in an organic medium.

4. *Green* MIPs synthesized in an aqueous medium

There are considerably fewer publications centered on molecularly imprinted polymers synthesized in aqueous media compared to those in

Table 1
A list of MIPs synthesized in an organic medium.

No.	Target Molecule	Solvent used in the synthesis	LOD	Recovery [%]	Temp. [°C]	Ref.
1.	2,4-D	EtOH	11.0 μg × L^{-1}	90	RT	[32]
2.		ACN	2.9 μg × L^{-1}	98-105	60	[31]
3.			79.6 μg × L^{-1}	97-113	70	[33]
4.	Atrazine	DMSO	3.9 μg × L^{-1}	91-107	60	[37]
5.		$PhCH_3$/ dodecanol	0.8 μg × L^{-1}	82-93	N/A	[34]
6.		DMF	1.1 μg × L^{-1}	N/A		[36]
7.		EtOH	0.1 μg × L^{-1}	N/A		[38]
8.	Ametryn	$PhCH_3$/ dodecanol	1.2 μg × L^{-1}	74-91	N/A	[34]
9.		$PhCH_3$	N/A	88-95	80	[35]
10.	Terbuthylazine	$PhCH_3$/ dodecanol	1.5 μg × L^{-1}	68-87	N/A	[34]
11.	2-amino-4-methoxy-6-methyl-1,3,5-triazine	$PhCH_3$/ dodecanol	1.7 μg × L^{-1}	77-92	N/A	[34]
12.	Deethylatrazine	EtOH	0.2 μg × L^{-1}	N/A	N/A	[38]
13.	Deisopropylatrazine	EtOH	0.3 μg × L^{-1}	N/A	N/A	[38]
14.	Cyanazine	$PhCH_3$	N/A	85-87	80	[39]
15.	Bentazon	TCM	5.0×10^{-2} μg × L^{-1}	91-94	60	[40]
16.	Glyphosate	TCM/ MeOH	4.6×10^{-2} μg × L^{-1}	99-104	60	[41]
17.		phosphate-buffered saline solution	0.2 μg × L^{-1}	N/A	N/A	[43]
18.		EtOH	2.0 μg × L^{-1}	81-120	60	[44]
19.	Diuron	ACN	2.3×10^{3} μg × L^{-1}	99	70	[45]
20.			2.1 μg × L^{-1}	96-100	60	[46]
21.			12.0 μg × L^{-1}	84-116		[47]
22.	Linuron	ACN	3.2×10^{3} μg × L^{-1}	95	70	[45]
23.	Isoproturon	ACN	3.7×10^{3} μg × L^{-1}	96	70	[45]
24.	Methiuron	ACN	3.1×10^{3} μg × L^{-1}	99	70	[45]
25.	Chlorsulfuron	$PhCH_3$/ MeOH/ DMF	1.0×10^{-3} μg × L^{-1}	81-110	60	[49]
26.		ACN	0.1 μg × kg^{-1}	97-110		[50]
27.			0.3 μg × kg^{-1}	90-114		[51]
28.	Monosulfuron	DMF	8.0 μg × kg^{-1}	94-110	RT	[48]
29.		ACN	2.5 μg × kg^{-1}	88-98	60	[50]
30.	Thifensulfuron-methyl	ACN/ $PhCH_3$	0.1 μg × L^{-1}	98-106	60	[54]
31.		ACN	5.0 μg × kg^{-1}	76-85		[50]
32.			0.3 μg × L^{-1}	96-108		[53]
33.	Bensulfuron	ACN	0.3 μg × kg^{-1}	90-114	60	[51]
34.	Tribenuron	ACN	0.3 μg × kg^{-1}	90-114	60	[51]
35.	Thifensulfuron	ACN	0.3 μg × kg^{-1}	90-114	60	[51]
36.	Nicosulfuron	ACN	2.9×10^{-3} μg × L^{-1}	100	70	[52]
37.	Alachlor	ACN/ DMF	1.4×10^{-2} μg × L^{-1}	96-104	65	[58]
38.		ACN	1.0×10^{-6} μg × kg^{-1}	83-88	60	[56]
39.	Butachlor	$PhCH_3$	38.0 μg × L^{-1}	71-88	60	[55]
40.			1.4 μg × L^{-1}	76-98		[57]
41.	Metolachlor	ACN	1.0×10^{-5} μg × kg^{-1}	81-85	60	[56]
42.		$PhCH_3$	2.8 μg × L^{-1}	76-98		[57]
43.			3.0 μg × L^{-1}	85-96		[55]
44.	Acetochlor	ACN	3.0×10^{-6} μg × kg^{-1}	85-90	60	[56]
45.	Pretilachlor	ACN	5.0×10^{-5} μg × kg^{-1}	85-97	60	[56]
46.	Propisochlor	$PhCH_3$	0.2 μg × L^{-1}	76-98	60	[57]
47.			9.6 μg × L^{-1}	79-91		[55]
48.	Maleic hydrazide	MeOH	60.0 μg × L^{-1}	98-103	60	[59]
49.		DMSO	40.0 μg × L^{-1}	80-106	N/A	[60]
50.	Propanil	Cyclohexane/ acetone	0.4 μg × L^{-1}	87-112	N/A	[61]
51.	Hexazinone	DCM	6.6×10^{-4} μg × L^{-1}	96	60	[62]
52.	Bispyribac	ACN	1.3×10^{3} μg × L^{-1}	N/A	75	[63]
53.	Pendimethalin	ACN	N/A	N/A	70	[64]
54.	Metribuzin	Acetone	1.0×10^{-4} μg × L^{-1}	97-103	60	[65]
55.	Imidacloprid	ACN	51.1 μg × L^{-1}	95-106	N/A	[66]

organic solvents. This is probably the result of several factors. One of them may be the lack of solubility of most monomers in water. However, the advantages resulting from the application of the principles of green chemistry, such as waste prevention, eco-friendliness, and less hazardous synthesis, encourage the search for solutions enabling the use of this type of polymerization. A kind of compromise may be the use of a polar organic solvent in a mixture with water [67,68].

4.1. 2,4-dichlorophenoxyacetic acid herbicide (2,4-D)

Water mixtures with ethanol or acetonitrile are most often used. This solvent mixture was used by Haupt and co-workers, who published the first paper describing the synthesis of MIPs in an aqueous environment in 1995. A molecularly imprinted polymer capable of determining 2,4-D was synthesized via bulk polymerization involving 4-VP as a functional monomer, EGDMA as a cross-linker, 2,2'-azobis(2,4-dimethylvaleronitrile) (ABDV) as a polymerization initiator, 2,4-D as a template, and a mixture of methanol/water as a porous agent. The sensor showed linearity in the range of 30 ng × mL^{-1} to 10 μg × mL^{-1}. [69] Another paper by Haupt et al. presents a fluorescent ligand displacement assay for the 2,4-D based on MIP, which was synthesized in the same way as before, but 7-carboxymethoxy-4-methylcoumarin (CMMC) was used as a fluorescent probe. The assay was capable of detecting the herbicide molecules with the limit of 100 nM and in the range of 100 nM to 50 μM in buffer and of 100 nM to 10 μM in acetonitrile. [70] Attieh et al. synthesized water-compatible molecularly imprinted polymer nanogels for 2,4-D recognition, by the enzyme-mediated initiation of free radical polymerization (FRP), by the principles of *green chemistry*. As an initiator, the horseradish peroxidase enzyme (HRP) was used instead of the commonly used synthetic inhibitors. 4-vinylpyridine was a functional monomer, 1,4-bis(acryloyl)piperazine (PDA) was a cross-linker, and hydrogen peroxide was used as an enzyme initiator. As a result, MIP nanoparticles with sizes ranging from 50 to 300 nm, having good binding properties and high selectivity for the target molecule, and being environmentally friendly, were achieved. [29] Pan et al. used the same pesticide for the synthesis of water-compatible narrowly dispersed MIPs with surface-grafted polymer brushes PNIPAM and polyethylene glycol (PEG). 4-VP and EGDMA were used for reversible addition fragmentation chain transfer (RAFT) precipitation polymerization and together with a template and AIBN dissolved in a mixture of methanol/water. Macromolecular chain-transfer agents (Macro-CTAs) and cumyl dithiobenzoate (CDB) were added to the reaction to obtain better hydrophilic properties of the received MIPs. [71] The following research paper published by Pan et al. describes the controlled synthesis of pure water-compatible MIP microspheres with an ultra-thin hydrophilic poly (2-hydroxyethyl methacrylate) (PHEMA) coating via surface-initiated RAFT polymerization. The 2,4-D MIP microspheres were prepared as previously described [71], but additionally, the reaction mixture was stirred in a water bath at 25 °C for 2 h. Applying a PHEMA layer onto the MIP surface improved the hydrophilicity and water-compatible binding properties of the MIP microspheres. [72] Wu et al. employed a 2,4-D target molecule for the synthesis of MIPs used in the monolith extraction process. Exactly as in the previously described work, 4-VP, EGDMA, AIBN, 2,4-D template, and a mixture of methanol/water were used for bulk polymerization. The resulting sensor was capable of the quantification of herbicide in the range of 0.006 to 0.5 mg × L^{-1} and with a limit of detection of 0.002 mg × L^{-1}. [73] In another study, Ton et al. reported on a disposable evanescent wave fiber optic sensor coated with a 2, 4-D-sensitive molecularly imprinted polymer. The MIP synthesis was conducted via precipitation polymerization and, as in the previously featured research, 4-VP, EGDMA, and a mixture of methanol/water was also utilized. Furthermore, N-(2-(6–4-methylpiperazin-1-yl)− 1,3-dioxo-1 H-benzo[de]isoquinolin-2(3 H)-ylethyl)acrylamide (FIM) was involved as a fluorescent functional monomer and ABDV as an initiator. The 2,4-D molecule was detected in the range of 2.5 to 100 nM. [74].

4.2. Azines

The previously described MIP sensors sensitive to triazine herbicides may also be synthesized in an aqueous environment. Qiao et al. presented a water-compatible magnetic imprinted microsphere (WCMM) for the determination of cyanazine and atrazine with a linear range of 2.5 to 200 ng × mL^{-1}. The limit of detection for cyanazine and atrazine was 0.25 ng × mL^{-1} and 0.37 ng × mL^{-1}, respectively. The WCMM synthesis was carried out in two steps. In the first, an aqueous solution of Fe_3O_4 was added to the mixture of AIBN, TRIM, and oleic acid dissolved in toluene, thus forming an inverse water-in-oil emulsion. In the second step, the resulting emulsion was added dropwise to a solution of methacrylic acid, hydroxyethylcellulose, and cyromazine (mimic template) in the ethanol/water mixture, thus obtaining water-in-oil-in-water multiple emulsions. In this way, good compatibility of WCMM with water was achieved. [75] Belmont et al. presented novel molecularly imprinted polymer films for reflectometric interference spectroscopic sensors sensitive to atrazine. MIPs were synthesized by miniemulsion polymerization mixing organic phase consisting of MAA, EGDMA or TRIM, AIBN, hexadecane, and solution atrazine in tetrachloroethane, with an aqueous phase – sodium dodecyl sulfate (SDS) in water. The limit of detection of atrazine was as low as 1.7 ppm. [76] In another study, Zhou et al. reported a novel hydrophilic molecularly imprinted resin (MIR) with high selectivity on triazines: simazine, atrazine, desmetryn, propazine, ametryn, and prometryn with LOD of 0.11, 0.02, 0.02, 0.15, 0.03 and 0.02 ng × g^{-1}, respectively. The MIRs for these herbicides were synthesized with the use of melamine and resorcinol as functional monomers, formaldehyde as a cross-linking agent, ametryn as a template, and a mixture of acetonitrile and water as porous agents. The sensor effectively marked the linearity of all six triazines studied in the honey samples in the range of 0.5 to 100 ng × g^{-1}. [77] In the following paper published by Zhou's group, magnetic MIRs were capable of detecting the triazines mentioned above, but in water, samples have been reported. The sensor synthesis was carried out as before but modified with the addition of Fe_3O_4 @NH_2, which contributed to obtaining a lower value of the detection limit and a linearity range as low as 0.65 – 333.33 μg × L^{-1}. The LOD was equal to 0.38, 0.06, 0.02, 0.05, 0.07, and 0.07 μg × L^{-1} for simazine, atrazine, desmetryn, propazine, ametryn, and prometryn, appropriately. [78] Two years later, Zhou's group presents the MWNTs@Fe_3O_4 @MIR as a new alteration of the triazine detection sensor applied on multi-walled carbon nanotubes (MWNTs). The resin with a molecular imprint was synthesized by methodology [77] and then applied to the surface of MWNTs@Fe_3O_4 in a one-pot condensation. The result was a material with better triazine recognition properties and a higher absorption capacity for these herbicides, compared to that previously described. The established method exhibited an even lower LOD of 0.043, 0.029, 0.007, 0.030, 0.068, and 0.026 μg × L^{-1} for simazine, atrazine, desmetryn, propazine, ametryn, and prometryn, accordingly. Good linearity was maintained in the range of 0.25 to 0.50 μg × L^{-1}. [79] The lowest LOD values for these triazines were characterized by the sensor developed by Zhao et al. and were 0.08, 0.07, 0.02, 0.07, 0.04, 0.07 ng × L^{-1}, in the same order as mentioned earlier. These results were obtained by applying MIP on the surface of SiO_2-encapsulated Fe_3O_4 as a magnetic core. The MIP was synthesized via free radical polymerization, using MAA as a functional monomer, EGDMA as a cross-linker, AIBN as an initiator, and prometryn as a template. The method has good linearity in the range of 0.25 to 500 ng × L^{-1}. [80].

4.3. Others

Gomez-Caballero et al. presented water-compatible magnetic stir-bar devices with a molecular imprint for cleaning samples from glyphosate. The MIP sensor was prepared as follows: functional monomers 2-dimethyl aminoethyl methacrylate (DMAEM) and N-allylthiourea (ATU), cross-linker EGDMA or diethylene glycol diacrylate (DEDA),

glyphosate template, benzophenone initiator, PEG, and 1,3-divinyltetramethyldisiloxane (DVTD) was dissolved in the mixture of methanol and water. PEG was used to increase the porosity of the material, while DVTD was employed to increase mechanical strength. The extraction device could determine the concentration with a detection limit of 0.140 μg × L^{-1} and a qualification limit of 0.468 μg × L^{-1}. [81].

2,4-Dichlorophenol (2,4-DCP) is a subsequent herbicide applied in agriculture to control weeds, but also as a precursor of 2,4-dichlorophenoxyacetic acid herbicide. Liu et al. obtained an electrochemical sensor for the detection of this herbicide in water, by using the molecularly imprinted membrane (MIM) technology combined with a system of the bipolar membrane (BPM) introduced onto a palladium-coated titanium mesh electrode (BPM/MIM@Pd/Ti). Thus, solving the problem of low efficiency in electrochemical reductive hydrodechlorination (ERHD) to wipe out chlorinated compounds from a sample of water. The removal of 2,4-DCP was received by oxidizing the Fenton's reagent in the ERHD procedure and the limit of detection was 0.7 μg × L^{-1}. 2,4-DCP molecularly imprinted membrane was synthesized with the use of a 2,4-DCP template, an aqueous solution of poly(vinyl alcohol) and carboxyl methyl cellulose, and iron (III) chloride solution. Sequentially, the mixture was spilt on the Pd/Ti mesh and a membrane was formed. [82].

Zhang et al. synthesized a MIP sensor in aqueous media with high selectivity to the chlorotoluron herbicide. The sensor was created by coating magnetic nickel hexacyanoferrate (NiHCF) nanoparticles on the molecularly imprinted polymers. During the MIP synthesis, methacrylic acid as functional monomer, N, N'-(methylene)-bisacrylamide as cross-linker, and chlorotoluron as a template were dissolved in water, and then the NiHCF particles and $(NH_4)_2S_2O_8$ as initiator was added. The determination of this herbicide is indirect and based on the linear dependence of the changes in the current resulting from the oxidation of hydrazine on the modified electrode and chlorotoluron in the range of 5×10^{-9} to 1×10^{-7} mol × L^{-1}, and the detection limit is 9.27×10^{-10} mol × L^{-1}. [83] The above-described syntheses in aqueous-organic media are summarized in Table 2, while Table 3 summarizes the MIPs syntheses in an aqueous media.

5. Application of MIPs

As mentioned in the introduction section, MIPs are widely used in both the scientific and industrial sectors. Undoubtedly, such widespread use of MIP is influenced by the advantages, including low-cost, easy, and quick synthesis, high thermal and chemical stability, high sensitivity and specificity to target molecules, and reusability. [85] MIPs are exploited for the sample preparation, including removal, detection, and isolation of molecular particles [35,39,40], and also as solid-phase extraction sorbents for preconcentration and purification of samples before determining the analyte and as selective extraction from the complex matrix [40,50,56], in membrane separation processes [33,63,82], and as molecular sieves. [19,26] Furthermore, MIPs have been used as sensors, in particular potentiometric sensors [33,63,66], electrochemical sensors [13,60,65,85,86], conductometric sensors [36], and chemiluminescence sensors [37,41,53,59] (Fig. 3). MIPs can operate based on various techniques, e.g. magnetic, electrochemical, and optical. Magnetic MIP sensors consist of MIPs and magnetic nanoparticles that impart magnetic properties and interact with an external magnet. [87] Electrochemical MIP sensors relate the interaction between matter and electricity. The following parameters are most often measured using electrochemical techniques: surface properties of the transducers, polymer rearrangements, or binding kinetics. [88] Optical MIPs can operate with a variety of sensing strategies: fluorescence, interferometry, and the surface plasmon effect. [89] MIPs are widely used sensors in both the scientific and industrial sectors, in the following branches: diagnostics, pharmaceuticals, drug delivery, environmental monitoring, detection of contaminants in food, or purification and separation of diverse types of analytes. [16].

In recent years, MIPs have attracted particular interest in the determination of micropollutants. In addition to capturing and specifying herbicides, MIPs are used for the detection and extraction of heavy metals, dyes, pesticides, insecticides, pharmaceuticals, drugs, and endocrine-disrupting chemicals (EDCs). [90].

Table 2
A list of MIPs synthesized in an aqueous-organic medium.

No.	Target Molecule	Solvent used in the synthesis	LOD	Recovery [%]	Temp. [°C]	Ref.
1.	2,4-D	water/MeOH	2.0 μg × L^{-1}	114-122	60	[73]
2.			2.2 μg × L^{-1}	N/A	50	[74]
3.		water/EtOH	2.2×10^{-4} μg × L^{-1}	98-104	60	[30]
4.	Atrazine	water/EtOH	0.4 μg × L^{-1}	100-104	70	[75]
5.		water/TeCA	1.7×10^{3} μg × L^{-1}	N/A	65	[76]
6.		water/ACN	7.0×10^{-5} μg × L^{-1}	90-93	60	[80]
7.			0.1 μg × L^{-1}	90-96	80	[78]
8.			2.0×10^{-2} μg × kg^{-1}	82-94		[77]
9.			2.9×10^{-2} μg × L^{-1}	91-94		[79]
10.	Cyanazine	water/EtOH	0.3 μg × L^{-1}	85-101	70	[75]
11.	Propazine	water/ACN	7×10^{-5} μg × L^{-1}	97-98	60	[80]
12.			0.2 μg × kg^{-1}	80-93	80	[77]
13.			5×10^{-2} μg × L^{-1}	90-97		[78]
14.			3.0×10^{-2} μg × L^{-1}	94-100		[79]
15.	Simazine	water/ACN	8.0×10^{-5} μg × L^{-1}	86-89	60	[80]
16.			0.1 μg × kg^{-1}	80-93	80	[77]
17.			0.4 μg × L^{-1}	86-90		[78]
18.			4.3×10^{-2} μg × L^{-1}	88-91		[79]
19.	Desmetryn	water/ACN	2.0×10^{-5} μg × L^{-1}	90-92	60	[80]
20.			2.0×10^{-2} μg × kg^{-1}	88-96	80	[77]
21.			2.0×10^{-2} μg × L^{-1}	96-101		[78]
22.			7.0×10^{-3} μg × L^{-1}	96-97		[79]
23.	Ametryn	water/ACN	4.0×10^{-5} μg × L^{-1}	97-100	60	[80]
24.			3.0×10^{-2} μg × kg^{-1}	91-99	80	[77]
25.			7.0×10^{-2} μg × L^{-1}	93-99		[78]
26.			6.8×10^{-2} μg × L^{-1}	91-98		[79]
27.	Prometryn	water/ACN	7×10^{-5} μg × L^{-1}	97-99	60 80	[80]
28.			2.0×10^{-2} μg × kg^{-1}	82-97		[77]
29.			7.0×10^{-2} μg × L^{-1}	85-95		[78]
30.			2.6×10^{-2} μg × L^{-1}	91-94		[79]
31.	Glyphosate	water/MeOH	0.1 μg × L^{-1}	91-97	RT	[81]

Table 3
A list of MIPs synthesized only in an aqueous medium.

No.	Target Molecule	Solvent used in the synthesis	LOD	Recovery [%]	Temp. [°C]	Ref.
1.	2,4-D	water	N/A	N/A	RT	[29]
2.	2,4-DCP	water	0.7 μg × L^{-1}	100	25	[82]
3.	Chlorotoluron	water	0.2 μg × L^{-1}	97-105	N/A	[83]
4.	Paraquat	water	0.5 μg × L^{-1}	94-102	RT	[84]

6. Discussion and conclusion

Molecularly imprinted polymers have been and still are widely researched and developed. It is possible to imprint various types of herbicides and the reached limits of detection are usually very low. This is especially important in environments where herbicides occur as micropollutants in trace amounts, often beyond the detection threshold of other methods. Most reports about polymers imprinted with herbicides concern 2,4-D. This seems to be justified due to the fact that, next to atrazine, it is one of the oldest-used herbicides. Most publications describing this type of MIPs are based on polymerization in an organic environment. This is understandable due to the good solubility of herbicides in organics, as well as of most monomers. Good solubility also facilitates the formation of stable monomer-standard complexes. In the process of creating MIP, the porogen also plays a key role by influencing the porous structure of the material and thus the availability of active sites. Therefore, an organic imprinting environment seems to be the easiest solution. However, the care for the environment and currently more and more dynamically developing trends in green chemistry force the search for new solutions and thus adapting the MIP synthesis to more ecological conditions. Additionally, in the case of MIPs that are intended for use in an aquatic environment, synthesis under similar conditions is desirable. However, imprinting in water is complicated also due to the water molecules character. If the imprinting is based on the hydrogen bonding water can compete to destroy hydrogen bonding between the template and functional monomer. Similar problems may occur when MIPs obtained in an organic environment will be used in an aqueous environment. Additionally, the imprinted sites can be destroyed due to the shrinking or swelling properties of MIPs. All of these limitations seem to be reflected in the amount of publications describing MIP synthesis in both environments. The solution to some problems seems to be the addition of organic solvents for polymerization in an aqueous environment. The number of publications describing synthesis in such an environment is constantly increasing, although they are still in the minority compared to those using organic solvents. Comparing the data contained in Tables 1 and 2, it can be concluded that with an appropriate selection of the composition of the polymerizing mixture, it is possible to obtain effectively operating MIPs both in aqueous and organic conditions. Moreover, in the case of 2,4-D, the detection limit of this compound by MIPs synthesized in a water/methanol mixture was much lower (2.2×10^{-4} μg × L^{-1}) than detection using MIPs obtained in organics (2.9 μg × L^{-1}). Similarly, in the case of atrazine, lower detection limits were also achieved using polymers imprinted in a water/acetonitrile mixture.

According to the literature review that we were able to perform, only four herbicides were imprinted in completely water-based environments. The presented review therefore represents a gap in the field of the synthesis of herbicide-sensitive MIPs in aquatic environments according to green chemistry. S-metolachlor is not among them. This herbicide was also not imprinted in the water/organic solvent mixture. This herbicide is significantly gaining popularity due to the increase in corn cultivation, especially in Poland, where in the late 1990 s, only 100,000 ha of fields were sown with this grain, while in 2022 - almost 1.9 million ha. Therefore, we believe that both the issue of herbicide imprinting by the principles of green chemistry as well as the development of effectively operating MIPs for monitoring the concentration of S-metolachlor in water may constitute a great challenge for scientists.

CRediT authorship contribution statement

Rapacz Dominika: Writing – review & editing, Writing – original draft, Visualization, Software, Resources, Investigation, Formal analysis. **Wolska Joanna:** Writing – review & editing, Writing – original draft, Supervision, Conceptualization. **Smolinska-Kempisty Katarzyna:** Writing – review & editing, Writing – original draft, Visualization, Supervision, Resources, Project administration, Funding acquisition, Conceptualization.

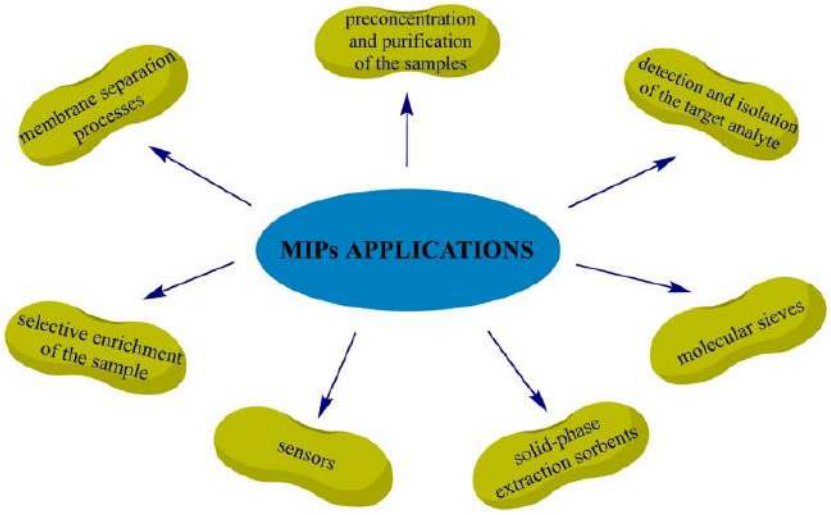

Fig. 3. Multiple roles of MIPs in herbicide application.

Declaration of Competing Interest

The authors declare that they have no known competing financial interests or personal relationships that could have appeared to influence the work reported in this paper.

Data Availability

No data was used for the research described in the article.

Acknowledgments

The authors wish to acknowledge the financial support of the National Science Centre Poland project Sonata Bis11, 2021/42/E/ST5/00019 (02NB/0002/22).

References

[1] A.H. Cobb, J.P.H. Reade. Herbicides and Plant Physiology, third ed., Wiley-Blackwell, Hoboken, 2021.
[2] R.J.W. Cremlyn, Agrochemicals: Preparation and Mode of Action, John Wiley and Sons, Chichester, 1991.
[3] H. Kraehmer, B. Laber, C. Rosinger, A. Schulz, Herbicides as weed control agents: state of the art I. Weed control research and safener technology: the path to modern agriculture, Plant Physiol. 166 (3) (2014) 1119–1131, https://doi.org/10.1104/pp.114.241901.
[4] Global Herbicide Classification Lookup. https://hracglobal.com/tools/classification-lookup/?s=&mode=10916&letter=&number=#classificationLookup. (Accessed 2022-10-03).
[5] P.F. Martins, C. Ortiz Martinez, G. de Carvalho, P. Irajara, B. Carneiro, R. A. Azevedo, S. Alvim, V. Pileggi, I. Soares De Melo, M. Pileggi, Selection of microorganisms degrading S-metolachlor herbicide, Braz. Arch. Biol. Technol. 50 (1) (2007) 153–159, https://doi.org/10.1590/S1516-89132007000100019.
[6] I.G. Cara, D. Topa, L. Raus, A.E. Calistru, F. Filipov, G. Jitareanu, L. Baranyai, V. Stoleru, Selective and sensitive quantification of acetochlor and S-metolachlor in maize and soybean plant samples by gas chromatography-tandem mass spectrometry, Agriculture 11 (4) (2021) 283–293, https://doi.org/10.3390/agriculture11040283.
[7] Rynek Zbóż w Polsce; *Krajowy Ośrodek wsparcia Rolnictwa* 2020. https://www.gov.pl/web/kowr/rynekzbozwpolsce. (Accessed 2023–02-03).
[8] Rynek Zbóż.; *Biuro Analiz i Strategii Krajowego Ośrodka Wsparcia Rolnictwa* 2023, 34. https://www.gov.pl/attachment. (Accessed 2023–10-30).
[9] Q. Mara Silva, M. Palmieri, L. Fonseca Andrade-Vieria, Effects of a S-metolachlor based herbicide on two plant mod-els: Zea mays L. and Lactuca sativa L. Preprints (2022) https://doi.org/10.20944/preprints202209.0351.v1.
[10] W.P. Liu, H.J. Liu, W. Zheng, J.H. Lu, Adsorption of chloroacetanilide herbicides on soil (I). Structural influence of chloroacetanilide herbicide for their adsorption on soils and its components, J. Environ. Sci. 13 (1) (2001) 37–45.
[11] D.M. Stamper, O.H. Tuovinen, Biodegradation of the acetanilide herbicides alachlor, metolachlor, and propachlor, Crit. Rev. Micro 24 (1) (1998) 1–22, https://doi.org/10.1080/10408419891294163.
[12] P.J. O'connell, C.T. Harms, J.R.F. Allen, Metolachlor, S-Metolachlor and their role within sustainable weed-management, Crop Prot. 17 (3) (1998) 207–212.
[13] N. Aydogdu, E. Demir, Chapter 13 – Development of electrochemical sensors for the analysis of herbicides. Electrochemical Sensors Based on Carbon Composite Materials, IOP Publishing., 2022, pp. 1–46, https://doi.org/10.1088/978-0-7503-5127-0ch13.
[14] C. Liang, H. Peng, L. Nie, S. Yao, Bulk acoustic wave sensor for herbicide assay on molecularly imprinted polymer, J. Od. Anal. Chem. 367 (2000) 551–555, https://doi.org/10.1007/s002160000396.
[15] R. Elshafey, A.E. Radi, Electrochemical impedance sensor for herbicide alachlor based on imprinted polymer receptor, J. Electroanal. Chem. 813 (2018) 171–177, https://doi.org/10.1016/j.jelechem.2018.02.036.
[16] R. Chepyala, Chapter 4 – applications and success of mips in optical-based nanosensors. Nanofabrication for Smart Nanosensor Applications, Elsevier, 2020, pp. 89–121, https://doi.org/10.1016/b978-0-12-820702-4.00004-0.
[17] X. Wu, J. Du, M. Li, L. Wu, C. Han, F. Su, Recent advances in green reagents for molecularly imprinted polymers, RSC Adv. 8 (2018) 311–327, https://doi.org/10.1039/c7ra11047b.
[18] L.I. Andersson, Molecular imprinting: developments and applications in the analytical chemistry field, J. Chromatogr. B: Biomed. Sci. Appl. 745 (1) (2000) 3–13, https://doi.org/10.1016/S0378-4347(00)00135-2.
[19] C. Algieri, E. Drioli, C. Ahmed, I.I. Nasser, L. Donato, Emerging tools for recognition and/or removal of dyes from polluted sites: molecularly imprinted membranes, J. Membr. Sep. Technol. 3 (4) (2014) 243–266, https://doi.org/10.6000/1929-6037.2014.03.04.3.
[20] R. Schirhagl. Bioapplications for molecularly imprinted polymers, Anal. Chem. 86 (1) (2014) 250–261, https://doi.org/10.1021/ac401251j.
[21] P. Rebelo, E. Costa-Rama, I. Seguro, J.G. Pacheco, H.P.A. Nouws, M.N.D. S. Cordeiro, C. Delerue-Matos, Molecularly imprinted polymer-based electrochemical sensors for environmental analysis, Biosens. Bioelectron. 172 (2021) 112719, https://doi.org/10.1016/j.bios.2020.112719.
[22] A. Azizi, C.S. Bottaro, A critical review of molecularly imprinted polymers for the analysis of organic pollutants in environmental water samples, J. Chromatogr. A (2020), https://doi.org/10.1016/j.chroma.2019.460603.
[23] A. Ferahtia, M.T. Halilat, F. Mimeche, E. Bensaci, Surface water quality assessment in Semi-Arid Region (El Hodna Watershed, Algeria) based on water quality index (Wqi), Stud. Univ. Babes-Bolyai. Chem. 66 (2021) 127–142. https://www.chem.ubbcluj.ro/~studiachemia/issues/chemia2021_1/10_Ferahtia_etal_127_142.pdf.
[24] M. Marć, T. Kupka, P.P. Wieczorek, J. Namieśnik, Computational modeling of molecularly imprinted polymers as a green approach to the development of novel analytical sorbents, Trends Anal. Chem. 98 (2018) 64–78, https://doi.org/10.1016/j.trac.2017.10.020.
[25] S. Suryana, Mutakin, Y. Rosandi, A.N. Hasanah, An update on molecularly imprinted polymer design through a computational approach to produce molecular recognition material with enhanced analytical performance, Molecules 26 (7) (2021) 1891, https://doi.org/10.3390/molecules26071891.
[26] N. Sanadgol, J. Wackerlig, Developments of smart drug-delivery systems based on magnetic eMolecularly imprinted polymers for targeted cancer therapy: a short review, Pharmaceutics 12 (9) (2020) 831, https://doi.org/10.3390/pharmaceutics12090831.
[27] E. Piletska, A. Guerreiro, M. Mersiyanova, T. Cowen, F. Canfarotta, S. Piletsky, K. Karim, S. Piletsky, Probing peptide sequences on their ability to generate affinity sites in molecularly imprinted polymers, Langmuir 36 (1) (2020) 279–283, https://doi.org/10.1021/acs.langmuir.9b03410.
[28] T. Cowen, E. Stefanucci, E. Piletska, G. Marrazza, F. Canfarotta, S.A. Piletsky, Synthetic mechanism of molecular imprinting at the solid phase, Macromolecules 53 (4) (2020) 1435–1442, https://doi.org/10.1021/acs.macromol.9b01913.
[29] M.D. Attieh, Y. Zhao, A. Elkak, A. Falcimaigne-Cordin, K. Haupt, Enzyme-initiated free-radical polymerization of molecularly imprinted polymer nanogels on a solid phase with an immobilized radical source, Angew. Chem. 129 (12) (2017) 3387–3391, https://doi.org/10.1002/ange.201612667.
[30] S. Wang, L. Ge, L. Li, M. Yan, S. Ge, J. Yu, Molecularly imprinted polymer grafted paper-based multi-disk micro-disk plate for chemiluminescence detection of pesticide, Biosens. Bioelectron. 50 (2013) 262–268, https://doi.org/10.1016/j.bios.2013.07.003.
[31] S. Xu, Y. Zou, H. Zhang, Well-defined hydrophilic "turn-on"-type ratiometric fluorescent molecularly imprinted polymer microspheres for direct and highly selective herbicide optosensing in the undiluted pure milks, Talanta 211 (2020), https://doi.org/10.1016/j.talanta.2020.120711.
[32] S. Feng, Y. Hu, L. Chen, X. Lu, Molecularly imprinted core-shell au nanoparticles for 2,4-dichlorophenoxyacetic acid detection in milk using surface-enhanced raman spectroscopy, Anal. Chim. Acta 1227 (2022), https://doi.org/10.1016/j.aca.2022.340333.
[33] M.M. El-Beshlawy, F.M. Abdel-Haleem, A.H. Kamel, A. Barhoum, Screen-printed sensors coated with polyaniline/molecularly imprinted polymer membranes for the potentiometric determination of 2,4-dichlorophenoxyacetic acid herbicide in wastewater and agricultural soil, Chemosensors 11 (2023) 3, https://doi.org/10.3390/chemosensors11010003.
[34] J. Chen, L. Bai, L. Zhang, M. Hu, Y. Zhang, Novel liquid-liquid-solid microextraction using molecularly imprinted polymer monolithic fibres and its application to the extraction of s-triazine herbicides from water samples, Adsorpt. Sci. Technol. 32 (4) (2014), https://doi.org/10.1260/0263-6174.32.4.331.
[35] R.M. Roland, S.A. Bhawani, M.N.M. Ibrahim, Synthesis of molecularly imprinted polymer by precipitation polymerization for the removal of ametryn, BMC Chem. 17 (165) (2023), https://doi.org/10.1186/s13065-023-01084-0.
[36] T.A. Sergeyeva, S.A. Piletsky, A.A. Brovko, E.A. Slinchenko, L.M. Sergeeva, A. El'skaya, Selective recognition of atrazine by molecularly imprinted polymer membranes. development of conductometric sensor for herbicides detection, Anal. Chim. Acta 392 (1999) 105–111, https://doi.org/10.1016/S0003-2670(99)00225-1.
[37] R. Liu, G. Guan, S. Wang, Z. Zhang, Core-shell nanostructured molecular imprinting fluorescent chemosensor for selective detection of atrazine herbicide, Analyst 136 (1) (2011) 184–190, https://doi.org/10.1039/C0AN00447B.
[38] Z. Salahshoor, K. Ho, S.Y. Hsu, C.H. Lin, M. Fidalgo de Cortalezzi, Detection of atrazine and its metabolites by photonic molecularly imprinted polymers in aqueous solutions, Chem. Eng. J. Adv. 12 (2022), https://doi.org/10.1016/j.ceja.2022.100368.
[39] R.M. Roland, S.A. Bhawani, M.N.M. Ibrahim, Synthesis of molecularly imprinted polymer for the removal of cyanazine from aqueous samples, Chem. Biol. Technol. Agric. 10 (92) (2023), https://doi.org/10.1186/s40538-023-00462-z.
[40] A. Geranmizadegan, L. Niknam, E. Pournamdari, Molecularly imprinted polymers for selective extraction and determination of toxic herbicide bentazon in water samples using liquid chromatography and assessment of mean square error using artificial neural network model, J. Anal. Chem. 78 (5) (2023) 572–581, https://doi.org/10.1134/S1061934823050052.
[41] P. Zhao, M. Yan, C. Zhang, R. Peng, D. Ma, J. Yu, Determination of glyphosate in foodstuff by one novel chemiluminescence- molecular imprinting sensor, Spectrochim. Acta Part A: Mol. Biomol. Spectrosc. 78 (5) (2011) 1482–1486, https://doi.org/10.1016/j.saa.2011.01.037.
[42] A.A. Coble, C. Silva-Sanchez, W.J. Arthurs, C.A. Flinders, Detection and accumulation of environmentally-relevant glyphosate concentrations delivered via pulse- or continuous-delivery on passive samplers, Part 2, Sci. Total Environ. 838 (2022), https://doi.org/10.1016/j.scitotenv.2022.156131.
[43] D. Balciunas, D. Plausinaitis, V. Ratautaite, A. Ramanaviciene, A. Ramanavicius, Towards electrochemical surface plasmon resonance sensor based on the

molecularly imprinted polypyrrole for glyphosate sensing, Talanta 241 (2022), https://doi.org/10.1016/j.talanta.2022.123252.
[44] P. Sawetwong, S. Chairam, P. Jarujamrus, M. Amatatongchai, Enhanced selectivity and sensitivity for colorimetric determination of glyphosate using mn–zns quantum dot embedded molecularly imprinted polymers combined with a 3D-microfluidic paper-based analytical device, Talanta 225 (2021), https://doi.org/10.1016/j.talanta.2020.122077.
[45] A.H. Kamel, Al Romian, F.M. Man-Tailored, Biomimetic sensors of molecularly polymers for selective recognition of some herbicides and their application to potentiometric transduction, Int. J. Chem. Mater. Sci. 1 (1) (2013) 1–12.
[46] A. Wong, M.V. Foguel, S. Khan, F.M. de Oliveira, C.R.T. Tarley, M.D.P. T. Sotomayor, Development of an electrochemical sensor modified with MWCNT-COOH and MIP for detection of diuron, Electrochim. Acta 182 (2015) 122–130, https://doi.org/10.1016/j.electacta.2015.09.054.
[47] Y.C. Lu, M.H. Guo, J.H. Mao, X.H. Xiong, Y.J. Liu, Y. Li, Preparation of core-shell magnetic molecularly imprinted polymer nanoparticle for the rapid and selective enrichment of trace diuron from complicated matrices, Ecotoxicol. Environ. Saf. 177 (2019) 66–76, https://doi.org/10.1016/j.ecoenv.2019.03.117.
[48] X. Dong, N. Wang, S. Wang, X. Zhang, Z. Fan, Synthesis and application of molecularly imprinted polymer on selective solid-phase extraction for the determination of monosulfuron residue in soil, J. Chromatogr. A 1057 (1–2) (2004) 13–19, https://doi.org/10.1016/j.chroma.2004.09.036.
[49] L. Guo, Q. Deng, G. Fang, W. Gao, S. Wang, Preparation and evaluation of molecularly imprinted ionic liquids polymer as sorbent for on-line solid-phase extraction of chlorsulfuron in environmental water samples, J. Chromatogr. A 1218 (37) (2011) 6271–6277, https://doi.org/10.1016/j.chroma.2011.07.016.
[50] Y. xin She, W. qiang Cao, X. mei Shi, X. ling Lv, J. jia Liu, R. yan Wang, F. Jin, J. Wang, H. Xiao, Class-specific molecularly imprinted polymers for the selective extraction and determination of sulfonylurea herbicides in maize samples by high-performance liquid chromatography-tandem mass spectrometry, J. Chromatogr. B Anal. Technol. Biomed. Life Sci. 878 (23) (2010) 2047–2053, https://doi.org/10.1016/j.jchromb.2010.05.038.
[51] F.N. Andrade, A.J. Santos-Neto, D.A.V. Medina, F.M. Lancas, A molecularly imprinted polymer for microextraction by packed sorbent of sulfonylureas herbicides from corn samples, J. Food Compos. Anal. 121 (2023) 105388, https://doi.org/10.1016/j.jfca.2023.105388.
[52] M. Piryaei, M.M. Abolghasemi, S. Jodatvand, Magnetic dispersive solid-phase extraction of nicosulfuron using surface immobilized molecularly imprinted polymer by RAFT polymerization on Fe3O4/graphene oxide nanosheets, Chem. Sel. 8 (2023) e20220402, https://doi.org/10.1002/slct.202204023.
[53] C.G. Xie, S. Gao, H.K. Zhou, H.F. Li, Chemiluminescence sensor for sulfonylurea herbicide using molecular imprinted microspheres as recognition element, Luminescence 26 (4) (2011) 271–279, https://doi.org/10.1002/bio.1224.
[54] H. Li, C. Xie, X. Fu, Electrochemiluminescence Sensor for Sulfonylurea Herbicide with Molecular Imprinting Core-Shell Nanoparticles/Chitosan Composite Film Modified Glassy Carbon Electrode, Sens. Actuators B Chem. 181 (2013) 858–866, https://doi.org/10.1016/j.snb.2013.02.094.
[55] X. Hu, G. Dai, J. Huang, T. Ye, H. Fan, T. Youwen, Y. Yu, Y. Liang, Molecularly imprinted polymer coated on stainless steel fiber for solid-phase microextraction of chloroacetanilide herbicides in soybean and corn, J. Chromatogr. A 1217 (38) (2010) 5875–5882, https://doi.org/10.1016/j.chroma.2010.07.011.
[56] Y. Wang, X. Jin, D. Zhao, X. Guo, R. Li, Molecularly imprinted solid-phase extraction coupled with gas chromatography for the determination of four chloroacetamide herbicides in soil, Anal. Methods 7 (15) (2015) 6411–6418, https://doi.org/10.1039/c5ay00281h.
[57] X. Hu, T. Ye, Y. Yu, Y. Cao, C. Guo, Novel liquid-liquid-solid microextraction method with molecularly imprinted polymer-coated stainless steel fiber for aqueous sample pretreatment, J. Chromatogr. A 1218 (25) (2011) 3935–3939, https://doi.org/10.1016/j.chroma.2011.04.069.
[58] M. Li, F. Shen, Z. Zhang, X. Ren, A novel 2-acrylamide-6-methoxybenzothiazole fabricated molecularly imprinted polymers for direct fluorescent sensing of alachlor, Chromatographia 79 (1–2) (2016) 71–78, https://doi.org/10.1007/s10337-015-2998-4.
[59] Y. Fang, S. Yan, B. Ning, N. Liu, Z. Gao, F. Chao, Flow injection chemiluminescence sensor using molecularly imprinted polymers as recognition element for determination of maleic hydrazide, Biosens. Bioelectron. 24 (6) (2009) 2323–2327, https://doi.org/10.1016/j.bios.2008.10.034.
[60] D. Elfadil, S. Palmieri, F. Silveri, F. della Pelle, M. Sergi, M. del Carlo, A. Amine, D. Compagnone, Fast sonochemical molecularly imprinted polymer synthesis for selective electrochemical determination of maleic hydrazide, Microchem. J. 180 (2022), https://doi.org/10.1016/j.microc.2022.107634.
[61] C.X. Liu, J. Zhao, R.R. Zhang, Z.M. Zhang, J.J. Xu, A.L. Sun, J. Chen, X.Z. Shi, Development and application of fluorescence sensor and test strip based on molecularly imprinted quantum dots for the selective and sensitive detection of propanil in fish and seawater samples, J. Hazard. Mater. 389 (2020), https://doi.org/10.1016/j.jhazmat.2019.121884.
[62] M.J.U. Toro, L.D. Marestoni, M. del Pilar Taboada Sotomayor, A new biomimetic sensor based on molecularly imprinted polymers for highly sensitive and selective determination of hexazinone herbicide, Sens. Actuators B Chem. 208 (2015) 299–306, https://doi.org/10.1016/j.snb.2014.11.036.
[63] N.S. Abdalla, M.A. Youssef, H. Algarni, N.S. Awwad, A.H. Kamel, All solid-state poly (Vinyl Chloride) membrane potentiometric sensor integrated with nano-beads imprinted polymers for sensitive and rapid detection of bispyribac herbicide as organic pollutant, Molecules 24 (4) (2019) 712–725, https://doi.org/10.3390/molecules24040712.
[64] M. Noor, K.M. Iqbal, T. Kanwal, K. Rehman, M. Ali, M.R. Shah, Synthesis and characterization of modified silica nanoparticles based molecularly imprinted polymers as a sensor for selective detection of pendimethalin from drinking water, J. Mol. Struct. 1287 (2023) 135635, https://doi.org/10.1016/j.molstruc.2023.135635.
[65] M.A.A. Fatnh, M.G.A. El-Moghny, M. El-Deab, R.M. El Nashar, Application of molecularly imprinted electrochemical sensor for trace analysis of Metribuzin herbicide in food samples, Food Chem. 404 (2023) 134708, https://doi.org/10.1016/j.foodchem.2022.134708.
[66] A.H. Kamel, H.S.M. Abd-Raggoh, Imprinted polymer/reduced graphene oxide-modified glassy carbon electrode-based highly sensitive potentiometric sensing module for imidacloprid detection, Microchem. J. 197 (2023) 109789, https://doi.org/10.1016/j.microc.2023.109789.
[67] T. Zhou, T. Zhou, L. Ding, G. Che, W. Jiang, L. Sang, Recent advances and trends of molecularly imprinted polymers for specific recognition in aqueous matrix: preparation and application in sample pretreatment, Trends Anal. Chem. 114 (2019) 11–28, https://doi.org/10.1016/j.trac.2019.02.028.
[68] S. Farooq, H. Wu, J. Nie, S. Ahmad, I. Muhammad, M. Zeeshan, R. Khan, M. Asim, Application, advancement and green aspects of magnetic molecularly imprinted polymers in pesticide residue detection, Sci. Total Environ. 804 (2022) 150293, https://doi.org/10.1016/j.scitotenv.2021.150293.
[69] K. Haupt, A. Dzgoev, K. Mosbach, Assay system for the herbicide 2,4-dichlorophenoxyacetic acid using a molecularly imprinted polymer as an artificial recognition element, Anal. Chem. 70 (3) (1998) 628–631, https://doi.org/10.1021/ac9711549.
[70] K. Haupt, A.G. Mayes, K. Mosbach, Herbicide assay using an imprinted polymer-based system analogous to competitive fluoroimmunoassays, Anal. Chem. 70 (18) (1998) 3936–3939, https://doi.org/10.1021/ac980175f.
[71] G. Pan, Y. Zhang, Y. Ma, C. Li, H. Zhang, Efficient one-pot synthesis of water-compatible molecularly imprinted polymer microspheres by facile RAFT precipitation polymerization, Angew. Chem. - Int. Ed. 50 (49) (2011) 11731–11734, https://doi.org/10.1002/anie.201104751.
[72] G. Pan, Y. Ma, Y. Zhang, X. Guo, C. Li, H. Zhang, Controlled synthesis of water-compatible molecularly imprinted polymer microspheres with ultrathin hydrophilic polymer shells via surface-initiated reversible addition-fragmentation chain transfer polymerization, Soft Matter 7 (18) (2011) 8428–8439, https://doi.org/10.1039/c1sm05497j.
[73] B. Wu, T. Muhammad, S. Aihebaier, K. Karim, Y. Hu, S. Piletsky, A molecularly imprinted polymer based monolith pipette tip for solid-phase extraction of 2,4-dichlorophenoxyacetic acid in an aqueous sample, Anal. Methods 12 (40) (2020) 4913–4921, https://doi.org/10.1039/d0ay01587c.
[74] X.A. Ton, V. Acha, P. Bonomi, B. Tse Sum Bui, K. Haupt, A disposable evanescent wave fiber optic sensor coated with a molecularly imprinted polymer as a selective fluorescence probe, Biosens. Bioelectron. 64 (2015) 359–366, https://doi.org/10.1016/j.bios.2014.09.017.
[75] F. Qiao, K.H. Row, M. Wang, Water-compatible magnetic imprinted microspheres for rapid separation and determination of triazine herbicides in environmental water, J. Chromatogr. B Anal. Technol. Biomed. Life Sci. 957 (2014) 84–89, https://doi.org/10.1016/j.jchromb.2014.02.041.
[76] A.S. Belmont, S. Jaeger, D. Knopp, R. Niessner, G. Gauglitz, K. Haupt, Molecularly imprinted polymer films for reflectometric interference spectroscopic sensors, Biosens. Bioelectron. 22 (12) (2007) 3267–3272, https://doi.org/10.1016/j.bios.2007.01.023.
[77] T. Zhou, J. Hou, D. Yuan, H. Li, P. Zhang, Y. Li, H. Ding, Y. Chen, L. Ding, Determination of triazine herbicides from honey samples based on hydrophilic molecularly imprinted resins followed by high performance liquid chromatography-tandem mass spectrometry, RSC Adv. 6 (101) (2016) 98663–98673, https://doi.org/10.1039/c6ra20698k.
[78] T. Zhou, J. Ding, L. Ni, J. Yu, H. Li, H. Ding, Y. Chen, L. Ding, Preparation of magnetic superhydrophilic molecularly imprinted resins for detection of triazines in aqueous samples, J. Chromatogr. A 1497 (2017) 38–46, https://doi.org/10.1016/j.chroma.2017.03.069.
[79] T. Zhou, J. Ding, Z. He, J. Li, Z. Liang, C. Li, Y. Li, Y. Chen, L. Ding, Preparation of magnetic superhydrophilic molecularly imprinted composite resin based on multi-walled carbon nanotubes to detect triazines in environmental water, Chem. Eng. J. 334 (2018) 2293–2302, https://doi.org/10.1016/j.cej.2017.11.165.
[80] Q. Zhao, T. Zhou, H. Li, H. Liu, N. Huang, Y. Xu, J. Ding, L. Ding, Y. Li, Preparation of magnetic surface molecularly imprinted polymers for the selective extraction of triazines in environmental water samples, Int. J. Environ. Anal. Chem. 98 (11) (2018) 1049–1062, https://doi.org/10.1080/03067319.2018.1520226.
[81] A. Gomez-Caballero, G. Diaz-Diaz, O. Bengoetxea, A. Quintela, N. Unceta, M. A. Goicolea, R.J. Barrio, Water compatible stir-bar devices imprinted with underivatised glyphosate for selective sample clean-up, J. Chromatogr. A 1451 (2016) 23–32, https://doi.org/10.1016/j.chroma.2016.05.017.
[82] Y. Liu, Z. Yan, R. Chen, Y. Yu, X. Chen, X. Zheng, X. Huang, 2,4-dichlorophenol removal from water using an electrochemical method improved by a composite molecularly imprinted membrane/bipolar membrane, J. Hazard. Mater. 377 (2019) 259–266, https://doi.org/10.1016/j.jhazmat.2019.05.064.
[83] L. Zhang, J. Li, Y. Zeng, Molecularly imprinted magnetic nanoparticles for determination of the herbicide chlorotoluron by gate-controlled electro-catalytic oxidation of hydrazine, Microchim. Acta 182 (1–2) (2015) 249–255, https://doi.org/10.1007/s00604-014-1326-2.
[84] J. Sun, C. Chen, Y. Zhang, X. Sun, A novel fluorescent molecularly imprinted polymer SiO2@CdTe QDs@MIP for paraquat detection and adsorption, Luminescence 36 (2) (2020) 345–352, https://doi.org/10.1002/bio.3949.

[85] Adsorption: fundamental processes and applications, in: M. Ghaedi (Ed.), Volume 33 in the Interface Science and Technology Series, Academic Press, 2021.
[86] S. Zhao, W. Liu, D. Song, Rapid detection and prediction model establishment of propachlor residues in food assisted by machine learning, J. Food Meas. Charact. 17 (2023) 5972–5979, https://doi.org/10.1007/s11694-023-02084-3.
[87] M.D. Arioni, A. Zuhrotun, P. Manesiotis, A.N. Hasanah, Magnetic molecularly imprinted polymers: an update on their use in the separation of active compounds from natural products, Polymers 14 (7) (2022) 1389–1413, https://doi.org/10.3390/polym14071389.
[88] Z.O. Uygun, H.D. Ertugrul Uygun, N. Ermis, E. Canbay, Molecularly imprinted sensors — new sensing technologies, Biosens. - Micro Nanoscale Appl. (2015) 85–108, https://doi.org/10.5772/60781.
[89] W. Yang, Y. Ma, H. Sun, C. Huang, X. Shen, Molecularly imprinted polymers based optical fiber sensors: a review, Trends Anal. Chem. 152 (2022), https://doi.org/10.1016/j.trac.2022.116608.
[90] M.G. Metwally, A.H. Benhawy, R.M. Khalifa, R.M. El Nashar, M. Trojanowicz, Application of molecularly imprinted polymers in the analysis of waters and wastewaters, Molecules 26 (21) (2021) 6515, https://doi.org/10.3390/molecules26216515.

7.2. Dobór warunków polimeryzacji w syntezie blokowych polimerów molekularnie wdrukowywanych reagujących na zmiany temperatury (Publikacja P2)

Rapacz D, Smolińska–Kempisty K, Wolska J. A novel green molecularly imprinted polymers synthesized in an aqueous medium as S–metolachlor sensitive materials. *Talanta*. 2024, vol. 280, art. 126674, s. 1-9. https://doi.org/10.1016/j.talanta.2024.126674.

Wprowadzenie

Drugi artykuł pod tytułem „**A novel green molecularly imprinted polymers synthesized in an aqueous medium as S–metolachlor sensitive materials”** opublikowany w *Talanta*, po raz pierwszy opisuje termoczułe polimery blokowe molekularnie wdrukowane selektywne wobec S–metolachloru, zsyntezowane według koncepcji tak zwanej „*zielonej chemii*”. Dotychczas opublikowane prace przedstawiały MIPy otrzymywane z wykorzystaniem rozpuszczalników organicznych, w podwyższonej temperaturze, co wskazuje na innowacyjność badań stanowiących treść niniejszej publikacji.

Wyniki

W tej pracy przedstawiono skład mieszaniny reakcyjnej, stosunek molowy reagentów oraz warunki syntezy polimerów blokowych selektywnych w stosunku do S–metolachloru. Najkorzystniejsze wyniki sorpcji uzyskano wykorzystując N–izopropyloakrylamid, kwas akrylowy i akryloamid (stosunek molowy odpowiednio 11:14:11) jako monomery funkcyjne, N,N'–metylenobis(akrylamid) użyto jako środek sieciujący, S–metolachlor jako cząsteczki szablonu, a wodę jako porofor oraz środowisko reakcji. Jako inicjator wykorzystano nadsiarczan amonu oraz N,N,N′,N′–tetrametyloetylenodiaminę. Oddziaływanie pomiędzy S–metolachlorem a monomerami funkcyjnymi zweryfikowano wykorzystując komputerowe modelowanie molekularne – przedstawione na Rysunku 1. Bazowano na algorytmie Leapfrog dostępnym na oprogramowaniu SYBYL 7.3. Badania te będą elementem oddzielnej publikacji. Stosunek molowy monomerów funkcyjnych do środka sieciującego wynosił 7:2, natomiast stosunek molowy monomerów funkcyjnych do cząsteczki szablonu był równy 39:1. Reakcja była prowadzona bez strat energii – w temperaturze otoczenia. W ten sam sposób, jednak bez dodatku S–metolachloru, otrzymano polimery bez odcisku molekularnego, stanowiące układ referencyjny. Jednym z głównych ograniczeń była rozpuszczalność S–metolachloru w wodzie (około 0,5 g × L^{-1}), która jest wystarczająca z punktu widzenia rolnictwa, natomiast stanowiła wyzwanie podczas syntezy, gdzie wymagana była duża zawartość analitu w mieszaninie reakcyjnej.

Proces sorpcji statycznej został przeprowadzony w celu charakterystyki zsyntezowanych sorbentów. Wartość sorpcji dla wyselekcjonowanego MIPu wynosiła 2,42 ± 0,04 mg × g^{-1}, natomiast dla NIPu była równa 0,46 ± 0,03 mg × g^{-1}. Z danych tych wynika, że MIP sorbuje S–metolachlor ponad pięciokrotnie lepiej niż układ referencyjny. Ponadto zbadano selektywność MIPów w stosunku do S–metolachloru. W tym celu wykonano proces sorpcji z roztworu wieloskładnikowego, zawierającego następujące herbicydy: S–metolachlor, atrazynę, glifosat oraz fenoksaprop–P–etylu. Na podstawie przeprowadzonych badań

oszacowano, iż MIP sorbuje S–metolachlor ponad trzykrotnie lepiej niż atrazynę oraz około sześciokrotnie lepiej niż glifosat i fenoksaprop–P–etylu, co wskazuje na dużą selektywność polimeru wdrukowanego molekularnie.

Ponadto, aby określić bardziej szczegółowe właściwości procesu sorpcji, wykonano analizę izoterm sorpcji, a otrzymane wyniki dopasowano do modeli izotermy Langmuira, Freundlicha oraz Dubinina–Radushkevicha. Określono, iż najlepszym dopasowaniem dla sorpcji MIPu był liniowy model izotermy Langmuira, wykazujący duży współczynnik determinacji (R^2 = 0,968) oraz maksymalną wartość sorpcji (3,15 mg × g^{-1}) zbliżoną do wartości eksperymentalnej (2,42 ± 0,04 mg × g^{-1}). Natomiast model izotermy Freundlicha opisywał sorpcję S–metolachloru przez NIP. Wartości współczynnika determinacji były bliskie 1, zarówno w liniowej (R^2 = 0,990), jak i nieliniowej (R^2 = 0,981) formie, natomiast wartości sorpcji były znacznie większe niż te otrzymane eksperymentalnie. Z kolei w modelu liniowym Dubinina–Radushkevicha maksymalna wartość sorpcji była zbliżona do eksperymentalnej, chociaż wartość współczynnik determinacji wynosiła R^2 = 0,431.

Otrzymane polimery przetestowano dodatkowo na próbkach rzeczywistych – sporządzonych z wody wodociągowej. Początkowo wartości przeprowadzonej sorpcji znacząco odbiegały od tej przeprowadzonej na roztworze modelowym i były równe 0,57 ± 0,33 mg × g^{-1} i 0,37 ± 0,01 mg × g^{-1}, odpowiednio dla MIPu i NIPu. Natomiast po obniżeniu pH roztworu rzeczywistego do około 5 – odpowiadającemu pH roztworu modelowego, wartości sorpcji były zbliżone do tych, otrzymanych dla roztworu modelowego i wynosiły 2,61 ± 0,35 mg × g^{-1} oraz 0,63 ± 0,21 mg × g^{-1}, odpowiednio dla MIPu i NIPu. Aby w pełni scharakteryzować właściwości sorbentów wykonano widma IR, zdjęcia SEM oraz oznaczono również chłonność wody. Celem spektroskopii w podczerwieni było porównanie budowy chemicznej sorbentów oraz potwierdzenie obecności grup funkcyjnych charakterystycznych dla użytych monomerów. Widma MIPu i NIPu wyglądały niemal identycznie, potwierdzając taką samą budowę chemiczną polimerów, jednakże znacząco różniących się właściwościami sorpcyjnymi. Analiza SEM zobrazowała morfologię powierzchni materiałów, przy czym powierzchnia MIPu była bardziej porowata niż NIPu, natomiast oba sorbenty cechowały się nieregularnymi kształtami. Wartości stopnia pęcznienia dla obu polimerów były podobne, co podkreśla, że cecha ta nie wpływa na właściwości sorpcyjne materiałów, jednocześnie potwierdzając obecność specyficznych miejsc wiążących w strukturze MIPu.

Podsumowanie

Otrzymane blokowe polimery wdrukowane molekularnie wykazują dużą selektywność w stosunku do S–metolachloru, sorbując go ponad trzykrotnie lepiej niż atrazynę oraz około sześciokrotnie lepiej niż glifosat i fenoksaprop–P–etylu. Ponadto MIP sorbuje S–metolachlor w próbkach modelowych pięciokrotnie lepiej niż układ referencyjny, czyli NIP, a w próbkach rzeczywistych – czterokrotnie lepiej, co potwierdza obecność swoistych wnęk w matrycy polimeru. Dodatkowo publikacja przedstawia po raz pierwszy, „*zielone*” polimery wdrukowane molekularnie selektywne wobec S–metolachloru, poszerzając tym samym czteroelementowy zbiór MIPów syntezowanych zgodnie z założeniami „*zielonej chemii*”.

Talanta 280 (2024) 126674

Contents lists available at ScienceDirect

Talanta

journal homepage: www.elsevier.com/locate/talanta

A novel *green* molecularly imprinted polymers synthesized in an aqueous medium as S-metolachlor sensitive materials

Dominika Rapacz *, Katarzyna Smolińska-Kempisty, Joanna Wolska

Wroclaw University of Science and Technology, Department of Process Engineering and Technology of Polymer and Carbon Materials, Wybrzeże Wyspiańskiego 27, 50-370, Wroclaw, Poland

ARTICLE INFO

Keywords:
S-metolachlor
Molecularly imprinted polymers
Green molecularly imprinted polymers
Sorption
Selectivity

ABSTRACT

A new molecularly imprinted polymer (MIP) sensitive and selective for S-metolachlor herbicide was synthesized by bulk polymerization with the use of N-isopropylacrylamide, acrylamide, and acrylic acid as functional monomers, and N,N′- methylenebis(acrylamide) as a cross-linker. A novel method for obtaining MIP toward S-metolachlor in an aqueous medium and at room temperature, according to the principles of *green chemistry*, has been discovered, in comparison to synthesis methods at high temperatures and using organic solvents. Under selected experimental conditions, the batch mode type of sorption was carried out efficiently, with S-metolachlor absorption of 2.4 mg per 1 g of MIP and 0.5 mg per 1 g of NIP. The selectivity of the sorbent towards other herbicides and pesticides was also tested, obtaining an ability to recognize S-metolachlor molecules 3.2 times better than atrazine, 6 times better than glyphosate, and 6.2 times better than fenoxaprop-P-ethyl. The FT-IR and SEM analyses were performed to characterize the structure of the synthesized polymers.

1. Introduction

In the United States, corn is the most commonly grown crop [1], while in Europe it ranks 2nd [2]. Poland is Europe's third largest producer of this grain [3]. Weeds are one of the main challenges in corn cultivation. Herbicides commonly used and effective in the fight against weeds include S-metolachlor [4].

S-metolachlor (2-chloro-N-(2-ethyl-6-methylphenyl)-N-(2-methoxy-1-methylethyl)acetanilide) is a preemergent chloroacetanilide herbicide widely used to control annual grass and broadleaf weeds, especially in corn, cotton, soybean, sunflower, and bean cultivation [5]. The mechanism of action is based on the inhibition of elongases and biosynthesis of gibberellic acid, as a result of which, after being absorbed by the roots and shoots, the weed plant dies, leaving the seed of the target plant intact [6]. S-metolachlor is slightly soluble in water (488 mg × L^{-1} at 25 °C) [7] and its hydrolysis half-life time is over 200 days at 20 °C, while the half-life in soil is 47–107 days [8].

Nowadays, a wide range of diverse methods and technologies for removing herbicides from aqueous solutions have been developed. Many of them are based on electrolysis [9], advanced oxidation processes, such as Fenton technology, or photochemical degradation [10], adsorbents, among them activated carbon [11], bioadsorbent, polymeric adsorbent, and agricultural waste, biological treatment techniques, or membrane techniques [12]. One promising technique is molecularly imprinted polymers (MIPs), which have specific binding sites for a particular analyte [13]. During the polymerization step, the molecule is incorporated into the matrix structure. After removing the template molecule, the cavities are observed on the polymer surface, perfectly matched in shape, size, and functional group to the chosen analyte [14].

Analytical techniques available today are capable of direct analysis of herbicides; however, multiple analytes often create a chemical cocktail, making the analysis significantly more difficult. Extracting individual analytes from a water sample will contribute to a more accurate analysis, excluding the share of analytes with properties similar to those of the analyzed molecule [15]. Therefore, this work reports a novel molecularly imprinted polymer sensitive to S-metolachlor herbicide synthesized in an aquagenic environment *via* bulk polymerization at room temperature. Furthermore, different factors, such as the type of monomer, the concentration of S-metolachlor, and the molar ratio of the reagent were investigated.

* Corresponding author.
E-mail address: dominika.rapacz@pwr.edu.pl (D. Rapacz).

https://doi.org/10.1016/j.talanta.2024.126674
Received 20 May 2024; Received in revised form 4 July 2024; Accepted 5 August 2024
Available online 6 August 2024

2. Materials and methods

2.1. Reagents and chemicals

N-isopropylacrylamide (NIPAM), methacrylic acid (MAA), N,N′-Methylenebis(acrylamide) (BIS) were purchased from Sigma-Aldrich. Acrylamide (AA) was provided by Thermo Scientific Chemicals. Ammonium persulfate (APS) and N,N,N′,N′-Tetramethylethylenediamine (TEMED) were purchased from Sigma-Aldrich. S-metolachlor (SMCh) was used as a plant protection product obtained from NOVA-GRA. Acrylic acid was purchased from Acros Organics, and 2,2′-Azobis (isobutyronitrile) (AIBN) was provided from Merck. The acetonitrile and water of HPLC grade were purchased from CHEMSOLUTE. The potassium sulfate (K_2SO_4), ethyl alcohol (EtOH), and methyl alcohol (MeOH) were purchased from POCH.

2.2. Methods

2.2.1. Synthesis of polymers

Molecularly imprinted polymers were prepared by bulk polymerization. To synthesize MIPs, BIS was used as a cross-linker, APS and TEMED as a catalytic system, and S-metolachlor as a template molecule. NIPAM, MAA, AA, and acrylic acid were tested as functional monomers, whereas water, ethanol, and methanol were tried out as porous agents. AA (3.52 or 4.64 mmol) or MAA (3.83 mmol) and NIPAM (3.52 mmol), acrylic acid (0.32 mmol or 72.86 mmol), BIS (2.34 mmol or 3.52 mmol), and template (from 0.08 mmol to 0.55 mmol) were dissolved into a glass vial. After nitrogen purging (1 min), APS (0.13 mmol) and TEMED (0.10 mmol) water solution (1 mL) or K_2SO_4 (high-temperature MIPs) (0.09 mmol, 0.17 mmol, 0.26 mmol) or AIBN (high-temperature MIPs) (0.13 mmol) were added to the polymerization mixture and deoxygenized with a stream of nitrogen again (2 min). The reaction vessel was placed on the shaker and polymerized for 24 h at room temperature, or in an oven at 60 °C (high-temperature MIPs). The bulk polymers were washed in a Soxhlet apparatus for 24 h using ethanol and dried at 60 °C. The same method was employed to prepare non-imprinted polymers (NIPs) without a template molecule. The composition of the reactants used is described in Table 2.

2.2.2. Analytical methods

2.2.2.1. High-performance liquid chromatography. HPLC system (Shimadzu high-performance liquid chromatograph model SCL-40) equipped with a PDA pump, an autosampler (model SIL-40), and a chromatographic column (3 μm ARION® Biphenyl, 150 × 4.6 mm) was employed. The isocratic elution was performed at 30 °C using the mixture of acetonitrile and water (50:50 v/v) as a mobile phase. The mobile phase was degassed for 10 min by sonification. The flow rate was maintained at 1 mL × min^{-1}, the injection volume was 30 μm, and the detection wavelength was 254 nm.

2.2.2.2. Scanning electron microscopy. The surface morphology of the selected pair of MIP and NIP sorbents was estimated using a Quanta 250 (FEI) SEM microscope. Firstly samples were sputtered with a 10–15 nm thick layer of gold. The analyses were conducted using a Large Field Detector (LFD) in the ESEM mode at an accelerated voltage of 15 kV, pressure of approximately 60 Pa, with a sample inclination of 60°.

2.2.2.3. Fourier-transform infrared spectroscopy. Fourier transform infrared spectra were performed in the 400-4000 cm^{-1} range to characterize the presence of functional groups in the sorption material. The spectra were taken on a Jasco FT-IR-4700 spectrophotometer by collecting 64 scans at a resolution of 4 cm^{-1}.

2.2.3. Batch mode sorption process

To study the efficiency of S-metolachlor removal from solutions by MIP and NIP, about 0.2 ± 0.003 g of dry polymer and 20 mL of 30 mg × L^{-1} S-metolachlor solution were mixed at room temperature for 24 h. After reaching equilibrium, the samples were filtrated by syringe filter Acrodisc 0.45 μm and the concentration of S-metolachlor that remained in the solution was determined on the HPLC apparatus. The sorption capacity, q_{SMCh} defined as (Eq. (1)) the amount of S-metolachlor absorbed at the equilibrium [mg × g^{-1}], was calculated as

$$q_{SMCh} = \frac{(C_0 - C_e) \times V}{m} \quad (1)$$

where C_0 and C_e are initial and equilibrium S-metolachlor concentrations respectively [mg × L^{-1}], V is a volume of solution [L], and m is a mass of dry polymer [g] [16].

2.2.4. Sorption isotherms

The selected, best pair of sorbents MIP and NIP were used to create sorption isotherms. In a glass flask, 0.2 ± 0.003 g of dry polymers were placed, and 20 mL of solutions containing 10–500 mg × L^{-1} S-metolachlor were added. The samples were shaken for 24 h at 22 ± 2 °C and filtered by syringe filter Acrodisc 0.45 μm afterward. The S-metolachlor concentration at an equilibrium state was determined on the HPLC apparatus. The obtained isothermal data were fitted to the Langmuir, Freundlich, Dubinin–Radushkevich, and Scatchard isotherms models (Table 1) [17,18].where.

C_e – the equilibrium concentration of adsorbate [mg × L^{-1}]

q_e – the absorption capacity at equilibrium [mg × g^{-1}]

K_L – Langmuir parameter, the affinity of the adsorption sites [L × mg^{-1}]

q_m – the maximum adsorption capacity [mg × g^{-1}]

K_F – the Freundlich constant related to adsorption capacity [mol × g^{-1}]

$1/n$ – a constant revealing the adsorption process strength

R – the gas constant [J × (mol × K)$^{-1}$]

T – the temperature of the solution [K]

K_{DR}– the activity coefficient related to free adsorption energy [mol^2 × kJ^{-2}]

ϵ - the Polanyi potential [kJ × mol]

2.2.5. Sorption from real samples

The ability to remove S-metolachlor from the solution of real samples was tested. In a glass flask, 0.2 ± 0.003 g of dry polymers and 20 mL of 30 mg × L^{-1} S-metolachlor tap water solution were shaken at room temperature for 24 h. After reaching equilibrium, the samples were filtrated by syringe filter Acrodisc 0.45 μm, and the concentration of S-metolachlor in the solution was determined using the HPLC technique. The sorption capacity was calculated based on Eq. (1).

2.2.6. Binding site selectivity

The binding selectivity of MIP and NIP sorbent was examined by placing approximately 0.2 g dry polymers in the glass flask and adding 20 mL of 0.05 mmol × L^{-1} solution consisting of three herbicides: atrazine, fenoxaprop-P-ethyl, and S-metolachlor. The samples were

Table 1
Mathematical linear and non-linear equations of the adsorption isotherm models [17,18].

Isotherm name	Linear form of isotherm	Non-linear form of isotherm
Langmuir	$\frac{1}{q_e} = \frac{1}{q_m K_L C_e} + \frac{1}{q_m}$	$q_e = \frac{q_m K_L C_e}{1 + K_L C_e}$
Freundlich	$lnq_e = lnK_F + \frac{1}{n} lnC_e$	$q_e = K_F C_e^{1/n}$
Dubinin-Radushkevich	$lnq_e = lnq_m - K_{DR}\epsilon^2$	$Q_e = q_m exp\left[RTln\left(1+\frac{1}{C_e}\right)\right]^2$

Table 2
Summary of MIPs synthesis conditions at room temperature.

Name	Solvent	Monomers	The molar ratio of template to monomers	Template
MIP-1	H_2O/EtOH (1.75:1)	NIPAM/MAA/ acrylic acid	1:55	Solution of template in EtOH
MIP-2	H_2O/EtOH (1.5:1)	11:12:1		
MIP-3	H_2O/EtOH (1.2:1)			
MIP-4	H_2O/EtOH (1:1)			
MIP-5	H_2O			
MIP-6	H_2O/ MeOH (1:1)			Solution of template in MeOH
MIP-7	H_2O			Pure S-metolachlor
MIP-8			1:39	Aqueous solution of template
MIP-9	H_2O/EtOH (1:1)		1:51	Solution of template in EtOH
MIP-10	H_2O/EtOH (0.8:1)		1:36	
MIP-11	H_2O/EtOH (6.3:1)	NIPAM/AA/ acrylic	1:70	Solution of template in EtOH
MIP-12	H_2O/EtOH (1:1)	acid11:14:1		
MIP-13				
MIP-14			1:20	
MIP-15			1:33	
MIP-16			1:36	
MIP-17			1:77	
MIP-18		11:11:1	1:12	
MIP-19	H_2O/EtOH (2:1)	11:14:1	1:255	
MIP-20			1:124	
MIP-21			1:77	
MIP-22			1:51	
MIP-23			1:38	
MIP-24			1:26	
MIP-25			1:19	
MIP-26	H_2O/EtOH (1.9:1)		1:70	
MIP-27	H_2O/EtOH (1.5:1)		1:124	
MIP-28			1:77	
MIP-29	H_2O/ MeOH (1:1)		1:55	Solution of template in MeOH
MIP-30	H_2O/ Acrylic	21:16:73	1:61	Pure S-metolachlor
MIP-31	acid (1:1)		1:36	
MIP-32	H_2O	11:14:1	1:39	Aqueous solution of
MIP-33			1:78	template

clappered for 24 h at 22 ± 2 °C and filtered by syringe filter Acrodisc 0.45 μm afterward. The S-metolachlor concentration at an equilibrium state was determined on the HPLC apparatus.

The distribution coefficient (K_{SMCh}) was calculated as a ratio of the amount of S-metolachlor absorbed on 1 g of polymer and the amount of S-metolachlor in equilibrium in 1 mL of solution as follow (Eq. (2))

$$K_{SMCh} = \frac{q_{SMCh} \times \rho}{C_e} \quad (2)$$

where ρ is the density of the S-metolachlor solution [$g \times L^{-1}$].

The imprinting factor (IF) value shows a particular analyte's distribution ratio of the imprinted polymer and non-imprinted polymer under exactly the same set of conditions [19]. IF (Eq. (3)) was calculated as [20].

$$IF = \frac{K_i^{MIP}}{K_i^{NIP}} \quad (3)$$

where $K_{i(j)}$ is distribution coefficient (i, j = S-MCh, ATR, FEN) of herbicide on imprinted polymer (K^{MIP}) and non-imprinted polymer (K^{NIP}). Specific selectivity factor (S) defined as (Eq. (4)) ratio of IFs of two different substances (IF_i, IF_j) was estimate as

$$S = \frac{IF_i}{IF_j} \quad (4)$$

2.2.7. Water regain

The weight of water absorbed by 1 g of dry polymer is known as water regain (*W*) [g $H_2O \times g^{-1}$ of sorbent], and was measured by centrifugation method and calculated as (Eq. (5))

$$W = \frac{(m_w - m_d)}{m_d} \quad (5)$$

where m_w – mass of wet polymer after centrifugation [g], m_d – mass of polymer after drying at 100 °C through the night [g] [21].

3. Result and discussion

3.1. Preparation of S-metolachlor molecularly imprinted polymers

Currently, available papers reported MIPs toward S-metolachlor [22–24], however, none of them described MIPs synthesized in an aqueous environment and at room temperature. The polymerization conditions such as monomers, solvent, and the molar ratio of reagents were optimized according to miscellaneous concepts. The best composition of a pair of materials (MIP-32 and appropriate NIP sorbent) was selected by the sorption capacity represented in Table 4, calculated from Eq. (1). The highest sorption capacity was obtained for MIP synthesized with the use of NIPAM, AA, and acrylic acid as functional monomers, BIS as a cross-linker agent, and APS and TEMED as a catalyst system. The molar ratio of functional monomers to cross-linker is 7:2, while the molar ratio of functional monomers to template molecule is 39:1. The biggest challenge was the relatively low solubility of S-metolachlor in water, approximately 0.5 $g \times L^{-1}$ [7], which is sufficient for spraying in agriculture. In contrast, the desire to obtain a concentrated aqueous solution of this herbicide, allowing for a relatively high percentage of template in the reaction mixture, poses a challenge to the synthetic engineer.

Similar polymer syntheses, but using a high-temperature, and K_2SO_4 or AIBN (for MIP-43 and MIP-44) as an initiator, were also carried out to compare the sorption capacities of the obtained sorbents. The reaction conditions for polymer synthesis at 60 °C are presented in Table 3.

Almost all reactions performed at 60 °C did not produce satisfactory results. Only in the case of the reaction MIP-41, an amount of polymer was obtained that enabled the sorption process to be carried out. However, the sorption properties was unsatisfactory because 1 g of MIP

Table 3
Summary of MIPs synthesis conditions at 60 °C.

	Solvent	Monomers	The molar ratio of template to monomers	Template
MIP-34	H_2O/EtOH (6.3:1)	NIPAM/MAA/ acrylic acid 11:12:1	1:70	Solution of template in EtOH
MIP-35				
MIP-36				
MIP-37	H_2O/EtOH (3:1)			
MIP-38	H_2O/EtOH (1:1)			
MIP-39				
MIP-40				
MIP-41	H_2O/EtOH (1:1)	NIPAM/AA/ acrylic acid 11:14:1	1:70	Solution of template in EtOH
MIP-42	H_2O/MeOH (1:1)		1:55	Solution of template in MeOH
MIP-43	Chloroform		1:70	Pure S-metolachlor
MIP-44	n-octane			

absorbed 0.931 ± 0.263 mg of S-metolachlor, while 1 g of NIP absorbed 1.352 ± 0.070 mg of this herbicide.

As the result of the first attempts to carry out the sorption process, the best pair of polymers (MIP-32 and appropriate NIP-22) was selected. This pair of materials MIP-32 and NIP-22 synthesized in an aqueous environment and ambient temperature sorbed S-metolachlor was much better than those synthesized at 60 °C, with a result of 2.415 ± 0.038 mg of herbicide by MIP and 0.463 ± 0.281 mg by NIP. More than 5 times better sorption of the molecularly imprinted polymer (MIP-32) determined the further characterization of this composition, including sorption isotherms, selectivity, FT-IR and SEM analyses, absorbency, and bed regeneration.

3.1.1. Sorption isotherms

More detailed sorption properties tests were performed for the selected pair of sorbents MIP-32 and NIP-22. In the first step, the adsorption isotherms were studied, which are presented in Fig. 1. To study the adsorption mechanisms of MIP-32 and NIP-22, the data obtained were fit to the Langmuir, Freundlich, and Dubinin–Radushkevich isotherms models.

3.1.2. Langmuir isotherms

The Langmuir isotherms model assumes that a monolayer of molecules is formed on the surface of the adsorbent. Moreover, a fixed number of adsorption sites are available on the surface of the adsorbent, and all binding sites are identical and interact with the same energy. Fig. 2 shows the non-linear fitting of the Langmuir isotherm for a selected pair of sorbents, while Fig. 3 shows the linear fit. The values of the estimated parameters and the R^2 coefficient for both types of isotherm fits are summarized in Table 5.

3.1.3. Freundlich isotherms

The Freundlich isotherms model is based on monolayer heterogeneous adsorption of adsorbate on the surface of the adsorbent without any interaction between adsorbed ions [25]. To determine the fit to the Freundlich adsorption models non-linear (Fig. 4) and linear (Fig. 5) regression analysis was performed. The values of the estimated parameters and the R^2 coefficient for both types of isotherm fits are presented in Table 6.

Table 4
Sorption capacity of metolachlor with MIP.

Name	Amount of S-Metolachlor absorbed on MIP (mg × g^{-1})	Amount of S-Metolachlor absorbed on NIP (mg × g^{-1})
MIP-3/ NIP-3	0.89 ± 0.37	1.21 ± 0.08
MIP-5/ NIP-5	1.59 ± 0.27	3.58 ± 0.36
MIP-8/ NIP-8	1.40 ± 0.03	1.43 ± 0.25
MIP-9/ NIP-9	1.28 ± 0.26	1.52 ± 0.03
MIP-10/ NIP-10	1.57 ± 0.87	1.95 ± 0.17
MIP-11/ NIP-11	3.61 ± 0.53	3.98 ± 0.04
MIP-12/ NIP-12	2.43 ± 0.43	2.02 ± 0.11
MIP-13/ NIP-13	0.07 ± 0.09	0.33 ± 0.09
MIP-14/ NIP-14	3.31 ± 0.42	3.20 ± 0.26
MIP-15/ NIP-14	2.32 ± 0.37	3.20 ± 0.26
MIP-16/ NIP-15	0.63 ± 0.07	0.43 ± 0.06
MIP-17/ NIP-15	0.59 ± 0.01	0.43 ± 0.06
MIP-18/ NIP-16	3.36 ± 0.64	4.53 ± 0.35
MIP-19/ NIP-17	1.31 ± 0.56	0.39 ± 0.04
MIP-20/ NIP-17	1.55 ± 0.16	0.39 ± 0.04
MIP-21/ NIP-17	0.81 ± 0.22	0.39 ± 0.04
MIP-22/ NIP-17	0.68 ± 0.03	0.39 ± 0.04
MIP-23/ NIP-17	1.14 ± 0.06	0.39 ± 0.04
MIP-24/ NIP-17	2.20 ± 1.28	0.39 ± 0.04
MIP-25/ NIP-17	1.16 ± 0.59	0.39 ± 0.04
MIP-27/ NIP-18	1.04 ± 0.18	1.99 ± 0.81
MIP-28/ NIP-18	1.34 ± 0.07	1.99 ± 0.81
MIP-29/ NIP-19	0.76 ± 0.05	0.59 ± 0.03
MIP-30/ NIP-20	2.29 ± 0.54	3.37 ± 0.64
MIP-31/ NIP-21	3.96 ± 0.07	3.61 ± 0.20
MIP-32/ NIP-22	**2.42 ± 0.04**	**0.46 ± 0.03**
MIP-33/ NIP-23	0.61 ± 0.32	0.58 ± 0.10

3.1.4. Dubinin – Radushkevich isotherms

The Dubinin-Radushkevich isotherms examine the interactions between the adsorbate and the sorbent and help distinguish mechanisms of chemisorption and physisorption [26]. The resultant data were fitted to the Dubinin-Radushkevich isotherm model using non-linear regression, as shown in Fig. 6, as well as linear regression (Fig. 7). The values of the estimated parameters and the R^2 coefficient for both types of isotherm fits are presented in Table 7.

Comparing the obtained isotherms and determined parameters, it is concluded that in the Langmuir isotherm for MIP in non-linear regression the maximum sorption is almost 9 mg × g^{-1}, while for linear regression three times lower. However, the R^2 values are higher for linear form (0.97) than for non-linear (0.94), as well as the affinity of the adsorption sites. Despite the good fit of the R^2 coefficient in both non-linear and linear models for NIP, the values of q_m and K_L are unlikely.

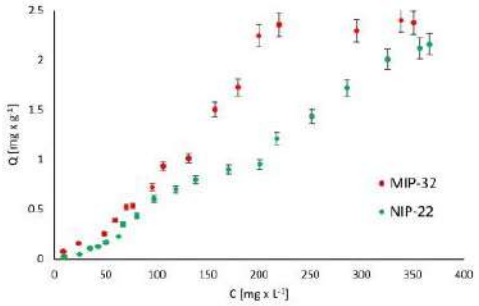

Fig. 1. Adsorption isotherms of MIP-32 (red) and NIP-22 (green).

For Freundlich isotherm in both non-linear and linear models Freundlich constant related to the binding affinity is significantly higher for MIP (0.016 and 0.007 for non-linear and linear models, respectively) than for NIP (0.003 and 0.001 for non-linear and linear models, respectively), even though the R^2 coefficient is higher for NIP (0.99 and 0.98 for non-linear and linear form, respectively) than for MIP (0.93 and 0.97 for non-linear and linear form, respectively). The heterogeneity index ranges from 0 to 1, where 1 indicates homogeneity and zero indicates heterogeneity of the adsorption sites [27]. This value for NIPs is higher than for MIPs, which confirms more heterogeneous properties of the molecularly imprinted polymer surfaces.

In the Dubinin-Radushkevich model, the values of theoretical maximum capacity are lower for linear regression than for non-linear. Furthermore, the q_m values for MIP are much lower than in the Langmuir model. The R^2 values in this fit are the lowest, especially for the linear form of the equation.

These diverse results show the complexity of the isotherm matching problem resulting from the heterogeneous surface of polymers. MIP sorption probably occurs according to both the Langmuir and Freundlich isotherms. However, in the case of NIP, the best-fitting model is the Freundlich isotherm.

3.1.5. Competitive binding

To demonstrate the presence of specific cavities on the MIP surface compatible with S-metolachlor, sorption was carried out in a solution containing other plant protection agents, exhibiting competitive binding. The tests were carried out by sorption of MIP and NIP polymers with a 0.05 M solution of a mixture of S-metolachlor, atrazine, Fenoxinn, and Halvetic. Fenoxinn is a herbicide containing fenoxaprop-P-ethyl, while Halvetic comprehends glyphosate as an active ingredient. The results (Table 8) presented a significantly lower imprinting factor (*IF*) for other chemicals than for S-metolachlor (2.6). Furthermore, the selectivity coefficients (*S*) for these substances are high, which means that the received MIP absorbed S-metolachlor 3 times better than atrazine, 6 times better than glyphosate, and 6 times better than fenoxaprop-P-ethyl. The presented data confirm the specific binding of S-metolachlor by the MIP molecule, caused by the presence of an imprint of this

Table 5
Parameter estimates for the Langmuir Isotherm.

Model		R^2	q_m [mg × g^{-1}]	K_L [L × mg^{-1}]
Non-linear form of Langmuir	MIP-32	0.940	8.9437	0.0012
	NIP-22	0.985	51706.8772	1.1190×10^{-7}
Linear form of Langmuir	MIP-32	0.968	3.1477	0.0029
	NIP-22	0.975	−0.7713	−0.0033

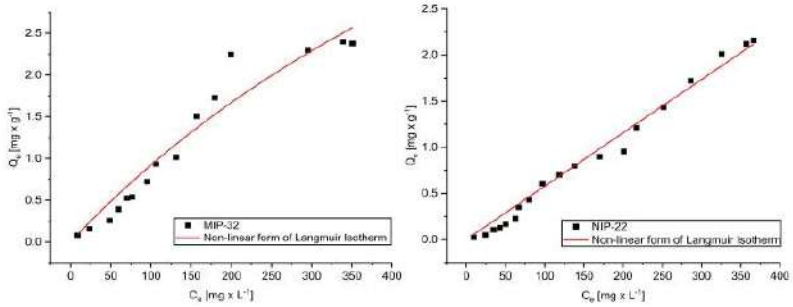

Fig. 2. The non-linear form of Langmuir isotherm for MIP-32 and NIP-22.

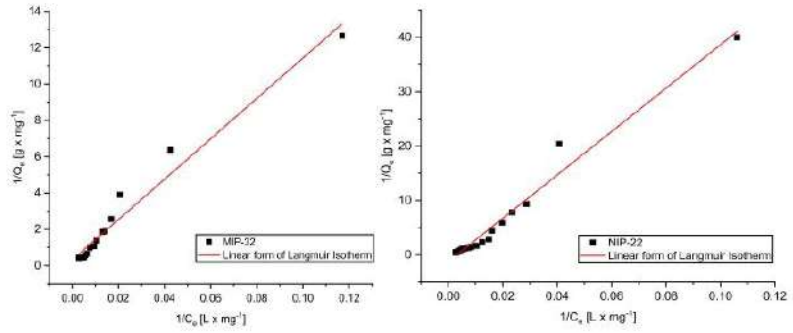

Fig. 3. The linear form of Langmuir isotherm for MIP-32 and NIP-22.

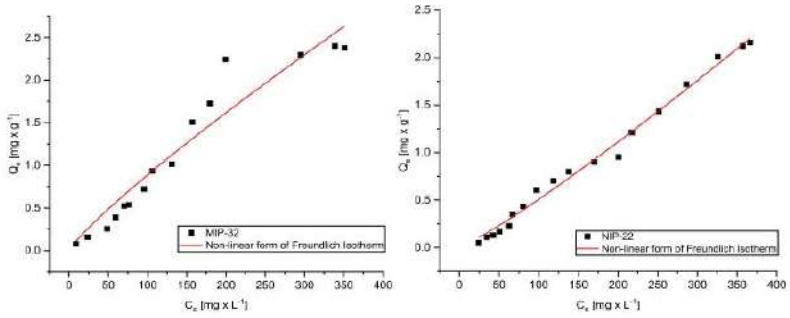

Fig. 4. The non-linear form of Freundlich isotherm for MIP-32 and NIP-22.

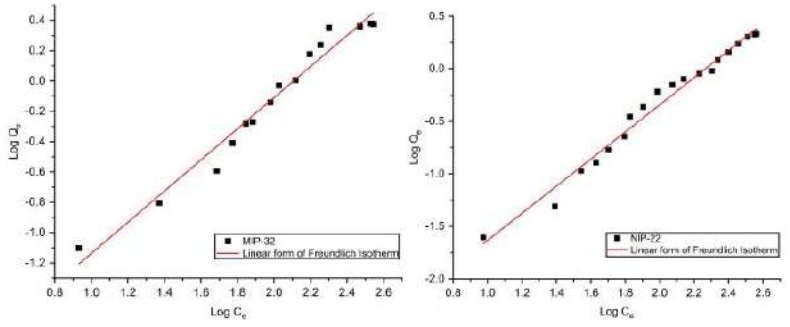

Fig. 5. The linear form of Freundlich isotherm for MIP-32 and NIP-22.

Table 6
Parameter estimates for the Freundlich Isotherm.

Model		R^2	K_F [mol × g^{-1}]	1/n
Non-linear form of Freundlich	MIP-32	0.929	0.0164	0.8662
	NIP-22	0.990	0.0026	1.1312
Linear form of Freundlich	MIP-32	0.968	0.0068	1.0278
	NIP-22	0.981	0.0012	1.2900

herbicide on the surface of the sorbent. At the same time, weak binding of the remaining compounds by MIP is observed, indicating the lack of specific interactions.

3.1.6. Application in real samples

The optimized synthesis conditions were used to check the sorption capacity in real samples prepared as a tap water solution of S-metolachlor (Table 9). The sorption process was carried out in the same manner as sorption on the model solution, however, did not initially produce the expected results. The value of S-metolachlor absorbed by 1 g of MIP was 0.566 ± 0.332 mg, while by 1 g of NIP it was 0.371 ± 0.001 mg. Therefore, an investigation of the influence of pH on the adsorption process was conducted. The pH of the solution was reduced to 5 using 0.1 M hydrochloric acid to obtain parameters similar to the PH value of deionized water. The amount of S-metolachlor bound to the MIP and NIP polymers was 2.614 ± 0.354 and 0.629 ± 0.213 mg of herbicide per gram of sorbent, respectively. The binding of S-metolachlor by MIP was more than 4 times better than that by NIP. This confirms the presence of cavities in the MIP structure that specifically bind to the imprinted analyte. For MIP and NIP, these values are 0.2 mg higher, than the sorption value for the model solution, which may be due to the complex matrix present in tap water.

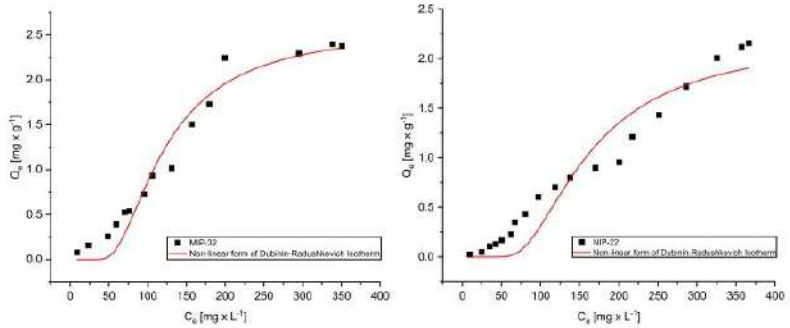

Fig. 6. The non-linear form of Dubinin-Radishkevich isotherm for MIP-32 and NIP-22.

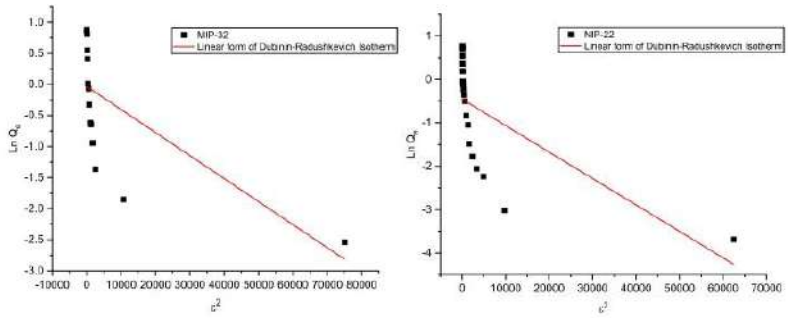

Fig. 7. The linear form of Dubinin-Radushkevich isotherm for MIP-32 and NIP-22.

Table 7
Parameter estimates for the Dubinin-Radushkevich Isotherm.

Model		R^2	q_m [mg × g^{-1}]	K_{DR} [mol^2 × kJ^{-2}]
Non-linear form of Dubinin-Radushkevich	MIP-32	0.954	2.5751	−11030.1556
	NIP-22	0.907	2.2085	−19744.6610
Linear form of Dubinin-Radushkevich	MIP-32	0.449	0.9676	0.0330
	NIP-22	0.431	0.6346	0.4548

Table 8
Competitive study.

Parameter	S-Metolachlor	Atrazine	Glyphosate	Fenoxaprop-P-ethyl
K_{MIP}	51.40 ± 4.58	16.63 ± 2.38	26.35 ± 2.72	14.10 ± 1.45
K_{NIP}	19.76 ± 4.40	17.48 ± 3.50	34.02 ± 2.02	12.22 ± 0.10
IF	2.63 ± 0.36	0.98 ± 0.24	0.89 ± 0.09	1.29 ± 0.31
S	–	3.2 ± 0.4	6.0 ± 0.8	6.2 ± 0.1

Table 9
Comparison of S-metolachlor sorption values from real and model solutions.

	MIP-32	NIP-22
Sorption from the real solution (pH 7) [mg × g^{-1}]	0.57 ± 0.33	0.37 ± 0.01
Sorption from the real solution (pH 5) [mg × g^{-1}]	2.61 ± 0.35	0.63 ± 0.21
Sorption from the model solution [mg × g^{-1}]	2.42 ± 0.04	0.46 ± 0.28

3.1.7. FT-IR analysis

The FT-IR spectra of the molecularly imprinted polymer toward S-metolachlor and non-imprinted polymer were performed to compare the structure of the sorbents. Analyzing both spectra Fig. 8, the peaks of MIP were nearly identical to the peaks from NIP. The presence of the N–H bending bond at 1650 cm^{-1} and 3470 cm^{-1}, as well as the C–N stretching bond at 1040 cm^{-1}, present in monomers, can be noticed. Both spectra have a peak at 1715 cm^{-1}, 2360 cm^{-1}, and 1140 cm^{-1} which showed the C=O stretching bond of the amide group and C–O–C stretching bound from the cross linker, respectively. The CH_3 bending bond was detected at 1460 cm^{-1}. At 2850 cm^{-1} as well as 1920 cm^{-1} C–H bonds are observed, while at 3550-3800 $^{-1}$ O–H stretching bonds are present. The information provided above proves that the chemical composition of the polymers is identical, however despite the similar structure, the sorption properties of this materials studied. Which may also confirm the existence of these specific S-metolachlor binding sites in the MIP structure.

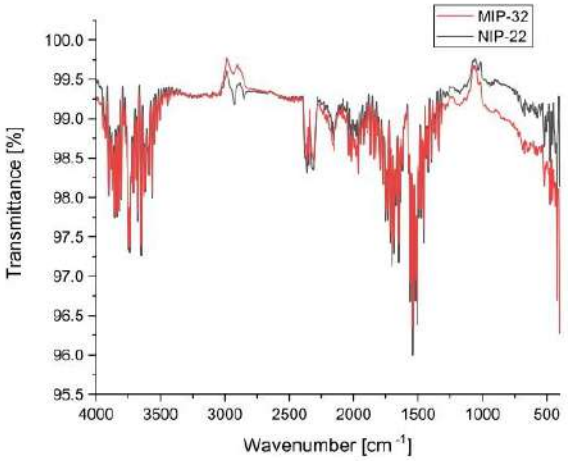

Fig. 8. The FT-IR spectra of selected MIP and NIP.

3.1.8. SEM analysis

The synthesized MIP and NIP sorbents were characterized by SEM analysis of the polymer matrix. SEM images are presented in Fig. 9 and show that the surface morphology of MIP is more porous than that of NIP, which could also explain the difference in S-metolachlor binding. From the SEM micrographs, it can be seen that the polymers have irregular surfaces and shapes.

3.1.9. Water regain

Determining the amount of adsorbed water was one of the tests regarding the material characterization, including swelling and mass changes. These values for both MIP and NIP materials were similar. Water regain by 1 g of NIP was calculated as 6.14 g, while by 1 g of MIP as 6.25 g. These values for both tested materials are similar, so it can also be emphasized here that this property does not affect the sorption properties and differs in the efficiency of SMCh removing from aqueous solutions, which probably also confirms the formation of these specific binding sites in the MIP structure.

4. Conclusions

In this work, the first molecularly imprinted polymer for S-metolachlor determination was prepared based on *green chemistry* principles. Various synthetic strategies as well as the compositions and molar ratios

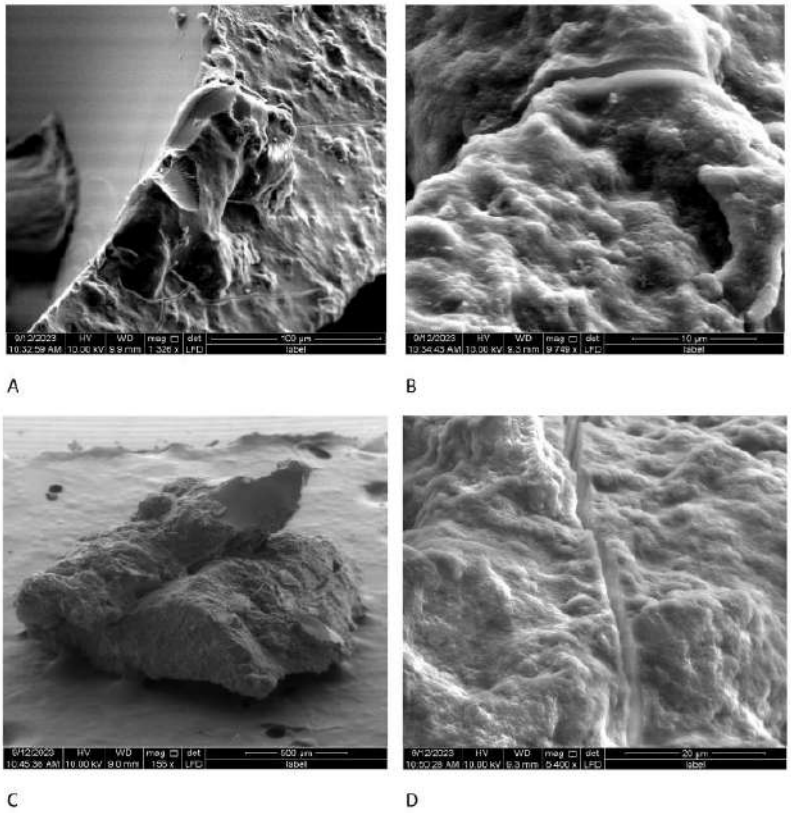

Fig. 9. The SEM images of selected MIP-32 (A, B) and NIP-22 (C, D) particles.

of the reaction mixture were tested. The highest sorption capacity and the difference between S-metolachlor sorption by MIP-32 and NIP-22 materials were obtained by polymerizing NIPAM, AA, acrylic acid, and BIS in an aqueous herbicide solution, synthesized at room temperature. The selectivity of the obtained sorbent is extremely high for S-metolachlor, while it is significantly lower for other plant protection products. One of the values that determine selectivity is the imprinting factor, which for S-metolachlor is 2.6, while for atrazine it is equal to 1, for fenoxaprop-P-ethyl it is 1.3 and for glyphosate it is 0.9.

Ethical Approval

Not applicable.

Consent to participate

All authors provided informed consent to participate in the study.

Consent to Publish

The authors have consented to the submission of the research to the journal.

Funding

The authors wish to acknowledge the financial support of the National Science Centre Poland project Sonata Bis11, 2021/42/E/ST5/00019 (02NB/0002/22).

We would also like to thank Dr. Juliusz Winiarski, prof. of WUST, for taking the SEM pictures.

CRediT authorship contribution statement

Dominika Rapacz: Writing – original draft, Validation, Methodology, Investigation, Formal analysis, Data curation. **Katarzyna Smolińska-Kempisty:** Writing – review & editing, Visualization, Supervision, Investigation, Funding acquisition, Conceptualization. **Joanna Wolska:** Writing – review & editing, Supervision, Conceptualization.

Declaration of competing interest

The authors declare the following financial interests/personal relationships which may be considered as potential competing interests:

Katarzyna Smolinska-Kempisty reports financial support was provided by National Science Centre Poland. Katarzyna Smolinska-Kempisty, Dominika Rapacz, Joanna Wolska has patent #P.447229 pending to Licensee. If there are other authors, they declare that they have no known competing financial interests or personal relationships that could have appeared to influence the work reported in this paper.

Data availability

Data will be made available on request.

References

[1] [USDA-NASS] U.S. Department of Agriculture, National agricultural statistics service, https://www.nass.usda.gov/index.php, 2022. (Accessed 11 August 2023).

[2] [USDA- IPAD] U.S. Department of Agriculture, Foreign agricultural statistics service, https://ipad.fas.usda.gov, 2022. (Accessed 11 August 2023).
[3] Trading economics. https://tradingeconomics.com/poland, 2023. (Accessed 11 August 2023).
[4] T.S. Silva, N.J. Arneson, R.P. DeWerff, D.V. Silva, D.H. Smith, R. Werle, Preemergence herbicide premixes reduce the risk of soil residual weed control failure in corn, Weed Technol. (2023), https://doi.org/10.1017/wet.2023.45.
[5] V. Feigenbrugel, S. Le Calvé, C. Loew, P. Mirabel, Near-UV molar absorptivities of acetone, alachlor, metolachlor, diazinon and dichlorvos in aqueous solution, J. Photochem. Photobiol. A. 174 (2005) 76–81, https://doi.org/10.1016/j.jphotochem.2005.03.014.
[6] A. Munoz, L. Cox, W.C. Koskinen, M.J. Sadowsky, Biodegradation and mineralization of metolachlor and alachlor by Candida xestobii, J. Agric. Food Chem. 59 (2011) 619–627, https://doi.org/10.1021/jf103508w.
[7] International Labour Organization (ILO) and World Health Organization, IC SC: 1360. https://www.ilo.org/dyn/icsc/showcard.display?p_version=2&p_card_id=1360, 2000. (Accessed 17 October 2023).
[8] World Health Organization, Guidelines for Drinking-Water Quality, second ed. Vol.2, Health criteria and other supporting information, Geneva, 1996.
[9] A. Abou-Shady, O. Abd-Elmottaleb, M.E.A. Ali, D. Eissa, H. El-Araby, A. El-Harairy, A.L.S. Elwa, A.A.M. Habib, R.H. Hegab, G.A.Z. Ibrahim, S. Ismail, Y.H. Kotp, M. A. Osman, A.M. Saudi, E.M.M. Selim, M.A. Tag-Elden, R. Yaseen, T.M.H. Yossif, Comprehensive review of progress made in soil electrokinetic research during 1993–2020, Part I: process design modifications with brief summaries of main output, S. Afr. J. Chem. Eng. 44 (2023) 156–256, https://doi.org/10.1016/j.sajce.2023.01.008.
[10] S.Y. Lee, S.J. Park, TiO_2 photocatalyst for water treatment applications, J. Ind. Eng. Chem. 19 (6) (2013) 1761–1769, https://doi.org/10.1016/j.jiec.2013.07.012.
[11] Diasa JM, Almeidaa MF, Alvim-Ferraza MCM, Rivera-Utrillab J. Manuel Sanchez-Polo (2007) Waste materials for activated carbon preparation and its use in aqueous-phase treatment: A Review. J. Environ. Manage. 85, 833-846. https://doi.org/10.1016/j.jenvman.2007.07.031.
[12] I.A. Saleh, M.A. Al-Ghouti, N. Zouari, Removal of pesticides from water and wastewater: chemical, physical and biological treatment approaches, Environ. Technol. Innov. 19 (2020) 101026, https://doi.org/10.1016/j.eti.2020.101026.
[13] R. Bakkour, J. Bolotin, T.B. Hofstetter, B. Sellergren, Molecularly-imprinted polymers for compound-specific isotope analysis of polar organic micropollutants in aquatic environments, Anal. Chem. 90 (12) (2018) 7292–7301, https://doi.org/10.1021/acs.analchem.8b00493.
[14] E.K. Reville, S.J. Benware, E.B. Berda, S.S. Negi, E.H. Sylvester, Customizable molecular recognition: advancements in design, synthesis, and application of molecularly imprinted polymers, Polym. Chem. 13 (2022) 3387–3411, https://doi.org/10.1039/D1PY01472B.
[15] P. Regal, R. Barreiro, A. Cepeda, M. Díaz-Bao, C. Fente, Application of molecularly imprinted polymers in food analysis: clean-up and chromatographic improvements, Cent. Eur. J. Chem. 10 (3) (2012) 766–784, https://doi.org/10.2478/s11532-012-0016-3.
[16] J. Wolska, P. Cyganowski, M. Kujawska, pH-responsive molecularly imprinted polymer for sorption and rapid desorption of dibutyl phthalate, Sep. Sci. Technol. 53 (7) (2018) 1076–1087, https://doi.org/10.1080/01496395.2017.1310235.
[17] K.V. Kumar, S. Sivanesan, Comparison of linear and non-linear method in estimating the sorption isotherm parameters for safranin onto activated carbon, J. Hazard Mater. 123 (1–3) (2005) 288–292. https://doi:10.1016/j.jhazmat.2005.03.040.
[18] O.I. Parisi, R. Malivindi, M. Ruffo, L. Scrivano, A. Vassallo, Smart bandage based on molecularly imprinted polymers (MIPs) for diclofenac controlled release, Pharmaceuticals 11 (4) (2018) 92, https://doi.org/10.3390/ph11040092.
[19] R.J. Ansell, Characterization of the binding properties of molecularly imprinted polymers, in: Bo Mattiasson, Lei Ye (Eds.), Molecularly Imprinted Polymers in Biotechnology. Advances in Biochemical Engineering/Biotechnology, vol. 150, Springer, 2015, pp. 51–93, https://doi.org/10.1007/10_2015_316.
[20] J. Wolska, P. Cyganowski, M. Kujawska, Selective sorption of diethyl phthalate on pH-responsive, molecularly imprinted polymeric adsorbents, Sep. Sci. Technol. 55 (12) (2020) 2137–2148, https://doi.org/10.1080/01496395.2019.1620778.
[21] M. Kujawska, A.W. Trochimczuk, Molecularly imprinted polymeric adsorbent for β-blockers removal synthesized using functionalized MSU-F silica as a sacrificial template, Sep. Sci. Technol. 51 (15–16) (2016) 2565–2575, https://doi.org/10.1080/01496395.2016.1200090.
[22] X. Hu, Y. Cao, C. Guo, T. Ye, Y. Yu, Novel liquid-liquid-solid microextraction method with molecularly imprinted polymer-coated stainless steel fiber for aqueous sample pretreatment, J. Chromatogr. A. 1218 (25) (2011) 3935–3939, https://doi.org/10.1016/j.chroma.2011.04.069.
[23] Y. Wang, X. Guo, X. Jin, R. Li, D. Zhao, Molecularly imprinted solid-phase extraction coupled with gas chromatography for the determination of four chloroacetamide herbicides in soil, Anal. Methods 7 (15) (2015) 6411–6418, https://doi.org/10.1039/c5ay00281h.
[24] X. Hu, G. Dai, H. Fan, J. Huang, Y. Liang, T. Ye, T. Youwen, Y. Yu, Molecularly imprinted polymer coated on stainless steel fiber for solid-phase microextraction of chloroacetanilide herbicides in soybean and corn, J. Chromatogr. A. 1217 (38) (2010) 5875–5882, https://doi.org/10.1016/j.chroma.2010.07.011.
[25] J. Wolska, N.J. Falizi, Membrane emulsification process as a method for obtaining molecularly imprinted polymers, Polymers 13 (16) (2021) 2830, https://doi.org/10.3390/polym13162830.
[26] T.A. Saleh, Chapter 4 - isotherm models of adsorption processes on adsorbents and nanoadsorbents in surface science of adsorbents and nanoadsorbents, Interface Sci. Technol. 34 (2022) 99–126, https://doi.org/10.1016/B978-0-12-849876-7.00009-9.
[27] Y. Zhao, H. Fan, Z. Feng, Y. Hu, S. Li, Y. Lu, X. Zhai, Preparation of magnetic molecularly imprinted polymers for selective recognition and determination of clenbuterol in pork samples, J. Chem. (2020) 8820262, https://doi.org/10.1155/2020/8820262.

7.3. Optymalizacja warunków działania kolumn SPE ze złożem składającym się z blokowych polimerów wrażliwych na zmiany temperatury (Publikacja P3)

Rapacz D, Smolińska–Kempisty K, Wolska J. Preparation and characterization of SPE column with smart green molecularly imprinted polymers materials for selective determination of S–metolachlor herbicide. *Scientific Reports*. 2025, vol. 15, art. 3153, s. 1-10. https://doi.org/10.1038/s41598-025-87685-2.

Wprowadzenie

Trzeci artykuł zatytuowany "**Preparation and characterization of SPE column with smart green molecularly imprinted polymers materials for selective determination of S–metolachlor herbicide**" opublikowany w *Scientific Reports* skupia się na zastosowaniu wcześniej zsyntezowanych polimerów wdrukowanych molekularnie (**P2**) jako selektywnego złoża w kolumnach typu SPE. W poprzedniej pracy (**P2**) proces sorpcji był prowadzony w trybie statycznym przez 24 godziny. Niniejsza publikacja natomiast, opisuje nie tylko sorpcję prowadzoną w trybie dynamicznym, pozwalającą na skrócenie czasu inkubacji ograniczającego się do przepłynięcia roztworu przez złoże, ale również przedstawia właściwości tak zwanych „*inteligentnych*" polimerów, wrażliwych na zmianę temperatury i cechujących się właściwościami samoregenerującymi.

Wyniki

W publikacji opisana została optymalizacja warunków sorpcji oraz desorpcji w trybie dynamicznym, uwzględniająca dobór odpowiedniego modelu pracy w kolumnach, czas inkubacji oraz temperaturę desorpcji. Przetestowano kolumny naczyń wyrównanych, kolumny typu SPE z polietylenowymi frytami oraz kolumny typu SPE z filtrem złożonym z bibuły filtracyjnej oraz waty. Proces sorpcji na kolumnach naczyń wyrównanych przebiegał do momentu przebicia złoża. Z kolei podczas drugiego eksperymentu, przeprowadzonego na tym samym, wcześniej oczyszczonym materiale, zaobserwowano niemal dwukrotnie większą wartość sorpcji w porównaniu do pierwszego etapu. Jednocześnie wyniki tego procesu wykazały brak powtarzalności. Ponadto długi czas penetracji roztworu oraz eluentu przez złoże oraz częste zatykanie się złoża, a także zużywanie dużej ilości eluentu przyczyniły się do poszukiwania lepszego rozwiązania.

W kolejnym kroku testowano kolumny typu SPE z frytami polietylenowymi. Obecność spieków PE uniemożliwiała swobodny przepływ roztworu przez złoże, wymuszając zastosowanie próżni, w celu przepchnięcia cieczy przez kolumnę, co znacząco skróciło czas sorpcji i desorpcji w trybie dynamicznym, w porównaniu z poprzednim modelem kolumny. Pomimo powtarzalności wyników, skróconego czasu zachodzącego procesu oraz dużego stopnia regeneracji złoża, metoda ta okazała się niezadowalająca, ponieważ pod wpływem podciśnienia generowanego przez próżnię, drobne kawałki polimeru blokowego wnikały w pory fryt, zatykając je i blokując dalszy przepływ.

Najlepsze rezultaty uzyskano dla kolumn typu SPE z wykorzystaniem filtra składającego się z warstwy bibuły, waty oraz kolejnej warstwy bibuły. Takie rozwiązanie

przyniosło pożądany efekt, umożliwiając przeprowadzenie procesu sorpcji i desorpcji bez blokowania się złoża, w krótkim czasie oraz z wykorzystaniem małej objętości eluentu. Ponadto zoptymalizowanie warunków sorpcji pozwoliło na uzyskanie niemal dwukrotnie większej wartości sorpcji dla MIPu niż dla NIPu, odpowiednio 0,91 mg × g^{-1} i 0,52 mg × g^{-1}. Proces sorpcji przeprowadzono również dla próbek przygotowanych na bazie wody z kranu, symulujących warunki rzeczywiste. Uzyskane wyniki wykazały zbliżoną wartość sorpcji dla MIPu, równą 0,85 mg × g^{-1}. Z kolei wartość sorpcji dla NIPu była większa w porównaniu z roztworem modelowym i wynosiła 0,71 mg × g^{-1}.

Przeprowadzono również optymalizację warunków desorpcji w kolumnach SPE. Ponieważ PNIPAM jest polimerem wrażliwym na zmianę temperatury, proces desorpcji był prowadzony w trzech temperaturach: 4, 22 i 50°C. Zgodnie z teorią LCST, w temperaturze 4°C proces desorpcji zachodził najefektywniej, a współczynnik regeneracji wynosił 66% (po przeprowadzeniu jednego cyklu procesu desorpcji), podczas gdy w temperaturze 22°C był równy 55%, a w 50°C osiągnął wartość 46%. Samoregeneracja tych sorbentów umożliwiła nie tylko określenie stężenia S–metolachloru w próbce badanej wody, ale również ich ponowne wykorzystanie.

Po opracowaniu warunków sorpcji oraz regeneracji złoża przetestowano, ile razy ten sam materiał może być ponownie wykorzystany. Złoże zachowało swoje właściwości przy przeprowadzeniu trzech cykli sorpcja–desorpcja. Taki rezultat jest zgodny z założeniami koncepcji „*zielonych*" polimerów wdrukowanych molekularnie. Ograniczenie ilości generowanych odpadów oraz wielokrotne wykorzystanie sorbentów świadczy o ich potencjale do realizacji zasad zrównoważonego rozwoju.

Ponadto przeprowadzono analizę kinetyki sorpcji, dopasowując otrzymane wyniki do odpowiednich modeli. Na podstawie obliczeń stwierdzono, że zarówno w przypadku MIPu, jak i NIPu, najlepsze dopasowanie uzyskano dla modelu kinetyki pseudo–drugiego rzędu. Wartości współczynnika determinacji wynosiły odpowiednio 0,992 dla MIPu i 0,981 dla NIPu. Dodatkowo ustalono, że proces sorpcji zachodzący na NIPie jest kontrolowany przez dyfuzję do powierzchni polimeru, podczas gdy w przypadku MIPu etapem ograniczającym szybkość sorpcji jest dyfuzja w głąb struktury sorbentu.

Podsumowanie

Zastosowanie polimerów wdrukowanych molekularnie jako złóż w kolumnach typu SPE, oraz optymalizacja warunków sorpcji i regeneracji złoża, umożliwiły stworzenie szybkiej metody detekcji oraz oznaczania stężenia S–metolachloru w próbkach wody. Pojemność sorpcyjna kolumny MIP–SPE była prawie dwukrotnie większa niż kolumny z układem referencyjnym, co potwierdza specyficzne interakcje pomiędzy polimerem a S–metolachlorem. Badania wykazały, że proces desorpcji, który jednocześnie pełni funkcję samoregeneracji kolumny, przebiega najefektywniej w temperaturze 4°C. Ponadto materiały te wpisują się również w założenia tak zwanych „*zielonych*" polimerów wdrukowanych molekularnie, ponieważ możliwe jest przeprowadzenie cyklu sorpcji–desorpcji nawet trzykrotnie, z zachowaniem średniego współczynnika regeneracji na poziomie 98%, ograniczając jednocześnie ilość generowanych odpadów.

scientific reports

OPEN

Preparation and characterization of SPE column with *smart green* molecularly imprinted polymers materials for selective determination of S-metolachlor herbicide

Dominika Rapacz✉, Katarzyna Smolińska-Kempisty & Joanna Wolska

The presence of traces of herbicides in ground and surface waters can have adverse impacts on humans and the environment. Therefore, developing a highly selective and reusable adsorbent for monitoring water quality has become important. This article describes smart *green* molecularly imprinted polymers (MIPs) as selective sorbents of S-metolachlor herbicide for solid phase extraction (SPE). Combining the MIP-SPE column with HPLC chromatography provided a quick and accurate method for determining the real concentration of S-metolachlor in water samples. The sorption capacity of the MIP-SPE column was almost twice that of the non-imprinted polymer column for SPE extraction. The bed can be regenerated up to three times before it loses its original sorption properties. A method has been developed whereby 6 ml of water can achieve an average recovery rate of 98% for sorbent. During the selectivity study from multicomponent solution, the calculate imprinting factor for MIPs was calculated to be 10, while MIPs sorb S-metolachlor 10 times better than atrazine, 12 times better than fenoxaprop-P-ethyl and 33 times better than glyphosate. The pseudo-second-order kinetic model was in good agreement with the experimental values obtained.

Keywords S-metolachlor, Solid phase extraction, *Green* molecularly imprinted polymers, Sorption, Desorption

Maize, wheat, and rice are the three main cereal crops grown on Earth, providing more than 40% of the world's caloric needs. Approximately 197 million hectares of corn are cultivated annually, and half of the world's maize production is accounted for in the Americas[1]. Agrochemicals, including fertilizers, herbicides, pesticides, insecticides, and plant-growth hormones, are widely used in agriculture to increase production efficiency to meet the needs of a steadily growing global population[2]. S-metolachlor is one of the most persistent soil-applied herbicides belonging to the chloroacetanilide group, used for the pre-emergence control of small-seeded broad-leafed weeds and annual grasses, among others, in maize, cotton, and soybean crops[3]. It is relatively well soluble in water and is weakly sorbed to soil particles, giving it the potential to permeate into groundwater[4].

The sustainable use of agrochemicals is important not only for boosting crop yield but also for human well-being and health, as well as the protection of water resources from farm pollution[5]. In addition to contamination from plant protection products, ground, surface, and drinking waters can contain micropollutants with heavy metals, medications and pharmaceuticals, dyes, drugs, and the endocrine disrupting system. The micropollutants present in water often occur at deficient concentrations, from ng × L^{-1} to µg × L^{-1}, which means that many traditional analytical methods are not sensitive enough to detect and remove these contaminants[6]. Widespread analytical tools used to determine micropollutants are liquid-chromatography coupled to mass spectrometry (LC-MS), gas chromatography linked to mass spectrometry (GC-MS)[7], and capillary electrophoresis[8]. The detection of S-metolachlor using molecularly imprinted polymers in samples containing micropollutants is

Department of Process Engineering and Technology of Polymer and Carbon Materials, Wroclaw University of Science and Technology, Wybrzeże Wyspiańskiego 27, Wrocław 50-370, Poland. ✉email: dominika.rapacz@pwr.edu.pl

typically conducted through the use of HPLC or GC. The precise parameters associated with this methodology are further delineated in the review[9].

Enrichment and pre-concentration methods used in preparing samples for analysis are crucial in determining the trace concentration, especially for complex environmental samples, regardless of the type of contaminant or sample matrix. Solid phase extraction is an extensively used clean-up, isolation, and concentration technique because of its ease of use, cost, and low solvent consumption[10]. The types of SPE sorbents include, among others, normal, reversed, and ionic phases, however, unsatisfactory selectivity caused by co-elutes with interfering compounds excludes their use in effective and reliable analyses. Molecularly imprinted polymers (MIPs) have proven to be a good selective SPE substrate due to their specific ability to recognize the target analyte molecule. Moreover, MIPs are stable, relatively inexpensive, easy to synthesize, and have potential affinity for a wide range of interest analyte molecules. The application of *green chemistry* principles has become increasingly popular in the field of molecular imprinting to improve the performance of MIPs by reducing their negative impacts. The design of *green* MIPs poses a significant challenge to researchers, primarily due to the lack of solubility of the majority of monomers in water[9,11]. The greenification list of principles encompasses the selective implementation of environmentally friendly materials and reagents in waste disposal[11,12].

Smart polymers are a class of functional materials that are able to respond to environmental stimuli such as temperature, pH, or light. Poly(N-isopropylacrylamide) (PNIPAM) is known to exhibit thermosensitive properties according to the theory of the lower critical solution temperature (LCST). PNIPAM has both hydrophilic amide groups and hydrophobic isopropyl groups in its molecule. At low temperatures, there is a strong hydrogen bond between the amide groups and water molecules, causing PNIPAM to swell. When the temperature rises above 32 °C the hydrogen bond between the amide group and the water molecules is broken, the isopropyl group takes over, and PNIPAM shrinks[13].

The present work presents a combination of solid phase extraction columns whose bed consists of smart molecularly imprinted polymers, and high-performance liquid chromatography as an analytical tool for detecting S-metolachlor herbicide from water samples. This study is subjected to human and environmental risk chemicals occurring in micro quantities, demonstrating the possibility of determining the real concentration of S-metolachlor in the *chemical cocktail* mixture. The composition of molecularly imprinted polymers synthesized according to the principles of *green chemistry*, published in our recent work[14], combined with the SPE technique, underlines the innovation of the research presented while focusing considerable attention on minimizing environmental risks. The greenification principles used in this work include self-cleaning MIPs, aqueous media as worthy porogen and solvent, generate minimal waste, controlling polymerization without energy waste, eliminate template through use of green solvent, as well as increase operator safety.

Materials and methods

Reagents and chemicals

Acrylamide (AA) was purchased from Thermo Scientific Chemicals. Acros Organics provided acrylic acid (AAc). Ammonium persulfate (APS), N-isopropylacrylamide (NIPAM), N,N′-methylenebis (acrylamide) (BIS), and N, N,N′,N′-tetramethylethylenediamine (TEMED) were supplied by Sigma-Aldrich. S-metolachlor (SMCh) was obtained from NOVAGRA. The HPLC grade acetonitrile was purchased from CHEMSOLUTE. Ultrapure water was obtained with a Milli-Q System (Merck Millipore).

Preparation of the polymers

The synthesis of MIP for S-metolachlor has been published in our previous work[13]. In brief, NIPAM (3.52 mmol), AA (4.64 mmol), and AAc (0.32 mmol) were placed in the vessel as functional monomers, BIS (2.34 mmol) as a cross-liner, and 10 mL of water solution of S-metolachlor (0.27 mmol) as a template molecule. Once dissolved, the mixture was purged with nitrogen for 1 min, and 1 mL of an aqueous solution of APS (0.13 mmol) and TEMED (0.10 mmol) was added to the polymerization mixture and blown with nitrogen for 2 min again. The polymerization reaction was carried out for 24 h on a shaker at room temperature. The bulk polymers were extracted for 24 h in Soxhlet using ethanol and dried at 60 °C. Non-imprinted polymers (NIPs) were synthesized similarly but without template molecules.

Sorption process

The adsorption capacity q (mg × g^{-1}), calculated according to the following Eq. (1), is defined as the amount of S-Metolachlor adsorbed at the equilibrium[15].

$$q = \frac{(C_i - C_{eq}) \times V}{m} \tag{1}$$

where C_i (mg × L^{-1})—initial concentration of S-metolachlor, C_{eq} (mg × L^{-1})—equilibrium concentration of S-metolachlor, V (L)—volume of the solution, m (g)—mass of the polymer.

Regeneration of sorbents

The HPLC apparatus determined the concentration of eluted herbicide. The regeneration factor (RF) was calculated following Eq. (2).

$$RF = \frac{M_e}{M_a} \times 100\% \tag{2}$$

where M_e (mg)—mass of eluted S-metolachlor, M_a (mg)– mass of absorbed S-metolachlor.

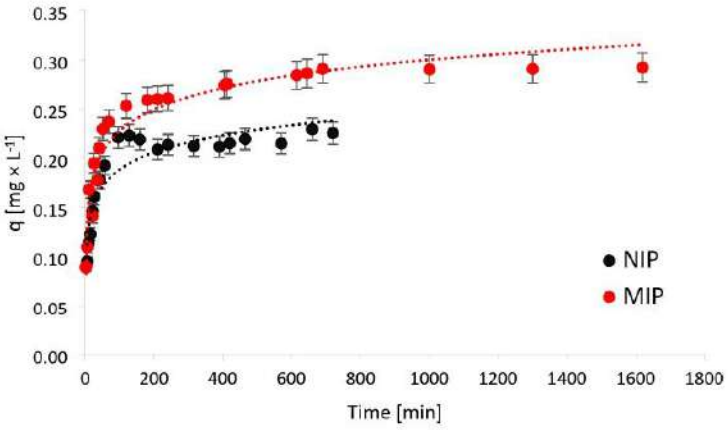

Fig. 1. Sorption kinetics for NIP and MIP.

	Film diffusion		Particle diffusion	
	k_a ($1 \times min^{-1}$)	R^2	k_b ($1 \times min^{-1}$)	R^2
NIP	0.032	**0.979**	0.028	0.967
MIP	0.002	0.276	0.012	**0.905**

Table 1. Parameters obtained from the calculation of the sorption kinetics according to *Fick's law*. Significant values are in bold.

Porosity of sorbents

Pore volume and surface area were obtained by examining nitrogen adsorption at the liquid nitrogen temperature using Micromeritics ASAP 2020 Plus version 2.0 analyzer. Prior to analysis samples (about 0.5 g) were degassed at 40 °C for 24 h. Dose of nitrogen was set to 3 $cm^3 g^{-1}$, free space of the analyzing tube was measured before performing the analysis. Resultant data were subjected to Braunauer–Emmet–Teller (BET) treatment.

High-performance liquid chromatography

Analyses were performed on the high-performance liquid chromatograph Shimadzu SCL-40 equipped with an autosampler (model SIL-40), PDA pump, and an ARION® Biphenyl chromatographic column (3 µm, 150 × 4.6 mm). The analysis was performed in isocratic elution using a mixture of water and acetonitrile (1:1, v:v) as a mobile phase. The temperature was kept to 30 °C, the injection volume was set at 30 µL, and the flow rate was maintained at 1 mL × min^{-1}. The wavelength has been fixed at 254 nm.

Result and discussion

Kinetics of adsorption

The characterization of the physicochemical properties of the polymers, such as scanning electron microscopy and Fourier transform infrared spectroscopy, was described in our a previous work[14]. In brief, the spectrum indicates the presence of an N–H bending bond at 1650 cm^{-1} and 3470 cm^{-1}, as well as a C–N stretching bond at 1040 cm^{-1}, which are characteristic of the monomers. Both spectra exhibited a peak at 1715 cm^{-1}, 2360 cm^{-1}, and 1140 cm^{-1}, which indicated the C–O stretching bond of the amide group and C–O–C stretching bond from the cross-linker, respectively. The CH_3 bending bond was identified at a wavelength of 1460 cm^{-1}. At 2850 cm^{-1} as well as 1920 cm^{-1}, C–H bonds are observed, while at 3550–3800 cm^{-1}, O–H stretching bonds are present. Additionally, the supplementary material contains SEM images. To completely characterize the sorption properties of these polymers sorption kinetic studies were conducted. The adsorption kinetics was investigated with 250 mL of S-metolachlor concentration of 30 mg × L^{-1} and sorbent mass of 2.5 g at room temperature. The concentration of samples taken at different time intervals was determined using the HPLC apparatus. The experimental data obtained from the sorption kinetics process are presented in Fig. 1.

To investigate the mechanism controlling sorption, the collected data were fitted to several kinetic models. *Fick's second law* models were first adapted to the experimental data to determine whether film diffusion or particle diffusion was the controlling process (Table 1). Equation (3) considers film diffusion as the rate-limiting step[16]. The sorption rate constant k_a was determined from a plot of $-ln(1 - \frac{q_t}{q_{eq}})$ versus time.

	NIP	MIP
k_{WM1} (mg × g^{-1} × min$^{0.5}$)	0.017	0.018
k_{WM2} (mg × g^{-1} × min$^{0.5}$)	0.038	0.063
k_{WM3} (mg × g^{-1} × min$^{0.5}$)	**0.014**	**0.011**

Table 2. Parameters from the Weber-Morris model calculation. Significant values are in bold.

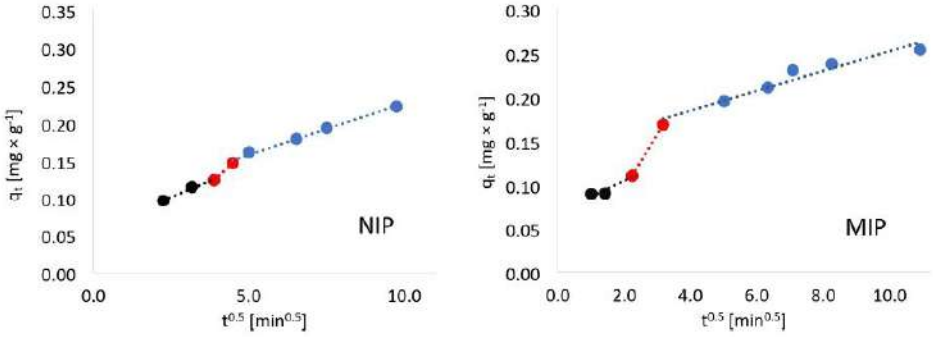

Fig. 2. Interparticle diffusion model of S-metolachlor adsorption on NIP and MIP.

$$k_a t = -ln\left(1 - \frac{q_t}{q_{eq}}\right) \tag{3}$$

where k_a (1 × min^{-1})—the pseudo-first-order rate constant, q_t and q_{eq} (mg × g^{-1})—the amount of adsorbate adsorbed at time t and at the equilibrium time, respectively.

Approximate expression for particle diffusion-controlled adsorption is given by Eq. (4)[16]. The sorption rate constant k_b was calculated from a plot of $-\ln(1 - \left(\frac{q_t}{q_{eq}}\right)^2)$ versus time.

$$k_b t = -\ln\left(1 - \left(\frac{q_t}{q_{eq}}\right)^2\right) \tag{4}$$

where k_b (1 × min^{-1})—the pseudo-second-order rate constant, q_t and q_{eq}(mg × g^{-1})—the amount of adsorbate adsorbed at time t and at the equilibrium time, respectively.

Analysis of the R^2 coefficients indicates which type of diffusion is in control of the process. For NIP, film diffusion is the dominant process, but the difference between the R^2 ratios for the two types of diffusion is negligible. However, for MIP there is a significant difference between the values of the R^2 coefficient, and particle diffusion controls the process more. A comparison of the data of the rate constants k_a and k_b is used to determine which process is faster. These values are very close for NIP, but the particle diffusion process occurs more quickly for MIP.

The limiting stage of the S-metolachlor adsorption process was also estimated using the Weber-Morris model of intraparticle diffusion (Eq. 5; Table 2), which assumes that in many adsorption circumstances, the solute uptake is approximately proportional to $t^{0.5}$ rather than to the contact time. The interparticle diffusion rate constant was calculated from a plot of q_t versus $t^{0.5}$, which should be a straight line if the intraparticle diffusion is the rate-limiting step[17]

$$q_t = k_{WM} t^{0.5} + B \tag{5}$$

where k_{WM}(mg × g^{-1} × min$^{0.5}$)—interparticle diffusion rate constant, q_t (mg × g^{-1})—the amount of adsorbate adsorbed at time t, B (mg × g^{-1})—boundary layer thickness.

However, when analyzing the plots shown in Fig. 2, it is noticeable that there are broken lines rather than straight lines. This is attributable to the fact that various processes are involved in the adsorption process, and not just intraparticle diffusion. Furthermore, none of the curves passes through the origin of the coordinate system, which also confirms that intramolecular diffusion is not the only controlling step. Adsorption on the outer surface of the adsorbent grain, or the immediate adsorption phase, is represented by the first steep section.

The second section is equivalent to a gradual, gentle adsorption step in which the process that controls the rate of the overall adsorption process is intraparticle diffusion[18].

The collected data were fitted to commonly used pseudo-first and pseudo-second-order kinetic models to better understand the mechanisms of sorption kinetics (Table 3). The pseudo-first-order model relies on the assumption that the sorption rate is directly proportional to the difference between the saturation concentration and the amount of solid uptake with time[19]. The linear form of the pseudo-first-order model is presented in following Eq. (6). From the $log\ (q_{eq} - q_t)$ versus time plot, the rate constant k_1 was calculated[20].

$$\log (q_{eq} - q_t) = \log (q_{eq}) - \frac{k_1 t}{2.303} \tag{6}$$

where k_1 ($1 \times \text{min}^{-1}$)—sorption rate constant, q_{eq} and q_t ($\text{mg} \times \text{g}^{-1}$)—the amount of adsorbate adsorbed at equilibrium time and at time t, respectively.

In the pseudo-second-order model, the process is under the control of the chemical sorption reaction at the liquid-solid interface in the adsorbent and predicts the behavior over the entire adsorption range. The linear form of the pseudo-second-order model is described in terms of Eq. (7). The rate constant k_2 was determined from the plot of $\frac{t}{q_t}$ versus time[20].

$$\frac{t}{q_t} = \frac{1}{k_2 q_{eq}^2} + \frac{1}{q_{eq}} t \tag{7}$$

where: k_2 ($\text{g} \times (\text{mg} \times \text{min})^{-1}$)—sorption rate constant, q_{eq} and q_t ($\text{mg} \times \text{g}^{-1}$)—the amount of adsorbate adsorbed at equilibrium time and at time t, respectively.

The absorption kinetics of S-metolachlor for both MIP and NIP can be described by a pseudo-second-order model based on higher values of the R^2 coefficients. Furthermore, the q_{max} values calculated according to the pseudo-second-order model are significantly closer to the sorption values from the performed experiment. The sorption rate constant k_2 is higher for the pseudo-second-order kinetics model than the rate constant k_1 for the pseudo-first-order model.

Optimization of the sorption conditions on SPE columns

Our previous work[14] described two types of molecularly imprinted polymers that exhibited outstanding sorption properties. Therefore, these materials were chosen for further studies. An investigation into the determination of S-metolachlor concentration using the MIP-SPE technique began with optimizing sorption conditions.

Sorption on the aligned vessel column

Initially, the sorption process was carried out on an aligned vessel column. About 0.13 ± 0.01 g of sorbent (MIP and NIP) was placed in a column equipped with wadding and the bed was activated by water. Then 30 $\text{mg} \times \text{L}^{-1}$ S-metolachlor aqueous solution was passed through the column until the bed was penetrated. After filtration through an Acrodisc 0.45 µm syringe filter, the concentration of S-metolachlor was measured by HPLC. The desorption process was carried out with water as an eluent solvent to determine the degree of bed regeneration. The sorption–desorption process on the same materials was repeated three times; the results are presented in Table 4.

To break through the bed of the column, 30 mL of S-metolachlor aqueous solution had to pass through the column for MIP sorbent and 20 mL for NIP sorbent. The desorption process was carried out until a minimum of 80% regeneration of the bed was achieved, with the eluent consumption ranging from 10 to 17 mL. The MIP-SPE column has a higher column capacity, possibly due to the specific binding sites resulting from the formation of imprints on the polymer matrix. This allows it to meet the measurement requirements of large-volume samples. However, this method also has disadvantages, including a long time for the solution and eluent to pass through the bed, driven only by the pressure generated by the liquid in the column of equalizing vessels. Moreover, frequent clogging of the bed and the consumption of large amounts of solvents contributed to the search for improved solutions.

Sorption on SPE column with PE frits

A 3 mL SPE column with a PE frit was loaded with approximately 0.09 ± 0.01 g of sorbent (MIP or NIP) and covered with a further PE frit. After activation of the MIP-SPE column with water, 30 $\text{mg} \times \text{L}^{-1}$ S-metolachlor aqueous solution was passed through the column until the bed was punctured and the concentration of the herbicide solution was determined over time using HPLC. To determine the degree of regeneration of the bed,

	Pseudo-first-order model			Pseudo-second-order model		
	k_1 ($1 \times \text{min}^{-1}$)	R^2	q_{max1} ($\text{mg} \times \text{g}^{-1}$)	k_2 ($\text{g} \times (\text{mg} \times \text{min})^{-1}$)	R^2	q_{max2} ($\text{mg} \times \text{g}^{-1}$)
NIP	0.032	0.979	0.016	0.413	**0.992**	0.226
MIP	0.004	0.874	0.017	0.458	**0.981**	0.263

Table 3. Parameters determined by calculating the sorption kinetics according to the pseudo-first and pseudo-second-order models. Significant values are in bold.

	MIP	NIP
Sorption I (mg × g^{-1})	0.71 ± 0.11	0.63 ± 0.05
Desorption I (mg × g^{-1})	0.71 ± 0.09	0.52 ± 0.07
RF (%)	100 ± 2	82 ± 4
Sorption II (mg × g^{-1})	1.33 ± 0.13	1.01 ± 0.08
Desorption II (mg × g^{-1})	1.18 ± 0.06	0.95 ± 0.04
RF (%)	89 ± 4	94 ± 3
Sorption III (mg × g^{-1})	1.31 ± 0.09	0.93 ± 0.07
Desorption III (mg × g^{-1})	1.23 ± 0.08	0.83 ± 0.05
RF (%)	94 ± 6	90 ± 2

Table 4. The results of the sorption–desorption process carried out on an aligned vessel column.

	MIP	NIP
Sorption I (mg × g^{-1})	1.15 ± 0.07	0.96 ± 0.02
Desorption I (mg × g^{-1})	1.04 ± 0.02	0.93 ± 0.01
RF (%)	91 ± 7	97 ± 3
Sorption II (mg × g^{-1})	0.98 ± 0.01	0.85 ± 0.03
Desorption II (mg × g^{-1})	0.97 ± 0.01	0.77 ± 0.04
RF (%)	99 ± 2	90 ± 2

Table 5. The results of the sorption–desorption process conducted on PE fritted SPE columns.

	MIP	NIP
Sorption (mg × g^{-1})	0.91 ± 0.28	0.52 ± 0.30
Desorption (mg × g^{-1})	0.88 ± 0.35	0.56 ± 0.25
RF (%)	98 ± 2	86 ± 1

Table 6. The results of the sorption–desorption process conducted on SPE columns with wadding.

the desorption process was carried out with water as the eluent. The sorption-desorption process was performed twice with the same materials. The data obtained are presented in Table 5.

The presence of PE frits in the SPE column prevented the solution from flowing freely through the bed, forcing the use of a vacuum to push the liquid through the column, significantly reducing the sorption and desorption time in the SPE columns compared to the previous system used. The MIP sorption results achieved are slightly lower than the previously discussed sorption on a column of aligned vessels; however, a smaller volume of S-metolachlor solution was required to penetrate the bed. Compared to the first described method, the volume of S-metolachlor solution was reduced from 30 to 18 mL in the first sorption process and to 12 mL in the second sorption process. The first NIP sorption was carried out using the same volume of S-metolachlor solution as in the case of sorption on the column of equalizing vessels, while in the second case, the volume was reduced to 12 mL. The desorption process, in turn, took place with a significant increase in the volume of the eluent – 34 mL for NIP and 31 mL for MIP in the first stage, and 16 and 15 mL for NIP and MIP respectively in the second stage. Despite the shorter analysis time and the high degree of bed regeneration, the sorption-desorption method on SPE columns with PE frits turned out to be unsatisfactory because the column bed consists of tiny pieces of the block polymer that, under the pressure generated by the vacuum, penetrate the pores of the frits, clogging them and blocking further penetration.

Sorption on SPE column with wadding and filter paper

To eliminate the effect of PE frits clogging, a layer of two filter papers, wadding, and another two filter papers were tested as a substitute for the standard frits. Approximately 0.08 ± 0.02 g of sorbent (MIP or NIP) was placed in a 3 mL SPE column equipped with a substitute for standard frit and the bed was activated with water. Then, 2 mL of S-metolachlor aqueous solution was dosed three times onto the column, regulating the liquid flow using the under pressure generated by the vacuum pump. The herbicide concentration was determined by high-performance liquid chromatography. The desorption process was carried out to determine the degree of bed regeneration. For this purpose, three portions of water, constituting the eluent, with a volume of 2 mL were passed through the column. The results of this are summarized in Table 6.

The use of wadding and filter paper had the desired effect, enabling the sorption-desorption process to take place without clogging. Moreover, the use of just 6 mL of the S-metolachlor solution resulted in MIP sorption values almost as high as those using 30 mL of the solution for sorption carried out on an aligned vessel column.

	MIP	NIP
RF 4 °C (%)	66 ± 12	92 ± 11
RF 22 °C (%)	55 ± 3	67 ± 2
RF 50 °C (%)	46 ± 9	76 ± 8

Table 7. The values of the desorption process conducted in various temperatures.

	MIP	NIP
Sorption I (mg × g^{-1})	0.50 ± 0.02	0.35 ± 0.06
RF (%)	93 ± 0	99 ± 1
Sorption II (mg × g^{-1})	0.51 ± 0.01	0.42 ± 0.02
RF (%)	98 ± 3	99 ± 1
Sorption III (mg × g^{-1})	0.53 ± 0.04	0.42 ± 0.03
RF (%)	98 ± 1	98 ± 1
Sorption IV (mg × g^{-1})	0.58 ± 0.17	0.43 ± 0.06
RF (%)	77 ± 1	100 ± 0

Table 8. The results of sorption-desorption process cycles performed on the MIP sorbent.

Furthermore, 6 mL of eluent was sufficient to regenerate almost 100% of the MIP bed and almost 90% of the NIP bed. The almost twofold difference between MIP and NIP sorption is evidence of the specific binding of template molecules by the molecularly imprinted polymer.

Due to the significantly reduced amount of solvents, in line with the *green chemistry* strategy, the shortened analysis time, and the evidence for the presence of particular cavities on the structure of MIP capable of binding of S-metolachlor molecules, the SPE column method using two layers of filter paper, cotton wool, and subsequent layers of filter paper was chosen as the most suitable method for carrying out sorption-desorption processes of S-metolachlor.

Desorption on SPE column in various temperatures

After optimizing the sorption and desorption conditions on SPE columns, the desorption process was carried out at various temperatures to confirm the thermosensitive properties of PNIPAM. The desorption of adsorbed S-metolachlor molecules was tested at three different temperatures: 4 °C, 22 °C (room temperature) and 50 °C for 75 min. The desorption process was carried out using 1 mL of water as eluent. The results of the research are presented in Table 7.

The above results confirm the change in the physicochemical properties of PNIPAM in response to a change in temperature. At lower temperatures, the polymer chain swells and becomes more flexible, due to the strong hydrogen bonds between the amide groups and water molecules. The release of adsorbed S-metolachlor molecules from the polymer structure is facilitated by the relaxation of the network and change of the polymer chain's conformation. Therefore, the temperature of 4 °C was selected as the optimal desorption temperature, in line with the LCST theory. At low temperatures, there is a strong hydrogen bond between the amide groups and water molecules, causing PNIPAM to swell. When the temperature rises above 32 °C the hydrogen bond between the amide group and water is broken, the isopropyl group takes over and PNIPAM shrinks.

Regeneration of the column bed

After optimizing the sorption and desorption conditions on the SPE columns, it was investigated how many cycles the column bed could be reused while maintaining the initial sorption parameters. Approximately 0.05 ± 0.01 g sorbent (MIP or NIP) was weighed into 3 mL SPE columns and the bed was activated by wetting with water. In the next step, 2 mL of S-metolachlor aqueous solution (C_e = 10 mg × L^{-1}) was added to the column and incubated for 3 h. In the next step, the adsorbed S-metolachlor particles were desorbed at 4 °C using water as eluent until at least 93% of the deposit was regenerated. The results are summarized in Table 8.

The column bed has been tested to be used as many as 3 times before it loses its sorption properties. By the fourth sorption–desorption cycle performed, the bed consist of MIP sorbent was blocked, preventing desorption above 80%.

Binding site selectivity

Once the conditions were optimized, the method was used for a selectivity analysis to assess the differences in the binding of the analyte between the MIP and NIP sorbents. Approximately 0.08 ± 0.02 g of sorbent (MIP or NIP) was introduced into a 3 mL SPE column and activated with water. The column was then treated with three 2 mL portions of a aqueous solution containing a mixture of plant protection products: atrazine (concentration 0.05 mmol × L^{-1}), S-metolachlor, glyphosate, and fenoxaprop-P-ethyl (concentration 0.1 mmol × L^{-1} for each), regulating the liquid flow using the underpressure generated by the vacuum pump. The concentration of the solution was determined by HPLC, and the chromatograms are provided in the supplementary information. The results are presented in Table 9.

Parameter	S-Metolachlor	Atrazine	Fenoxaprop-*P*-ethyl	Glyphosate
K_{MIP}	5.94	2.37	1.74	0.57
K_{NIP}	0.61	2.48	2.06	1.93
IF	9.7	1.0	0.8	0.3
S	–	10.1 ± 0.1	11.5 ± 0.2	33.0 ± 0.4

Table 9. The results of the competitive study.

	MIP	NIP
Sorption (mg × g^{-1})	0.85 ± 0.08	0.71 ± 0.07
RF (%)	100	100

Table 10. Results of the sorption-desorption process carried out on real samples.

The recognition selectivity is rated by the distribution coefficient ($K_{i(j)}$) demonstrating the difference between the concentration (i—S-metolachlor, j—other plant protection products) in solution before and after absorption, calculated according to the following Eq. (8)[21].

$$K_{i(j)} = \frac{(C_{i(j)} - C_{i(j)eq}) \times \rho}{C_{i(j)eq}} \tag{8}$$

Where: $C_{i(j)}$ (mg × L^{-1})—initial concentration (i—S-metolachlor, j—other plant protection products), $C_{i(j)eq}$ (mg × L^{-1})—equilibrium concentration (i—S-metolachlor, j—other plant protection products) ρ(g × L^{-1})—density of the solution.

The imprinting factor (IF) is the ratio of the distribution coefficients of imprinted polymer and the non-imprinted polymer was calculated with Eq. (9)[20]

$$IF = \frac{K_i^{MIP}}{K_i^{NIP}} \tag{9}$$

Where: $K_{i(j)}$—distribution coefficient (i—S-metolachlor, j—other plant protection products) of a substance on an imprinted polymer (K^{MIP}) and non-imprinted polymer (K^{NIP}).

The selectivity factor (S) was calculated using the following Eq. (10)[21]

$$S = \frac{IF_i}{IF_j} \tag{10}$$

where: IF_i—imprinting factor of the S-metolachlor, IF_j—imprinting factor of analogue molecules.

From the sorption data collected, the distribution coefficients were calculated for each of the compounds. The imprinting factor was used as a measure of MIP recognition characteristics. The *IF* for the synthesized MIP was calculated as 9.7, which is approximately 10 times higher than for atrazine, almost 12 times higher than for fenoxaprop-P-ethyl, and above 30 times higher than for glyphosate. The high selectivity values confirm the specific recognition properties of S-metolachlor by MIP due to specific cavities on the polymer matrix.

Sorption from real samples

After optimization of the conditions, the method has been applied to the analysis of real samples. The solution was prepared from tap water to which S-metolachlor was added and the pH of the solution was adjusted with HCl to the pH of distilled water. A more detailed description of the conditions for selecting the pH can be found in our previous work[14], and chromatograms are provided in the supplementary information. Approximately 0.05 ± 0.01 g of the sorbent was loaded into a 3 mL SPE column and activated with water. Then 2 mL portions of a tap water solution of S-metolachlor were passed through the column, adjusting the liquid flow by vacuum, and the concentration of herbicide was indicated using HPLC. The desorption of S-metolachlor was carried out with water as an eluent. The results are given in Table 10.

The results obtained (Table 9) show that there were no significant differences between the real and the experimental data and confirm the validity of the proposed polymer composition for the determination of S-metolachlor from real samples.

Porous structure analysis of obtained polymers

To complete the physicochemical characterization of the materials obtained which was started in our last paper[13], the porous structure analysis was performed. This analysis was also supposed to give us an indirect answer to the question that the unique sorption properties of MIP in relation to S-metolachlor were ensured by the imprints produced during polymerization in the polymer matrix. The measurement results with ASAP are presented in Table 11. The porous structure of the analyzed materials was characterized using nitrogen adsorption. The

Sample	BET surface ($m^2 \times g^{-1}$)	Pore volume ($cm^3 \times g^{-1}$)	Average pore size (nm)
NIP	0.15 ± 0.02	4.0×10^{-5}	3.3
MIP	0.19 ± 0.02	6.0×10^{-5}	3.3

Table 11. Characteristic of the selected pair of polymers.

values of the average pore volume and the specific surface area for the selected pair of MIP and NIP were also very similar. According to IUPAC, both polymers studied, characterized by average pore size in a range of 2 and 50 nm, can be classified as mesoporous materials[22]. It can be observed that the porosity value is very small; however, it was determined for a dry sample, and our material is a typical hydrogel with a high water capacity (after swelling, 1 g of NIP weighed 6.14 g, and 1 g of MIP weighed 6.25 g)[14], where the surface develops in an aqueous environment and provides access to potential sorption sites for S-metolachlor, hence such a relatively high sorption capacity despite the small active surface area.

Conclusions

The article describes the further characterization of the synthesized smart *green* molecularly imprinted polymers as selective sorbents for S-metolachlor herbicide in a solid phase extraction column. In connection with HPLC, this method can be used for the detection of traces of S-metolachlor in water samples. The extraction procedure was optimized using different columns, the best being an SPE column with a layer of two filter papers and wadding as a substitute for standard PE frits. Molecularly imprinted polymers have a high IF value for metolachlor (IF = 10), while for the other plant protection products the value does not exceed 1. The sorption capacity of the MIP-SPE column was almost twice that of the non-printed polymer column, confirming the specific interactions between the matrix and S-metolachlor. The desorption process was optimized at 4 °C, confirming the thermosensitive properties of NIPAM. MIPs have been tested to be recyclable up to three times, with an average regeneration factor of 98%. The MIP-SPE column is a good method for sample enrichment and preconcentration, characterized by speed, high selectivity, easier analysis, and no requirement for expensive instrumentation.

Data availability

The data will be available on the request. To obtain research data, please contact Dominika Rapacz; email: dominika.rapacz@pwr.edu.pl.

Received: 29 October 2024; Accepted: 21 January 2025
Published online: 24 January 2025

References

1. Erenstein, O., Jaleta, M., Sonder, K., Mottaleb, K. & Prasanna, B. M. Global maize production, consumption and trade: trends and R&D implications. *Food Secur.* **14**, 1295–1319. https://doi.org/10.1007/s12571-022-01288-7 (2022).
2. Mandal, A. et al. Chapter 7—Impact of agrochemicals on soil health. In *Agrochemicals Detection, Treatment and Remediation* (ed. Prasa, M. N. V.) 161–187, ISBN 9780081030172 (Butterworth-Heinemann, 2020). https://doi.org/10.1016/B978-0-08-103017-2.00007-6
3. de Avila, L. A. et al. Mineralization of S-metolachlor in soil as affected by moisture content, application history, and association with glyphosate. *Adv. Weed Sci.* **41**, e020230033. https://doi.org/10.51694/AdvWeedSci/2023;41:00014 (2023).
4. Sanyal, D. & Kulshrestha, G. Effects of repeated metolachlor applications on its persistence in field soil and degradation kinetics in mixed microbial cultures. *Biol. Fertil. Soils* **30**, 124–131. https://doi.org/10.1007/s003740050598 (1999).
5. Tanumihardjo, S. A. et al. Maize agro-food systems to ensure food and nutrition security in reference to the Sustainable Development Goals. *Global Food Secur.* **25**, 100327. https://doi.org/10.1016/j.gfs.2019.100327 (2020).
6. Metwally, M. G., Benhawy, A. H., Khalifa, R. M., El Nashar, R. M. & Trojanowicz, M. Application of molecularly imprinted polymers in the analysis of Waters and Wastewaters. *Molecules* **26**(21), 6515. https://doi.org/10.3390/molecules26216515 (2021).
7. Warner, W., Licha, T. & Nödler, K. Qualitative and quantitative use of micropollutants as source and process indicators. A review. *Sci. Total Environ.* **686**, 75–89. https://doi.org/10.1016/j.scitotenv.2019.05.385 (2019).
8. Carreras, H. Z. An introduction to Capillary Electrophoresis: theory, practice and applications. *Technol. Networks* (2023). https://www.technologynetworks.com/analysis/articles/an-introduction-to-capillary-electrophoresis-theory-practice-and-applications-378737
9. Rapacz, D., Smolińska-Kempisty, K. & Wolska, J. Molecularly imprinted polymers toward herbicides—progress in development and the current state of the art depending on the polymerization environment—short review. *J. Environ. Chem. Eng.* **12**, 112159. https://doi.org/10.1016/j.jece.2024.112159 (2024).
10. David, V., Galaon, T. & Bacalum, E. Sample enrichment by solid-phase extraction for reaching parts per quadrillion levels. *Environ. Anal. Chromatogr.* **82**, 1139–1150. https://doi.org/10.1007/s10337-019-03696-y (2019).
11. Arabi, M. et al. Molecular imprinting: green perspectives and strategies. *Adv. Mater.* **33**(30), 210054. https://doi.org/10.1002/adma.20210054 (2021).
12. Ostovan, A. et al. Greenificated molecularly imprinted materials for advanced applications. *Adv. Mater.* **34**(42), 2203154. https://doi.org/10.1002/adma.202203154 (2022).
13. He, W. et al. Application of poly(N-isopropylacrylamide) as thermosensitive smart materials. *J. Phys. Conf. Ser.* **1676**, 012063. https://doi.org/10.1088/1742-6596/1676/1/012063 (2020).
14. Rapacz, D., Smolińska-Kempisty, K. & Wolska, J. A novel green molecularly imprinted polymers synthesized in an aqueous medium as S-metolachlor sensitive materials. *Talanta*, 126674. https://doi.org/10.1016/j.talanta.2024.126674 (2024).
15. El-Bery, H. M., Saleh, M., El-Gendy, R. A., Saleh, M. R. & Thabet, S. M. High adsorption capacity of phenol and methylene blue using activated carbon derived from lignocellulosic agriculture wastes. *Sci. Rep.* **12**, 5499. https://doi.org/10.1038/s41598-022-09475-4 (2022).

16. Pilśniak-Rabiega, M. & Wolska, J. Removal of silver from chloride solutions using new polymer materials. *Physicochem. Probl. Mineral. Process.* **56**(9), 174357. https://doi.org/10.37190/ppmp/174357 (2023).
17. Jasani, N. et al. Theoretical, equilibrium, kinetics and thermodynamic investigations of methylene blue adsorption onto lignite coal. *Molecules* **27**(6), 1856. https://doi.org/10.3390/molecules27061856 (2022).
18. Ulatowska, J. Adsorption behaviour of as(III) onto synthetic iron-based minerals: a comparative study of akaganeite, goethite and magnetite. *Physicochem. Probl. Mineral. Process.* 58(2), 144818. https://doi.org/10.37190/ppmp/144818 (2022).
19. Sahoo, T. R. & Prelot, B. Chap. 7—Adsorption processes for the removal of contaminants from wastewater: the perspective role of nanomaterials and nanotechnology. In Micro and Nano Technologies, Nanomaterials for the Detection and Removal of Wastewater Pollutants (eds. Bonelli, B. et al.) 161–222 (Elsevier, 2020). https://doi.org/10.1016/B978-0-12-818489-9.00007-4
20. Revellame, E. D., Fortela, D. L., Sharp, W., Hernandez, R. & Zappi, M. E. Adsorption kinetic modeling using pseudo-first order and pseudo-second order rate laws: a review. *Clean. Eng. Technol.* **1**, 100032. https://doi.org/10.1016/j.clet.2020.100032 (2020).
21. Wolska, J., Kujawska, M. & Cyganowski, P. Selective sorption of diethyl phthalate on pH-responsive, molecularly imprinted polymeric adsorbents. *Sep. Sci. Technol.* 1–12. https://doi.org/10.1080/01496395.2019.1620778 (2019).
22. Rouquerol, J. et al. Recommendations for the characterization of porous solids (Technical Report). *Pure Appl. Chem.* **66**, 1739–1758. https://doi.org/10.1351/pac199466081739 (1994).

Acknowledgements
This research was funded in whole by National Science Centre Poland 2021/42/E/ST5/00019 (02NB/0002/22). For the purpose of Open Access, the author has applied a CC-BY public copyright licence to any Author Accepted Manuscript (AAM) version arising from this submission.

Author contributions
D.R. Conceptualization, Data curation, Formal analysis, Investigation, Methodology, Validation, Writing—original draft. K.S.K. Conceptualization, Funding acquisition, Investigation, Methodology, Project administration, Resources, Supervision, Visualization, Writing—review and editing. J.W. Conceptualization, Investigation, Methodology, Supervision, Validation, Visualization, Writing—review and editing.

Declarations

Competing interests
The authors declare no competing interests.

Additional information
Supplementary Information The online version contains supplementary material available at https://doi.org/10.1038/s41598-025-87685-2.

Correspondence and requests for materials should be addressed to D.R.

7.4. Dobór warunków syntezy blokowych polimerów molekularnie wdrukowywanych reagujących na zmiany pH oraz ich zastosowanie jako selektywnych sorbentów w kolumnach SPE (Publikacja P4)

Rapacz D, Smolińska–Kempisty K, Wolska J. Detection of S–metolachlor herbicide in water samples using new molecularly imprinted polymer for solid–phase extraction. *Journal of Water Process Engineering*. 2025, vol. 75, art. 107980, s. 1-10. https://doi.org/10.1016/j.jwpe.2025.107980.

Wprowadzenie

Kolejny artykuł pod tytułem "**Detection of S–metolachlor herbicide in water samples using new molecularly imprinted polymer for solid–phase extraction"** opublikowany w *Journal of Water Process Engineering*, po raz pierwszy opisuje pH–czułe blokowe polimery molekularnie wdrukowane selektywne wobec S–metolachloru, zsyntezowane zgodnie z założeniami „*zielonej chemii*". Publikacja jest wprowadzeniem do drugiego rodzaju, tak zwanych, „*inteligentnych*" sorbentów – wrażliwych na zmianę pH. Jednym z powszechnie znanych polimerów wykazujących odpowiedź na zmianę pH jest hydrofilowy poli(kwas akrylowy). Obecność grup karboksylowych w łańcuchach polimeru jest odpowiedzialna za jego wrażliwość na pH, powodując odwracalne przejście konformacyjne, zachodzące pod wpływem jonizacji grupy karboksylowej, z kształtu bardziej zbliżonego do kłębka polimerowego, do rozluźnionej formy.

Wyniki

Badania rozpoczęto od doboru składu oraz warunków syntezy pH–czułych polimerów wdrukowanych molekularnie, a na podstawie przeprowadzonych procesów sorpcji wyselekcjonowano najbardziej optymalny skład. Najkorzystniejsze wyniki sorpcji uzyskano wykorzystując jako monomery funkcyjne kwas akrylowy i akryloamid (odpowiednio 5,76 i 6,96 mmol), N,N'–metylenobis(akrylamid) (4,93 mmol) jako środek sieciujący, S–metolachlor jako szablon, natomiast woda stanowiła porofor. Inicjatorem reakcji był nadsiarczan amonu oraz N,N,N′,N′–tetrametyloetylenodiamina (dodawane w ilości odpowiednio 0,20 i 0,30 mmol). Reakcja była prowadzona w temperaturze otoczenia. W odróżnieniu od syntezy polimerów blokowych wrażliwych na temperaturę, przeprowadzonej na wytrząsarce, niniejszy proces polimeryzacji przebiegał z zastosowaniem mieszadła mechanicznego. To rozwiązanie umożliwiło ciągłe mieszanie oraz zapewniło większą jednorodność sorbentów. Wartość przeprowadzonej sorpcji dla MIPu wynosiła 0,260 ± 0,121 mg × g^{-1}, a dla NIPu była równa 0,166 ± 0,002 mg × g^{-1}.

Ponieważ otrzymany sorbent jest pH–czuły, proces sorpcji wykonano w różnych pH, wynoszących: 2,5; 4,5; 6,5; 8,5 oraz 10,5. Na podstawie przeprowadzonych badań stwierdzono, iż, największe wartości sorpcji uzyskano w pH równym 4,5 i 6,5. Jest to potwierdzeniem zachodzącego zjawiska transformacji sieci PAAc.

Aby w pełni scharakteryzować proces sorpcji przeprowadzono również badania kinetyki oraz izoterm sorpcji. Najlepsze dopasowanie uzyskano dla modelu kinetyki pseudo–drugiego rzędu, zarówno dla MIPu (R^2=0,998), jak i dla NIPu (R^2=0,999). Ponadto oszacowane wartości sorpcji (0,173 i 0,107 mg × g^{-1} odpowiednio dla MIP i NIP) są zbliżone do wartości eksperymentalnych. Informacje dotyczące mechanizmu procesu adsorpcji mogą być dostarczone poprzez zbadanie izoterm sorpcji. Otrzymane wyniki zostały dopasowane do modeli izoterm Langmuira, Freundlicha, Dubinin– Radushkevicha i Scatcharda. Przy czym model Scatcharda stanowił najlepsze dopasowanie do danych eksperymentalnych.

Sorbenty następnie upakowano w kolumnach typu SPE w celu przeprowadzenia procesu sorpcji w trybie dynamicznym. Badania rozpoczęto od optymalizacji czasu inkubacji sorbentu z roztworem S–metolachloru, obejmującego zakres od 15 minut do 5 godzin. Najlepsze wyniki – niemal dwukrotnie większą wartość sorpcji dla MIPu niż dla NIPu uzyskano po czterech godzinach kontaktowania. W kolejnym kroku zoptymalizowano warunki desorpcji. Na podstawie doniesień literaturowych oraz wcześniejszych badań, jako eluent wybrano wodę o pH wynoszącym około 9,2, a optymalny czas inkubacji ustalono na 15 minut. Dodatkowo przeanalizowano wpływ temperatury na przebieg procesu desorpcji. Zaobserwowano, że wymywanie przebiegało najskuteczniej w temperaturze pokojowej, gdzie osiągnięto 75% desorpcji, podczas gdy w temperaturze 4°C uzyskano 71% wymycia. Takie warunki umożliwiły uproszczenie całego procesu. Po zoptymalizowaniu parametrów, sprawdzono, ile razy proces sorpcji–desorpcji może być przeprowadzony na tym samym materiale. Wykazano, że właściwości sorbentów oraz powtarzalność wyników utrzymują się podczas wykonaniu dwóch cykli sorpcji–desorpcji.

Polimery przetestowano również na próbkach symulujących warunki rzeczywiste, przeprowadzając proces sorpcji zarówno w trybie dynamicznym, jak i statycznym. W obu przypadkach zaobserwowano, że wartości sorpcji S–metolachloru przez MIP z próbek rzeczywistych (0,65 mg × g^{-1} w trybie statycznym i 0,5 mg × g^{-1} w trybie dynamicznym), były nieco mniejsze w porównaniu do wartości uzyskanych dla roztworu modelowego (odpowiednio 0,75 mg × g^{-1} i 0,73 mg × g^{-1}). Takie wyniki mogą być związane z obecnością większej ilości jonów w roztworze rzeczywistym. Mimo to, wartości sorpcji pozostają na tyle duże, że sorbenty z powodzeniem mogą być wykorzystywane do oznaczania S–metolachloru w próbkach środowiskowych. Dodatkowo zbadano selektywność polimerów w stosunku do S–metolachloru dla dwóch różnych trójskładnikowych roztworów herbicydów. W pierwszym roztworze S–metolachlor był sorbowany około trzykrotnie lepiej niż atrazyna i 2,4–D, natomiast w drugim roztworze około dwukrotnie lepiej niż atrazyna i trzykrotnie lepiej niż mezotrion.

Pełną charakterystykę właściwości fizyko–chemicznych pH–wrażliwych polimerów wdrukowanych molekularnie selektywnych wobec S–metolachloru otrzymano wykonując widma IR, fotografie SEM oraz mierząc stopień pęcznienia sorbentów w różnych pH. Podobnie jak w przypadku blokowych polimerów reagujących na zmianę temperatury, widma IR obu sorbentów były do siebie porównywalne, potwierdzając taką samą budowę chemiczną materiałów. Zbliżone cechy do „*termoczułych*” MIPów zaobserwowano również na

fotografiach SEM, ukazujących nieregularną strukturę powierzchni zarówno dla MIPu, jak i NIPu, oraz zwiększoną porowatość powierzchni dla polimeru molekularnie wdrukowanego. Dodatkowo MIP wykazywał większy stopień pęcznienia w porównaniu z NIPem, we wszystkich badanych wartościach pH, co również potwierdza większą porowatość jego powierzchni.

Podsumowanie

Przedstawione blokowe polimery wdrukowane molekularnie, reagujące na zmiany pH i selektywne wobec S–metolachloru, mogą z powodzeniem znaleźć zastosowane w detekcji oraz oznaczaniu stężenia tego herbicydu zarówno w próbkach modelowych, jak i w złożonych matrycach środowiskowych. Sorbenty te stanowią alternatywę dla „*termoczułych*" blokowych MIPów, przy czym, jak wspomniano wcześniej, zmieniono metodę syntezy. W poprzedniej procedurze do mieszania mieszaniny reakcyjnej używano tradycyjnej wstrząsarki, natomiast w opisanej tutaj metodzie zastosowano mieszadło mechaniczne, które umożliwiło zsyntezowanie materiału o zwiększonej jednorodności.

Journal of Water Process Engineering 75 (2025) 107980

Contents lists available at ScienceDirect

Journal of Water Process Engineering

journal homepage: www.elsevier.com/locate/jwpe

Detection of S-metolachlor herbicide in water samples using new molecularly imprinted polymer for solid-phase extraction

Dominika Rapacz *, Katarzyna Smolińska-Kempisty, Joanna Wolska

Wrocław University of Science and Technology, Department of Process Engineering and Technology of Polymer and Carbon Materials, Wybrzeże Wyspiańskiego 27, 50-370 Wrocław, Poland

ARTICLE INFO

Editor: Zhugen Yang

Keywords:
Green molecularly imprinted polymers
pH-responsible polymers
S-metolachlor
Sorption process
Solid phase extraction
Smart polymers

ABSTRACT

The application of herbicides has been proven to enhance crop yield. Nevertheless, the use of plant protection products has been associated with the migration of chemicals into water systems, thereby reducing their quality. The present study proposes a novel methodology for the detection of S-metolachlor within water samples, utilizing pH-sensitive molecularly imprinted polymers (MIPs) as highly selective and sensitive sorbents. The MIPs demonstrated a higher absorption capacity of S-metolachlor (0.75 ± 0.34 mg $\times$ g^{-1}) in comparison to the non-imprinted polymers (0.17 ± 0.04 mg $\times$ g^{-1}). The adsorption isotherms were analyzed using the Freundlich, Langmuir, Dubinin-Radushkevich, and Scatchard models. The Scatchard model was found to be the best fit, as the parameters obtained were closest to the experimental values, confirming the heterogeneity of the binding sites present on the MIP surface. The data obtained from the kinetic study were fitted to the pseudo-first-order and pseudo-second-order models. The pseudo-second-order model provided the most appropriate fit (R^2 = 0.998). The obtained sorbent exhibited high selectivity for S-metolachlor, absorbing it approximately 3 times better than atrazine, 2,4-dichlorophenoxyoctic acid (2,4-D), and mesotrione. The results indicate that pH-sensitive molecularly imprinted polymers, exhibit excellent sensitivity and selectivity towards S-metolachlor, making them a novel material for preconcentrating and determining the concentration of sample.

1. Introduction

The term pesticides refers to a very wide range of chemical substances used to control insects, fungi and weeds in crops. The employment of herbicides significantly increased crop yields. However, this use has also been associated with significant negative environmental and human health impacts, owing to their toxicity and high persistence. [1] A growing awareness of the consequences of irresponsible herbicide use has led to improvements in the quality and dose of herbicides, as well as in the environmentally friendly production of crop protection products. [2] One of the chloroacetamide herbicides is S-metolachlor [2-chloro-N-(2-ethyl-6-methylphenyl)-N-(2-methoxymethylethyl)acetamide], inhibits the formation of a very long chain fatty acid (VLCFA). [3,4] It is an important soil-applied herbicide that has been used on more than 70 crops worldwide for many decades. [5,6] In USA, S-metolachlor is distributed extensively through the environment. Indeed, 50.3 % of surface water and 2 % of groundwater have been found to be contaminated with this herbicide. [7] The Minnesota Department of Agriculture analyzed a total of 249 surface water samples, of which 67 % contained metolachlor, at a maximum detected concentration of 37.9 μg $\times$ L^{-1}. The presence of metolachlor in groundwater was identified in 14 out of 249 samples, with a maximum detected concentration of 5.89 μg $\times$ L^{-1}. [8] According to the regulation of the World Health Organization, the maximum allowable concentration of S-metolachlor in drinking water is 0.01 mg $\times$ L^{-1}. Therefore, the issue of removing this herbicide from water solutions is of significant environmental health concern. [7]

In recent years, molecular imprinting has gained popularity as an effective technique for creating highly specific binding sites in a polymer matrix to recognize target molecules. MIPs are used in a variety of application, including chromatography, detection, purification, chemical separation, binding assays, drug delivery and sorbents for solid phase extraction. [9–11] The employment of functional materials, including magnetic, pH-sensitive, temperature-sensitive, photo-sensitive and bio-macromolecule-sensitive materials, can be utilized to achieve the intelligent MIPs. [12–20] The combination of molecular imprinting and stimulus-response can significantly improve the adsorption/desorption process according to changes in the external environment. [21] Monitoring water quality often requires special analytical procedures to

* Corresponding author.
E-mail address: dominika.rapacz@pwr.edu.pl (D. Rapacz).

https://doi.org/10.1016/j.jwpe.2025.107980
Received 10 March 2025; Received in revised form 23 April 2025; Accepted 18 May 2025
Available online 27 May 2025

determine concentrations within their detection limits. The sample preparation step is particularly important and may cause errors in subsequent analyses. A frequently employed method is sample preconcentration by solid phase extraction (SPE) using molecularly imprinted polymers as selective sorbents. [22]

The implementation of *green chemistry* strategies in the domain of molecular imprinting has been delineated by Arabi et al. in their conceptualization of GREENIFICATION, which provides a foundation for the principles of *green* MIPs. The novel imprinting strategies prioritize the safety of the operator and the environment by aligning *green chemistry* with molecular imprinting technology (MIT). A significant focus was placed on the selection of functional monomers, templates, and the aqueous medium as porogens. Moreover, the study investigates the aspects of conducting polymerization in mild conditions and at reduced reaction times. It further explores the principles of polymerization without energy dissipation, the conception of self-cleaning MIPs, and the enhancement of degradability of sorbents within natural environments. Additionally, it discusses the generation of minimal waste. [23]

Poly(acrylic acid) (PAAc) is a hydrophilic polymer, containing carboxylic groups with vinyl groups at each end. The presence of a carbon-carbon double bond in acrylic acid results in its high reactivity. It is able to readily react with free radicals and undergo crosslinking through a radical polymerization process. The presence of carboxylic groups in the chains is responsible for the pH-responsive behavior, causing it to swell at pHs between 4.5 and 5. [24,25] PAAc undergoes a reversible conformational transition from a coil to a globule transition, at a pH of about 5, driven by the state of ionization of the carboxylic group. At low pH, PAAc exhibits a compacted (although not fully collapsed) globular conformation. Conversely, an increase in pH results in ionization, leading to the polymer expanding into a fully solvated open coil conformation. [25,26]

To the best of the authors' knowledge, several articles describing molecularly imprinted polymers sensitive to S-metolachlor are available in the scientific literature. However there is a distinct gap in the area of application of *smart* MIPs synthesized according to *green chemistry* principles for the selective detection of S-metolachlor. [27] The extant literature on the subject is limited to the authors' papers describing temperature-sensitive MIPs. [17,28,29] In contrast, pH-sensitive MIPs are a complete novelty. Therefore the present study focuses on the pH-responsible molecularly imprinted polymers as a sensitive and selective sorbent for the detection of S-metolachlor in water samples, synthesized according to conceptualization of GREENIFICATION. To this purpose, the effect of polymerization variables such as the type and ratio of monomers, the amount of initiator and crosslinker, and the reaction time on the synthesis is investigated. The mechanism of specific analyte recognition and selective adsorption were investigated by adsorption kinetics and sorption isotherms. The sorbents were tested on model solutions and applied to water samples simulating a real solution. FT-IR spectroscopy and SEM images have been used for the characterization of the prepared polymers.

2. Materials and methods

2.1. Reagents and chemicals

S-metolachlor (SMCh) was obtained from NOVAGRA. The chemicals utilized for the polymers synthesis were acrylamide (AA), purchased from Thermo Scientific Chemicals, acrylic acid (AAc), provided by Acros Organics, ammonium persulfate (APS) and N, N'- methylenebis (acrylamide) (BIS) supplied by Sigma-Aldrich. Ethyl alcohol (EtOH) and the HPLC grade acetonitrile was obtained from POCH S.A. Ultrapure water was obtained with a Milli-Q System (Merck Millipore).

Table 1
The amount of reagents used for the synthesis process.

MIP designation	Functional monomers [mmol]	Cross-linker BIS [mmol]	Initiator [mmol]	Porogen [mL]
MIP-1	AAc: AA [5.76: 6.96]	3.50	APS: TEMED [0.20: 0.30]	H_2O [10]
MIP-2	AAc: AA [5.76: 6.96]	4.93	APS: TEMED [0.20: 0.30]	H_2O [15]
MIP-3*	AAc: AA [5.76: 6.96]	4.93	APS: TEMED [0.20: 0.30]	H_2O [15]
MIP-4	AAc [19.98]	2.00	APS: TEMED [0.20: 0.30]	H_2O [10]
MIP-5	AAc: AA [19.98: 19.98]	2.00	APS: TEMED [0.20: 0.30]	H_2O [10]
MIP-6	AAc: AA[19.98: 19.98]	5.00	APS: TEMED [0.20: 0.30]	H_2O [10]
MIP-7*	AAc: AA [5.76: 6.96]	4.93	APS: TEMED [0.40: 0.60]	EtOH [15]
MIP-8	AAc: AA [3.89: 4.64]	2.34	$K_2S_2O_8$ [0.06]	H_2O [10]

* Reaction conducted on a mechanical stirrer.

2.2. Synthesis of the polymers

The molecularly imprinted polymers were synthesized by the bulk polymerization. The experimental amounts of the reagents used for the preparation of the different types of polymers are listed in Table 1. In brief, S-metolachlor, the appropriate functional monomers, and BIS were dissolved in the porogen in a flask. The mixture was purged with nitrogen (3 min), and then APS and TEMED water solution (1 mL) or $K_2S_2O_8$ were added to the mixture and deoxygenized with a stream of nitrogen again (5–10 min). The reaction was then conducted on a stirrer for 24 h at room temperature or at 60 °C (for reactions with $K_2S_2O_8$). The obtained bulk polymers were subsequently extracted in a Soxhlet apparatus for 24 h using ethanol, and finally dried at 60 °C. The non-imprinted polymers (NIPs) were synthesized using the same procedure, but without a template molecule.

2.3. Analytical and characterization methods

2.3.1. High performance liquid chromatography

The concentration of the herbicides was determined by high performance liquid chromatography (HPLC) method. The analysis was performed on a Shimadzu high performance liquid chromatograph (model SCL-40) equipped with a photodiode array (PDA) detector, and a 3 µm ARION® Biphenyl, 150 × 4.6 mm column. The mobile phase was acetonitrile – water (50/50 *v*/v) mixed in the isocratic mode at a flow rate of 1 mL × min^{-1}. Prior to analysis, the mobile phase was degassed by sonication for 10 min. The injection of a sample volume of 30 µL was conducted using an autosampler (model SIL-40), with the detection wavelength set at 254 nm.

2.3.2. Scanning electron microscopy

The morphologies and structures of the polymers were characterized by scanning electron microscopy (SEM). Specimens were mounted on aluminum stubs with double-sided carbon tape and gold-coated for 400 s using an Edwards Scancoat Six Sputter Coater. A scanning electron microscope (Zeiss Evo LS15) operating at 16 kV was used for imaging.

2.3.3. Fourier-transform infrared spectroscopy

The functional groups of the polymers were characterized by Fourier-transform infrared spectroscopy (FT-IR). The spectral data were collected on a Jasco FT-IR-4700 spectrophotometer using 64 scans with a resolution of 4 cm^{-1}, in the 400–4000 cm^{-1} range.

2.4. Adsorption experiments

The adsorption capacities q (mg × g^{-1}) of MIPs and NIPs were estimated using the following equation (Eq. (1)), which defines the amount of absorbed S-metolachlor at equilibrium:

$$q = \frac{(C_i - C_{eq}) \times V}{m} \quad (1)$$

where C_i (mg × L^{-1}) – the initial concentration of S-metolachlor, C_{eq} (mg × L^{-1}) – the equilibrium concentration of S-metolachlor, V (L) – the volume of the solution, m (g) – the mass of the sorbent.

2.4.1. Kinetics of adsorption

The kinetics of the adsorption process was studied using 250 mL of a solution of S-metolachlor at a concentration of 30 mg × L^{-1} and a mass of polymer (MIP and NIP) of 2.5 g. The experiment was carried out at room temperature and the concentration of the samples was measured at various time intervals (ranging from 5 min to 24 h) using HPLC methods. The adsorption capacity was calculated using Eq. (1). The pseudo-first-order and pseudo-second-order models were employed to ascertain the key process controlling the adsorption rate.

2.4.1.1. Pseudo-first-order model. The linear form of the pseudo-first-order model is presented in the following equation (Eq. (2)). The rate constant k_1 was calculated from the $log\left(q_{eq} - q_t\right)$ versus time plot.

$$\log\left(q_{eq} - q_t\right) = \log\left(q_{eq}\right) - \frac{k_1 t}{2.303} \quad (2)$$

where k_1 (1 × min^{-1}) – sorption rate constant, q_{eq} and q_t (mg × g^{-1}) – the amount of adsorbate adsorbed at equilibrium time and at time t, respectively. [30]

2.4.1.2. Pseudo-second-order model. The linear form of the pseudo-second-order model is described in terms of the following equation (Eq. (3)).

$$\frac{t}{q_t} = \frac{1}{k_2 q_{eq}^2} + \frac{1}{q_{eq}} t \quad (3)$$

where k_2 (g × (mg × min)$^{-1}$) – sorption rate constant, q_{eq} and q_t (mg × g^{-1}) – the amount of adsorbate adsorbed at equilibrium time and at time t, respectively. [31]

2.4.2. Sorption isotherms

To ascertain the sorption isotherm of sorbents (MIP and NIP), 0.200 ± 0.001 g of polymers were placed into the flask, and 20 mL of solutions with a concentration range of 10–250 mg × L^{-1} of S-metolachlor were added. The samples were then shaken for 24 h and filtered through a syringe filter. The equilibrium concentration of S-metolachlor was determined by HPLC, and the adsorption capacity was calculated using Eq. (1). The Langmuir, Freundlich, Dubinin–Radushkevich and Scatchard isotherm models were utilized for the fitting the obtained data with the specific interaction between the analyte and the adsorbent.

2.4.2.1. Langmuir isotherms. The mathematical linear form of the Langmuir model can be expressed as follows (Eq. (4)):

$$\frac{1}{q_e} = \frac{1}{q_m K_L C_e} + \frac{1}{q_m} \quad (4)$$

where q_e – the absorption capacity at equilibrium (mg × g^{-1}), q_m – the maximum adsorption capacity (mg × g^{-1}), K_L – Langmuir parameter – the affinity of the adsorption sites (L × mg^{-1}), and C_e – the equilibrium concentration of adsorbate (mg × L^{-1}). [32]

2.4.2.2. Freundlich isotherms. The mathematical linear form of the Freundlich model is given by the following equation (Eq. (5)):

$$log q_e = m \, log C_e + log K_F \quad (5)$$

where q_e – the absorption capacity at equilibrium (mg × g^{-1}), K_F – the Freundlich constant related to adsorption capacity (mg × g^{-1}), m – a heterogeneity index, C_e – the equilibrium concentration of adsorbate (mg × L^{-1}). [33]

2.4.2.3. Dubinin–Radushkevich isotherms. The following equation represents the linear mathematical formulation of the Dubinin–Radushkevich model (Eq. (6)):

$$ln q_e = ln q_m - K_{DR}\varepsilon^2 \quad (6)$$

where q_e – the absorption capacity at equilibrium (mg × g^{-1}), q_m – the maximum adsorption capacity (mg × g^{-1}), K_{DR} – the activity coefficient related to free adsorption energy (mol^2 × kJ^{-2}), and ε – the Polanyi potential (kJ × mol^{-1}). [34]

2.4.2.4. Scatchard isotherms. The mathematical linear form of the Scatchard model is given by the following equation (Eq. (7)):

$$\frac{q_e}{C_e} = PN - Pq \quad (7)$$

where q_e – the absorption capacity at equilibrium (mg × g^{-1}), C_e – the equilibrium concentration of adsorbate (mg × L^{-1}), P – binding affinity (L × $mmol^{-1}$), N – number of binding sites (mmol × g^{-1}). [33]

2.4.3. Competitive study

In order to determine the binding selectivity, approximately 0.200 ± 0.001 g of MIP and NIP was placed in the flask. Thereafter, 20 mL of a solution comprising a combination of plant protection products was added to the flask; I: atrazine, 2,4-D and S-metolachlor and II: atrazine, mesotrione and S-metolachlor, with a concentration of 0.05 mmol × L^{-1} for each. The same analyses were conducted in the dynamic mode type of sorption. For this, approximately 0.050 ± 0.005 g of sorbent (MIP or NIP) was introduced into a 1 mL SPE column and activated with water. Thereafter, the column was incubated for 4 h with 2 mL of a I or II solution. The concentration of the solution was determined by HPLC, and the adsorption capacity was calculated using Eq. (1).

The distribution coefficient ($K_{i(j)}$), representing the difference between the concentration (i – S-metolachlor, j – other plant protection products) in the solution before and after the sorption process, was calculated according to the following equation (Eq. (8)):

$$K_{i(j)} = \frac{q_{i(j)} \times \rho}{C_{i(j)eq}} \quad (8)$$

where $q_{i(j)}$ (μmol × g^{-1}) – the sorption capacity (i – S-metolachlor, j – other plant protection products), $C_{i(j)eq}$ (μmol × L^{-1}) – the equilibrium concentration (i – S-metolachlor, j – other plant protection products, and ρ (g × L^{-1}) – the density of the solution. [35]

The imprinting factor (IF) indicates the efficiency of the imprinting on the matrix molecule. It was calculated as the ratio of the distribution of the particular analyte on the polymer with molecular imprint to the polymer without molecular imprint, under the same conditions (Eq. (9)).

$$IF = \frac{K_i^{MIP}}{K_i^{NIP}} \quad (9)$$

where $K_{i(j)}$ – the distribution coefficient (i – S-metolachlor, j – other plant protection products) of an analyte on an imprinted polymer (K^{MIP}) and a non-imprinted polymer (K^{NIP}). [35]

The selectivity factor (S) defined as the ratio of the imprinting factor

of S-metolachlor to the imprinting factor of other herbicides, was calculated as follows (Eq. (10)):

$$S = \frac{IF_i}{IF_j} \quad (10)$$

where IF_i and IF_j – imprinting factor of the S-metolachlor and other herbicides, respectively. [35]

2.4.4. Sorption from reals samples

The sorption study was carried out on both a model sample and solution, with the objective of simulating the real sample. These were analyzed in both in batch and dynamic modes. For batch mode, approximately 0.200 ± 0.001 g of polymer (MIP or NIP) was placed into the flask and mixed for 24 h with 20 mL of S-metolachlor solution at a concentration of 30 mg × L^{-1}. The same analyses were carried out in the dynamic mode type of sorption. For this, approximately 0.050 ± 0.005 g of sorbent (MIP or NIP) was introduced into a 1 mL SPE column and activated with water. Thereafter, the column was incubated for 4 h with 2 mL of a S-metolachlor solution with a concentration of 30 mg × L^{-1}. The concentration of the solution after sorption was determined by HPLC, and the adsorption capacity was calculated using Eq. (1).

2.5. Sorbent regeneration process

The desorption process was carried out employing SPE columns. For this purpose, the MIP or NIP sample following the sorption process was treated with 1 mL of water, as a regenerating solution, for 15 min. The desorption was calculated according to the equation given below (Eq. (11)).

$$D = \frac{C_{(ij)} \times V}{m} \quad (11)$$

where $C_{(ij)}$ (mg × L^{-1}) – the concentration of (i – S-metolachlor, j – other plant protection products), V (mL) – the volume of the regenerating solution, m (g) – the mass of the sorbent.

The sorbent regeneration factor (R_f), which is defined as the ratio of eluted analyte molecules to adsorbed analyte molecules, was calculated according to following equation (Eq. (12)).

$$R_f = \frac{m_e}{m_a} \times 100\% \quad (12)$$

where m_e (mg) – the mass of eluted S-metolachlor, m_a (mg) – the mass of absorbed S-metolachlor.

2.6. Swelling degree

The swelling study was carried out using distilled water at a pH of 4.2, 7.9 and 9. The sorbents were first incubated in water for 24 h and then centrifuged. The wet mass of each sorbent was weighed. The samples were then dried to achieve a constant mass and weighed again. The swelling ability was determined according to the following equation (Eq. (13)).

$$DS = \frac{m_w - m_d}{m_d} \times 100\% \quad (13)$$

where m_w (g) and m_d (g) represents mass of wet and dry sorbent, respectively. [36]

3. Results and discussion

3.1. Optimization of the condition

3.1.1. Development of sorbent

In order to select a suitably composed sorbent, a static sorption process was carried out on the synthesized polymers. The calculation of absorption capacities was conducted in accordance with Eq. (1). The results are presented in Table 2.

Table 2
The absorption capacities of MIPs and NIPs.

Designation of polymer	Adsorption capacities [mg × g^{-1}]	
	MIP	NIP
1	0.108 ± 0.029	0.101 ± 0.024
2	0.230 ± 0.172	0.128 ± 0.029
3	0.260 ± 0.121	0.166 ± 0.002
4*	–	–
5	0.174 ± 0.019	0.130 ± 0.003
6	0.148 ± 0.031	0.105 ± 0.011
7	0.068 ± 0.038	0.055 ± 0.002
8	0.080 ± 0.006	0.143 ± 0.041

* Polymerization has not occurred sufficiently.

Table 3
The absorption data obtained.

pH	Adsorption [mg × g^{-1}]	
	MIP	NIP
2.5	0.260 ± 0.007	0.287 ± 0.006
4.5	0.246 ± 0.064	0.108 ± 0.021
6.5	0.343 ± 0.042	0.174 ± 0.038
8.5	0.212 ± 0.032	0.121 ± 0.027
10.5	0.450 ± 0.103	0.286 ± 0.026

A polymer pair, designated 3, was selected from the obtained data as the most optimal, and further studies were conducted with this pair. In the remainder of this work, MIP-3 and NIP-3 will be referred to as MIP and NIP, respectively, in order to enhance the clarity of the text. In the case of the polymer designated 4, it was not possible to carry out a sorption process because the polymer obtained after synthesis was excessively fluid, which was probably due to the polymer chains being too short, thus preventing adaptation to work in columns. The repeatability of results for some polymers is less than expected, which may be due to the fact that block polymers are characterized by a non-homogeneous structure and surface morphology, which is also reflected in the sorption values.

3.1.2. Selection of the pH of the S-metolachlor solution

To ascertain an appropriate pH value for the S-metolachlor solution, a sorption process was conducted on the MIP and NIP polymers in static mode. The obtained data are summarized in Table 3.

The sorption values obtained from a solution with a pH of 4.5 and 6.5 are the most favorable, as MIP sorbs S-metolachlor approximately two times better than NIP. This can be attributed to the transformation of the PAAc network, as previously discussed. At a pH of approximately 4.5–5, carboxyl groups release H^+ ions, convert to COO^- groups and, as a consequence, the polymer swells. [24,25] This, in turn, increases the availability of all binding sites and consequently leads to an improved sorption process of S-metolachlor.

Table 4
Data obtained from the optimization of incubation time.

Time [h]	Adsorption [mg × g^{-1}]	
	MIP	NIP
0.25	0.467 ± 0.088	0.389 ± 0.007
0.5	0.422 ± 0.151	0.392 ± 0.005
1	0.496 ± 0.015	0.477 ± 0.077
2	0.561 ± 0.066	0.452 ± 0.024
3	0.454 ± 0.006	0.464 ± 0.031
4	**0.549 ± 0.058**	**0.289 ± 0.132**
5	0.439 ± 0.045	0.389 ± 0.034

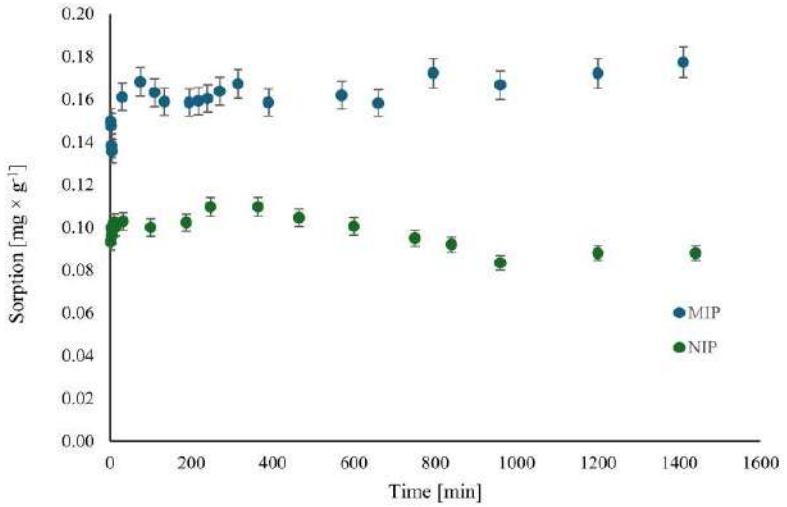

Fig. 1. The kinetics of sorption of MIP and NIP.

Table 5
Parameters obtained from pseudo-first-order and pseudo-second-order models.

	Pseudo-first-order model			Pseudo-second-order model		
	k_1 [1 × min^{-1}]	R^2	q_{eq1} [mg × g^{-1}]	k_2 [g × [mg × min]$^{-1}$]	R^2	q_{eq2} [mg × g^{-1}]
MIP	0.001	0.508	0.002	0.446	0.998	0.173
NIP	0.003	0.054	0.001	8.504	0.999	0.107

3.1.3. Optimizing of the incubation time in the dynamic mode

In the next stage of the study, the sorbents were introduced into SPE columns and sorption was conducted in dynamic mode. It was necessary to optimize the incubation time of the deposit with the S-metolachlor solution. As a fundamental basis for this study, it was initially assumed that 3 h would be the optimal sorption time, based on experience gained in previous work with thermosensitive polymers [29]. However, it was subsequently determined that this time was too short, and the incubation time was extended accordingly. The resulting data are presented in Table 4. Following the analysis of the obtained data, it was determined that a 4-h incubation period (bold in Table 4) was the most suitable for the polymer with the bed, as this resulted in the most significant difference between the sorption value calculated for MIP and NIP.

3.2. Kinetics of adsorption

Adsorption kinetics is a valuable tool for the analysis of potential adsorption mechanisms and the identification of rate-limiting steps during the adsorption process. The kinetics of adsorption of S-metolachlor on MIP and NIP, presented in the Fig. 1, were evaluated employing pseudo-first-order and pseudo-second-order model. The obtained data are summarized in Table 5.

The pseudo-second-order model was determined to provide a more suitable fit for both the MIP and NIP sorbents. The adsorption of S-metolachlor on these materials exhibited a linear function t/q against t with the coefficient $R^2 = 0.998$ for MIP and $R^2 = 0.999$ for NIP. The calculated q_{eq2} data are comparable to those obtained from the experiments, and are equal 0.173 mg × g^{-1} and 0.107 mg × g^{-1} for MIP and NIP, respectively. The calculated values k_2 are 0.446 g × (mg × min)$^{-1}$ and 8.504 g × (mg × min)$^{-1}$ for MIP and NIP, respectively.

Table 6
The parameters of Langmuir, Freundlich, Dubinin– Radushkevich models.

Adsorption isotherm	Parameter	Value	
		MIP	NIP
Langmuir	K_L [L × mg^{-1}]	0.015	0.007
	q_m [mg × g^{-1}]	2.682	13.774
	R^2	0.988	0.990
Freundlich	K_F [mg × g^{-1}]	0.032	0.009
	m	0.686	0.934
	R^2	0.875	0.928
Dubinin– Radushkevich	K_{DR} [mol^2 × kJ^{-2}]	5.144	5.404
	q_m [mg × g^{-1}]	0.006	0.005
	R^2	0.944	0.911
Scatchard	P_1 [L × mg^{-1}]	0.021	–
	N_1 [mg × g^{-1}]	0.865	–
	R_1^2	1.000	–
	P_2 [L × mg^{-1}]	0.004	0.004
	N_2 [mg × g^{-1}]	4.138	0.306
	R_2^2	0.729	0.708

3.3. Sorption isotherms

The adsorption isotherm models can provide mechanism information of the adsorption process. The obtained data were fitted to the Langmuir, Freundlich, Dubinin– Radushkevich, and Scatchard models. The Langmuir isotherm model postulates the formation of a monolayer of molecules on the surface of the adsorbent, with a defined number of adsorption sites that interact with identical binding energies. The Freundlich isotherm model is founded upon the monolayer heterogeneous adsorption of adsorbate on the surface of the adsorbent, in the absence of interaction between adsorbed ions. The Dubinin-Radushkevich isotherms are a valuable tool for examining the interactions between the adsorbate and the sorbent, providing insights into the distinction between chemisorption and physisorption mechanisms. [28] The Scatchard isotherms permitted the determination of both the binding affinity and the number of binding sites. The limiting slopes method yields two separate sets of binding parameters (P_1, N_1) and (P_2, N_2) for two classes of sites. [33] The result of this analysis are presented in the Table 6.

The Langmuir isotherm model was employed to estimate the maximum sorption capacity. This value for the MIP was calculated to be 2.682, a significant improvement over the NIP. The maximum sorption

Table 7
Selectivity study data obtained from I solution.

	Batch sorption			Dynamic sorption		
Parameter	S-Metolachlor	Atrazine	2,4-D	S-Metolachlor	Atrazine	2,4-D
K_{MIP}	8.807	11.286	2.833	19.410	15.327	15.932
K_{NIP}	3.102	10.632	3.216	9.697	13.389	13.389
IF	2.84	1.06	0.88	2.00	1.15	1.19
S	–	2.7	3.2	–	1.8	1.7

Table 8
Selectivity study data obtained from II solution.

	Batch sorption			Dynamic sorption		
Parameter	S-Metolachlor	Atrazine	Mesotrione	S-Metolachlor	Atrazine	Mesotrione
K_{MIP}	5.694	5.318	2.741	25.981	16.431	11.533
K_{NIP}	2.390	4.319	2.990	10.829	12.809	11.621
IF	2.38	1.23	0.92	2.40	1.28	0.98
S	–	**1.9**	**2.6**	–	**1.9**	**2.5**

capacity obtained in experimental studies is approximately 1.2, while that ascertained through the Langmuir model is nearly 14. Despite the coefficient of determination for NIP approaching 1 ($R^2 = 0.99$), the significantly different q_m renders the model unsuitable for describing NIP sorption. It is evident that a value of m in the Freundlich isotherm that is closer to 1 indicates a highly homogeneous material. For NIP, the value of m is equal to 0.934, indicating high homogeneity, while for MIP it is 0.686, which is related to the heterogeneity of this material. Furthermore, the K_F factor, which is indicative of the sorption capacity, demonstrates a fourfold increase in the MIP capacity compared to the NIP. While the R^2 factor does not approximate 1, as observed in the Langmuir model, this model can nevertheless be applied to the description of the material's sorption properties. In the Dubinin-Radushkevich model, the theoretical maximum capacity values are lower than in the Langmuir model and deviate from the experimental values. The Scatchard isotherm model for MIP demonstrates the presence of binding sites with high affinity for S-metolachlor ($N_1 = 0.865$ mg × g^{-1}), which are not observed in NIP. Furthermore, significantly more low affinity binding sites is observed on the MIP surface ($N_2 = 4.138$ mg × g^{-1}) in comparison to the NIP surface ($N_2 = 0.045$ mg × g^{-1}). The Scatchard model is the standard method for assessing the binding site heterogeneity of a solid material, such as MIPs. This study found that, based on the parameters obtained, the Scatchard model was the most suitable for the MIPs described in this article, as the calculated values were closest to those obtained experimentally. The Scatchard isotherm model is dedicated to the study of specific interactions in receptor materials, which include MIPs, to demonstrate the existence of two types of binding sites. The Scatchard plot obtained for MIPs is curvilinear, indicating that the binding sites on their surface are heterogeneous, whereas the plot for NIPs is linear, confirming the presence of only homogeneous binding sites. Furthermore, there are two types of binding sites on the surface of MIPs, confirmed by the Scatchard model, which provide evidence of the binding affinity of the target molecule. Despite not exhibiting the highest regression coefficient of all the models discussed, the Scatchard model can be successfully applied based on the values presented.

3.4. Competitive study

In order to investigate the selectivity of the sorbent, sorption tests were carried out with two solutions containing S-metolachlor and other pesticides utilized in the cultivation of maize. The results are presented in Tables 7 and 8.

The MIP exhibited superior selectivity in comparison to the NIP, as demonstrated by a selectivity coefficient of towards S-metolachlor in the presence of other herbicides. The selectivity coefficient is elevated in

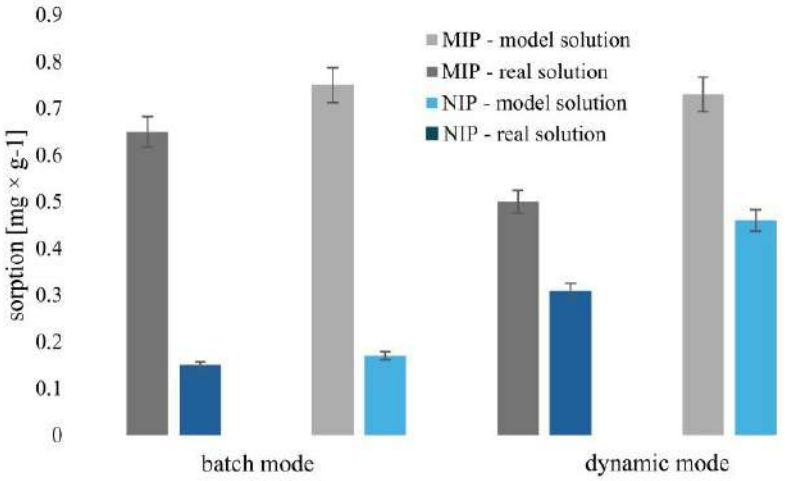

Fig. 2. Comparison of data obtained from sorption from real and model solutions.

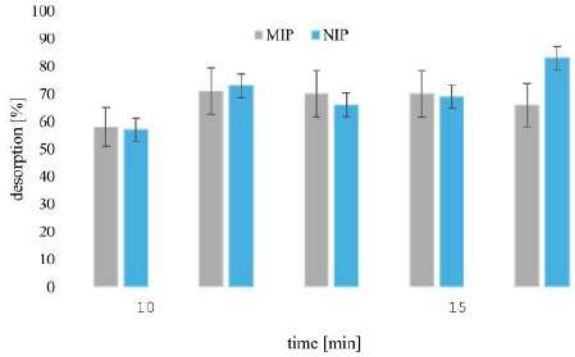

Fig. 3. % desorption after different time periods.

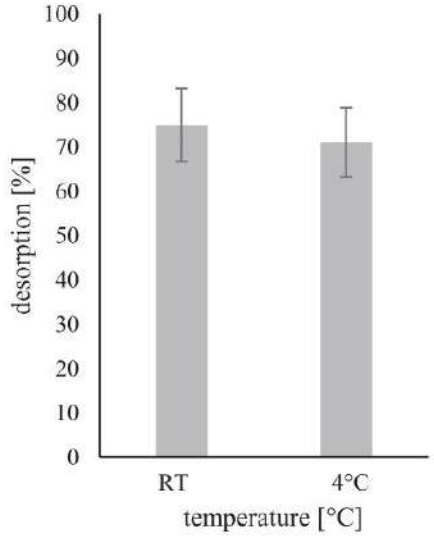

Fig. 4. % desorption performed in different temperatures.

batch experiments, which may be the reason for the increased contact time of the deposit with the herbicide mixture. In the I solution, MIP exhibited higher sorption affinity for S-metolachlor compared to atrazine and 2,4-D, with a selectivity factor of approximately 3 in batch mode and approximately 2 in dynamic mode. In the II solution, MIP demonstrated a twofold enhancement in the sorption of S-metolachlor compared to atrazine, and a threefold increase compared to mesotrione, in both static and dynamic modes.

3.5. Sorption from reals samples

In order to verify the applicability of the MIP sorbents to the detection of S-metolachlor herbicide in environmental samples, a series of experiments were conducted. To this end, tap water was spiked with S-metolachlor and the results obtained are presented in Fig. 2.

The sorption values for the solution simulating the real one, are only slightly lower than for the model solution. The sorption values obtained from batch mode, are higher than those from dynamic, which can be explained by the shorter incubation time. It can therefore be concluded that the obtained sorbent can be successfully used for the detection of S-metolachlor in environmental water samples.

Table 9
The results of sorption-desorption process cycles.

	MIP	NIP
sorption I [mg × g^{-1}]	0.613 ± 0.268	0.313 ± 0.043
R_f [%]	99 ± 1	99 ± 1
sorption II [mg × g^{-1}]	0.687 ± 0.169	0.370 ± 0.085
R_f [%]	92 ± 1	96 ± 4
sorption III [mg × g^{-1}]	0.773 ± 0.032	0.513 ± 0.021
R_f [%]	65 ± 2	96 ± 4

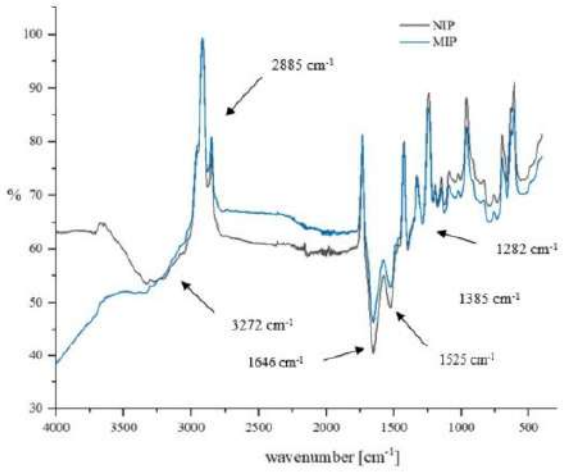

Fig. 5. FT-IR spectra of MIP and NIP.

3.6. Desorption

The desorption process was conducted in dynamic mode on an SPE column. The elution solution was water with a pH of approximately 9. The choice of these conditions is described in more detail in our work. [37,38] To optimize the desorption process, the incubation time of the regenerating solution with the deposit, as well the temperature, were selected. The obtained data are presented in the Fig. 3.

The optimal desorption time was determined to be 15 min, as this period was associated with the highest number of adsorbed analyte molecules. The desorption values for subsequent times are comparable. It is also notable that a comparatively brief desorption time has a favorable impact on the analysis rate. The next step was to investigate the effect of the incubation temperature. Desorption was performed at 4 °C and at room temperature (RT). The data obtained are shown in Fig. 4.

The difference between desorption at 4 °C (71 %) and at room temperature (75 %) is not that significant. Therefore, in order to minimize energy wastage, desorption at room temperature was selected as the optimum, in accordance with the assumptions of GREENIFICATION.

3.7. Regeneration of the column bed

Following the optimization of the sorption and desorption conditions on the SPE columns, the investigation focused on the number of cycles the column deposit could be reused while maintaining the initial sorption parameters. The obtained results are presented in Table 9.

The findings of the study indicate that the bed can be used up to two times before its sorption properties are lost. It is conceivable that a third sorption may occur, however, the bed has reached a point where desorption is no longer possible. Consequently, the number of desorbed molecules cannot be determined.

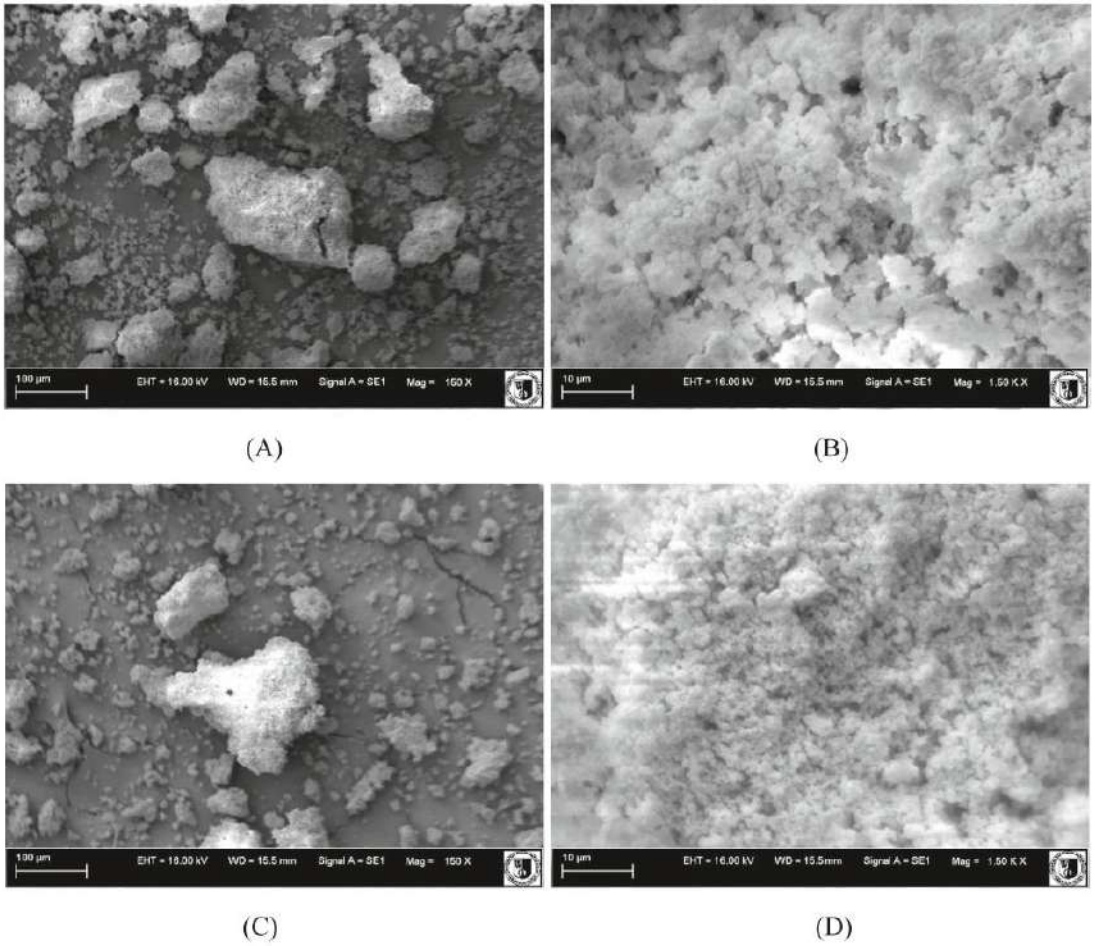

Fig. 6. SEM images of MIP (A, B) and NIP (C, D).

3.8. FT-IR analysis

As illustrated in Fig. 5, the infrared spectra of the MIPs and NIPs are presented. A comparison of the two spectra reveals a high degree of similarity, indicating that these polymers possess a comparable chemical structure. In both spectra, a band at approximately 3272 cm^{-1} can be identified, which has been associated with O—H or N—H stretching vibrations. The presence of a band at 2885 cm^{-1} is indicative of an aliphatic C—H stretching vibration, and is observed in both polymers. The peak observed at 1646 cm^{-1} can be related to stretching vibrations derived from C=O, while the peak at 1525 cm^{-1} is consistent with N—H deformation vibrations. The band at 1385 cm^{-1} is attributed to the O—H deformation vibration, while the band at 1282 cm^{-1} corresponds to the C—N stretching vibration.

3.9. SEM analysis

Analysis of the SEM images indicated a surface with irregular shapes and surface morphology, accompanied by a significant number of surface depressions for both MIP and NIP. Furthermore, the MIP surface exhibits increased porosity in comparison to the NIP surface. As illustrated in Fig. 6 (A and C), a 150 times magnified image of the MIP and NIP surfaces is presented, with a scale bar measuring 100 μm. Fig. 6 (B and D) presents a 1500 fold magnified images of MIP and NIP surfaces, overlaid on a bar scale of 10 μm. The degree of swelling of the polymers at different pH was also studied to complete the characterization of the surface. The result are presented in the Fig. 7. MIP exhibited a higher

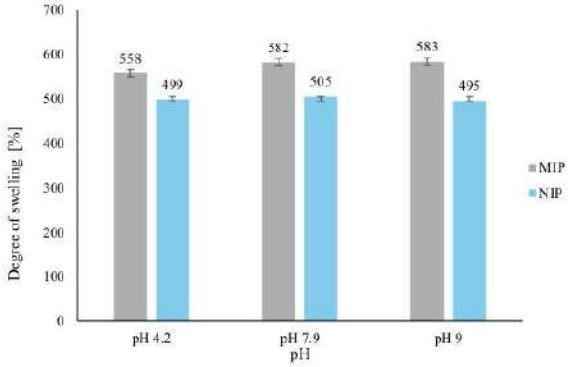

Fig. 7. Swelling degree at pH 4.2, 7.9, and 9.

degree of swelling in comparison to NIP at all pH values tested, thereby confirming the increased porosity of the MIP surface. At a pH of approximately 4–4.5, the conformational transition of PAAc from a globular to an open coil structure is observed. An increase in pH results in polymer loosening, as evidenced by the elevated degree of swelling values observed at higher pH levels. However, the phenomenon of chain relaxation has been observed to occur up to a pH value of approximately 8–9, as evidenced by the comparable degree of swelling of MIPs at these pH values.

4. Conclusions

A series of pH-sensitive molecularly imprinted polymers have been synthesized with the objective of obtaining a MIP-SPE sorbent material that possesses the necessary characteristics for the rapid and selective extraction of S-metolachlor from water samples. Among the synthesized compositions, the most satisfactory results were achieved through the utilization of acrylic acid and acrylamide as functional monomers, BIS as a cross-linker, S-metolachlor as a template and water as a porogen, with the reaction being conducted at room temperature in accordance with the principles of *green chemistry*. MIP exhibits high selectivity, with the ability to absorb S-metolachlor approximately three times more effectively than atrazine, 2,4-D and mesotrione. The desorption process was optimized at pH about 9, confirming the pH-sensitive properties of AAc. It is evident that the developed material can be employed for the sorption of S-metolachlor from both model and real solutions, in both static and dynamic modes. The kinetics study showed that the adsorption of S-metolachlor followed a pseudo-second-order model, with R^2 approximately 0.998. It has been determined that MIP can be used twice while maintaining its sorption and desorption (R_f = 96 %) properties. Compared to our previously published temperature-sensitive block MIP (sorption = 2.4 mg per 1 g) [28], the described sorbent has about three times lower sorption capacity (sorption = 0.75 mg per 1 g). Nevertheless, its capacity remains satisfactory for adsorbing S-metolachlor molecules from water samples, where it is present at much lower concentrations. In a related study, the MIP described in this paper sorbs S-metolachlor about three times better than atrazine, similar to a prior polymer [28]. In previous studies, the selectivity was investigated with glyphosate and fenoxaprop-P-ethyl, with sorption rates approximately six times lower than for S-metolachlor. In the present study, 2,4-D and mesotrione were used in addition to atrazine for selectivity study. However, a comparison of the sorption carried out on SPE columns reveals that the obtained MIP, for both the model and real solution, exhibits a greater difference between the sorption value for MIP and for NIP than previous described [29]. In dynamic mode, the sorption of S-metolachlor from solution simulating the real one by the MIP was found to be approximately 0.5 mg, while the NIP only absorbed 0.31 mg of S-metolachlor. In contrast, the temperature-sensitive polymer absorbed 0.85 mg and 0.71 mg, respectively by MIP and NIP. [29] In comparison with core-shell particles, a greater quantity of reactants is consumed in block polymers. Furthermore, the tendency of block polymers to clog the column is significantly higher than for the core-shell structures. However, these limitations are balanced by a number of other advantages that allow the user the to work with a wide range of materials.

CRediT authorship contribution statement

Dominika Rapacz: Writing – original draft, Methodology, Investigation, Formal analysis, Data curation, Conceptualization. **Katarzyna Smolińska-Kempisty:** Writing – review & editing, Supervision, Resources, Project administration, Methodology, Investigation, Funding acquisition, Conceptualization. **Joanna Wolska:** Writing – review & editing, Validation, Supervision, Methodology, Investigation, Conceptualization.

Declaration of competing interest

The authors declare the following financial interests/personal relationships which may be considered as potential competing interests: Katarzyna Smolinska-Kempisty reports financial support was provided by National Science Centre Poland. Dominika Rapacz Katarzyna Smolinska-Kempisty Joanna Wolska has patent pending to Licensee. If there are other authors, they declare that they have no known competing financial interests or personal relationships that could have appeared to influence the work reported in this paper.

Acknowledgments

This research was funded in whole by National Science Centre Poland 2021/42/E/ST5/00019 (02NB/0002/22). For the purpose of Open Access, the author has applied a CC-BY public copyright licence to any Author Accepted Manuscript (AAM) version arising from this submission.

Data availability

Data will be made available on request.

References

[1] R.Y. Qu, B. He, J.F. Yang, H.Y. Lin, W.C. Yang, Q.Y. Wu, Q.X. Li, G.F. Yang, Where are the new herbicides? Pest Manag. Sci. 77 (6) (2021) 2620–2625, https://doi.org/10.1002/ps.6285.
[2] Gianessi., The increasing importance of herbicides in worldwide crop production, Pest Manag. Sci. 69 (10) (2013) 1099–1105, https://doi.org/10.1002/ps.3598.
[3] Koffi Badou-Jeremie Kouame, Mary C. Savin, Cammy D. Willett, Thomas R. Butts, Erin Grantz, Matthew B. Bertucci, Samantha E. Robinson, Rodrigo Werle, Nilda Roma-Burgos, Biphasic models improved S-metolachlor dissipation endpoint predictions, Agrosyst. Geosci. Environ. 8 (1) (2024) e70026, https://doi.org/10.1002/agg2.70026.
[4] J. Wei, Toxicity and glutathione s-transferase-catalyzed metabolism of r-/s-metolachlor in rice, J. Agric. Food Chem. 72 (45) (2024) 25001–25014, https://doi.org/10.1021/acs.jafc.4c06711.
[5] Peter J. O'Connell, Christian T. Harms, James R.F. Allen, Metolachlor, *S*-metolachlor and their role within sustainable weed management, Crop Prot. 17 (3) (1998) 207–212, https://doi.org/10.1016/S0261-2194(98)80011-2.
[6] R. Busi, Resistance to herbicides inhibiting the biosynthesis of very-long-chain fatty acids, Pest Manag. Sci. 70 (9) (2014) 1378–1384, https://doi.org/10.1002/ps.3746.
[7] S. Hartnett, S. Musah, K.R. Dhanwada, Cellular effects of metolachlor exposure on human liver (HepG2) cells, Chemosphere 90 (3) (2013) 1258–1266, https://doi.org/10.1016/j.chemosphere.2012.09.077.
[8] Metolachlor and Drinking Water, Minnesota Department of Health Health Risk Assessment, 2018. https://www.health.state.mn.us/communities/environment/risk/docs/guidance/dwec/metolinfo.pdf.
[9] Hossein Hosseinzadeh, Siamak Javanbakht, Reza Mohammadi, Molecularly imprinting polymethacrylamide onto cu-based metal-organic framework as a pH-sensitive core-shell nanocarrier for potential anti-cancer drug delivery, J. Drug Deliv. Sci. Technol. 102 (2024) 106404, https://doi.org/10.1016/j.jddst.2024.106404.
[10] J.W. Lowdon, H. Diliën, P. Singla, M. Peeters, T.J. Cleij, B. van Grinsven, K. Eersels, Mips for commercial application in low-cost sensors and assays – an overview of the current status quo, Sens. Actuators, B Chem. 325 (2020) 128973, https://doi.org/10.1016/j.snb.2020.128973.
[11] Wang, et al., Fabrication of fluorescence sensor based on semi-covalent dummy molecularly imprinted silica on silane-modified carbon quantum dot for highly selective and sensitive detection of bisphenol a in spirits, Colloids Surf. A Physicochem. Eng. Asp. 696 (2024) 134292, https://doi.org/10.1016/j.colsurfa.2024.134292.
[12] P.K. Paul, Biomimetic insulin-imprinted polymer nanoparticles as a potential oral drug delivery system, Acta Pharm. 67 (2) (2017) 149–168, https://doi.org/10.1515/acph-2017-0020.
[13] G. Marcelo, I.C. Ferreira, R. Viveiros, T. Casimiro, Development of itaconic acid-based molecular imprinted polymers using supercritical fluid technology for pH-triggered drug delivery, Int. J. Pharm. 542 (1–2) (2018) 125–131, https://doi.org/10.1016/j.ijpharm.2018.03.010.
[14] Li, et al., Synthesis of novel photoresponsive molecularly imprinted polymer microspheres with special binding properties, J. Appl. Polym. Sci. 130 (2) (2013) 869–876, https://doi.org/10.1002/app.39233.
[15] L. Li, L. Chen, H. Zhang, Y. Yang, X. Liu, Y. Chen, Temperature and magnetism bi-responsive molecularly imprinted polymers: preparation, adsorption mechanism and properties as drug delivery system for sustained release of 5-fluorouracil,

Mater. Sci. Eng. C 61 (2016) 158–168, https://doi.org/10.1016/j.msec.2015.12.027.
[16] T. Miyata, M. Jige, T. Nakaminami, T. Uragami, Tumor marker-responsive behavior of gels prepared by biomolecular imprinting, Proc. Natl. Acad. Sci. 103 (5) (2006) 1190–1193, https://doi.org/10.1073/pnas.0506786103.
[17] K. Smolinska-Kempisty, T. Cowen, J. Duda, M. Bryjak, Environmentally friendly molecularly imprinted polymers as an insert for SPE type columns in the gentamicin monitoring process, Talanta 282 (2025) 126966, https://doi.org/10.1016/j.talanta.2024.126966.
[18] Yunlei Yin, Dual-sensing nano-yarns for real-time pH and temperature monitoring in smart textiles, Chem. Eng. J. 500 (2024) 157115, https://doi.org/10.1016/j.cej.2024.157115.
[19] N. An, Rational electrochemical design of cuprous oxide hierarchical microarchitectures and their derivatives for SERS sensing applications, Small Methods 8 (5) (2024) 2300910, https://doi.org/10.1002/smtd.202300910.
[20] Feng Qian, Ruyi Jia, Maoding Cheng, Ashish Chaudhary, Saad Melhi, Saleh Dessouky Mekkey, Neng Zhu, Chao Wang, Fidaus Razak, Xiaowei Xu, Chao Yan, Xiong Bao, Qinglong Jiang, Jie Wang, Mingmao Hu, An overview of polylactic acid (PLA) nanocomposites for sensors, Adv. Compos. Hybrid Mater. 7 (3) (2024) 75, https://doi.org/10.1007/s42114-024-00887-6.
[21] Suna He, Advances of molecularly imprinted polymers (MIP) and the application in drug delivery, Eur. Polym. J. 143 (2021) 110179, https://doi.org/10.1016/j.eurpolymj.2020.110179.
[22] Monika Sobiech, Piotr Luliński, Molecularly imprinted solid phase extraction – recent strategies, future prospects and forthcoming challenges in complex sample pretreatment process, Trends Anal. Chem. 174 (2024) 117695, https://doi.org/10.1016/j.trac.2024.117695.
[23] M. Arabi, A. Ostovan, J. Li, X. Wang, Z. Zhang, J. Choo, L. Chen, Molecular imprinting: green perspectives and strategies, Adv. Mater. 33 (30) (2021) 2100543, https://doi.org/10.1002/adma.202100543.
[24] M.S. Hashem, Rokaya A. Sobh, M.A. Abd El-Ghaffar, pH-responsive bionanocomposite pectin grafted with dimethylaminoethyl methacrylate and acrylic acid copolymer along with silver nanoparticles for breast cancer drug delivery, Polym. Eng. Sci. 64 (12) (2024) 6115–6128, https://doi.org/10.1002/pen.26975.
[25] T. Swift, L. Swanson, M. Geoghegan, S. Rimmer, The pH-responsive behaviour of poly(acrylic acid) in aqueous solution is dependent on molar mass, Soft Matter 12 (9) (2016) 2542–2549, https://doi.org/10.1039/C5SM02693H.
[26] Ishak, et al., pH-responsive gamma-irradiated poly(acrylic acid)-cellulose-nanocrystal-reinforced hydrogels, Polymers 12 (9) (2020) 1932, https://doi.org/10.3390/polym12091932.
[27] Dominika Rapacz, Katarzyna Smolinska-Kempisty, Joanna Wolska, Molecularly imprinted polymers toward herbicides – progress in development and the current state of the art depending on the polymerization environment – short review, J. Environ. Chem. Eng. 12 (2) (2024) 112159, https://doi.org/10.1016/j.jece.2024.112159.
[28] D. Rapacz, K. Smolińska-Kempisty, J. Wolska, A novel *green* molecularly imprinted polymers synthesized in an aqueous medium as s-metolachlor sensitive materials, Talanta 280 (2024) 126674, https://doi.org/10.1016/j.talanta.2024.126674.
[29] D. Rapacz, K. Smolińska-Kempisty, J. Wolska, Preparation and characterization of SPE column with smart green molecularly imprinted polymers materials for selective determination of S-metolachlor herbicide, Sci. Rep. 15 (1) (2025) 3153, https://doi.org/10.1038/s41598-025-87685-2.
[30] S. Zafar, N. Khalid, M. Daud, M.L. Mirza, Kinetic studies of the adsorption of thorium ions onto rice husk from aqueous media: linear and nonlinear approach, Nucleus 52 (1) (2015) 14–19, https://doi.org/10.71330/thenucleus.2015.659.
[31] Moussout, et al., Critical of linear and nonlinear equations of pseudo-first order and pseudo-second order kinetic models, Karbala Int. J. Modern Sci. 4 (2) (2018) 244–254, https://doi.org/10.1016/j.kijoms.2018.04.001.
[32] Seyed Ali Akbar Mansoori, Zoherboomi Reza, Hosseinzadeh Mohammad, Mansoori Seyed Mohammad, Jomekian Abolfazl, Sedaghat Sadegh, Ehsaninezhad Akbar, HSS anions reduction combined with the analytical test of aqueous MDEA in south pars gas complex, Natural Gas Industry B 9 (3) (2022) 318–324, https://doi.org/10.1016/j.ngib.2022.06.004.
[33] Joanna Wolska, Marek Bryjak, Removal of bisphenol a from aqueous solution by molecularly imprinted polymers, Sep. Sci. Technol. 49 (11) (2014) 1643–1653, https://doi.org/10.1080/01496395.2014.906459.
[34] Ghaffari, et al., Linear and nonlinear two-parameter adsorption isotherm modeling: a case-study, Int. J. Eng. Sci. 6 (9) (2017) 1–11, https://doi.org/10.9790/1813-0609010111.
[35] Joanna Wolska, Piotr Cyganowski, Tomasz Kożlecki, Fine polymer imprinted layers for the monitoring of bisphenol a in aqueous solutions, Sep. Sci. Technol. 53 (2) (2018) 206–218, https://doi.org/10.1080/01496395.2017.1385627.
[36] P.T. Sudheesh Kumar, G. Praveen, Mincy Raj, K.P. Chennazhi, R. Jayakumar, Flexible, micro-porous chitosan–gelatin hydrogel/nanofibrin composite bandages for treating burn wounds, RSC Adv. 4 (110) (2014) 65081–65087, https://doi.org/10.1039/C4RA11969J.
[37] Joanna Wolska, Katarzyna Smolinska-Kempisty, Marek Bryjak, Wojciech Kujawski, Polypropylene membranes with the double sensitivity effect, J. Appl. Polym. Sci. 132 (14) (2014) 99, https://doi.org/10.1002/app.41763.
[38] Katarzyna Smolinska, Marek Bryjak, Joanna Wolska, Wojciech Kujawski, Ph-sensitive membranes for lithium separation, Mater. Chem. Phys. 148 (3) (2014) 548–553, https://doi.org/10.1016/j.matchemphys.2014.08.003.

7.5. Określenie parametrów reakcji polimeryzacji cząstek typu rdzeń–otoczka z warstwą polimeru z odciskiem molekularnym wrażliwego na zmiany temperatury oraz ich zastosowanie do ekstrakcji w kolumnach SPE (Publikacja P5)

Rapacz D, Smolińska–Kempisty K, Wolska J. Eco friendly core–shell particles coated with molecularly imprinted polymers for S–metolachlor recognition and separation. Analytica Chimica Acta. 2025, vol. 1367, art. 344310, s. 1-10. https://doi.org/10.1016/j.aca.2025.344310.

Wprowadzenie

Piąty artykuł zatytułowany "**Eco friendly core–shell particles coated with molecularly imprinted polymers for S–metolachlor recognition and separation**" opublikowany w *Analytica Chimica Acta* opisuje cząstki typu rdzeń–otoczka (ang. core–shell) z warstwą polimeru molekularnie wdrukowanego wrażliwego na zmianę temperatury, selektywne w stosunku do S–metolachloru. W procesie nanoszenia warstwy MIPu na ziarna PVC, bazowano na opracowanym składzie mieszaniny reakcyjnej wykorzystanej do syntezy polimerów blokowych, przedstawionych w pierwszej pracy badawczej **P2**.

Wyniki

Polimery typu rdzeń–otoczka zsyntezowano wykorzystując ziarna poli(chlorku winylu), na które została naniesiona warstwa molekularnie wdrukowanych polimerów wykazujących odpowiedź na zmianę temperatury, selektywnych wobec S–metolachloru. Badania rozpoczęto od procesu dehydrochlorowania PVC, a następnie opracowano metodologię syntezy sorbentów. Rozważano następujące parametry: rodzaj rozpuszczalnika – organiczny izooktan lub przyjazną środowisku wodę, ilość naniesionych warstw polimeru, a także objętość mieszaniny reakcyjnej dodanej do ziaren PVC. Mieszaninę polimeryzacyjną sporządzono zgodnie z procedurą opisaną w pierwszej pracy badawczej **P2**. Skuteczność zsyntezowanych materiałów określono za pomocą oceny ich właściwości sorpcyjnych. Jako optymalne warunki wyselekcjonowano naniesienie jednej warstwy MIPu oraz wodę jako rozpuszczalnik. Uzyskane wartości sorpcji wynosiły 1,06 mg × g^{-1} dla CS–MIP oraz 0,82 mg × g^{-1} dla CS–NIP i cechowały się mniejszymi wartościami odchylenia standardowego niż w przypadku sorbentów zsyntezowanych z wykorzystaniem izooktanu, dla których wartość sorpcji dla CS–MIP była nieznacznie większa i wynosiła 1,07 mg × g^{-1}. Największą wartość sorpcji zaobserwowano dla materiałów z trzema warstwami naniesionego polimeru, równą 1,11 mg × g^{-1}. Jednakże różnice w wartościach sorpcji były na tyle niewielkie, że proces syntezy z zastosowaniem jednej warstwy polimeru uznano za najbardziej optymalny. Dodatkowymi zaletami była zmniejszona ilość używanych reagentów oraz skrócony czas niezbędny do przeprowadzenia rekcji.

Następnie sorbenty upakowano w kolumnach typu SPE i przeprowadzono proces sorpcji dynamicznej, dobierając czas inkubacji polimerów z roztworem S–metolachloru. Analizując otrzymane wyniki, stwierdzono, że najbardziej optymalnym rozwiązaniem jest kontaktowanie przez 30 minut. Dodatkowo scharakteryzowano proces sorpcji, przeprowadzając badania kinetyki oraz izoterm sorpcji. Najlepsze dopasowanie mechanizmu

adsorpcji uzyskano dla modelu izotermy Freundlicha, gdzie współczynnik korelacji wynosił 0,973 dla CS–MIP oraz 0,959 dla CS–NIP. Korzystną adsorpcję w tym modelu izotermy uzyskuje się, gdy wartość parametru 1/n, odnoszącego się do homogeniczności powierzchni, mieści się w przedziale od 0 do 1. Parametr ten jest równy 0,908 dla CS–NIP i 0,848 dla CS–MIP, co wskazało, że bardziej jednorodną powierzchnię posiadał układ referencyjny. Na podstawie badań kinetyki, oszacowano, iż sorpcja przebiega według modelu kinetyki pseudo–drugiego rzędu, podobnie jak w blokowych polimerach molekularnie wdrukowanych. Ponadto przetestowano selektywność sorbentów w stosunku do S–metolachloru. Zsyntezowany materiał sorbował S–metolachlor prawie czterokrotnie lepiej niż atrazynę, ponad dwukrotnie lepiej niż glifosat oraz około pięciokrotnie lepiej niż fenoksaprop–P–etylu, co wskazuje na dużą selektywność sorbentu. Ponadto polimery przetestowano na próbkach symulujących rzeczywiste, sporządzonych z wody z kranu, przeprowadzając sorpcję zarówno w trybie statycznym, jak i w dynamicznym.

Dobrane zostały warunki desorpcji zaadsorbowanych cząsteczek S–metolachloru z roztworu jednoskładnikowego. Jako eluent testowano wodę o temperaturze 4°C i 60°C oraz wodne roztwory etanolu o stężeniach 10, 20 i 30%. Najlepsze wyniki desorpcji, wynoszącej 19%, uzyskano dla 30% wodnego roztworu etanolu. Natomiast równie dobre rezultaty otrzymano wymywając S–metolachlor wodą o temperaturze 4°C – wartość pierwszej desorpcji była równa 15%. Mając na uwadze założenia tak zwanej „*zielonej chemii*” oraz przyjazność środowisku, uznano, iż desorpcja wodą o temperaturze 4°C będzie korzystniejszą metodą. W kolejnym kroku opracowano warunki desorpcji S–metolachloru w obecności innych środków ochrony roślin. Początkowo przeprowadzono desorpcję 10% wodnym roztworem etanolu, co pozwoliło na wymycie większości mikrozanieczyszczeń oraz jedynie 23% S–metolachloru. Następnie desorbowano S–metolachlor wodą o temperaturze 4°C, wykorzystując mechanizm „*smart*” PNIPAMu. Opracowano również równanie, pozwalające na określenie stężenia S–metolachloru w wodzie:

$$C = 6.66 \times D_{H2O},$$

gdzie D_{H2O} symbolizuje sumę stężeń S–metolachloru w dwóch procesach desorpcji wodą o temperaturze 4°C. Pełną charakterystykę sorbentów rozszerzono o widma IR, obrazy SEM oraz stopień pęcznienia. Spektroskopia IR potwierdziła, iż modyfikacja ziaren PVC przebiegła pomyślnie, a naniesione na ich powierzchnię warstwy MIPu i NIPu nie wykazują różnic w budowie chemicznej. Mikroskopia SEM zobrazowała morfologię oraz strukturę powierzchni sorbentów. Zarówno cząstki CS–MIP, jak i CS–NIP cechują się zbliżonym rozmiarem, a ich powierzchnia ma nieregularną strukturę i kształt. Obrazy SEM umożliwiły również zaobserwowanie naniesionej warstwy polimeru z odciskiem molekularnym na rdzeń PVC, co potwierdziło obecność tej warstwy i pozwoliło oszacować jej grubość. Stopień pęcznienia polimerów badano w temperaturze pokojowej, 4°C i 60°C. Uzyskane dane wskazały na brak zależności stopnia pęcznienia od temperatury, co prawdopodobnie może wynikać z obecności bardzo cienkiej warstwy polimeru na powierzchni rdzenia PVC.

Podsumowanie

Na podstawie wyników otrzymanych badań, stwierdzono, że polimery typu rdzeń–otoczka z warstwą molekularnie wdrukowanego polimeru, wykazujące odpowiedź na zmianę temperatury, są selektywne wobec S–metolachloru. CS–MIP sorbuje S–metolachlor około czterokrotnie lepiej niż atrazynę, ponad dwukrotnie lepiej niż glifosat oraz około pięciokrotnie lepiej niż fenoksaprop–P–etylu. Sorbenty zostały zsyntezowane również zgodnie z założeniami tak zwanej „*zielonej chemii*". Do reakcji, prowadzonej w temperaturze otoczenia, wykorzystano wodę jako rozpuszczalnik, a zregenerowane sorbenty były gotowe do ponownego wykorzystania. Badane materiały charakteryzowały się mniejszą różnicą w wartościach sorpcji pomiędzy MIPem i NIPem, w porównaniu do polimerów blokowych. Ich główną zaletą jest jednak mała ilość reagentów stosowanych podczas syntezy, co wynika z nanoszenia cienkiej warstwy polimeru na ziarna zmodyfikowanego PVC, a także skrócony czas sorpcji.

Analytica Chimica Acta 1367 (2025) 344310

Contents lists available at ScienceDirect

Analytica Chimica Acta

journal homepage: www.elsevier.com/locate/aca

Eco friendly core-shell particles coated with molecularly imprinted polymers for S-metolachlor recognition and separation

Dominika Rapacz *, Katarzyna Smolińska-Kempisty, Joanna Wolska

Wrocław University of Science and Technology, Department of Process Engineering and Technology of Polymer and Carbon Materials, Wybrzeże Wyspiańskiego 27, 50-370, Wrocław, Poland

HIGHLIGHTS

- Core-shell particles coated with MIPs for S-metolachlor recognition and separation.
- The sensor shows high selectivity for S-metolachlor in both real and model solutions.
- CS-MIP synthesis in accordance with the principles of green chemistry.

GRAPHICAL ABSTRACT

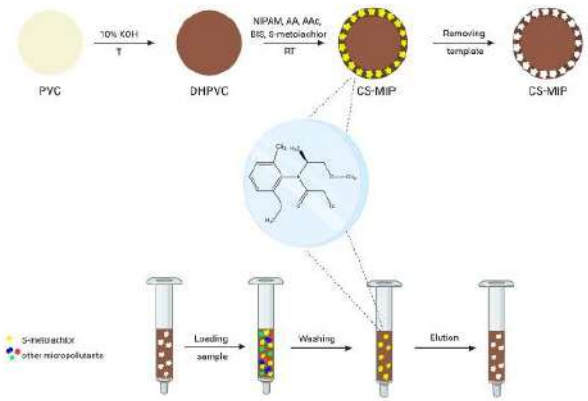

ARTICLE INFO

Keywords:
Green molecularly imprinted polymers
Smart polymers
S-metolachlor
Sorption process
Core-shell polymers
Solid phase extraction

ABSTRACT

Background: The presence of a variety of micropollutants in aquatic environments is currently resulting in a significant degree of deterioration in water quality. Furthermore, these micropollutants can be found in concentrations ranging from ng to μg per liter, which frequently fall below the detection limit for the relevant analytes. This renders the analysis considerably more complex and time-consuming. The present work proposes the utilization of molecularly imprinted polymers applied to poly(vinyl chloride) (PVC) particles, thereby creating a novel materials for the detection of S-metolachlor, synthesized according to *green chemistry* principles. *Results:* The sorbents obtained were then tested for the suitability of the appropriate sorption model. The adsorption isotherms were subsequently fitted using the Freundlich, Langmuir and Dubinin-Radushkevich models. This indicated that the Freundlich model was the most suitable. The maximum adsorption capacity, as calculated according to the Freundlich isotherm model, was estimated to be 6.24 and 3.12 mg × g^{-1}, for core-shell molecularly imprinted polymers, and core-shell non-imprinted polymers, respectively. The data obtained from the kinetic study were fitted to the pseudo-first-order and pseudo-second-order models, with the pseudo-second-order model providing the best fit. The obtained material exhibit high selectivity for S-metolachlor,

* Corresponding author.
E-mail address: dominika.rapacz@pwr.edu.pl (D. Rapacz).

https://doi.org/10.1016/j.aca.2025.344310
Received 25 February 2025; Received in revised form 2 June 2025; Accepted 6 June 2025
Available online 8 June 2025

absorbing it approximately 5 times than fenoxaprop-P-ethyl, 4 times better than atrazine, and 2 times than glyphosate. The sorbents successfully absorbed S-metolachlor from both model solutions and real samples.
Significance: Sample preparation for determination of individual analytes, especially from micropollutant solutions, is a challenge for modern analytical chemistry. The utilization of core-shell particles coated with molecularly imprinted polymers for the separation of S-metolachlor has the potential to enhance the methodology for the determination of this herbicide from multicomponent solutions, thereby markedly reducing analysis time.

1. Introduction

The acceleration of urbanization and technological development across a range of industries, coupled with the increase in the diversity of pollutants present in water environments, has resulted in an enhanced necessity to monitor these pollutants. The presence of a variety of chemical substances in water has been identified, including pharmaceuticals, surfactants [1], heavy metals, metalloids, plant protection products (such as pesticides and herbicides), endocrine-disrupting chemicals (EDCs), and personal care products. The concentrations of microcontaminants present in water samples frequently lie below the limits of detection, with levels ranging from $ng \times L^{-1}$ to $\mu g \times L^{-1}$ [2]. It is of the utmost importance to determine the presence of these substances in order to prevent their accumulation and to protect human health and the environment [3].

A wide range of techniques have been developed for the detection of small quantities of compounds. These include high-performance liquid chromatography, gas chromatography, liquid chromatography-mass spectrometry/mass spectrometry [4], biological detection, and immunological approaches. Nevertheless, these methods have inherent drawbacks and limitations, such as a lengthy processing time, the necessity for highly skilled personnel, and the subsequent elevated costs associated with analysis [5]. The residual concentration of micropollutants present in water makes it necessary to enrich and concentrate the samples. One of the most frequently employed techniques for preparation of solutions is solid-phase extraction (SPE) [6]. Nowadays, the commonly used solid-phase extraction cartridges in the laboratory are predominantly silica-based cartridges represented by C18, polymer - based cartridges, and mixed-type strong cation cartridges [7].

Nevertheless, classic SPE sorbents lack selectivity, a property that has led to a growing reliance on molecularly imprinted polymers (MIPs) [8–11], which have recognition cavities that are perfectly matched in shape, size and functionality to the target molecule and due to are capable of retaining analytes through specific interactions [12]. MIPs present a variety of advantages such as easy of production, reusability, low-cost, improved thermal and chemical stability and short synthesis time [13,14]. Nevertheless, MIPs also exhibit several drawbacks, including an uneven distribution of binding sites, the presence of deeply embedded cavities, an irregular surface morphology, destroyed binding sites, and the incomplete removal of template molecules [15,16]. These limitations can be surmounted by virtue of the distinctive structure of the core-shell particles, which comprises the deposition of a thin layer of molecularly imprinted polymer on the solid core of the molecule. This results in a large surface area with a uniform distribution of binding sites, which facilitates the removal of analyte molecules and the subsequent re-binding of the target molecule [17].

Smart materials are type of functional materials capable of responding to external stimuli such as temperature, pH, light, and ionic strength. One thermosensitive polymer that has been widely described and studied is poly(N-isopropylacrylamide) (PNIPAM) [18]. PNIPAM is capable of undergoing sudden alterations in its conformations in response to changes in temperature. The reduction in solubility that occurs with an increase in temperature is a phenomenon known as the lower critical solution temperature (LCST). A reduction in temperature will result in the solution becoming more transparent due to the formation of a single phase. The aqueous solution of PNIPAM undergoes a transition from a coil to a globule structure upon heating. At temperatures below the LCST (32 °C), the PNIPAM chains adopt a coil configuration due to the hydrogen bonding of amide groups with water [19].

Herbicides are chemical substances that are employed for the purpose of preventing or inhibiting the growth of plants, or for the destruction of weeds in agricultural fields [20]. S-metolachlor is a pre-emergent herbicide used for controlling grasses and broadleaf weeds in over 70 crops worldwide [21]. The objective of sustainable agriculture is not to eradicate environmental disturbance but to guarantee that the environmental dynamics of disturbance and recovery remain within acceptable limits. Furthermore, it aims to achieve a balance between environmental conservation, agricultural production, farm profit and community well-being [22].

In accordance with the above theory, a layer of molecularly imprinted polymers was applied on a poly(vinyl chloride) core, thereby creating a core-shell MIP with the capacity to selectively detect S-metolachlor from water samples. Moreover, the synthesis was conducted in accordance with the conceptualization of GREENIFICATION. This entailed conducting polymerization in mild conditions at room temperature, thereby reducing the amount of energy required. In addition, water was utilized as a porophore instead of the conventional organic solvents, which are often toxic. Moreover, the materials obtained were synthesized according to the concept of self-cleaning MIPs, thereby leading to a reduction in waste generation. MIPs were synthesized by using S-metolachlor as template, N-isopropylacrylamide, acrylamide and acrylic acid as a functional monomers, respectively. Core-shell MIPs was employed as adsorbents to extract molecules from the solution mixture through SPE. The samples were analyzed by high performance liquid chromatography. Consequently, a novel methodology that enables rapid analysis of S-metolachlor at a reduced cost has been developed.

2. Materials and methods

2.1. Reagents and chemicals

Acrylamide (AA) was obtained from Thermo Scientific Chemicals. Acrylic acid (AAc) were supplied by Acros Organics. Ammonium persulfate (APS), N-isopropylacrylamide (NIPAM), N, N′- methylenebis (acrylamide) (BIS), N, N, N′, N′- tetramethylethylenediamine (TEMED), isooctane, and potassium hydroxide (KOH) were provided by Sigma-Aldrich. Ethyl alcohol (EtOH) and isopropyl alcohol was supplied by POCH S.A. S-metolachlor (SMCh) was obtained from NOVAGRA. Poli (vinyl chloride) (Ongrovil® S-5167) was provided by BorsodChem, with medium molecular weight, and with a K value (an indicator of molecular weight) of 66–68. The HPLC grade acetonitrile was purchased from CHEMSOLUTE. Ultrapure water was obtained with a Milli-Q System (Merck Millipore).

2.2. Dehydrochlorination of PVC

The dehydrochlorination of PVC was performed according to the methodology described by Wolska et al. [23] In brief, a total of 67.5 g of PVC was dispersed in 500 mL of 10 % KOH solution of isopropyl alcohol–water (4:1 w/w). This mixture was heated to the boiling point under the reflux condenser for 24 h. The color of the reaction mixture was changed from colorless to dark brown during the reaction. Then,

degraded PVC was filtered and washed with a large excess of water and finally with ethanol. The obtained product was extracted with ethanol for 24 h. After extraction, DHPVC was dried at 60 °C in a dryer.

2.3. Preparation of core-shell polymers

The most favorable results were obtained for core-shell polymers synthesized in accordance with the following methodology. About 2 g of PVC after previously described modification was mixed with the polymerization mixture. The monomer composition for the preparation of the polymer layer was selected on the basis of our previous studies [24]. A water solution of 3 mL of reaction mixture, comprising NIPAM (1.06 mmol), AA (1.39 mmol), AAc (0.10 mmol), S-metolachlor (0.08 mmol) and BIS (0.70 mmol), was contacted with 2 g of PVC for a total of 30 min. Subsequently, 7 mL of water was added to the mixture and the solution was allowed to stand for 10 min. The mixture was purged with nitrogen for a total of 3–5 min, during which 2.5 mL of the initiator solution (APS, 0.17 mmol, and TEMED 0.13 mmol), were introduced. The reaction was conducted for 24 h on a stirrer at ambient temperature. The core-shell polymers were washed with water on a G-1 funnel, then extracted for 24 h in a Soxhlet apparatus using ethanol, followed by drying at 40 °C. Non-imprinted polymers (NIPs) were synthesized similarly but without template molecules.

2.4. Analytical and characterization methods

2.4.1. High performance liquid chromatography

High performance liquid chromatography (HPLC) system (Shimadzu high performance liquid chromatograph model SCL-40) equipped with an autosampler (model SIL-40), a PDA detector and a chromatographic column (3 μm ARION® Biphenyl, 150 × 4.6 mm) was used. Isocratic elution was performed at 30 °C using a mixture of water and acetonitrile (50:50 v/v) as the mobile phase. The mobile phase was degassed by sonication for 10 min. A flow rate of 1 mL × min^{-1} was maintained, with an injection volume of 30 μm and a detection wavelength of 254 nm.

2.4.2. Fourier-transform infrared spectroscopy

Fourier transform infrared spectra (FT-IR) were performed in the 400-4000 cm^{-1} range to characterize the presence of functional groups in the sorbent materials. The spectral data were collected on a Jasco FT-IR-4700 spectrophotometer using 64 scans at a resolution of 4 cm^{-1}.

2.4.3. Scanning electron microscopy

The surface morphology of the CS-MIP and CS-NIP sorbents was characterized using a Quanta 250 (FEI) scanning electron microscope (SEM). Prior to analysis, samples were sputtered with a 10–15 nm thick layer of gold. The analysis were carried out using a Large Field Detector (LFD) in the environmental scanning electron microscope (ESEM) mode at an accelerating voltage of 15 kV, pressure of approximately 60 Pa, with a sample inclination of 60°.

2.5. Optimizing the condition of the synthesis

To optimize all of the following synthesis conditions, solvent and number of polymer layers applied to the core, the sorption process was carried out in the same way. For this purpose, approximately 0.2 g of the sorbents (core-shell molecularly imprinted polymers and core-shell non-imprinted polymers) were weighed and mixed with 20 mL of 30 mg × L^{-1} S-metolachlor solution for 24 h. The concentration of the solution after sorption was then determined by HPLC.

2.6. Optimization of the time of the absorption process on SPE columns

Approximately 0.200 ± 0.001 g of CS-MIP or CS-NIP was placed into SPE column and activated with water. Subsequently, the sorbent was incubated with a 10 mg × L^{-1} solution of S-metolachlor for periods of time ranging between 1 and 180 min. The concentration of the solution was determined by HPLC.

2.7. Sorption study

The specificity and efficiency of the core-shell molecularly imprinted polymers was determined by measuring the sorption of S-metolachlor. During the batch mode sorption process, 0.200 ± 0.001 g of the sorbent was placed into the flask and mixed with the S-metolachlor solution at room temperature for 24 h. Subsequently, the solution was filtered through a 0.45 μm cellulose syringe filter in order to separate it from the nanoparticles. Then the solution was analyzed by HPLC, utilizing the previously described analytical parameters. The sorption capacity was calculated as the following equation (Eq. (1)):

$$q = \frac{(C_i - C_{eq}) \times V}{m} \quad \text{(Eq. 1)}$$

where C_i and C_{eq} (mg × L^{-1}) represent the initial and equilibrium concentrations of S-metolachlor, respectively, V (L) denotes the volume of the solution, while m (g) symbolizes the mass of the sorbent [25].

2.7.1. Kinetics of adsorption

The kinetics of the adsorption process were investigated using 250 mL of a solution of S-metolachlor with a concentration of 30 mg × L^{-1} and a mass of the sorbent (CS-MIP and CS-NIP) of 2.5 g. The experiment was conducted at room temperature, with the concentration of the samples taken at different time intervals (from 5 to 180 min) determined using HPLC methods.

2.7.2. Sorption isotherms

To determine the sorption isotherm of CS-MIP and CS-NIP, 0.200 ± 0.003 g of polymers were placed in the flask, and 20 mL of solutions with a concentration range of 10–200 mg × L^{-1} of S-metolachlor were added. The samples were shaken for 24 h at 22 ± 2 °C and subsequently filtered using a syringe filter. The equilibrium concentration of S-metolachlor was determined using HPLC.

2.7.3. Competitive study

In order to ascertain the binding selectivity, approximately 0.200 ± 0.001 g of sorbent (CS-MIP or CS-NIP) was placed into a flask. Subsequently, the 20 mL of solution comprising a combination of plant protection products, namely atrazine, glyphosate, fenoxaprop-P-ethyl, and S-metolachlor, with a concentration of 10.78, 8.45, 18.09, and 14.19 mg × L^{-1}, respectively, was added. The concentration of the solution was determined by HPLC.

2.7.4. Sorption from reals samples

The sorption study was conducted on the model sample and solution, which were designed to simulate the real sample. For this purpose, approximately 0.200 ± 0.001 g of sorbent (CS-MIP or CS-NIP) was introduced into a 1 mL SPE column and activated with water. Thereafter, the column was incubated for 30 min with 1 mL of a S-metolachlor solution with a concentration of 10 mg × L^{-1}. The concentration of the solution was determined by HPLC. The same analyses were carried out in the batch mode type of sorption. For this, approximately 0.200 ± 0.001 g of sorbent (CS-MIP or CS-NIP) was introduced into the flask and mixed for 24 h with 20 mL of S-metolachlor solution at a concentration of 10 mg × L^{-1}. The concentration of the solution after sorption was determined by HPLC.

2.8. Desorption process

The desorption process of the absorbed analytes was conducted using SPE columns. To achieve this, the CS-MIP or CS-NIP sample, after the sorption process, was subjected to a regenerating solution, and the

Table 1
Optimizing the condition of the synthesis process.

Type of solvent	Number of polymer layers	core-shell molecularly imprinted polymers sorption (mg × g^{-1})	core-shell non-imprinted polymers sorption (mg × g^{-1})
isooctane	1	1.074 ± 0.029	0.808 ± 0.011
	3	0.871 ± 0.007	0.756 ± 0.024
	6	1.072 ± 0.016	1.070 ± 0.019
distilled water	1	**1.063 ± 0.002**	**0.815 ± 0.024**
	3	1.112 ± 0.053	0.784 ± 0.010
	6	1.111 ± 0.045	1.092 ± 0.011

desorption calculated according to following equation (Eq. (2)). The deposit was incubated with 1 mL of the solution for the period of 20 min.

$$D = \frac{C_{(i;j)} \times V}{m} \quad \text{(Eq. 2)}$$

where $C_{(i;j)}$ (mg × L^{-1}) represents the concentration (i – S-metolachlor, j – other plant protection products), V (L) symbolizes the volume of the regenerating solution, m (g) represents the mass of CS-MIP or CS-NIP.

Additionally, the regeneration factor (RF) of the deposit was estimated in accordance with the following equation (Eq. (3)).

$$RF = \frac{m_e}{m_a} \times 100\% \quad \text{(Eq. 3)}$$

where m_e (mg) symbolizes mass of eluted S-metolachlor, m_a (mg) represents mass of absorbed S-metolachlor.

2.9. Degree of swelling

The swelling study was carried out in distilled water at room temperature, 60 °C and at 4 °C. The sorbents were firstly incubated in water for 24 h, following which they were subjected to a centrifugation process. Thereafter, the wet mass of each sorbent was weighed. Subsequent to this, the samples were dried to constant mass and weighed again. The swelling ability was estimated using the following equation (Eq. 4.).

$$DS = \frac{m_w - m_d}{m_d} \times 100\% \quad \text{(Eq. 4)}$$

Where m_w and m_d (g) represents mass of wet and dry sorbent, respectively [26].

3. Results and discussion

3.1. Optimizing the condition of the synthesis process

3.1.1. Selection of the solvent for the synthesis

Parameters investigated to optimize the synthesis conditions included the solvent used for synthesis and the number of polymer layers applied to the poly(vinyl chloride) core. Two solvents were selected for the study on the basis of their environmentally friendly properties: isooctane and distilled water. The core-shell synthesis was conducted in accordance with the methodology outlined in section 2.3. However, following the contact polymerization of the mixture with PVC, one sample was added isooctane and the other distilled water. The subsequent steps of the synthesis were then performed. Subsequently, the sorption process was undertaken in order to compare the sorption properties.

3.1.2. Optimizing the number of polymer layers applied to the core

The number of polymer layers applied to the PVC core was also investigated. For this purpose, a variety of numbers of polymer layers synthesized as described in section 2.3. were applied to the PVC core, and then a static sorption process was carried out. The obtained results are presented in Table 1.

Table 2
The data of the optimization of sorption times.

Time (min)	CS-MIP sorption (mg × g^{-1})	CS-NIP sorption (mg × g^{-1})
1	0.007 ± 0.003	0.004 ± 0.003
3	0.006 ± 0.004	0.007 ± 0.006
5	0.020 ± 0.019	0.019 ± 0.018
10	0.021 ± 0.015	0.021 ± 0.017
15	0.026 ± 0.012	0.022 ± 0.011
20	0.021 ± 0.017	0.021 ± 0.014
30	**0.035 ± 0.001**	**0.030 ± 0.001**
45	0.033 ± 0.001	0.032 ± 0.001
60	0.035 ± 0.001	0.030 ± 0.001
90	0.037 ± 0.001	0.034 ± 0.001
120	0.042 ± 0.001	0.036 ± 0.001
160	0.037 ± 0.001	0.031 ± 0.001

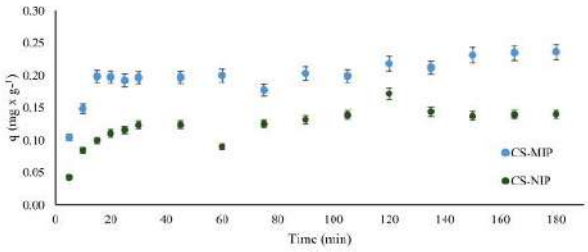

Fig. 1. The sorption kinetics of CS-MIP and CS-NIP.

The minimal discrepancy in sorption values for core-shell molecularly imprinted polymers and core-shell non-imprinted polymers for sorbents synthesized with water and isooctane indicated that water would be a preferable solvent for syntheses in accordance with green chemistry principles. Furthermore, it was established that the optimal number of layers would be one, as all the cavities formed are available for the sorption of S-metolachlor. For further studies, a molecularly imprinted polymers core-shell material, synthesized using water as a solvent and with one layer of polymer applied, designated CS-MIP (for the molecularly imprinted polymer applied on the PVC core) and CS-NIP (for the polymer without molecular imprint applied on the PVC core), was selected as the optimal material for the purposes of this investigation. Moreover, the sorption of S-metolachlor by PVC under aforementioned conditions was calculated to be 0.750 ± 0.021 mg × g^{-1}, indicating that CS-NIP sorbs S-metolachlor to a minimal extent.

3.2. Optimization of the sorption conditions on SPE columns

One of the parameters that has been subjected to optimization in the process of determining the concentration of S-metolachlor is the incubation time of the sorbent with the solution. The sorption results obtained after different incubation times are presented in Table 2.

30 min incubation time was identified as the optimal period for analysis of the presented data. Following this time, a distinction in sorption values between CS-MIP and CS-NIP became repeatable. Furthermore, the results exhibited enhanced reproducibility compared to earlier analyses. Following 30 min incubation duration, the difference in sorption between the CS-MIP and CS-NIP samples remains consistent, and the sorption value shows minimal variation. Accordingly, in order to achieve a reduced analysis time, it was determined that 30 min incubation time represents the optimal condition for this procedure.

3.3. Kinetics of adsorption

Mathematical equations, known as adsorption kinetic models, can be used to describe the rate at which a solute is adsorbed onto a surface. In order to elucidate the mechanisms of sorption kinetics, the data

Table 3
Parameters estimated from pseudo-first-order and pseudo-second-order kinetics models.

	Pseudo-first-order model			Pseudo-second-order model		
	k_1 (1 × min^{-1})	R^2	q_{eq1} (mg × g^{-1})	k_2 (g × (mg × min)$^{-1}$)	R^2	q_{eq2} (mg × g^{-1})
CS-MIP	0.018	0.685	0.011	0.306	0.975	0.222
CS-NIP	0.026	0.831	0.007	0.597	0.969	0.151

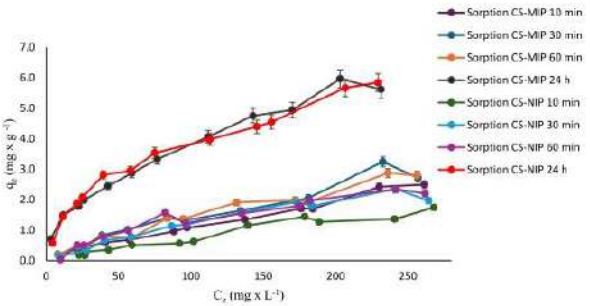

Fig. 2. The adsorption isotherms of CS-MIP and CS-NIP at different time.

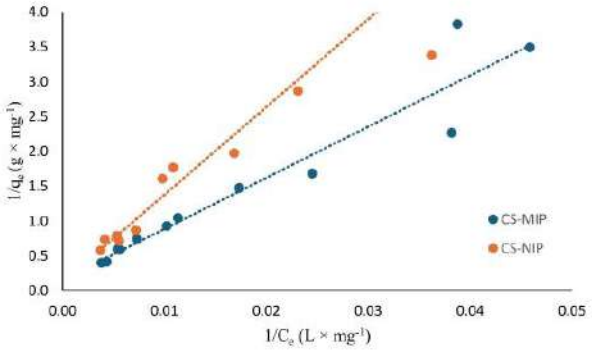

Fig. 3. Linear fit to the Langmuir isotherm model.

collected and presented in Fig. 1, were fitted to pseudo-first-order and pseudo-second-order kinetic models. The estimated parameters are outlined in Table 3.

The pseudo-first-order model is predicated on the assumption that the rate of sorption is directly proportional to the difference between the saturation concentration and the amount of solid uptake over time [27]. The linear form of the pseudo-first-order model is presented in the following equation (Eq. (5)). The rate constant k_1 was calculated from the $log\left(q_{eq} - q_t\right)$ versus time plot [28].

$$\log\left(q_{eq} - q_t\right) = \log\left(q_{eq}\right) - \frac{k_1 t}{2.303} \quad \text{(Eq. 5)}$$

where k_1 (1 × min^{-1}) represents sorption rate constant, q_{eq} and q_t (mg × g^{-1}) symbolizes the amount of adsorbate adsorbed at equilibrium time and at time t, respectively.

In the pseudo-second-order model, the process is under the control of the chemical sorption reaction at the liquid-solid interface in the adsorbent, which allows for the estimation of the behavior over the entire adsorption range. The linear form of the pseudo-second-order model is described in terms of the following equation (Eq. (6)). The rate constant k_2 was determined from a plot of $\frac{t}{q_t}$ versus time [27].

$$\frac{t}{q_t} = \frac{1}{k_2 q_{eq}^2} + \frac{1}{q_{eq}} t \quad \text{(Eq. 6)}$$

where k_2 (g × (mg × min)$^{-1}$) symbolizes sorption rate constant, q_{eq} and q_t (mg × g^{-1}) represents the amount of adsorbate adsorbed at equilibrium time and at time t, respectively.

The results showed that the pseudo-second-order equation was the best fitting model for both CS-MIP and CS-NIP (R^2 = 0.975 and 0.969 respectively) and the data obtained from this model were more reasonable. The q_{max} values calculated in accordance with the pseudo-second-order model are markedly closer to the sorption values derived from the conducted experiment. Analysis of k_1 and k_2 values shows the material on which the sorption process was more effectively. For both CS-MIP and CS-NIP, the sorption rate constant k_2 for the pseudo-second-order kinetic model is higher than the rate constant k_1 for the pseudo-first-order model.

3.4. Sorption isotherms

There exist a several types of adsorption isotherm models, each of which describes a specific aspects of the adsorption process. The obtained isothermal data were fitted to the Langmuir, Freundlich, and Dubinin–Radushkevich models. The adsorption isotherms were conducted in a series of experiments over time in order to identify the optimal conditions (Fig. 2).

For further, more detailed adjustments, the 10-min sorption isotherms were selected due to the largest difference between the sorption of CS-MIP and CS-NIP in the entire concentration range.

Table 4
Parameters estimated for the Langmuir isotherm model.

Model		R^2	q_m (mg × g^{-1})	K_L (L × mg^{-1})
Linear form of Langmuir	CS-MIP	0.917	6.614	0.014
	CS-NIP	0.908	8.772	0.008

3.4.1. Langmuir isotherms

The Langmuir isotherm model postulates the formation of a monolayer of molecules on the surface of the adsorbent. Furthermore, a fixed number of adsorption sites are available on the surface of the sorbent, and all binding sites are identical and interact with the same energy. The mathematical linear form of the model is defined by the following equation (Eq. (7)):

$$\frac{1}{q_e} = \frac{1}{q_m K_L C_e} + \frac{1}{q_m} \quad \text{(Eq. 7)}$$

where q_e symbolizes the absorption capacity at equilibrium (mg × g^{-1}), q_m represents the maximum adsorption capacity (mg × g^{-1}), K_L denotes Langmuir parameter – the affinity of the adsorption sites (L × mg^{-1}), and C_e symbolizes the equilibrium concentration of adsorbate (mg × L^{-1}) [28]. The linear fitting of the isotherm to the Langmuir model is presented in Fig. 3, and the values of the estimated parameters are summarized in Table 4.

3.4.2. Freundlich isotherms

The Freundlich isotherms model is characterized by monolayer heterogeneous adsorption of the adsorbate on the surface of the adsorbent, wherein no interaction occurs between the adsorbed ions. The mathematical linear form of this model is described by the following equation (Eq. (8)):

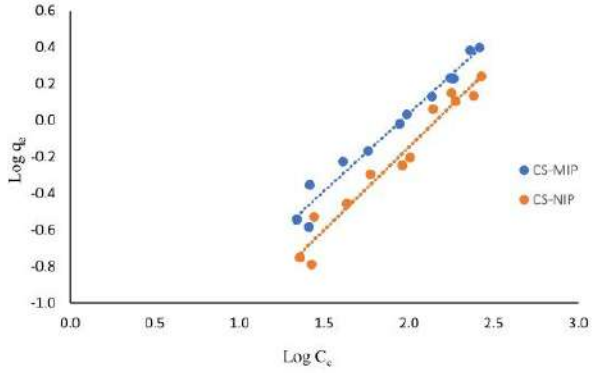

Fig. 4. Linear fit to the Freundlich isotherm model.

Table 5
Parameters estimated for the Freundlich isotherm model.

Model		R^2	K_F (mg × g^{-1})	$1/n$
Linear form of Freundlich	CS-MIP	0.973	6.243	0.848
	CS-NIP	0.959	3.121	0.908

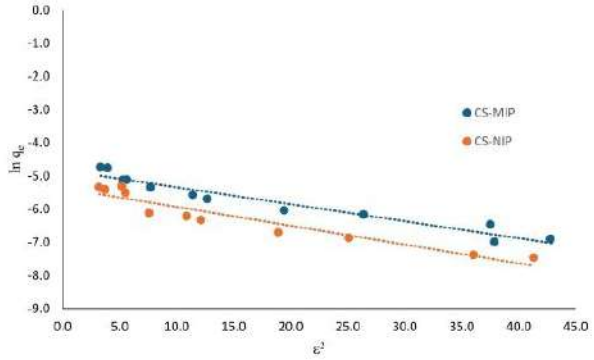

Fig. 5. Linear fit to the Dubinin– Radushkevich isotherm model.

$$log\ q_e = \frac{1}{n}\ log\ C_e + log\ K_F \quad \text{(Eq. 8)}$$

where q_e represents the absorption capacity at equilibrium (mg × g^{-1}), K_F symbolizes the Freundlich constant related to adsorption capacity (mg × g^{-1}), $\frac{1}{n}$ represents a constant revealing the adsorption process strength, C_e symbolizes the equilibrium concentration of adsorbate (mg × L^{-1}) [29]. The linear fitting of the isotherm to the Freundlich model is presented in Fig. 4, and the values of the estimated parameters are summarized in Table 5.

3.4.3. Dubinin– Radushkevich isotherms

The Dubinin-Radushkevich isotherms investigate the interactions between the adsorbate and the sorbent, with the objective of distinguishing between the mechanisms of chemisorption and physisorption. The linear mathematical formulation of this model is given as follow (Eq. (9)):

$$lnq_e = lnq_m - K_{DR}\varepsilon^2 \quad \text{(Eq. 9)}$$

where q_e symbolizes the absorption capacity at equilibrium (mg × g^{-1}), q_m represents the maximum adsorption capacity (mg × g^{-1}), K_{DR} symbolizes the activity coefficient related to free adsorption energy (mol^2 × kJ^{-2}), and ε represents the Polanyi potential (kJ × mol) [30]. The linear fitting of the isotherm to the Dubinin– Radushkevich model is illustrated in Fig. 5, and the values of the calculated parameters are provided in Table 6.

Table 6
Parameters estimated for the Dubinin– Radushkevich isotherm model.

Model		R^2	q_m (mg × g^{-1})	K_{DR} (mol^2 × kJ^{-2})
Linear form of Dubinin–Radushkevich	CS-MIP	0.937	0.008	4.828
	CS-NIP	0.906	0.005	5.365

Table 7
Competitive study data.

Parameter	S-Metolachlor	Atrazine	Glyphosate	Fenoxaprop-P-ethyl
K_{MIP}	11.71	0.62	8.83	2.49
K_{NIP}	4.08	0.79	6.92	4.30
IF	2.87	0.79	1.28	0.58
S	–	3.64	2.25	4.95

The high *IF* value for S-metolachlor in comparison to other plant protection products provides confirmation of the strong affinity of S-metolachlor for MIP. The results demonstrated that selectivity factors exceeding 1.0 indicated a notable improvement in the inherent selectivity of the polymer, which was enhanced through the imprinting process.

The subsequent order of preference (from best to worst fit) with reference to R^2 is Freundlich > Dubinin–Radushkevich > Langmuir. The results substantiate the appropriateness of the Freundlich model for elucidating the adsorption of S-metolachlor. The favorable adsorption in Freundlich isotherm model is obtained when the values of $1/n$ is in the range of 0–1. A value closer to 1 indicates a more homogeneous surface, denoting that NIP surfaces are more homogeneous than MIP surfaces. Furthermore, the value of the Freundlich constant in relation to the adsorption capacity most closely correlates with the sorption values for the investigated CS-MIP and CS-NIP materials.

3.5. Competitive study

A competitive study was evaluated to compare the binding efficiency of S-metolachlor and other herbicides commonly used in maize crops. The obtained results are summarized in Table 7.

One of the parameters used to assess recognition selectivity is the distribution coefficient ($K_{i(j)}$), which demonstrates the difference in concentration (*i* – S-metolachlor, *j* – other plant protection products) in solution before and after absorption, calculated according to the following equation (Eq. (10)):

$$K_{i(j)} = \frac{q_{i(j)} \times \rho}{C_{i(j)eq}} \quad \text{(Eq. 10)}$$

Where $q_{i(j)}$ (µg × g^{-1}) symbolizes the sorption capacity (*i* – S-metolachlor, *j* – other plant protection products), $C_{i(j)eq}$ (µg × L^{-1}) represent the equilibrium concentration (*i* – S-metolachlor, *j* – other plant protection products, and ρ (g × L^{-1}) denoted the density of the solution [23].

The efficiency of the imprint on the matrix molecule is determined by the imprinting factor (*IF*). It is calculated as the ratio of the particular analyte's distribution on the polymer with molecular imprint as well as polymer without molecular imprint, under the same conditions (Eq. (11)).

$$IF = \frac{K_i^{MIP}}{K_i^{NIP}} \quad \text{(Eq. 11)}$$

where $K_{i(j)}$ symbolizes the distribution coefficient (*i* – S-metolachlor, *j* – other plant protection products) of an analyte on an imprinted polymer

Table 8
The sorption data for S-metolachlor in both real and model solutions.

	CS-MIP	CS-NIP
Sorption from the real solution – dynamic mode (mg × g^{-1})	0.038 ± 0.001	0.032 ± 0.001
Sorption from the real solution – batch mode (mg × g^{-1})	0.470 ± 0.021	0.407 ± 0.030

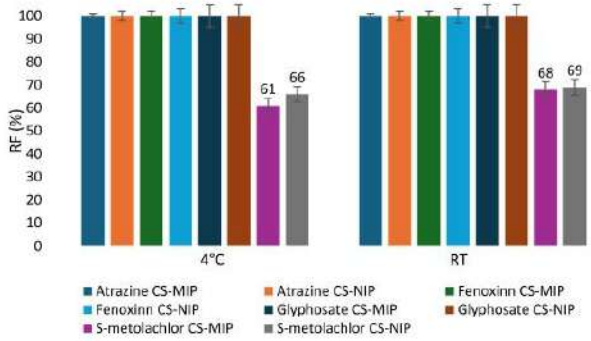

Fig. 6. Desorption of analytes using pure ethanol.

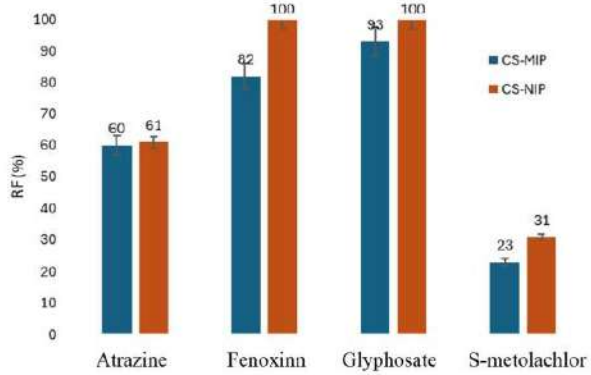

Fig. 7. Desorption of analytes using 10 % ethanol solution.

(K^{MIP}) and a non-imprinted polymer (K^{NIP}) [23].

The selectivity factor (S) was calculated as (Eq. (12)):

$$S = \frac{IF_i}{IF_j} \quad \text{(Eq. 12)}$$

where IF_i and IF_j represent imprinting factor of the S-metolachlor and other herbicides, respectively [23].

3.6. Sorption from reals samples

In this work, two different types of samples were subjected to analysis. S-metolachlor solution was prepared using distilled water, and a second solution was prepared with tap water, representative of the samples that would be encountered in a real-world setting. The pH of the tap water solution was set to approximately 5, reflecting the pH of distilled water. The selection of pH conditions for real solutions was described in our previous work [24]. The sorption data are presented Table 8.

The sorption values obtained in batch mode are higher than those obtained in dynamic mode, which can be attributed to the longer contact time. However, the CS-MIP and CS-NIP sorption ratio is maintained the same, indicating the better sorption properties of CS-MIP.

Table 9
Desorption data for different eluting solutions.

	CS-MIP	CS-NIP
RF (%) – desorption with 10 % EtOH	6 ± 1	7 ± 1
RF (%) – desorption with 20 % EtOH	14 ± 2	17 ± 1
RF (%) – desorption with 30 % EtOH	19 ± 1	19 ± 2
RF (%) – desorption with water 4°C	**15 ± 2**	**17 ± 3**
RF (%) – desorption with water 60 °C	10 ± 2	10 ± 1

3.7. Desorption

The key to detecting a single compound from a mixture is to remove all other chemicals present in the water. The idea behind this process was to desorpte other pesticides left after the filtration process. In this way, only the metolachlor selectively bound to the imprints remained in the polymer structure, the rest of micropollutants would be removed. In order to optimize the process conditions for purging the column of residual plant protection products, regeneration solutions of pure ethanol (Fig. 6) and 10 % aqueous ethanol solution (Fig. 7) were tested.

The analytes were desorbed using pure ethanol as a regeneration solution, at temperatures of 4 °C and at room temperature. The use of the EtOH regeneration solution permitted the complete elution of the residual plant protection products. However, it also resulted in the desorption of approximately 70 % of the S-metolachlor. As the desorption was non-selective, it was decided to use a 10 % ethanol solution.

The application of double desorption with a 10 % aqueous ethanol solution proved an effective method for the removal of the majority of impurities from the deposit. However, the S-metolachlor remained present in the matrix and in specific cavities. Subsequently, the desorption of S-metolachlor was carried out using the smart PNIPAM mechanism, with water at a temperature of 4 °C employed as the regenerating solution. Furthermore, the effect of ethanol addition to the aqueous elution solution and changes in the temperature of the water used after the removal of other impurities from the SPE column, on the value of the regeneration factor was also investigated. The outcomes of the sum of two desorption processes are presented in Table 9.

Given that the difference between desorption with water and desorption with ethanol is not significant, the desorption process with cold water was selected as the optimal condition. This aligns with the intelligent mechanism of PNIPAM and the principles of *green chemistry*, thus making this method eco-friendly. Moreover, this method allows for monitoring of S-metolachlor concentration, eliminating the need for complete desorption. In order to determine the real concentration of S-metolachlor present in a sample, the following equation (Eq. (13)) should be employed:

$$C = 6.66 \times D_{H2O} \quad \text{(Eq. 13)}$$

where C (mg × L^{-1}) symbolizes the concentration of S-metolachlor, D_{H2O} (mg × L^{-1}) represents the sum of the concentration of S-metolachlor in two desorption processes with water at 4 °C.

Moreover, the same sorbent can be reused. For this purpose, a twice wash with ethanol is required to remove any remaining contaminants, followed by nine additional desorption cycles with cold water. The RF factor for the CS-MIP sorbent was determined to be 83 ± 7 %, while that for CS-NIP was 94 ± 5 %. As an alternative, the deposit can be regenerated through the use of 100 % ethanol, which requires a four washing cycles. In this method, the RF factor for the CS-MIP was found to be 89 ± 11 %, while for CS-NIP it was 87 ± 11 %.

3.8. Method validation

The analytical characteristics of the HPLC method, such as limit of detection (LOD), limit of quantification (LOQ), linearity range and

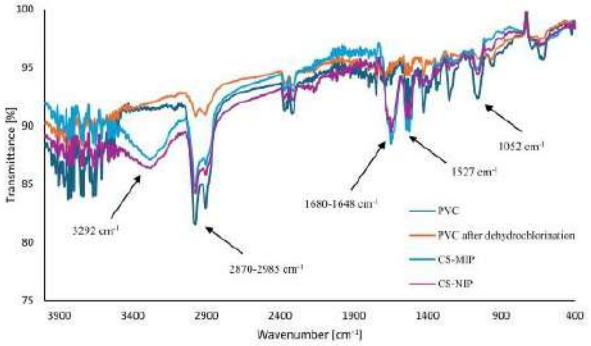

Fig. 8. The FT-IR spectra of PVC, CS-MIP and CS-NIP.

regression coefficient (R^2), have been determined. A linear calibration plot with a regression coefficient greater than 0.9999 was established between the peak area and the concentration of S-metolachlor over the range 0.141–215.016 mg × L^{-1}. The LOD and LOQ were determined to be 0.113 mg × L^{-1} and 0.142 mg × L^{-1}, respectively. The formula $y = 3703.87x$ was used to describe the equation of the calibration curve.

3.9. FT-IR analysis

The chemical structures of the PVC, PVC after dehydrochlorination and amination, CS-MIP and CS-NIP were investigated through the utilization of the FTIR method, and are presented in Fig. 8.

In the spectrum of core-shell structures with an applied polymer layer (CS-MIP and CS-NIP), a band was observed at 3292 cm^{-1}, which is likely associated with the vibrations of O–H binding as well as N–H stretching. In the spectrum of the CS-MIP, CS-NIP bands in the range of 2985 cm^{-1} and 2870 cm^{-1} were identified, which could be indicative of

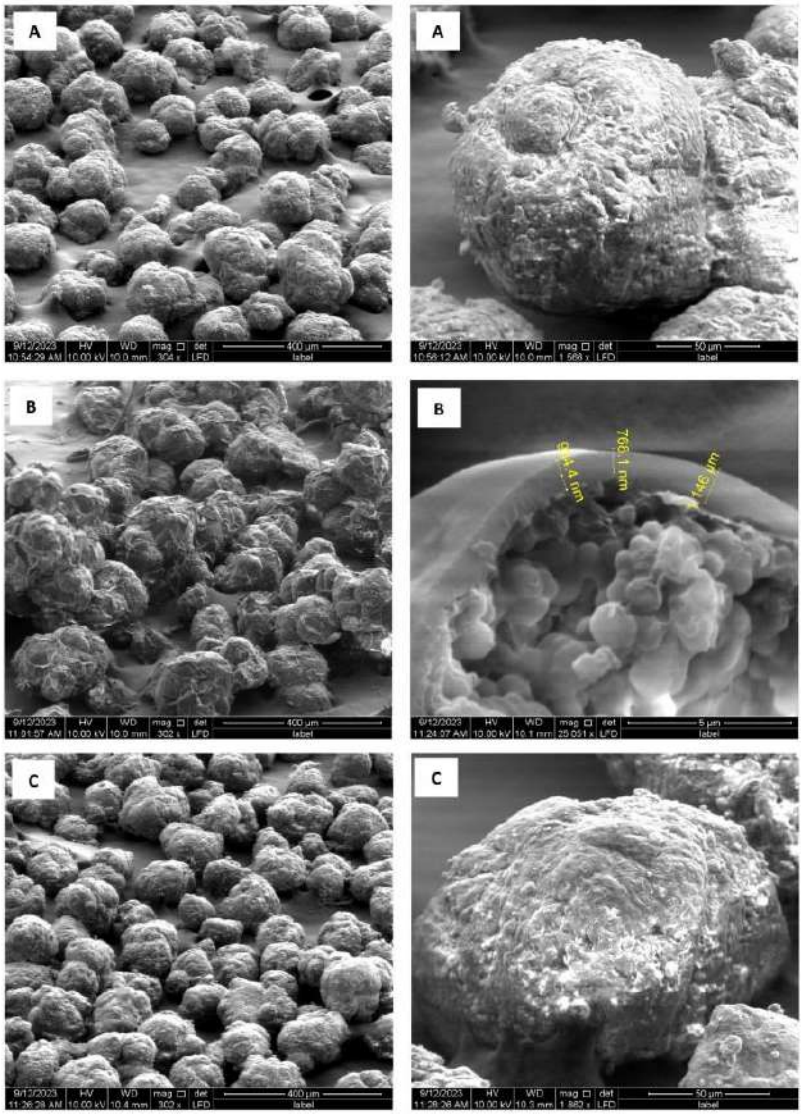

Fig. 9. SEM images of: A: PVC after modification; B: CS–MIP; C: CS–NIP.

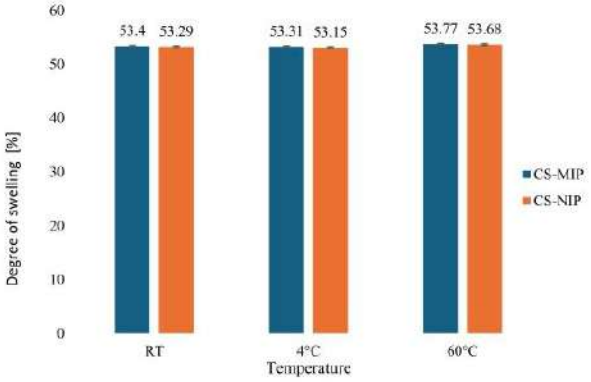

Fig. 10. Degree of swelling at various temperatures.

the aliphatic C–H vibrations. Moreover, the previously mentioned molecules exhibited peaks within the range of 1680 cm^{-1} and 1648 cm^{-1}, as well as 1527 cm^{-1} which are likely attributable to the presence of the amine group. The observed bands at 1052 cm^{-1} could be indicative of the presence of vinyl C–H binding.

3.10. SEM analysis

The surface morphology of PVC, CS-MIP and CS-NIP, is presented in Fig. 9, was characterized by SEM analysis. It was observed that the structures of all three samples are very similar. Figure B is an example of the deposition of a polymer layer on PVC, thereby confirming its existence. All three samples exhibited a porous and irregular surface. In order to complete the characterization of the surface, the degree of swelling of the polymers at room temperature, 4 °C and 60 °C was also investigated. The resulting data are presented in Fig. 10. The data obtained demonstrate that there is no temperature dependence of the swelling degree, which may be due to the presence of a very thin polymer layer on the core surface as well as temperature equalization at the spinning stage.

4. Conclusions

The present study was focused on the development of environmentally friendly core-shell molecularly imprinted polymer for the selective adsorption of S-metolachlor from model and real samples. The utilization of sorbent as a deposit to the SPE cartridges and the development of a procedure for the determination of S-metolachlor enabled the creation of a rapid detection method for this herbicide. In comparison to our previous work [24,31], the utilization of MIP-CS as a deposit has resulted in the elimination of complications associated with column clogging. The clogging was attributed to the presence of block polymers as column fill, given the tendency of these sorbents to form precipitates. Furthermore, the larger particle size of these polymers causes that they can accumulate on the filter material, blocking the pores of the filter, reducing filtration efficiency, or even preventing it. This issue is addressed in core-shell structures, wherein a thin layer of polymer is applied exclusively to the surface of the core. Moreover, the material is more homogeneous than the block polymer, attributable to the thin layer of the applied polymer. This results in a markedly higher degree of repetition in the results obtained. The sorption value obtained for CS-MIP was calculated as 1.063 ± 0.002 mg $\times$ g^{-1}, whereas for block MIP as 2.415 ± 0.038 mg $\times$ g^{-1}, making the standard deviation value for core-shell materials almost 20 times smaller. Furthermore, a reduced quantity of monomers is utilized in the synthesis of CS-MIP, a factor which has positive effects on price and environmental friendliness. To illustrate this, the synthesis of a single portion of core-shell sorbents necessitates the utilization of only half of the polymerization mixture employed for the synthesis of a single portion of block polymers. Furthermore, it has been determined that a quantity of only 0.05 g of CS-MIP polymers is sufficient for the purposes of sorption studies, with the majority of this mass being composed of PVC grains. However, during the sorption of S-metolachlor by block polymers, it is possible to adsorb a larger number of molecules of this herbicide. The thin polymer layer applied on the PVC core shows high selectivity towards S-metolachlor. Furthermore, the selectivity exhibited by the core-shell material is analogous to that of the block polymer. CS-MIP demonstrated a higher sorption for S-metolachlor in comparison to atrazine (3.6 times), glyphosate (2.3 times), and fenoxaprop-P-ethyl (5 times). The block polymer exhibited enhanced sorption, with a 3.2, 6, and 6.2 times increase, respectively. The kinetics study showed that the adsorption of S-metolachlor followed a pseudo-second-order model, with R^2 approximately 0.98. The Freundlich model fits well with the isothermal data, as indicated by R^2 value of 97.

CRediT authorship contribution statement

Dominika Rapacz: Writing – original draft, Visualization, Methodology, Investigation, Formal analysis, Data curation, Conceptualization. **Katarzyna Smolińska-Kempisty:** Writing – review & editing, Supervision, Resources, Project administration, Methodology, Investigation, Funding acquisition, Conceptualization. **Joanna Wolska:** Writing – review & editing, Supervision, Methodology, Investigation, Conceptualization.

Declaration of competing interest

The authors declare the following financial interests/personal relationships which may be considered as potential competing interests: Katarzyna Smolinska-Kempisty reports financial support was provided by National Science Centre Poland. Dominika Rapacz, Katarzyna Smolinska-Kempisty, Joanna Wolska has patent Sposób otrzymywania polimerowych cząsteczek z nadrukiem molekularnym typu rdzeń-powłoka selektywnych wobec Smetolachloru pending to Licensee. If there are other authors, they declare that they have no known competing financial interests or personal relationships that could have appeared to influence the work reported in this paper.

Acknowledgements

This research was funded in whole by National Science Centre Poland 2021/42/E/ST5/00019 (02NB/0002/22). For the purpose of Open Access, the author has applied a CC-BY public copyright licence to any Author Accepted Manuscript (AAM) version arising from this submission.

We would also like to gratefully acknowledge the contribution of Dr. Juliusz Winiarski, prof. of WUST, in the taking of the SEM pictures.

Data availability

Data will be made available on request.

References

[1] N. Bolong, A.F. Ismail, M.R. Salim, T. Matsuura, A review of the effects of emerging contaminants in wastewater and options for their removal, Desalination (Amst.) 239 (2009) 229–246, https://doi.org/10.1016/j.desal.2008.03.020.
[2] F. Altaf, M.Z. Hashmi, U. Farooq, Z.U. Rehman, M.U. Hmeed, R. Batool, S. Pongpiachan, Chapter: nanotechnology to treat the environmental micropollutants, in: M.Z. Hashmi, S. Wang, Z. Ahmed (Eds.), Advances in Pollution Research, Environmental Micropollutants, Elsevier, 2022, pp. 407–441, https://doi.org/10.1016/B978-0-323-90555-8.00017-9.
[3] S.M. Rhind, Anthropogenic pollutants: a threat to ecosystem sustainability? Phil. Trans. Biol. Sci. 364 (2009) 3391–3401, https://doi.org/10.1098/rstb.2009.0122.

[4] M. Necibi, A. Atayat, N. Mzoughi, Chapter: methods of determination of micropollutants indifferent marine matrices, in: L. Charles (Ed.), Marine Environments: Diversity, Threats and Conservation, Nova, 2022.
[5] Y. Shao, D. Jinqi, M. Wang, J. Cao, Y. She, Z. Cao, G. Li, F. Jin, J. Wang, A.M. Edb El-Aty, Application of molecularly imprinted electrochemical biomimetic sensors for detecting small molecule food contaminants, Polymers (Basel) 15 (2022) 187, https://doi.org/10.3390/polym15010187.
[6] N. Fontanals, R.M. Marce, F. Borrull, Materials for solid-phase extraction of organic compounds, Separations 6 (4) (2019) 56, https://doi.org/10.3390/separations6040056.
[7] G. Wang, J. Shen, S. Wei, D. Cai, J. Liu, Identification of heavy metals and organic micropollutants in drinking water sources in typical villages and towns in Northeast China, Molecules (Basel) 27 (22) (2022) 8033, https://doi.org/10.3390/molecules27228033.
[8] A. Adumitrăchioaie, M. Tertis, A. Cernat, R. Sandulescu, C. Cristea, Electrochemical methods based on molecularly imprinted polymers for drug detection. A review, Int. J. Electrochem. Sci. 13 (3) (2018) 2556–2576, https://doi.org/10.20964/2018.03.75.
[9] N. Pérez-Moral, A.G. Mayes, Direct rapid synthesis of MIP beads in SPE cartridges, Biosens. Bioelectron. 21 (2006) 1798–1803, https://doi.org/10.1016/j.bios.2005.08.014.
[10] G.N. Wang, K. Yang, H.Z. Liu, M.X. Feng, J.P. Wang, Molecularly imprinted polymer-based solid phase extraction combined high performance liquid chromatography for determination of fluoroquinolones in milk, Anal. Methods 8 (2016) 5511–5518, https://doi.org/10.1039/C6AY00810K.
[11] H.A. Mulder, A.C. Pearcy, M.S. Halquist, Characterization of molecularly imprinted polymers for the extraction of tobacco alkaloids and their metabolites in human urine, Biomed. Chromatogr. 36 (2022) 6, https://doi.org/10.1002/bmc.5361.
[12] B. Onal Acet, T. Inanan, K. Salieva, B. Borkoev, M. Odabasi, O. Acet, Molecular imprinted polymers: important advances in biochemistry, biomedical and biotechnology, Polym. Bull. 81 (2024) 10439–10459, https://doi.org/10.1007/s00289-024-05238-5.
[13] A. Doostmohammadi, K. Youssef, S. Akhtarian, E. Tabesh, G. Kraft, S.K. Brar, P. Rezai, Molecularly imprinted polymer (MIP) based core-shell microspheres for bacteria isolation, Polymer 251 (2022) 124917, https://doi.org/10.1016/j.polymer.2022.124917.
[14] T. Sajini, B. Mathew, A brief overview of molecularly imprinted polymers: highlighting computational design, nano and photo-responsive imprinting, Talanta Open 4 (2021) 100072, https://doi.org/10.1016/j.talo.2021.100072.
[15] W. Zhao, N. Sheng, R. Zhu, F. Wei, Z. Cai, M. Zhai, S. Du, Q. Hu, Preparation of dummy template imprinted polymers at surface of silica microparticles for the selective extraction of trace bisphenol A from water samples, J. Hazard Mater. 179 (1–3) (2010) 223–229, https://doi.org/10.1016/j.jhazmat.2010.02.083.
[16] Y. Fu, F. Pessagno, P. Manesiotis, F. Borrull, N. Fontanals, R.M. Marcé, Preparation and evaluation of molecularly imprinted polymers as selective SPE sorbents for the determination of cathinones in river water, Microchem. J. 175 (2022) 107100, https://doi.org/10.1016/j.microc.2021.107100.
[17] M. Niu, C. Pham-Huy, H. He, Core-shell nanoparticles coated with molecularly imprinted polymers: a review, Microchim. Acta 183 (2016) 2677–2695, https://doi.org/10.1007/s00604-016-1930-4.
[18] W. He, Y. Ma, X. Gao, X. Wang, X. Dai, J. Song, Application of Poly(N-isopropylacrylamide) as thermosensitive smart materials, J. Phys. Conf. 1676 (2020) 012063, https://doi.org/10.1088/1742-6596/1676/1/012063.
[19] K. Jain, R. Vedarajan, M. Watanabe, M. Ishikiriyama, N. Matsumi, Tunable LCST behavior of poly(N-isopropylacrylamide/ionic liquid) copolymers, Polym. Chem. 6 (2015) 6819–6825, https://doi.org/10.1039/C5PY00998G.
[20] P. Koli, N.R. Bhardwaj, S.K. Mahawer, Chapter 4 - agrochemicals: harmful and beneficial effects of climate changing scenarios, in: K.K. Choudhary, A. Kumar, A. K. Singh (Eds.), Climate Change and Agricultural Ecosystems, Woodhead Publishing, 2019, pp. 65–94, https://doi.org/10.1016/B978-0-12-816483-9.00004-9.
[21] C.R. Zemolin, L.A. Avila, G.V. Cassol, J.H. Massey, E.R. Camargo, Environmental fate of S-metolachlor - a Review, Planta Daninha, Viçosa-MG 32 (3) (2014) 655–664, https://doi.org/10.1590/S0100-83582014000300022.
[22] P.J. O'Connell, C.T. Harms, J.R.F. Allen Metolachlor, S-metolachlor and their role within sustainable weed-management, Crop Prot. 17 (3) (1998) 207–212, https://doi.org/10.1016/S0261-2194(98)80011-2.
[23] J. Wolska, P. Cyganowski, T. Kożlecki, Fine polymer imprinted layers for the monitoring of bisphenol A in aqueous solutions, Separ. Sci. Technol. 53 (2) (2018) 206–218, https://doi.org/10.1080/01496395.2017.1385627.
[24] D. Rapacz, K. Smolińska-Kempisty, J. Wolska, A novel green molecularly imprinted polymers synthesized in an aqueous medium as S-metolachlor sensitive materials, Talanta 280 (2024) 126674, https://doi.org/10.1016/j.talanta.2024.126674.
[25] J. Wolska, P. Cyganowski, M. Kujawska, pH-responsive molecularly imprinted polymer for sorption and rapid desorption of dibutyl phthalate, Separ. Sci. Technol. 53 (7) (2018) 1076–1087, https://doi.org/10.1080/01496395.2017.1310235.
[26] C.A.O. Moreno, Z. Altintas, Bioselective PES membranes based on ChitosanFunctionalization and virus-imprinted NanoMIPs for HighlyEfficient separation of human pathogenic viruses from water, Membranes 12 (2022) 1117, https://doi.org/10.3390/membranes12111117.
[27] T.R. Sahoo, B. Prelot, Chapter 7 - adsorption processes for the removal of contaminants from wastewater: the perspective role of nanomaterials and nanotechnology, in: B. Bonelli, F.S. Freyria, I. Rossetti, R. Sethi (Eds.), Micro and Nano Technologies, Nanomaterials for the Detection and Removal of Wastewater Pollutants, Elsevier, 2020, pp. 161–222, https://doi.org/10.1016/B978-0-12-818489-9.00007-4.
[28] E.D. Revellame, D.L. Fortela, W. Sharp, R. Hernandez, M.E. Zappi, Adsorption kinetic modeling using pseudo-first order and pseudo-second order rate laws: a review, Clean. Eng. Technol. 1 (2020) 100032, https://doi.org/10.1016/j.clet.2020.100032.
[29] J. Wolska, N.J. Falizi, Membrane emulsification process as a method for obtaining molecularly imprinted polymers, Polymers (Basel) 13 (16) (2021) 2830, https://doi.org/10.3390/polym13162830.
[30] T.A. Saleh, Chapter 4 - isotherm models of adsorption processes on adsorbents and nanoadsorbents, in: T.A. Saleh (Ed.), Interface Science and Technology, Elsevier, 2022, https://doi.org/10.1016/B978-0-12-849876-7.00009-9.
[31] D. Rapacz, K. Smolińska-Kempisty, J. Wolska, Preparation and characterization of SPE column with smart green molecularly imprinted polymers materials for selective determination of S-metolachlor herbicide, Sci. Rep. 15 (2025) 3153, https://doi.org/10.1038/s41598-025-87685-2.

7.6. Dobór warunków syntezy cząstek typu rdzeń–otoczka z warstwą polimeru z odciskiem molekularnym wrażliwego na zmiany pH (Publikacja P6)

Rapacz–Kinas D, Smolińska–Kempisty K, Wolska J. Core–shell molecularly imprinted polymer for selective recognition and detection of S–metolachlor in aqueous samples. *Scientific reports*. 2026, vol. 16, art. 14750, s. 1-11. https://doi.org/10.1038/s41598-026-44780-2.

Wprowadzenie

Szósty artykuł zatytułowany "**Core–shell molecularly imprinted polymer for selective recognition and detection of S–metolachlor in aqueous samples**" opublikowany w *Scientific Reports* omawia cząstki typu rdzeń–otoczka z naniesioną warstwą polimeru molekularnie wdrukowanego, która wykazuje odpowiedź na zmianę pH i jest selektywna wobec S–metolachloru. Do syntezy warstwy MIPu na ziarnach rdzenia, wykorzystano stosunek molowy monomerów trzech najlepszych składów polimerów blokowych reagujących na pH, stanowiących treść publikacji **P4**.

Wyniki

Cząstki PVC, na które nanoszono warstwę polimeru wdrukowanego molekularnie lub polimeru bez odcisków molekularnych musiały zostać poddane modyfikacji. W pierwszym etapie przeprowadzono proces dehydrochlorowania poli(chlorku winylu), a następnie reakcję aminowania. Wykorzystując opracowane trzy najlepsze składy polimerów blokowych reagujących na zmianę pH, zsyntezowano trzy rodzaje sorbentów, w oparciu o doświadczenie zdobyte podczas syntezy cząstek CS wykazujących odpowiedź na zmianę temperatury. Wszystkie zsyntezowane sorbenty charakteryzowały się zdolnością do wiązania S–metolachloru. Jednakże stosunek wartości sorpcji pomiędzy CS–MIP i CS–NIP był największy dla polimeru oznaczonego jako 1 (dla którego stosunek molowy AAc:AA:MBAA:SMCh był równy odpowiednio 14:17:12:1) i wynosił 8,23. Dla polimeru oznaczonego jako 2 (stosunek molowy AAc:AA:MBAA:SMCh równy odpowiednio 17:17:12:1) stosunek wartości sorpcji CS–MIP:CS–NIP wynosił 2,83, a dla polimeru oznaczonego jako 3 (stosunek molowy AAc:AA:MBAA:SMCh wynosił 74:74:19:1) wartość współczynnika wdrukowania (IF) CS–MIP do CS–NIP była równa 1,74. Dlatego dalsze, bardziej szczegółowe badania przeprowadzono z użyciem pierwszego sorbentu. Następnie określono, jaka liczba warstw polimeru naniesionych na rdzeń zmodyfikowanego PVC będzie wystarczająca. Wartość sorpcji w przypadku CS–MIP z zaaplikowaną jedną warstwą polimeru wdrukowanego molekularnie była równa 0,364 mg × g^{-1}, a dla CS–NIP wynosiła 0,201 mg × g^{-1}. Natomiast po naniesieniu dwóch warstw, sorpcja osiągnęła wartości 0,287 i 0,183 mg × g^{-1}, odpowiednio dla CS–MIP i CS–NIP. Na podstawie przeprowadzonych badań, stwierdzono, iż proces syntezy z naniesieniem jednej warstwy polimeru jest najbardziej optymalny zarówno pod względem uzyskanych wartości współczynnika wdrukowania, ale także z perspektywy ekonomicznej.

Dodatkowo testowano zakres pH, wynoszący od 2,5 do 9, w którym proces sorpcji będzie zachodził najefektywniej. Największą wartość współczynnika IF odnotowano przy pH

wynoszącym około 7,9, odpowiadającemu pH wody z kranu, co zadecydowało o kontynuowaniu dalszych badań w tym zakresie pH. W kolejnym kroku opracowano warunki sorpcji dynamicznej na kolumnach typu SPE. Proces inkubacji roztworu S–metolachloru z zastosowaniem badanego złoża prowadzono w przedziale czasowym od 5 do 90 minut, przy czym za optymalny uznano czas trwania wynoszący 10 minut. Desorpcję cząsteczek S–metolachloru przeprowadzono z wykorzystaniem 96% etanolu jako eluentu. Dobrą powtarzalność cykli sorpcja–desorpcja uzyskano dla dwóch przeprowadzonych powtórzeń, co potwierdza, że materiał wpisuje się w założenia „*greenification*" zarówno w procesie syntezy, jak i w zastosowaniu MIPów.

Zbadano selektywność zsyntezowanych cząstek, przeprowadzając proces sorpcji z roztworu wieloskładnikowego. Na podstawie wyników tych badań oszacowano, iż CS–MIP sorbuje S–metolachlor około 2 krotnie lepiej niż atrazynę i 2,4–D. Następnie sprawdzono, czy sorbenty można wykorzystać do oznaczania S–metolachloru z próbek symulujących rzeczywiste. Badania przeprowadzono dla dwóch naważek równych 0,2 g i 0,05 g. Dla obu naważek sorpcja z próbki rzeczywistej zachodziła porównywalnie do tej z roztworu modelowego. Dla naważki 0,2 g w roztworze rzeczywistym CS–MIP sorbował S–metolachlor około 3,5 razy lepiej niż CS–NIP, a w roztworze modelowym dwukrotnie lepiej. Natomiast dla naważki 0,05 g CS–MIP wykazał dziewięciokrotnie większą sorpcję niż CS–NIP z roztworu modelowego i około 2,5 większą wartość w roztworze rzeczywistym. Aby w pełni scharakteryzować opisane sorbenty, zbadano ich właściwości fizyko–chemiczne: wykonano widma IR, zdjęcia SEM, analizę TGA i DLS, a także porowatość. Po naniesieniu warstwy polimeru bez odcisku molekularnego na powierzchnię rdzenia, zaobserwowano zmniejszenie powierzchni właściwej PVC, ponieważ prawdopodobnie pory obecne na jego powierzchni zostały zabudowane. Natomiast w przypadku CS–MIP odnotowano wzrost powierzchni właściwej, co prawdopodobnie było efektem obecności specyficznych miejsc wiążących. Ze względu na małą powierzchnię właściwą nie było możliwe określenie średniej wielkości porów. Stabilność termiczna polimerów została określona za pomocą analizy termograwimetrycznej. Dla CS–NIP całkowity rozkład masy nastąpił w przedziale od około 700°C do 1000°C, natomiast dla CS–MIP dopiero około 1000°C. Różnica w wartościach temperatury rozkładu mogła wynikać z nieco większej średniej średnicy cząstek CS–MIP (150 μm) w stosunku do CS–NIP (118 μm), zmierzonej za pomocą techniki dynamicznego rozpraszania światła.

Podsumowanie

Niniejsza publikacja opisuje po raz pierwszy cząstki typu rdzeń–otoczka z warstwą molekularnie wdrukowanego polimeru wrażliwego na zmianę pH, selektywnego w stosunku do S–metolachloru. Otrzymane sorbenty, podobnie jak i inne otrzymane w ramach realizacji pracy doktorskiej, wpisują się w założenia tak zwanych „*zielonych MIPów*", ponieważ synteza została przeprowadzona z wykorzystaniem wody, w temperaturze pokojowej, a materiały nadają się do ponownego wykorzystania. Do syntezy cząstek typu rdzeń–otoczka zużywane są mniejsze ilości reagentów, w porównaniu do polimerów blokowych. Jednakże, ze względu na naniesioną cienką warstwę MIPu, wartości sorpcji S–metolachloru są mniejsze, niż te uzyskane

dla polimerów blokowych reagujących na zmianę pH. Mimo to, pojemność sorpcyjna materiałów jest wystarczająca do efektywnego oznaczenia i monitorowania zawartości S–metolachloru w roztworach wodnych, a proces syntezy jest przyjazny środowisku.

scientific reports

Check for updates

OPEN

Core-shell molecularly imprinted polymer for selective recognition and detection of S-metolachlor in aqueous samples

Dominika Rapacz-Kinas✉, Katarzyna Smolińska-Kempisty & Joanna Wolska

In the present study, an eco-friendly approach for preparing molecularly imprinted polymers (MIPs) applying on poly(vinyl chloride) (PVC) core is reported. The synthesis of pH sensitive MIPs was accomplished utilizing S-metolachlor as a template molecule, acrylic acid and acrylamide as a functional monomers, N,N′- methylenebis(acrylamide) as a cross-linking agent, and water as a porous agent. The morphology and shape of the particles were examined using a scanning electron microscope. The sorbents were subjected to detailed analysis using FT-IR spectroscopy, dynamic light scattering and thermogravimetric analysis techniques. The synthesized CS-MIPs exhibited a high degree of selectivity towards the target molecule S-metolachlor, sorbing it more than twice as effectively as atrazine and 2,4-D. The obtained CS-MIPs were successfully employed to the detection of S-metolachlor in both model and real samples. A methodology for the regeneration of sorbents has been developed, allowing for the reuse of the same material several times.

Keywords *Green* molecularly imprinted polymers, pH-responsible polymers, S-metolachlor, Sorption process, *Core-shell* polymers, Solid phase extraction

The utilization of coupled analytical techniques has been identified as a highly effective method for the detection and separation of traces of various analytes, including pharmaceuticals, heavy metals, pesticides, and industrial or household chemicals, in aquatic ecosystems[1–3]. The combination of liquid chromatography and mass spectrometry is widely applied in the qualitative and quantitative analysis of a variety of micropollutants present in complex samples[3]. Nevertheless, this method demands the expertise of skilled technicians, the employment of costly instrumentation, and time-consuming sample pretreatment procedures[4–6].

As a cost-effective approach, the use of molecularly imprinted polymers (MIPs) as a selective analyte extraction material is proposed. During the polymerization process of MIPs, specific binding sites are created on the polymer frameworks. Then, the template molecules are removed, and molecular cavities are generated that can recognize and capture only those analytes that fit them specially. These binding sites are complementary to the target analyte in their morphology, size and molecular interactions[7]. The selection of appropriate monomers, termed functional monomers, for polymerization is of significance in increasing the selectivity of the molecular imprinting process. These monomers possess recognition sites, such as heteroatoms, functional groups, and π-π conjugated systems, which interact with the binding sites of template molecules through covalent bonds, and non-covalent bonds like hydrogen bonds, electrostatic attractions, π-π stacking, and van der Walls and hydrophobic interactions[8,9]. MIPs are applied in a wide range of fields, including medicine, biochemistry, biology, chromatography, solid-phase extraction, separation techniques, imaging methods, immunoassays, drug delivery systems, and optical and electrochemical sensors, due to their specific properties[9–12].

Despite many advantages associated with MIPs, conventional methods of synthesizing these compounds are regarded as non-eco-friendly. In the traditional synthesis process, a considerable volume of organic solvents is employed, in addition to the utilization of toxic chemicals. This has the potential to pose a health risk to operators, generate substantial chemical waste, and have a detrimental effect on the environment[3]. Accordingly, a novel eco-friendly approach for MIPs synthesis is gaining popularity, including the use of renewable, innocuous reagents, the control of polymerization without energy waste, and the utilization of aqueous media as porogen and solvent. Furthermore, the design of self-cleaning MIPs, enhanced degradability of MIPs at environmental

Department of Process Engineering and Technology of Polymer and Carbon Materials, Wroclaw University of Science and Technology, Wybrzeże Wyspiańskiego 27, Wrocław 50-370, Poland. ✉email: dominika.rapacz-kinas@pwr.edu.pl

conditions after use, implementation of polymerization at mild conditions, and optimization via computational modelling are assumptions of the greenification concept[13].

Traditionally, MIPs are synthesized by bulk polymerization. However, the irregular size and small surface area of the obtained polymers, as well as the heterogeneous binding sites, render this method less attractive[14]. As an alternative strategy, the MIPs layer can be grown as a shell on a nanoparticle core, creating *core-shell* particles. This type of structure undoubtedly exhibits several notable advantages, including uniform morphology, homogeneous binding site distribution, and a comparatively large surface area[15]. The combination of materials that form *core-shell* particles results in the demonstration of remarkable properties, which could not be attained through the utilisation of the constituent materials in their separate forms[16].

Herbicides are the most commonly used pesticides in agriculture for the management of weeds. Nevertheless, the synthesis of these compounds results in significant environmental and water contamination[17]. The presence of trace amounts of pesticides in water, ranging from undetectable to a few micrograms per liter, has been termed micropollutants[18]. S-metolachlor ((*S*)-2-Chloro-*N*-(2-ethyl-6-methyl-phenyl)-*N*-(1-methoxypropan-2-yl) acetamide) is one of the most widely used herbicide in the cultivation of maize[19]. The absorption of S-metolachlor by soil particles is facilitated by a range of interactions, including Van der Waals forces, hydrophobic partitioning, charge-transfer complexes, ligand exchange, and covalent bonding. These interactions may occur individually or in combination, depending on the specific conditions of the environment[20]. The herbicidal activity of metolachlor is caused primarily by S-isomers, which are now widely employed due to their enhanced herbicidal activity in comparison to their racemate forms[21].

In the present study, pH-responsible *core-shell* polymers with S-metolachlor imprints in the shell have been prepared according to the strategies of *greenification*. More specifically, the pre-polymerization mixture consists of acrylic acid, sensitive to pH, and acrylamide as a functional monomers, N,N′- methylenebis(acrylamide) as a cross-linking agent, and water as a porous agent. The resultant mixture was then applied as a layer on the poly(vinyl chloride) core. In this paper, we describe the design and preparation of *core-shell* particles and their applications as functional sorbents of S-metolachlor from an aqueous samples.

Materials and methods

Reagents and chemicals

The following chemicals were utilized in the synthesis of the *core-shell* polymers: acrylamide (AA), obtained from Thermo Scientific Chemicals; acrylic acid (AAc), received from Acros Organics; ammonium persulfate (APS), N,N′-methylenebis(acrylamide) (BIS), and N, N,N′,N′-tetramethylethylenediamine (TEMED) purchased from Sigma-Aldrich. S-metolachlor (SMCh) was received from NOVAGRA. Atrazine was supplied by ABCR GmbH & Co. 2,4-dichlorophenoxyacetic acid (2,4-D) was received from Corteva. Poly(vinyl chloride) (Ongrovil® S-5167) was purchased from BorsodChem, with medium molecular weight, and with a K value (an indicator of molecular weight) of 66–68. Ethyl alcohol (EtOH) and the HPLC grade acetonitrile was supplied by POCH S.A. Ultrapure water was obtained with a Milli-Q System (Merck Millipore).

Dehydrochlorination of PVC

The process of dehydrochlorination of PVC was conducted in accordance with the methodology delineated by Wolska et al.[22] To summarize the procedure, 67.5 g of PVC was dispersed in a 500 mL 10% KOH solution (4:1 w/w isopropyl alcohol: water). The mixture was then subjected to heating at its boiling point under the reflux condenser for a period of 24 h. During this process, the color of the reaction mixture underwent a transition from a colorless to a dark brown hue. Subsequently, the degraded PVC was filtered and washed with a large volume of water, followed by a final wash with ethanol. The obtained product was extracted with ethanol for 24 h. Following this extraction process, DHPVC was subjected to drying at a temperature of 60 °C in a dryer.

Amination of DHPVC

The amination of PVC was undertaken in accordance with the methodology established by Wolska et al.[22] A quantity of 25 g of DHPVC was added to 200 mL of amine in a 500 mL flask. The flask containing the mixture was then subjected to heating at its boiling point for a period of 10 min and subsequently stored in a reaction mixture for 24 h at room temperature. Then, the resin was filtered, washed with distilled water to remove ethylenediamine (EDA), and dried in a 60 °C a dryer.

Preparation of core-shell polymers

The preparation of *core-shell* molecularly imprinted polymers was achieved through the following procedure. Approximately 5 g of poly(vinyl chloride) grains, which had undergone the amination process, were contacted with 14 mL of an aqueous solution of the prepolymerization mixture. This mixture consists of the two functional monomers: acrylic acid and acrylamide (5.76–19.98 mmol and 5.84–19.98 mmol, respectively), as well as a cross-linking agent N, N′-methylenebis (acrylamide) (4.93–5.00 mmol), and S-metolachlor (0.27–0.40 mmol). The prepolymerization mixture was subsequently sonicated for a period of 10–15 min in order to dissolve BIS. Thereafter, 15.3 mL of water was added to the reactor and the mixture was left to incubate for a further 10–15 min. In the next step of the process, the prepolymerization mixture was purged with nitrogen for 5–10 min. Following this, the initiator ammonium persulfate (0.20–0.30 mmol) and tetramethylethylenediamine (0.15–0.23 mmol), was added. The reaction was conducted for 24 h at ambient temperature. The mixture was subsequently washed onto Buchner funnel and extracted on a Soxhlet apparatus for a period of 24 h. Following this, the polymers were dried at room temperature. The non-imprinted *core-shell* polymers (CS-NIPs) was synthesized in an identical way to CS-MIPs, with the exception that S-metolachlor molecules were not added during the process. The compositions of individual polymers are presented in Table 1.

CS-MIPs marking	AAc (mmol)	AA (mmol)	BIS (mmol)	SMCh (mmol)	APS (mmol)	TEMED (mmol)
1	5.76	6.96	4.93	0.40	0.30	0.23
2	6.87	5.84	4.93	0.40	0.20	0.15
3	19.98	19.98	5.00	0.27	0.20	0.15

Table 1. The composition of the polymers.

Analytical and characterization methods

High performance liquid chromatography

High performance liquid chromatography (HPLC) system (Shimadzu high performance liquid chromatograph model SCL-40) equipped with an autosampler (model SIL-40), a photodiode array (PDA) detector and a chromatographic column (3 µm ARION® Biphenyl, 150 × 4.6 mm) was used. Isocratic elution was carried out at a temperature of 30 °C, with a mixture of water and acetonitrile (50:50 v/v) employed as the mobile phase. The maintenance of a flow rate of 1 mL × min^{-1} was achieved, with an injection volume of 30 µL and a detection wavelength of 254 nm. The mobile phase was degassed by sonication for 10 min.

Scanning electron microscopy

The characterization of polymer morphologies and structures was performed by scanning electron microscopy (SEM). The samples were mounted on aluminum stubs using double-sided carbon tape. Following this, the specimens were gold-coated for 400 s by utilizing an Edwards Scancoat Six Sputter Coater. A scanning electron microscope (Zeiss Evo LS15) operating at 16 kV was used for imaging.

Fourier-transform infrared spectroscopy

The characterization of the chemical structures of the polymers was performed by Fourier-transform infrared spectroscopy (FT-IR). The acquisition of spectral data was conducted on a Jasco FT-IR-4700 spectrophotometer, employing a total of 64 scans with a resolution of 4 cm^{-1} within the 400–4000 cm^{-1} spectral range.

Thermogravimetric analysis

The thermal stability characteristics of CS-MIPs and CS-NIPs were investigated by thermogravimetric analysis (TGA). This analysis was conducted using the TGA 8000 apparatus from Perkin Elmer. The heating of the polymers was performed within an nitrogen atmosphere, with a constant flow rate of 10 mL × min^{-1}, ranging from 30 to 1000 °C. The rate of heating was maintained at 10 °C × min^{-1}.

Dynamic light scattering

Determination of size distribution of PVC, CS-MIPs, and CS-NIPs was achieved through implementation of a dynamic light scattering (DLS) technique. The analysis was carried out using the LS 13 320 XR Laser Diffraction Particle Size Analyzer. The measurements were obtained by dispersing particles in water, with this process repeated three times. SPAN number was calculated as

$$SPAN = \frac{d_{90} - d_{10}}{d_{50}}$$

where d_{90}, d_{50}, d_{10} are the diameters for 90, 50, and 10% of the particle population[23].

Porosity of sorbents

The specific surface area (S_{BET}) and pore volume (V_{N2}) were determined through the analysis of nitrogen adsorption at the liquid nitrogen temperature, utilizing Autosorb IQ gas sorption analyzer (Quantachrome, Boynton Beach, FL, USA). Before analysis, degassing of the samples was conducted at a temperature of 50 °C for duration of 10 h. The nitrogen dosage was set at 3 $cm^3 \times g^{-1}$. The free space of the analytical tube was measured before performing the analysis.

Adsorption experiments

Batch mode sorption process

For all batch mode sorption experiments, a quantity of sorbents (CS-MIPs and CS-NIPs) with a mass of approximately 0.05–0.2 g was weighed into the flask. Thereafter, 30 mL f a solution of S-metolachlor at a concentration of 30 mg × L^{-1} was added and the contents of the flask were stirred for a period of 24 h. The concentration of the solution after sorption was then determined by HPLC. Sorption capacity (q) – defined as the amount of S-metolachlor adsorbed at the equilibrium – was calculated using following equation:

$$q = \frac{(C_0 - C_e q) \times V}{m} \quad (1)$$

where C_0 and C_{eq} (mg × L^{-1}) are the concentrations of the herbicide at the initial solution and at the equilibrium, respectively, m (g) is the mass of the dry sorbents, V (L) is a volume of the solution[24].

Dynamic mode sorption on the SPE columns

For all dynamic mode sorption experiments, conducted on the SPE columns, approximately 0.05 g of sorbents (CS-MIPs and CS-NIPs) was weighed and placed into the SPE columns. Subsequently, the sorbents were washed with water to dampen the surface. Thereafter, 2 mL of S-metolachlor solution was added and incubated with the sorbents for varying periods of time. The concentration of the solution after sorption was then determined by HPLC, and the sorption was calculated according to Eq. 1.

Competitive study

An investigation was conducted into the binding selectivity of the polymers from multicomponent tap water solution (pH~7.9), consisting of the herbicides: atrazine, glyphosate and S-metolachlor (concentration: 15 mmol $\times L^{-1}$) in dynamic mode. The introduction of approximately 0.050 ± 0.001 g of sorbent (CS-MIPs or CS-NIPs) into a 1 mL SPE column and activation with water was performed. Thereafter, the column was incubated for 10 min with 2 mL of a S-metolachlor solution with a concentration of 30 mg $\times L^{-1}$. The solution concentration was determined by HPLC.

The calculation of the distribution coefficient (K) was undertaken in order to characterize the selective properties, according to the following equation:

$$K_{i(j)} = \frac{q_{i(j)} \times \rho}{C_{i(j)eq}} \tag{2}$$

where $q_{i(j)}$ (μg $\times g^{-1}$) is the sorption capacity (i – S-metolachlor, j – other plant protection products), ρ(g $\times L^{-1}$) is the density of the solution, and $C_{i(j)eq}$ (μg $\times L^{-1}$) is the equilibrium concentration (i – S-metolachlor, j – other plant protection products[25].

Moreover, the calculation of the imprinting factor (IF) was conducted using Eq. 3:

$$IF = \frac{K_i^{MIP}}{K_i^{NIP}} \tag{3}$$

where $K_{i(j)}$ is the distribution coefficient (i – S-metolachlor, j – other plant protection products) of an analyte on an imprinted polymer (K^{MIP}) and a non-imprinted polymer (K^{NIP})[25].

The specific selectivity factor (S) was calculated according to the following equation (Eq. 4):

$$S = \frac{IF_i}{IF_j} \tag{4}$$

where IF_i and IF_j are imprinting factor of the S-metolachlor and other plant protection products, respectively[25].

Sorption from real samples

The sorption study was conducted on both the model solution and the sample, which were prepared to simulate the properties of a real sample, in dynamic mode. Approximately 0.050 ± 0.001 g of sorbent (CS-MIPs or CS-NIPs) was introduced into a 1 mL SPE column and activated with water. Thereafter, the column was incubated for 10 min with 2 mL of a S-metolachlor solution with a concentration of 30 mg $\times L^{-1}$. The concentration of the solution was determined by HPLC, and the sorption was calculated according to Eq. 1.

Bed regeneration

The estimation of the regeneration factor (R_f) of the deposit was conducted through the implementation of the following equation (Eq. 5):

$$R_f = \frac{m_e}{m_a} \times 100\% \tag{5}$$

where m_e (mg) is mass of eluted S-metolachlor, and m_a (mg) is mass of absorbed S-metolachlor.

Results and discussion

Characterization of adsorbents

FT-IR analysis

FT-IR spectroscopy was performed to further confirm the grafting of molecularly imprinted polymer and non-imprinted polymer layer on the poly(vinyl chloride) core. The results are illustrated in Fig. 1. Notably, bands in the range of 2975 cm^{-1} and 2898 cm^{-1} were observed in the spectra of PVC, CS-MIPs, and CS-NIPs, which could indicate aliphatic C–H vibrations. Furthermore, both CS-MIPs and CS-NIPs showed a peak at 1747 cm^{-1} which is presumably attributable to C=O vibrations. The presence of the amine group is likely to be responsible for the peaks within the range of 1541 cm^{-1} and 1523 cm^{-1}. The observed band at 1065 cm^{-1} could be indicative of the presence of C–N bonding. In the PVC spectra, the C–Cl band was identified at 608 cm^{-1}. After the amination process of PVC, spectra exhibited bands at 1020 cm^{-1} which are probably related to the presence of the amine group.

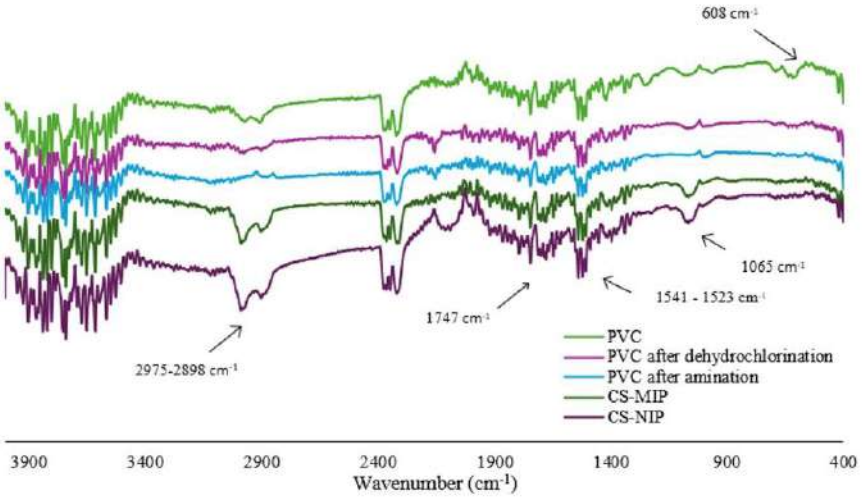

Fig. 1. The FT-IR spectra of the core (PVC), and *core-shell* structures (CS-MIPs and CS-NIPs).

SEM analysis

The structure and morphology of the obtained materials are important parts for the exploration of their properties. The SEM images of CS-MIPs (I) and CS-NIPs (II) are shown in Fig. 2. It can be seen that CS-MIPs and CS-NIPs particles exhibit comparable sizes, however, their surfaces are characterized by a rough and irregular texture.

TGA analysis

The thermal stability of the synthesized polymers was investigated by thermogravimetric analysis. Initially, up to a temperature of approximately 315 °C, the graphs for CS-MIPs and CS-NIPs appear almost identical. It is evident that both polymers undergo a loss of water in the initial phase, up to approximately 100 °C, with the most significant loss of mass occurring at approximately 230 °C. For CS-NIPs, the loss of mass in the temperature range from approximately 700 °C to 1000 °C indicates the destruction of the polymers, while for CS-MIPs, complete mass loss was achieved at approximately 1000 °C (Fig. 3).

Dynamic light scattering

The average diameter of the sorbent particles and the SPAN number were measured using the dynamic light scattering method The mean diameter of the PVC particles following the amination process was found to be 162.1 µm, with a SPAN value of 0.74. For CS-MIPs particles, the average diameter was measured to be 150.2 µm, and for CS-NIPs it was 117.7 µm. The SPAN value for CS-MIPs was 0.50, and for CS-NIPs it was 0.81. The PVC particles were composed of two different batches, each exhibiting varied average diameters. It can be assumed that the batch containing smaller grains was utilised for the synthesis of CS-NIPs, which would account for the observed decrease in their average diameter and faster decomposition of the sorbent, as evident in the graph.

Porosity study

The porosity of the materials was studied (including PVC after amination process, CS-MIPs and CS-NIPs) in order to ascertain their specific surface area and pore volume. The results of the study are presented in Table 2. Following the application of a layer of molecularly imprinted polymers to the core, there was a decrease in the surface area of CS-NIPs, as the pores present on the surface of PVC were probably occluded. However, in the case of CS-MIPs, an increase in the specific surface area was observed, thereby possibly confirming the presence of selective binding cavities. Due to the small surface area, it was not possible to determine the average pore size.

Optimizing the condition of the synthesis process

The synthesis process was carried out in compliance with the procedure described in paragraph 2.4 and the experience gained from our previous studies[26]. All of the *core-shell* polymers obtained exhibit the ability to adsorb S-metolachlor. However, for sorbent marked as 1 (see Fig. 4), the sorption ratio for CS-MIPs and CS-NIPs is 8.23, while for sorbent 2 it is 2.83, and for sorbent 3 it is 1.74. Given that CS-MIPs sorb S-metolachlor about 8 times better than CS-NIPs, sorbent marked as 1 was selected for the further, more detailed studies. In a subsequent section of this work, the selected *core-shell* composition with molecular imprint will be designated as CS-MIPs, while the molecule without molecular imprint will be designated as CS-NIPs.

One of the parameters investigated was the number of the polymer layers applied on the poly(vinyl chloride) core. The results are presented in Table 3. The sorption of S-metolachlor by CS-MIPs after the application of

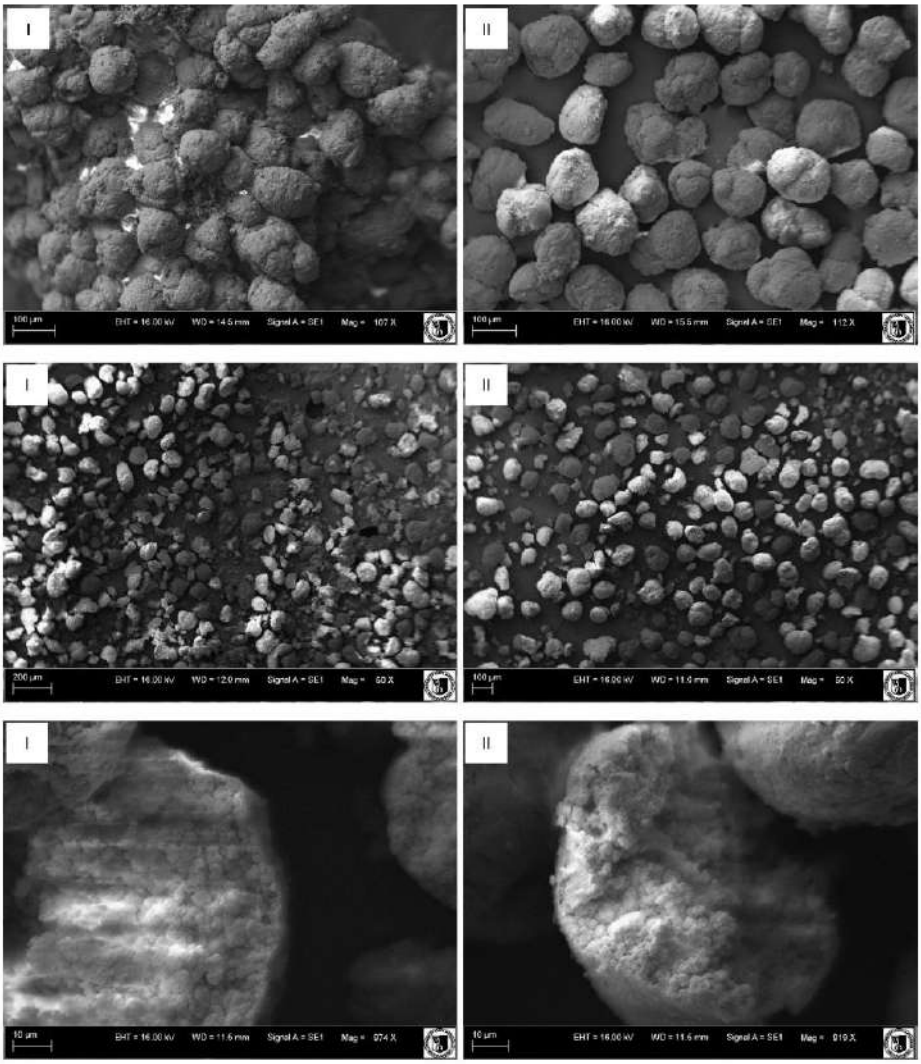

Fig. 2. The scanning electron microscope images of: CS-MIPs (I); CS-NIPs (II).

one layer of polymer to the PVC core is greater than after the application of two layers of polymer. Moreover, the difference between sorption by CS-MIPs and CS-NIPs is more significant when only one layer is applied. In addition, the lower consumption of reactants and the reduced synthesis time were taken into consideration, which together indicated that the optimal application would be one layer of polymer on the core particle.

Another parameter that was optimized was the pH of the solution from which sorption is carried out (see Table 4). In all pH ranges examined, CS-MIPs exhibited approximately twofold enhanced sorption capacity for S-metolachlor in comparison to CS-NIPs, thereby confirming the efficacy of sorption processes for this herbicide within the pH range of 2.5 to 9.0. However, given that the material is intended for use in the detection of S-metolachlor from real samples, and IF value was the most favorable, further studies were conducted at a pH of approximately 7.9.

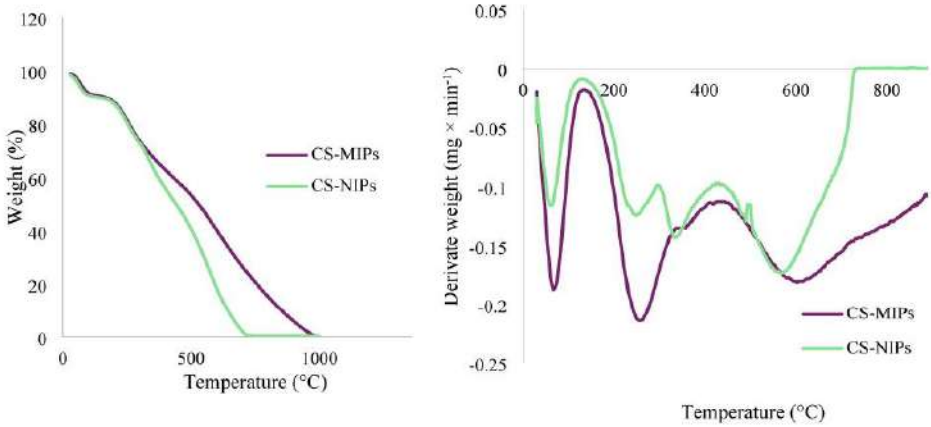

Fig. 3. The results of TGA analysis for CS-MIPs and CS-NIPs.

	S_{BET} ($m^3 \times g^{-1}$)	V_{N2} ($cm^3 \times g^{-1}$)
PVC	5.8	0.018
CS-MIPs	7.4	0.019
CS-NIPs	3.4	0.017

Table 2. The porosity study data.

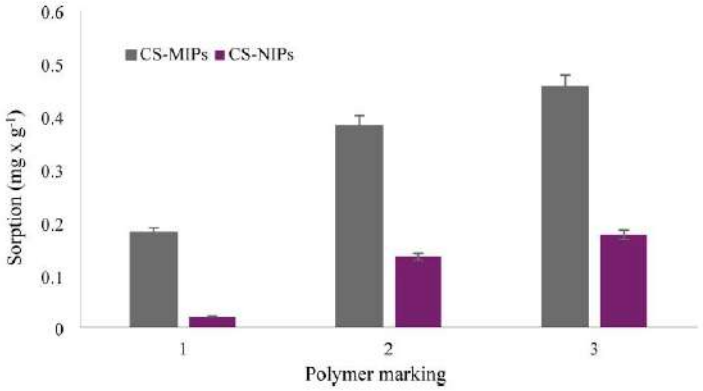

Fig. 4. The results of sorption process.

	Sorption of CS-MIPs ($mg \times g^{-1}$)	Sorption of CS-NIPs ($mg \times g^{-1}$)
1 layer of applied polymer	0.364 ± 0.028	0.201 ± 0.034
2 layers of applied polymer	0.287 ± 0.033	0.183 ± 0.035

Table 3. The results of the optimization of the number of applied polymer layers.

pH	Sorption (mg × g^{-1})		IF
	CS-MIPs	CS-NIPs	
2.5	0.35 ± 0.04	0.16 ± 0.01	2.2
4.5	0.41 ± 0.10	0.17 ± 0.11	2.4
7.9	0.18 ± 0.01	0.02 ± 0.02	9.0
9	0.32 ± 0.08	0.15 ± 0.05	2.1

Table 4. Sorption values for CS-MIPs and CS-NIPs from solutions at different pH.

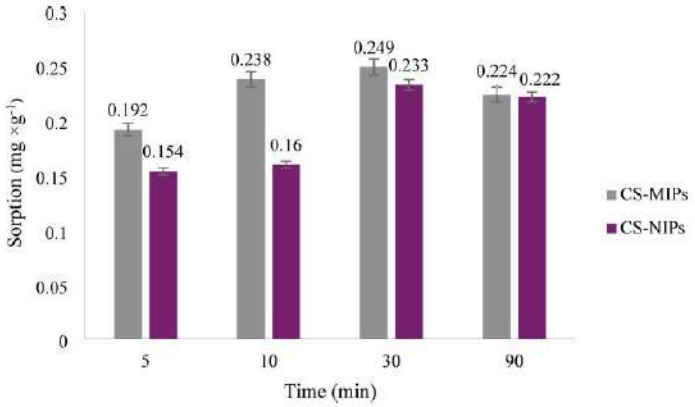

Fig. 5. The results of the optimization of the incubation time on the SPE columns.

	CS-MIPs	CS-NIPs
Sorption I (mg × g^{-1})	**0.35 ± 0.07**	**0.22 ± 0.09**
R_f (%)	96 ± 4	95 ± 2
sorption II (mg × g^{-1})	0.28 ± 0.02	0.16 ± 0.02
R_f (%)	95 ± 5	97 ± 3
sorption III (mg × g^{-1})	0.39 ± 0.15	0.31 ± 0.11
R_f (%)	98 ± 2	99 ± 1

Table 5. The results of the sorption–desorption process.

Optimization of sorption time

A crucial parameter that necessitated optimization during dynamic sorption on SPE columns was the incubation time of the bed with the S-metolachlor solution. The results of the research are presented in Fig. 5. Following analysis of the data presented below, it was determined that 10 min of contact between the sorbents and the S-metolachlor solution would be the optimal time, as the difference in sorption values for CS-MIPs and CS-NIPs after this time is the greatest. Moreover, the reduced experimental time permits almost immediate analysis of the sample.

Sorption and desorption cycles

The regeneration properties of the bed were also examined to ascertain the number of times the material could be reused. The pure ethanol was employed as an eluent. The results obtained can be found in Table 5. As illustrated by the data presented above, the CS-MIPs can be utilized up to three times while maintaining its sorption properties. This has the advantage of reducing the cost of production, analysis and obtaining a favorable environmental impact.

Selectivity study

In addition to the difference in sorption values between CS-MIPs and CS-NIPs, it is critically important that the synthesized material exhibits selective sorption of S-metolachlor. In order to achieve this objective, a solution

Parameter	S-metolachlor	Atrazine	2,4-D
IF	3.034	1.389	1.452
S	–	2.18	2.09

Table 6. The results of the selectivity study.

	Sorption from model solution (mg × g^{-1})	Sorption from real samples (mg × g^{-1})
CS-MIPs[1]	**0.24 ± 0.01**	**0.28 ± 0.02**
CS-NIPs[1]	0.12 ± 0.01	0.08 ± 0.02
CS-MIPs[2]	0.18 ± 0.01	0.18 ± 0.05
CS-NIPs[2]	0.02 ± 0.02	0.07 ± 0.03

Table 7. The sorption results of S-metolachlor from both model and real solutions. [1]The data for the weighting of 0.2 g [2]The data for the weighting of 0.05 g

comprising various plant protection agents was formulated: atrazine, the commercially available Mustang containing 2,4-dichlorophenoxyacetic acid, and S-metolachlor. The results obtained are collated in Table 6. Despite the application of a thin layer of molecularly printed polymer to the PVC core, the material exhibits high selectivity, with the ability to absorb S-metolachlor over two times more effectively than atrazine and 2,4-D.

Sorption from real samples

In order to verify that the resulting material sorbs S-metolachlor not only from the model solution, but also from real samples, a simulated real solution was prepared from tap water. The sorption process was conducted in dynamic mode, and the results obtained are presented in Table 7. The data presented demonstrates the efficacy of the material in absorbing S-metolachlor from both types of solution. In addition, following the principles of greenification, it is possible to reduce the mass of the sorbent used by a factor of 4, while maintaining the material's high affinity for S-metolachlor.

Method validation

The analytical parameters of the HPLC method, including the limit of detection (LOD), limit of quantification (LOQ), the regression coefficient (R^2), and the linearity range have been ascertained. The establishment of a linear calibration plot was undertaken, the regression coefficient of which was equal 0.9999. This objective was achieved through the correlation of the peak area with the concentration of S-metolachlor, within the range of 0.141–215.016 mg × L^{-1}. The LOD was determined to be 0.113 mg × L^{-1}, indicating the minimum concentration at which the S-metolachlor can be detected but not reliably quantified. The LOQ was estimated to be 0.142 mg × L^{-1}, representing the lowest concentration of the analyte that could be accurately quantified. The calibration curve was described by the formula y = 3703.87x.

Conclusions

The *core-shell* structure combined with molecularly imprinted polymers exhibit a specific recognition ability for S-metolachlor. Based on the results, it could be concluded that CS-MIPs could selectively isolate S-metolachlor from both model and simulated real solutions. Furthermore, the strong binding affinity of CS-MIPs for S-metolachlor was well established even after three times adsorption–desorption cycles. The reusability of the sorbents and synthesis method is indicative of the *greenification* of MIPs. The optimum conditions of S-metolachlor sorption on CS-MIPs on SPE columns were achieved at an incubation time of 10 min. In addition, the potential applications of presented CS-MIPs in the rapid separation of S-metolachlor, as well as in the purification and enrichment of the water samples, are promising. The sorbents were characterized using a range of techniques, including FT-IR, SEM, TGA and DLS.

Data availability

Data will be made available upon request.

Received: 17 December 2025; Accepted: 13 March 2026
Published online: 01 April 2026

References

1. Yang, L. et al. Assessment of trace elements contamination and human health risk based on Monte Carlo simulation in a karst groundwater system affected by industrial activities. *Ecotoxicol. Environ. Saf.* (2025). https://doi.org/10.1016/j.ecoenv.2024.117550
2. Nanusha, M. Y. et al. Unravelling the occurrence of trace contaminants in surface waters using semi-quantitative suspected non-target screening analyses. *Environ. Pollut.* (2022). https://doi.org/10.1016/j.envpol.2022.120346
3. Martins, R. O. et al. Greener molecularly imprinted polymers: Strategies and applications in separation and mass spectrometry methods. *Nov 01 2023 Elsevier B V* https://doi.org/10.1016/j.trac.2023.117285

4. Li, R., Zhu, Q., Sun, X., Li, Z. & Liu, X. Electrochemical biosensor based on the integration of maple leaf-like gold nanocrystal and truncated aptamer for detection of α-amanitin with high sensitivity, selectivity and rapidity. *Food Chem.* (2024). https://doi.org/10.1016/j.foodchem.2024.139639
5. Tran, H. N., Nguyen, N. B., Ly, N. H., Joo, S. W. & Vasseghian, Y. Core-shell Au@ZIF-67-based pollutant monitoring of thiram and carbendazim pesticides. *Environ. Pollut.* (2023). https://doi.org/10.1016/j.envpol.2022.120775
6. Song, Z. et al. Lateral flow chromatography strip system for rapid fluorescence determination of phycocyanin in water samples. *J. Hazard. Mater.* (2024). https://doi.org/10.1016/j.jhazmat.2024.135927
7. Ali, Y. A. E. H. et al. Progress and prospects in the green synthesis of molecularly imprinted polymers for sorptive extraction and sensing applications toward emerging contaminants in various sample matrices. *Elsevier B V.* (2024). https://doi.org/10.1016/j.trac.2023.117466
8. Ayerdurai, V. et al. An advantageous application of molecularly imprinted polymers in food processing and quality control. *Taylor Francis Ltd.* https://doi.org/10.1080/10408398.2022.2132208 (2024).
9. Zuo, J. et al. *Application of Molecularly Imprinted Polymers in Plant Natural Products: Current Progress and Future Perspectives* (John Wiley and Sons Inc., 2023). https://doi.org/10.1002/mame.202200499
10. Cabaleiro-Lago, C., Hasterok, S., Gjörloff, A., Tassidis, H. & Wingren & *Recent Advances in Molecularly Imprinted Polymers and Their Disease-Related Applications* (Multidisciplinary Digital Publishing Institute (MDPI), 2023). https://doi.org/10.3390/polym15214199
11. Gkika, D. A. et al. Application of molecularly imprinted polymers (MIPs) as environmental separation tools. *RSC Appl. Polym.* 2 (2), 127–148. https://doi.org/10.1039/d3lp00203a (2024).
12. Chai, P. et al. Fabrication and application of molecularly imprinted polymer doped carbon dots coated silica stationary phase. *Anal. Chim. Acta.* (2023). https://doi.org/10.1016/j.aca.2023.341611
13. Arabi, M. et al. Molecular Imprinting: Green Perspectives and Strategies, John Wiley and Sons Inc. (2021). https://doi.org/10.1002/adma.202100543
14. Orbay, S., Kocaturk, O., Sanyal, R. & Sanyal, A. Molecularly imprinted polymer-coated inorganic nanoparticles: fabrication and biomedical applications. *MDPI* (2022). https://doi.org/10.3390/mi13091464
15. Niu, M., Pham-Huy, C. & He, H. *Core-shell nanoparticles coated with molecularly imprinted polymers: a review*. (Springer-Verlag Wien, 2016). https://doi.org/10.1007/s00604-016-1930-4
16. Ramli, R. A., Laftah, W. A. & Hashim, S. Core-shell polymers: A review. *Sep. 28*. https://doi.org/10.1039/c3ra41296b (2013).
17. Cheng, F. et al. *Advances in biosynthesis of chiral amide herbicides and the key enzymes: dimethenamid-P and S-metolachlor as case studies* (Springer, 2025). https://doi.org/10.1186/s40643-025-00851-2
18. Vadiraj, K. T., Achar, R. R. & Sirigeri, S. A review on emerging micropollutants: sources, environmental concentration and toxicity. *Centro de Biotecnologia y Biomedicina, Clinical Biotec. Universidad Católica del Oriente (UCO), Univesidad Yachay Tech.* (2021). https://doi.org/10.21931/RB/2021.06.04.29
19. Joly, P., Bonnemoy, F., Charvy, J. C., Bohatier, J. & Mallet, C. Toxicity assessment of the maize herbicides S-metolachlor, benoxacor, mesotrione and nicosulfuron, and their corresponding commercial formulations, alone and in mixtures, using the Microtox® test. *Chemosphere* **93** (10), 2444–2450. https://doi.org/10.1016/j.chemosphere.2013.08.074 (2013).
20. Daninha, P. & Viçosa, M. Environmental fate of S-metolachlor-a review ENVIRONMENTAL FATE OF S-METOLACHLOR-A REVIEW-Dinâmica Ambiental do Herbicida S-metolachlor-Revisão, (2014).
21. Ye, J., Zhao, M., Niu, L. & Liu, W. Enantioselective environmental toxicology of chiral pesticides. *Am. Chem. Soc.* (2015). https://doi.org/10.1021/tx500481n
22. Wolska, J., Cyganowski, P. & Kożlecki, T. Fine polymer imprinted layers for the monitoring of bisphenol A in aqueous solutions. *Sep. Sci. Technol. (Philadelphia).* **53** (2), 206–218. (2018). https://doi.org/10.1080/01496395.2017.1385627
23. Wolska, J. & Bryjak, M. Removal of Bisphenol A from Aqueous Solution by Molecularly Imprinted Polymers. *Sep. Sci. Technol. (Philadelphia).* **49** (11), 1643–1653. https://doi.org/10.1080/01496395.2014.906459 (2014).
24. Wolska, J., Kujawska, M. & Cyganowski, P. Selective sorption of diethyl phthalate on pH-responsive, molecularly imprinted polymeric adsorbents. *Sep. Sci. Technol. (Philadelphia).* **55** (12), 2137–2148. (2020). https://doi.org/10.1080/01496395.2019.1620778
25. Smolinska-Kempisty, K., Wolska, J. & Bryjak, M. Molecularly Imprinting Microfiltration Membranes Able to Absorb Diethyl Phthalate from Water. *Membr. (Basel.* (2022). https://doi.org/10.3390/membranes12050503
26. Rapacz, D., Smolinska-Kempisty, K. & Wolska, J. Eco friendly core-shell particles coated with molecularly imprinted polymers for S-metolachlor recognition and separation. *Anal. Chim. Acta.* (2025). https://doi.org/10.1016/j.aca.2025.344310

Acknowledgements
We would also like to gratefully acknowledge the contributions of Dr. Daria Minta in the performing porosity study and Ms. Małgorzata Ulatowska in conducting the TGA analysis, as well as Dr. Mateusz Kruszelnicki in carrying out the DLS analysis.

Author contributions
D.R.K. wrote the manuscript, collected and processed the data, performed the analysis, K.S.K and J.W. reviewed the manuscript, D.R.K, K.S.K, J.W. methodology, investigation, visualisation, K.S.K project manager, fundraising.

Funding
This research was funded in whole by National Science Centre Poland 2021/42/E/ST5/00019 (02NB/0002/22). For the purpose of Open Access, the author has applied a CC-BY public copyright licence to any Author Accepted Manuscript (AAM) version arising from this submission. The research was also supported by Wroclaw University of Science and Technology as part of the Academia Professorum Iuniorum.

Declarations

Conflict of interests
The authors declare no competing interests.

Additional information
Correspondence and requests for materials should be addressed to D.R.-K.

Reprints and permissions information is available at www.nature.com/reprints.

7.7. Zastosowanie sorbentów typu rdzeń–otoczka z warstwą polimeru z odciskiem molekularnym wrażliwego na zmiany pH jako złoża w kolumnach SPE, do oznaczania S-metolachloru z próbek pochodzących z akwenów wodnych (Publikacja P7)

Rapacz–Kinas D, Smolińska–Kempisty K, Urbanowska A, Wolska J. Detection of S–metolachlor in Surface Water Near Cornfields Using pH-Sensitive Green Molecularly Imprinted Polymers. *Molecules.* 2026, vol. 31, art. 932, s. 1-17. https://doi.org/10.3390/molecules31060932.

Wprowadzenie

Siódmy artykuł zatytułowany "**Detection of S–metolachlor in Surface Water Near Cornfields Using pH-Sensitive Green Molecularly Imprinted Polymers**" opublikowany w *Molecules* przedstawia zastosowanie cząstek typu rdzeń–otoczka z warstwą molekularnie wdrukowanego polimeru reagującego na zmianę pH, opisanych w poprzedniej pracy **P6**, do analizy S–metolachloru w próbkach pobranych z akwenów wodnych, znajdujących się w pobliżu upraw kukurydzy. Dodatkowo próbki wody poddano procesowi membranowego oczyszczania, obejmującego mikrofiltrację oraz ultrafiltrację, a także scharakteryzowano właściwości fizyczne i jonowe tych próbek na każdym etapie filtracji. Celem filtracji była weryfikacja możliwości wykorzystania kolumn zależnie od złożoności matrycy próbki wody. Artykuł charakteryzuje również modele kinetyki oraz izoterm sorpcji, a także omawia warunki desorpcji cząsteczek herbicydu.

Wyniki

W niniejszej pracy scharakteryzowano proces sorpcji pod kątem mechanizmu kinetyki sorpcji oraz dopasowania do czterech modeli izoterm. Na podstawie badań kinetyki oszacowano, iż proces sorpcji zarówno dla CS–MIP, jak i CS–NIP zachodzi według modelu pseudo–pierwszego rzędu. Jednakże obliczona maksymalna pojemność sorpcyjna (0,096 mg × g $^{-1}$ dla CS–MIP, R^2= 0,984; i 0,116 mg × g $^{-1}$ dla CS–NIP, R^2= 0,925), jest znacznie mniejsza niż dla wartości wyznaczonych eksperymentalnie (0,364 mg × g $^{-1}$ dla CS–MIP i 0,201 mg × g $^{-1}$ dla CS–NIP), dlatego w dalszym etapie rozważano prawo Ficka. Określono, że w przypadku CS–MIP mechanizmem kontrolującym proces sorpcji jest dyfuzja cząsteczkowa, podczas gdy dla CS–NIP ograniczeniem szybkości procesu jest dyfuzja filmowa. Natomiast w przypadku wyznaczenia mechanizmu sorpcji rozważano cztery modele izoterm: Langmuira, Freundlicha, Dubinin–Radushkevicha i Scatcharda. Na podstawie przeprowadzonych badań, określono, iż najlepsze dopasowanie dla mechanizmu sorpcji CS–MIP określa model izotermy Scatcharda. Wykazano, iż cząstki typu rdzeń–otoczka z warstwą polimeru molekularnie wdrukowanego posiadają dwa rodzaje miejsc wiążących. Ponadto liczba miejsc wiążących o dużym powinowactwie jest znacząco większa niż liczba miejsc wiążących o małym powinowactwie, a współczynnik determinacji dla obu krzywych jest duży i wynosi R_1^2 = 0,969 oraz R_1^2 = 0,985. Dla CS–NIP model izotermy Dubinin–Radushkevicha został wybrany jako najbardziej optymalny. Wyznaczona maksymalna pojemność sorpcyjna była podobna do wartości eksperymentalnej i wnosiła 0,359 mg × g $^{-1}$, a współczynnik R^2 był równy 0,962.

Kolejny etap badań stanowiło opracowanie warunków desorpcji dynamicznej na kolumnach typu SPE. Początkowo dobrano warunki elucji S–metolachloru z roztworu jednoskładnikowego. Testowano wodę o pH około 9 oraz wodne roztwory etanolu o stężeniu 20, 30, 50 i 70%, również o pH zbliżonym do 9. Najbardziej skutecznym eluentem okazał się 50% wodny roztwór etanolu o pH około 9, ponieważ dwa cykle desorpcji pozwoliły na wymycie blisko 50% zaadsorbowanych cząsteczek herbicydu. Jednakże największym wyzwaniem okazał się dobór warunków desorpcji S–metolachloru z wieloskładnikowego roztworu mieszaniny środków ochrony roślin. Weryfikowano różnorodne podejścia oraz roztwory wymywające, natomiast jako najbardziej efektywny eluent wyselekcjonowano 30% roztwór etanolu o pH zbliżonym do 9, który umożliwił wymycie większości mikrozanieczyszczeń, jednocześnie desorbując mniejszy procent cząsteczek S–metolachloru związanych w porach polimeru. W celu ponownego wykorzystania złoża, niezbędne jest jego oczyszczenie poprzez przeprowadzenie czterech cykli desorpcji 96% roztworem etanolu.

Zsyntezowane sorbenty zostały przetestowane na próbkach rzeczywistych: wodzie z rzeki Stobrawy oraz ze stawu znajdujących się w pobliżu upraw kukurydzy. Wody poddano procesowi mikrofiltracji oraz ultrafiltracji, mającemu na celu wstępne ich oczyszczenie. Określono parametry jonowe próbek wody, zarówno przed oczyszczaniem, jak i po każdym etapie filtracji. Oznaczono, m.in. zawartość fluorków, chlorków, azotanów (V), czy siarczanów (VI) oraz sodu i potasu. Dodatkowo zbadano właściwości fizyczne wody takie jak: kolor, pH, przewodność i mętność oraz oznaczono TOC i COD. W celu detekcji S–metolachloru w zebranych próbkach, przepuszczono 50 cm^3 wody przez kolumnę typu SPE ze złożem CS–MIP oraz przez kolumnę stanowiącą układ referencyjny. Pomimo zatężenia próbki, w wodzie nie wykryto S–metolachloru. Niemniej jednak, aby sprawdzić, czy sorbenty działają na próbkach rzeczywistych, zarówno do nieoczyszczonej wody, jak i do wody po procesie filtracji, dodano S–metolachlor i przeprowadzono ponownie proces sorpcji. Wartości sorpcji S–metolachloru zarówno z wody pochodzącej z rzeki, jak i ze stawu, były większe niż wartości sorpcji z roztworu modelowego, co może być spowodowane większą siłą jonową roztworu. Dla trzech rodzajów próbek z rzeki: bez oczyszczania, po MF i po UF, wartości sorpcji przez CS–MIP były równe 0,530 $mg \times g^{-1}$, podczas gdy wartość sorpcji przez CS–NIP zwiększała się po kolejnym etapie oczyszczania. Natomiast dla próbek wody ze stawu, wartości sorpcji zarówno dla CS–MIP, jak i CS–NIP, zwiększały się wraz z kolejnym etapem filtracji. Mając na uwadze duże wartości sorpcji S–metolachloru z próbek nieoczyszczonej wody, stwierdzono, iż detekcja S–metolachloru może zachodzić efektywnie bez wcześniejszego przygotowywania próbek. Przeprowadzono również proces desorpcji S–metolachloru. W pierwszym etapie złoże przemyto wodą destylowaną o pH około 9, aby pozbyć się mikrozanieczyszczeń, a następnie przeprowadzono trzy cykle desorpcji 96% roztworem etanolu. Proces desorpcji najefektywniej przebiegał dla surowych próbek wody, co potwierdza, iż nie ma konieczności poddawania próbek oczyszczaniu za pomocą filtracji membranowej.

Podsumowanie

Cząstki typu rdzeń–otoczka z warstwą polimeru molekularnie wdrukowanego z powodzeniem przetestowano na próbkach wody pochodzących z rzeki oraz ze stawu, znajdujących się w pobliżu upraw kukurydzy, co dowodzi, iż materiały mogą być

wykorzystywane nie tylko w laboratorium uczelnianym na roztworach modelowych, ale również mogą mieć bezpośrednie zastosowanie w laboratoriach analiz środowiskowych, czy w badaniach wody i ścieków. Dodatkowo scharakteryzowano właściwości wody pochodzącej z rzeki oraz ze stawu, a następnie ją oczyszczono, przeprowadzając proces mikrofiltracji i ultrafiltracji. Ponadto opracowano warunki desorpcji S–metolachloru z roztworu wieloskładnikowego, wykorzystując 30% wodny roztwór etanolu o pH około 9. Natomiast jako eluent S–metolachloru z roztworu jednoskładnikowego najlepiej sprawdził się 50% wodny roztwór etanolu o takim samym pH.

molecules

MDPI

Article

Detection of S-Metolachlor in Surface Water near Cornfields Using pH-Sensitive *Green* Molecularly Imprinted Polymers

Dominika Rapacz-Kinas [1,*], Katarzyna Smolińska-Kempisty [1], Agnieszka Urbanowska [2] and Joanna Wolska [1]

[1] Department of Process Engineering and Technology of Polymer and Carbon Materials, Wroclaw University of Science and Technology, Wybrzeże Wyspiańskiego 27, 50-370 Wrocław, Poland
[2] Department of Water and Wastewater Management and Waste Technology, Wroclaw University of Science and Technology, Wybrzeże Wyspiańskiego 27, 50-370 Wrocław, Poland
* Correspondence: dominika.rapacz-kinas@pwr.edu.pl

Abstract

In this study, *core–shell* molecularly imprinted polymers (CS-MIP) were utilized for the detection of the herbicide S-metolachlor in surface water samples, collected from a river and pond that are in the proximity of cornfields. The study revealed that no traces of herbicide were detected in the samples that were analyzed. The collected water samples were treated with membrane filtration—microfiltration and ultrafiltration. The adsorption isotherms were fitted using the Langmuir, Freundlich, Dubinin–Radushkevich, and Scatchard models. This indicated that the Scatchard model is the most appropriate for CS-MIP. The data obtained from the kinetic study were analyzed using the pseudo-first-order and pseudo-second-order models, as well as Fick's second law. For CS-MIP, the most suitable model was determined to be the particle diffusion model, while for *core–shell* non-imprinted polymers (CS-NIP), the film diffusion model was identified as the limiting step. A method for the desorption of S-metolachlor from the pH-sensitive sorbent bed has been developed, thereby enabling the material to be reused. The optimum eluent from the multicomponent solution was determined to be a 30% aqueous ethanol solution with a pH of approximately 9. This solution effectively removed the majority of contaminants, with the exception of S-metolachlor, which was retained within polymer pores.

Keywords: micropollutants detection; sorption; desorption; surface water; smart polymers

1. Introduction

Plant protection products perform a crucial function in the protection of crops against diseases, insects, and weeds [1]. Herbicides are of significant importance in present-day agriculture, as they control weeds and ensure the sustainable productivity of crops. Nevertheless, the employment of herbicides has given rise to concerns regarding their contamination, which poses a grave threat to the environment, biodiversity, and food safety [2]. At present, the global consumption of pesticides is estimated to be in excess of 4.10 million tonnes, with herbicides accounting for 47.50% of this total. The utilization of pesticides has undergone a marked increase, with a growth of over 40% observed in the last two decades [2–4]. Aquatic ecosystems are defined as complex biotic systems that include a variety of organisms. The impact of herbicides on such ecosystems is twofold: firstly, as a direct result of their physiological effects on organisms, and secondly, through indirect ecological interactions between species [5].

Check for updates

Academic Editor: M. Gilles Mailhot

Received: 10 February 2026
Revised: 3 March 2026
Accepted: 8 March 2026
Published: 11 March 2026

S-metolachlor is a chloroacetamide herbicide that is extensively utilized on a global scale due to its low cost and wide spectrum of activity, particularly in the cultivation of corn crops [6,7]. On an international level, the excessive application of S-metolachlor and metolachlor has resulted in significant environmental contamination issues [7]. S-metolachlor was classified as moderately toxic—Class III [6]. It was found that the majority of S-metolachlor and metolachlor residues are retained within the soil matrix. Owing to their heightened water solubility and reduced adsorption properties, these substances are susceptible to leaching into surface water and groundwater [7]. Following the transfer of S-metolachlor and metolachlor from soil to aquatic systems, there is an observed increase in their half-life, which is prolonged from 15 to 70 days to 97–200 days. This effect is indicative of an increased persistence of the pollutants [8].

Numerous research studies have been carried out across the globe that have focused on the elevated levels of herbicides present within water bodies. These studies provide valuable insights into the environmental impact of herbicides. For example, the mean S-metolachlor concentration in the sediments from the cultivated areas of the Ebro River in Spain was 0.33 ng $\times$ g^{-1} [9], which is similar to the value documented in the study by Yi-hao Qin et al.—0.49 ng $\times$ g^{-1} [10]. In a study conducted by Vera-Candioti et al., metolachlor was identified as the second most prevalent detected pesticide in surface and groundwater samples collected from agricultural areas in the Pampas region of Argentina. This analysis was carried out between November 2016 and May 2018 [11]. In a different study, several herbicides were examined. The analysis of river water samples from European countries revealed the presence of 2,4-dichlorophenoxyacetic acid (2,4-D) in 52% of the samples, while atrazine was detected in 68% of the samples and isoproturon in 70%. Notably, the research was conducted in autumn, which is an uncommon application period for herbicides. Consequently, these compounds were detected in relatively low concentrations [12]. Nevertheless, a separate study revealed that the concentration of metolachlor in winter was comparable to that measured during rain events, which can be attributed to the prolonged degradation time of this herbicide [13].

The extent of herbicide transport within a given environment is contingent upon a number of factors, including the degree of herbicide persistence and mobility, the application rate, meteorological conditions, precipitation, and topographical features [14]. The movement of pesticides to diverse environmental areas may occur via runoff erosion, volatilisation, and leaching. It is important to note that transport by runoff and leaching has the potential to result in the contamination of surface water and groundwater [15]. The contamination of surface and ground waters is a significant issue, given their utilization as drinking water supplies. Pesticide contamination of irrigation water has the potential to pollute agricultural farms in areas where they have not been applied. The quality of the ground or the drinking water beneath agricultural areas may be subject to degradation due to the irrigation of water contaminated with pesticides [16].

In addition to pesticide contamination, other compounds such as pharmaceuticals, surfactants, hormones, industrial chemicals, and heavy metals have also been detected in water [17]. The presence of a wide variety of potentially harmful substances in water resources has led to the formation of complex chemical mixtures, so-called chemical cocktails, which have been identified as a significant contributing factor to the degradation of water quality. Furthermore, the similarity of these compounds in terms of molecular weights often renders their separation and identification a very challenging task [18]. Chromatographic techniques, including liquid and gas chromatography, in combination with a variety of detection methods, like GC-MS, LC-MS/MS, UPLC-QTOFMS, and GC-ECD, are utilized for the analysis of trace quantities of pesticides in water. These methods are

https://doi.org/10.3390/molecules31060932

time-consuming [19], costly, and their implementation necessitates the expertise of skilled personnel [20].

Molecularly imprinted polymers are substances that exhibit a specific recognition ability for target pollutants, thereby improving the limit of detection and removal efficiency [21]. The process of molecular imprinting involves the polymerization of functional monomers in the presence of a template molecule, resulting in the formation of MIPs. Following the process of polymerization, the template is removed. As a result, the cavities that are complementary in terms of functional groups, shape, and size to the target molecule are formed on the polymer matrix [22]. MIPs exhibit both chemical and mechanical stability in the presence of extreme chemical and physical conditions. MIPs were selected for application in analytical separation and purification processes, utilizing techniques such as solid-phase extraction and chromatography due to their notable advantages [23].

In this paper, pH-sensitive *core–shell* polymers selective to S-metolachlor have been applied in the detection and separation of S-metolachlor herbicide in water samples from the river Stobrawa and a pond that are near cornfields in Poland. This work fully characterizes the sorbent described in our previous study [24]. The sorbent is then employed as a deposit within the SPE column for real sample applications.

2. Results and Discussion

2.1. Kinetics of Adsorption

The kinetics curves of S-metolachlor adsorption onto CS-MIP and CS-NIP particles were investigated using several kinetic models. The obtained data are summarized in Tables 1 and 2.

Table 1. The result obtained from the calculation according to the pseudo-first and pseudo-second order models.

	Pseudo-First-Order Model			Pseudo-Second-Order Model		
	k_1 $(1 \times \text{min}^{-1})$	R^2	q_{max1} $(\text{mg} \times \text{g}^{-1})$	k_2 $(\text{g} \times (\text{mg} \times \text{min})^{-1})$	R^2	q_{max2} $(\text{mg} \times \text{g}^{-1})$
CS-MIP	0.005	0.984	0.096	0.129	0.949	0.517
CS-NIP	0.007	0.925	0.116	0.024	0.512	0.782

Table 2. The parameters obtained from the calculation according to Fick's law.

	Film Diffusion		Particle Diffusion	
	k_a $(1 \times \text{min}^{-1})$	R^2	k_b $(1 \times \text{min}^{-1})$	R^2
CS-MIP	0.005	0.972	0.002	0.988
CS-NIP	0.007	0.925	0.003	0.854

It was concluded from the kinetic studies that sorption of S-metolachlor occurs in accordance with the *pseudo-first-order model* for both CS-MIP and CS-NIP. Nevertheless, the maximum sorption capacity of the sorbents is considerably lower than the experimental one. Furthermore, the sorption value for CS-NIP is higher than that for CS-MIP. In our previous work [25], we described a block molecularly imprinted polymer with a composition very similar to that of the CS-MIP under consideration. The kinetics of adsorption for the block MIP and NIP occurred according to the *pseudo-second order model*. However, in order to ascertain which type of kinetics of adsorption is decisive for CS-MIP and CS-NIP, Fick's law was employed.

https://doi.org/10.3390/molecules31060932

The analysis of the coefficients of determination enables the determination of which diffusion mechanisms are the most suited to the sorbent obtained. It is observed that the particle diffusion model is the optimal mechanism for controlling the sorption process for CS-MIP ($R^2 = 0.988$), while the film diffusion model is more suitable for CS-NIP ($R^2 = 0.925$), although the distribution coefficient is not close to one. The parameters k_a and k_b are used to ascertain which process occurs faster. It has been demonstrated that, in both cases of CS-MIP and CS-NIP, film diffusion is the faster of the two diffusion processes, which is a result of the presence of a thin polymer layer applied to the core particle.

2.2. Sorption Isotherms

In order to characterize the sorption process in complete detail, the sorption isotherms of S-metolachlor were investigated using four isotherm models. The following theories were considered: Langmuir, Freundlich, Dubinin–Radushkevich, and Scatchard isotherm models. The data obtained from this study are presented in Table 3.

Table 3. Isotherm models data for the S-metolachlor sorption process.

	Langmuir Model			Freundlich Model			Dubinin–Radushkevich Model			Scatchard Model					
	K_L	q_m	R^2	K_F	$1/n$	R^2	K_{DR}	q_m	R^2	P_1	N_1	R_1^2	P_2	N_2	R_2^2
CS-MIP	0.02	21.8	0.827	0.7	0.69	0.999	1.1	0.35	0.907	6.8	16.4	0.969	1.1	5.2	0.985
CS-NIP	0.32	36.2	0.996	0.6	0.71	0.999	1.0	0.36	0.962	-	-	-	0.6	3.4	0.943

Initially, the data were matched to the Langmuir isotherm model. The data obtained indicates an R^2 coefficient for CS-NIP of 0.996. This could initially be interpreted as evidence that sorption occurs in accordance with this model. However, it was observed that the maximum sorption values for both sorbents (CS-MIP and CS-NIP) were found to be 50–140 times higher than the experimental values. Consequently, it was determined that this model was not applicable to either sorbent. In the Freundlich model, the parameter $1/n$, which is indicative of surface heterogeneity, is higher for CS-NIP, indicating a more homogeneous surface compared to the surface of CS-MIP. Moreover, it is observed that the determination coefficient for both sorbents is equal to 0.999. Nevertheless, the value of K_F (0.611 mg $\times$ g^{-1}) related to adsorption capacity is much higher for CS-NIP than the experimental one (0.265 mg $\times$ g^{-1}). For CS-MIP, the R^2 (0.999) and K_F (0.698 mg $\times$ g^{-1}) results are very promising. However, it should be noted that CS-MIP has a heterogeneous surface; therefore, the value of $1/n$ should be higher than 1. The Dubinin–Radushkevich model was further considered. The value of K_{DR}, which is constantly related to the free energy, is found to range from 1 to 8 kJ $\times$ mol^{-1} for both CS-MIP and CS-NIP. This indicates the physical mode of sorption. Furthermore, the maximum sorption calculated from this model is comparable to the experimental one. In addition, the determination coefficient is found to be 0.962. This indicates that the Dubinin–Radushkevich model can be utilized to characterize the sorption process of CS-NIP. In the case of CS-MIP, the value of R^2 is equal to 0.907, and the maximum sorption capacity is slightly lower than the experimental one (0.425 mg $\times$ g^{-1}). Therefore, this model was not selected. Finally, the Scatchard isotherm model was investigated. CS-MIP revealed two types of curves that were obtained, indicating the presence of two types of binding sites. For both curves, the determination coefficient is high, as well as the number of high-affinity binding sites, which is significantly higher than the number of low-affinity binding sites. Moreover, in the case of CS-NIP, low-affinity binding sites are not present. Therefore, it was determined that the Scatchard isotherm model would be the most suitable for CS-MIP.

https://doi.org/10.3390/molecules31060932

2.3. Desorption Study

In our previous work [24], we optimized the parameters of dynamic sorption on SPE columns and determined that the same material may be utilized up to three times, yielding an average regeneration factor of 96%. This study will focus on developing desorption procedures in detail. Initially, the conditions for the desorption of S-metolachlor from a single-component solution were selected. The desorption process was examined using pure water with a pH~9 and aqueous ethanol solutions with concentrations of 20, 30, 50, and 70% (pH~9). The data obtained are presented in Figure 1.

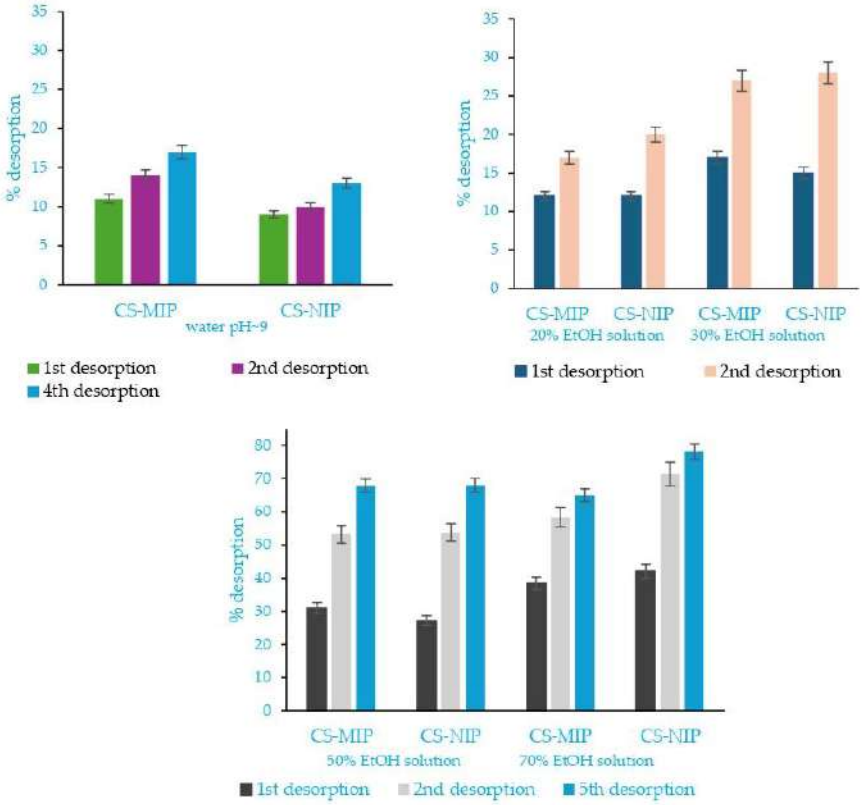

Figure 1. The desorption of S-metolachlor from a single-component solution.

Acrylic acid is a pH-sensitive polymer. According to the results of our previous research and experience [25], water with a pH~9 was utilized for desorption. However, this eluent did not yield the expected results. The four-step process resulted in only 17% of S-metolachlor being desorbed. Consequently, the addition of ethanol was incorporated into further tests. The most suitable eluent was found to be a 50% aqueous ethanol solution with a pH~9. Two desorption cycles using this eluent resulted in the desorption of approximately 50% of the adsorbed herbicide molecules. However, further studies on the desorption of S-metolachlor from a multicomponent matrix were conducted in order to enable the utilization of the sorbent in real samples. The most challenging aspect of the study was the selection of an eluent capable of removing the residual herbicides while maintaining the S-metolachlor within the cavities. The various approaches were tested: 10%, 20%, 30%, 40%, and 100% aqueous solution of ethanol (pH~9) and pure water at pH~9. The results are presented in Figures 2–4.

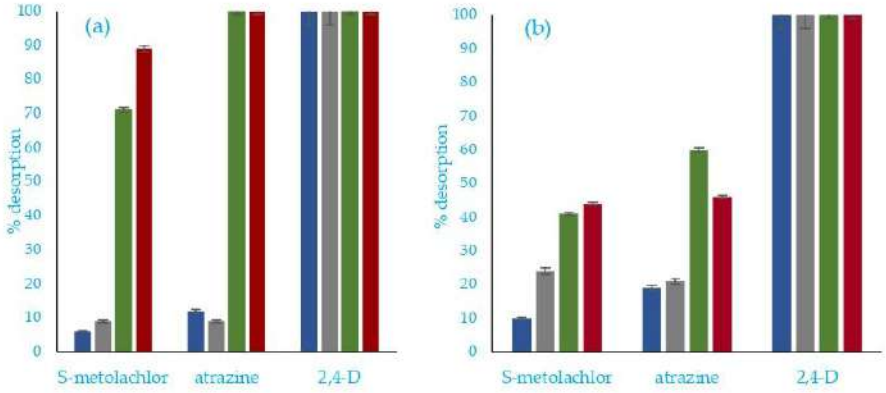

Figure 2. The desorption study: (**a**) First desorption using water with pH~9, and second and third desorption with 100% ethanol. (**b**) Desorption using 10% ethanol. ■ CS-MIP first desorption; ■ CS-NIP first desorption; ■ CS-MIP sum of first, second, and third desorption; and ■ CS-NIP sum of first, second, and third desorption.

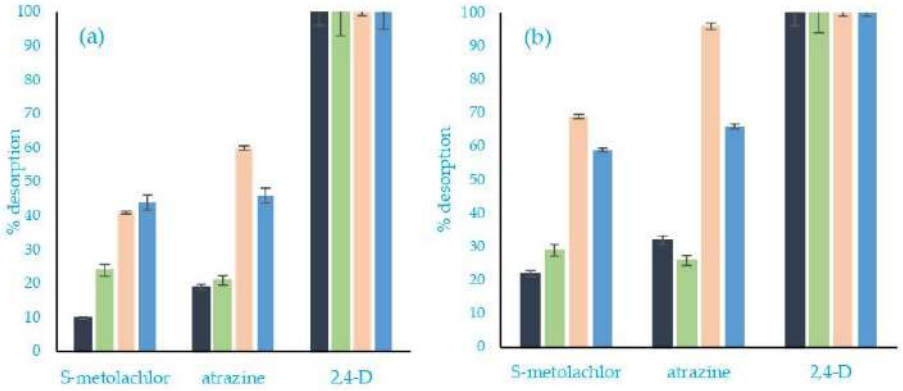

Figure 3. The desorption data: (**a**) Desorption using 20% ethanol; (**b**) Desorption using 30% ethanol. ■ CS-MIP first desorption; ■ CS-NIP first desorption; ■ CS-MIP sum of first, second, and third desorption; and ■ CS-NIP sum of first, second, and third desorption.

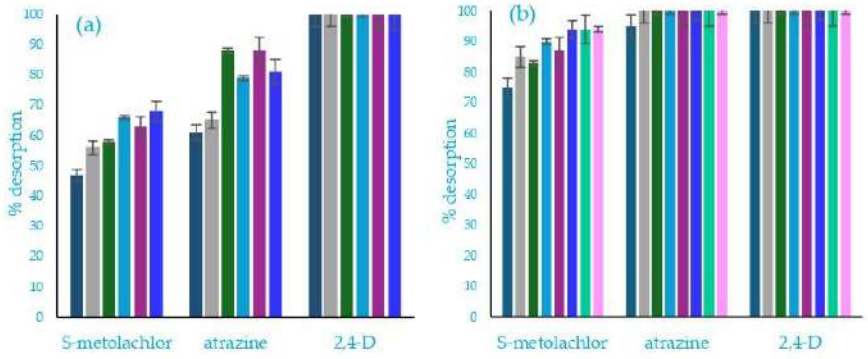

Figure 4. The desorption data: (**a**) first desorption using 40% ethanol, second desorption with 20% ethanol, and third desorption using water with pH~9; (**b**) Desorption using 100% ethanol. ■ CS-MIP first desorption; ■ CS-NIP first desorption; ■ CS-MIP second desorption; ■ CS-NIP second desorption; ■ CS-MIP third desorption; ■ CS-NIP third desorption; ■ CS-MIP fourth desorption; and ■ CS-NIP fourth desorption.

https://doi.org/10.3390/molecules31060932

The tests were repeated on several occasions. The analysis of the data obtained indicates that the most effective eluent, which resulted in the almost complete removal of other herbicides present in the sample, while S-metolachlor remained bound in the pores, was 30% aqueous ethanol solution (pH~9). Following three desorption cycles, atrazine and 2,4-D desorbed 96% and 100%, respectively, while S-metolachlor desorbed 69%. However, in order to desorb almost all of the adsorbed S-metolachlor and clean the bed, four desorption cycles with pure 100% alcohol are required.

2.4. *River and Pond Water Characteristics*

The study examined water samples from two distinct locations: the Stobrawa River and a pond situated in proximity to cornfields in the Opolskie Province of Poland. An analysis was conducted on the water samples obtained from both the river and the pond with the objective of evaluating their ionic and physical properties. The tests were performed in its natural state, as well as undergoing treatment with microfiltration and ultrafiltration. The examination of the content of fluorides, chlorides, nitrates (V), and sulfur (VI) was conducted through the process of ionic analysis. The values of these compounds (see Table 4) decreased after each purification stage, but were not significantly lower.

Table 4. Ionic parameters of water from the river and the pond.

Type of Sample	Type of Purification	Flourides [mg × L^{-1}]	Chlorides [mg × L^{-1}]	Nitrates (V) [mg × L^{-1}]	Sulfur (VI) [mg × L^{-1}]	Na [mg × L^{-1}]	K [mg × L^{-1}]
River	Without	0.06	46.10	4.27	81.20	8.30	2.50
	MF	<0.02	45.50	4.20	80.10	6.10	2.00
	UF	<0.02	45.10	4.16	79.00	5.40	1.90
Pond	Without	0.30	52.00	19.01	103.40	1.00	6.80
	MF	0.14	50.90	6.18	100.90	0.50	6.70
	UF	0.13	50.30	5.90	98.10	0.03	5.90

A further analysis was conducted on the Total Organic Carbon and Chemical Oxygen Demand, the values of which are presented in Figure 5. In accordance with the stipulations outlined in the Regulation of the Minister of Infrastructure of Poland [26], the maximum permissible concentration of Total Organic Carbon in a lowland river, such as the Stobrawa, is set at a value below 8.2 mg × L^{-1} for I class surface water quality. The result of the conducted tests indicates a concentration of 6.85 mg × L^{-1}, falling within the prescribed parameters. However, the determined COD value significantly exceeds the parameters even for Class II surface water quality. The aforementioned regulation does not include water from ponds.

Subsequently, a series of physical properties was examined, including conductivity, turbidity, absorbance, pH, and color (see Table 5). The measurement of the absorbances was conducted at a wavelength of 254 nm, facilitating the assessment of water contamination in relation to the presence of organic compounds. As detailed in regulation [26], the specific conductivity value for water quality class I is less than 420 μS × cm^{-1}. However, the value obtained through the test conducted is 421.1 μS × cm^{-1}, which is in proximity to this threshold. It is important to note that the remaining parameters specified are not incorporated within the regulation. The turbidity and color values decrease with each subsequent stage of purification. The river water exhibited increased transparency at the initial stage, while the pond water demonstrated significantly elevated levels of turbidity. Therefore, for the river water sample, a slight decrease in color value was observed; however, a particularly significant change in color and turbidity was observed for the water sample from the pond after the ultrafiltration process. In consideration of the data

https://doi.org/10.3390/molecules31060932

presented, it can be deduced that the water of the Stobrawa River exhibits characteristics of Class I water quality for specific parameters. For other parameters, it demonstrates characteristics of lower classes, thus indicating that the water can be characterized as medium quality.

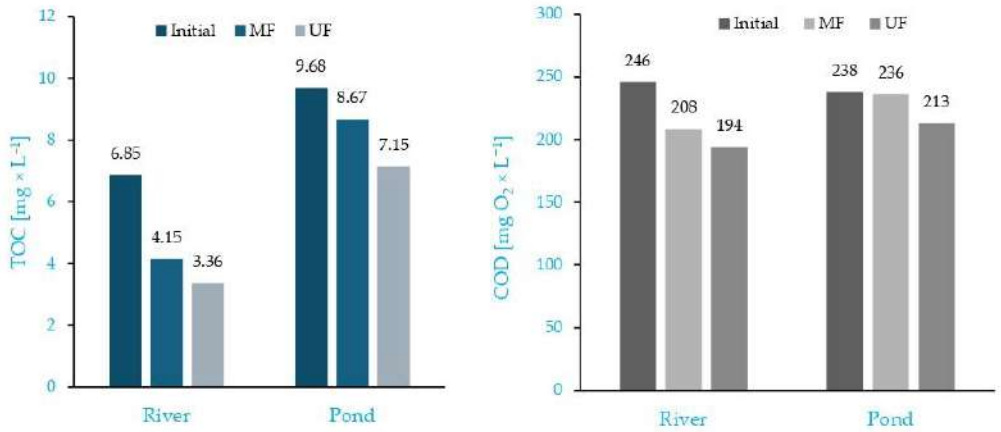

Figure 5. Analysis of Total Organic Carbon (**left**) and Chemical Oxygen Demand (**right**).

Table 5. Analysis of physical properties of water.

Type of Sample	Type of Purification	Conductivity [μS × cm^{-1}]	Turbidity [NTU]	Absorbance [cm^{-1}]	pH	Color [mg Pt × L^{-1}]
River	Without	421.1	9.87	0.031	8.28	17.83
	MF	432.9	6.60	0.021	8.41	17.52
	UF	346.6	2.17	0.015	8.33	15.07
Pond	Without	478.1	11.30	0.038	8.57	32.16
	MF	353.2	9.30	0.032	8.4	31.31
	UF	458.9	0.70	0.014	8.65	13.17

2.5. Real Sample Detection

In our previous study [24], we examined the simulated real-one conditions by testing a tap water solution of S-metolachlor. However, the composition of tap water is less complex than that of samples taken from rivers or ponds. The standard SPE procedure was utilized for the detection of S-metolachlor in both types of samples. However, this procedure did not reveal the presence of the herbicide in the water. Consequently, a methodology was designed to concentrate the S-metolachlor in the water. This was achieved by passing 50 mL of water from the river and the pond through a column. However, the test also did not detect the presence of S-metolachlor in the water samples. S-metolachlor was added to the collected water samples that were used in this study, thus creating a simulated herbicide system in real samples, which was then subjected to further testing.

2.5.1. Analysis of Water from the River and Pond

S-metolachlor (concentration ~35 mg × L^{-1}) was added to the untreated water sample in order to determine whether the sorbent would be capable of catching herbicide molecules in the presence of other interference compounds. The water was also purified by membrane filtration through a 200 and 20 nm PP membrane. S-metolachlor (concentration ~35 mg × L^{-1}) was then added to the purified water, and the sorption process was carried out. The results are presented in Table 6.

Table 6. The results of the real sample study.

	River Stobrawa		Pond	
	CS-MIP [mg × g^{-1}]	CS-NIP [mg × g^{-1}]	CS-MIP [mg × g^{-1}]	CS-NIP [mg × g^{-1}]
Water without purifying	0.530 ± 0.022	0.446 ± 0.058	0.448 ± 0.015	0.360 ± 0.038
Water after MF	0.530 ± 0.059	0.472 ± 0.088	0.494 ± 0.043	0.449 ± 0.027
Water after UF	0.530 ± 0.079	0.553 ± 0.064	0.657 ± 0.080	0.560 ± 0.077

The above data show that, for river samples, the membrane purification process does not influence the sorption capacity of S-metolachlor by molecularly imprinted polymers. The average sorption value was the same in all three samples, equating to 0.530 mg × g^{-1}. This proves that the selective sorption of S-metolachlor does not require membrane filtration. The values obtained from the river samples are higher than those obtained from model solutions, which may be due to the higher ionic strength. In the case of water samples from a pond, the sorption values are also higher than those obtained from model solutions. With subsequent water purification, the sorption value for both sorbents (CS-MIP and CS-NIP) increases, and the difference between the values obtained for CS-MIP and CS-NIP decreases. This phenomenon may be attributed to the initial high turbidity and color values, indicating high pollution, which reduced marginally following microfiltration but increased considerably after the ultrafiltration process. Subsequent to each treatment stage, a reduced number of interfering compounds was observed in the water, thereby yielding increased sorption values. However, in the case of pond water, the sorption process of S-metolachlor can also be successfully carried out without purifying the sample because the sorption value is high enough to detect potential contamination with S-metolachlor. In the following stage of the experiment, the adsorbed S-metolachlor molecules undergo desorption, with the results illustrated in Figures 6 and 7.

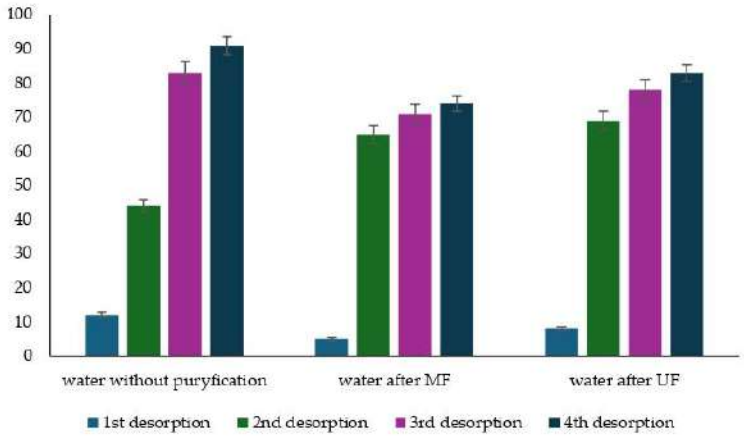

Figure 6. Desorption of S-metolachlor from river samples.

The desorption process was carried out in accordance with the developed procedure. Desorption was performed on all types of samples, including river water and pond water, both before and after treatment. The initial desorption was conducted with distilled water, having a pH of approximately 9. The subsequent three desorptions were carried out using 100% ethanol, with the objective of completely removing all adsorbed molecules. The initial desorption process was designed to eliminate contaminants, achieving an average desorption rate of 8% for S-metolachlor in river water samples and 7% for the herbicide in pond samples. With regard to river water samples, the second desorption process proved

https://doi.org/10.3390/molecules31060932

to be the least effective for untreated water (only 44%), and for samples after membrane treatment, an average of 67% was achieved. However, the desorption process for untreated samples was the most successful, with over 90% of the herbicide molecules desorbed. In contrast, for samples treated with 200 and 20 nm membranes, 74 and 83% were desorbed, respectively. This outcome confirms the previously proposed thesis that the sorption and desorption of S-metolachlor from complex water matrices can be achieved without the necessity of prior sample preparation. In the case of water samples from the pond, S-metolachlor desorbed the least favorably from samples after filtration through a 20 nm membrane, purifying the deposit by only 60%. As in the case of river water samples, the desorption process was most favorable in samples without prior purification, regenerating the deposit by 93%. The data presented indicate the efficacy of the sorbent in analyzing environmental samples without the necessity for prior purification.

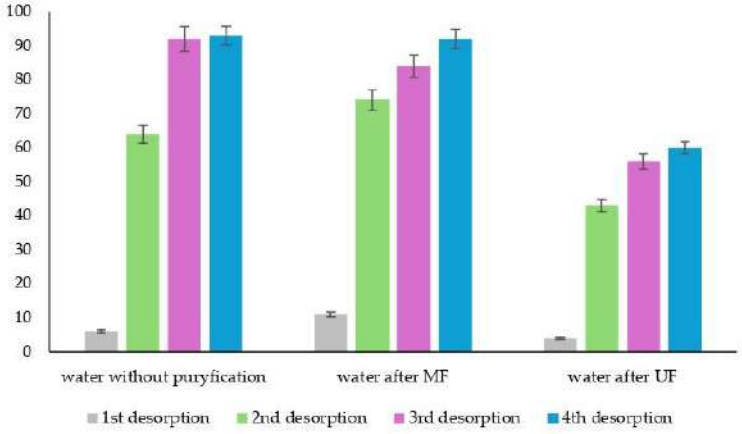

Figure 7. Desorption of S-metolachlor from pond samples.

2.5.2. The Permeate Flux

The flux was measured in relation to the increasing filtered volume of permeate through the membrane. The results obtained are presented in Figure 8. The data collected demonstrates a direct correlation between the increase in permeate volume and the resulting decrease in permeate flux.

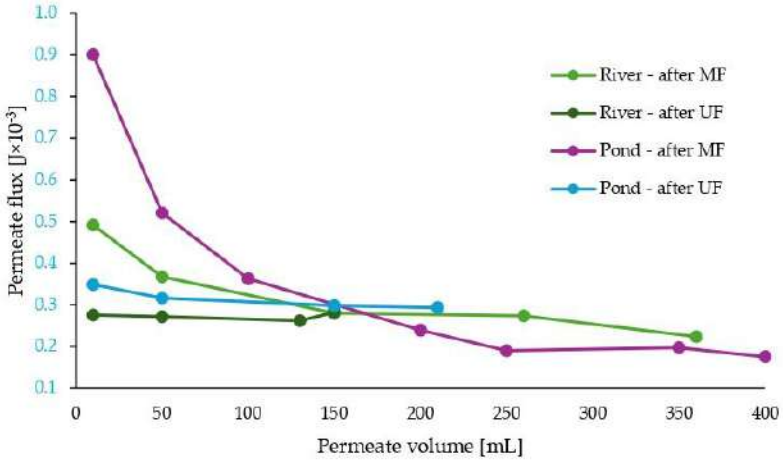

Figure 8. The permeate flux for water from the river and the pond.

https://doi.org/10.3390/molecules31060932

3. Materials and Methods

3.1. Reagents and Chemicals

The following agents were used without any further treatment. Acrylamide (AA) was purchased from Thermo Scientific Chemicals (Warsaw, Poland), and Acrylic acid (AAc) was obtained from Acros Organics (Warsaw, Poland). Ammonium persulfate (APS), N, N′-methylenebis (acrylamide) (BIS), and N, N, N′, N′-tetramethylethylenediamine (TEMED) were received from Sigma-Aldrich (Warsaw, Poland). S-metolachlor (SMCh) was sourced from NOVAGRA (Błonie, Poland). Atrazine was acquired from ABCR GmbH and Co. (Karlsruhe, Germany), and 2,4-dichlorophenoxyacetic acid (2,4-D) was supplied from Corteva (Indianapolis, IN, USA). Sodium hydroxide (NaOH) was purchased from POCH S.A. (Gliwice, Poland). Poly(vinyl chloride) (Ongrovil® S-5167) was procured from BorsodChem (Kazincbarcika, Hungary), with medium molecular weight, and with a K value (an indicator of molecular weight) of 66–68. High-performance liquid chromatography (HPLC) grade acetonitrile (ACN) and ethyl alcohol (EtOH) were purchased by POCH S.A. (Gliwice, Poland). Ultrapure water was obtained with a Milli-Q System (Merck Millipore, Warsaw, Poland).

3.2. Preparation of Core–Shell Molecularly Imprinted Polymers

The synthesis of the *core–shell* molecularly imprinted polymer was conducted in accordance with the procedure delineated in our previous work [24]. The experimental process involved the contact of approximately 5 g of poly(vinyl chloride) grains, which had undergone the amination process, with 14 mL of an aqueous solution of the prepolymerization mixture. The mixture consists of the two functional monomers: acrylic acid (5.75 mmol) and acrylamide (6.96 mmol), as well as the cross-linking agent N, N′- methylenebis(acrylamide) (4.93 mmol) and S-metolachlor (0.40 mmol). The prepolymerization mixture was then subjected to sonication for a period of 10–15 min, with the objective of achieving the dissolution of BIS. Subsequently, 15.3 mL of water was added to the reactor, after which the mixture was left to incubate for an additional 10–15 min. In the following stage of the process, the prepolymerization mixture was purged with nitrogen for a period of 5–10 min. Subsequently, ammonium persulfate (0.30 mmol) and tetramethylethylenediamine (0.23 mmol) were introduced as an initiator. The reaction was carried out for 24 h at ambient temperature. The mixture was then transferred to a Buchner funnel and extracted on a Soxhlet apparatus for 24 h. Subsequently, the polymers were dried at room temperature. The non-imprinted core–shell polymer (CS-NIP) was synthesized in an identical method to CS-MIP, with the exception that S-metolachlor molecules were not incorporated during the process.

3.3. Adsorption Experiments

3.3.1. Dynamic Mode Sorption on the SPE Columns

In the case of all dynamic mode sorption tests carried out on the SPE columns, approximately 0.05 g of polymers (CS-MIP and CS-NIP) was inserted into the 1 mL SPE columns. Thereafter, samples were subjected to a water wash in order to activate the surface. Subsequently, 2 mL of S-metolachlor solution was added, and the sorbents were incubated for varying periods of time. Subsequently, the concentration of the solution following sorption was ascertained by high-performance liquid chromatography. The calculation of sorption was then performed in accordance with the following equation:

$$q = \frac{(C_0 - C_{eq}) \times V}{m} \quad (1)$$

https://doi.org/10.3390/molecules31060932

where C_0 is the initial concentration of S-metolachlor (mg × L^{-1}), C_{eq} is the equilibrium concentration of S-metolachlor (mg × L^{-1}), V is the volume of the solution (L), and m is the mass of the polymer (g).

3.3.2. Kinetics of Adsorption

Investigations into the kinetics of adsorption were conducted using a 250 mL S-metolachlor solution (concentration 30 mg × L^{-1}) and a mass of 2.5 g of the sorbent (CS-MIP and CS-NIP). The experiment was carried out at room temperature, and the concentration of the samples was measured at different time intervals (from 5 to 180 min) using HPLC methods. The *pseudo-first-order* and *pseudo-second-order* models, as well as Fick's law, were employed to ascertain the key process parameters.

Pseudo-First-Order Model

In the *pseudo-first-order model*, the difference between the amount of adsorbed adsorbate molecules on the adsorbents at equilibrium adsorption time and a defined time is determined by the adsorption process rate. In this model, the process of adsorption is independent of the nature of the adsorbates. The linear form of the pseudo-first-order model is presented below in the form of Equation (2). The value of the rate constant k_1 was determined through calculation based on the plot $log(q_{eq} - q_t)$ versus time.

$$\log(q_{eq} - q_t) = \log(q_{eq}) - \frac{k_1 t}{2.303} \quad (2)$$

where k_1 is the sorption rate constant (1 × min^{-1}) and q_{eq} and q_t are the mass of S-metolachlor adsorbed at the equilibrium time and at time t, respectively (mg × g^{-1}) [27,28].

Pseudo-Second-Order Model

In the *pseudo-second-order model*, it is assumed that the sharing or exchanging of electrons between the adsorbent and the adsorbate is a rate-limiting step. This kinetics model postulates that the adsorption process is controlled by chemisorption. The following Equation (3) is used to describe the linear form of the pseudo-second-order model:

$$\frac{t}{q_t} = \frac{1}{k_2 q_{eq}^2} + \frac{1}{q_{eq}} t \quad (3)$$

where k_2 is the sorption rate constant (g × (mg × min)$^{-1}$) and q_{eq} and q_t are the mass of S-metolachlor adsorbed at equilibrium time and at time t, respectively (mg × g^{-1}) [28,29].

Fick's Second Law

To ascertain whether particle or film diffusion is the rate-limiting process, Fick's second law was employed to determine the diffusion mechanisms. The kinetics of the sorption process controlled by diffusion through the film are expressed as follows (4)

$$k_a t = -ln(1 - \frac{q_t}{q_{eq}}) \quad (4)$$

where k_a is the sorption rate constant (1 × min^{-1}) and q_t and q_{eq} are the amount of S-metolachlor adsorbed at time t and at the equilibrium time, respectively (mg × g^{-1}).

The particle diffusion-controlled adsorption process is estimated by Equation (5). The sorption rate constant k_b was calculated from a plot of $-\ln(1 - (\frac{q_t}{q_{eq}})^2)$ versus time [30].

$$k_b t = -\ln(1 - (\frac{q_t}{q_{eq}})^2) \quad (5)$$

https://doi.org/10.3390/molecules31060932

where k_b is the sorption rate constant ($1 \times min^{-1}$) and q_t and q_{eq} are the amount of S-metolachlor adsorbed at time t and at the equilibrium time, respectively ($mg \times g^{-1}$) [30].

3.3.3. Sorption Isotherms

The interaction between adsorbent and adsorbate in the aqueous solution is explained by uptake isotherms. The data obtained from the sorption study were fitted to four linear adsorption isotherm models: Langmuir, Freundlich, Dubinin–Radushkevich, and Scatchard. These models are the most well-known and frequently employed, so we ascertained whether any of them would also align with the experimental data presented.

Langmuir Model

The Langmuir isotherm is based on the assumption that all binding sites on the surface are equivalent, thus demonstrating the relationship between the amount of bound analyte and the amount of free analyte in the system at the equilibrium. The mathematical linear form of the Langmuir model can be expressed as follows (6):

$$\frac{1}{q_e} = \frac{1}{q_m K_L C_e} + \frac{1}{q_m} \quad (6)$$

where q_e is the absorption capacity at equilibrium ($mg \times g^{-1}$), q_m is the maximum adsorption capacity ($mg \times g^{-1}$), K_L is the Langmuir parameter—the affinity of the adsorption sites ($L \times mg^{-1}$)—and C_e is the equilibrium concentration of S-metolachlor ($mg \times L^{-1}$) [31].

Freundlich Equation

The Freundlich isotherm model is based on the sorption on a heterogeneous surface and the interaction between adsorbed molecules. In the case of a slope value between 0 and 1, it measures the surface heterogeneity or the intensity of adsorption. The slope value is indicative of the type of material: if it is close to 1, the material is homogeneous, and if the calculated value is higher than 1, the material is heterogeneous. The mathematical linear form of the Freundlich model is given by the following Equation (7):

$$logq_e = \frac{1}{n} logC_e + logK_F \quad (7)$$

where q_e is the absorption capacity at equilibrium ($mg \times g^{-1}$), K_F is the Freundlich constant related to adsorption capacity ($mg \times g^{-1}$), n is a heterogeneity index, and C_e is the equilibrium concentration of S-metolachlor ($mg \times L^{-1}$) [32].

Dubinin–Radushkevich Model

The Dubinin–Radushkevich model was investigated to estimate whether the adsorption process was chemisorption or physical adsorption. When the ε value is found to be in the range of 1–8 $kJ \times mol^{-1}$, this is indicative of physical adsorption. In the range of 8 to 16 $kJ \times mol^{-1}$, the sorption process is assumed to occur through ion exchange. However, for values exceeding 16 $kJ \times mol^{-1}$, the sorption process is deemed to be of a chemical character. The following Equation (8) represents the linear mathematical formulation of the Dubinin–Radushkevich model:

$$lnq_e = lnq_m - K_{DR}\varepsilon^2 \quad (8)$$

where q_e is the absorption capacity at equilibrium ($mg \times g^{-1}$), q_m is the maximum adsorption capacity ($mg \times g^{-1}$), K_{DR} is the activity coefficient related to adsorption-free energy ($mol^2 \times kJ^{-2}$), and ε is the Polanyi adsorption potential ($kJ \times mol^{-1}$) [32,33].

https://doi.org/10.3390/molecules31060932

Scatchard Equation

The Scatchard isotherm model is a reliable method for determining the nature of active sites on the adsorbent. In the event of a linear fit being obtained from the Scatchard model, it can be deduced that the adsorbent contains one type of active site (homogenous surface). Whereas a non-linear fit will reveal that the adsorbent contains more than one type of binding site (heterogeneous surface). The mathematical linear form of the Scatchard model is given by the following Equation (9):

$$\frac{q_e}{C_e} = PN - Pq \tag{9}$$

where q_e is the absorption capacity at equilibrium (mg × g^{-1}), C_e is the equilibrium concentration of S-metolachlor (mg × L^{-1}), P is the binding affinity (L × $mmol^{-1}$), and N is the number of binding sites (mmol × g^{-1}) [34].

3.3.4. Bed Regeneration

The calculation of the regeneration factor (R_f) of the deposit was undertaken using the following Equation (10):

$$R_f = \frac{m_e}{m_a} \times 100\% \tag{10}$$

where m_e is the mass of eluted S-metolachlor (mg), and m_a is the mass of absorbed S-metolachlor (mg).

3.4. Membrane Process

The water samples from the river and pond were treated using a membrane filtration process. The microfiltration (MF) and ultrafiltration (UF) processes were conducted on Amicon Millipore cell model 8200, utilizing polypropylene (PP) membranes with an average pore size of 200 nm (MF) and 20 nm (UF), respectively, supplied by Celgard. The diameters of the membranes employed in the process were approximately 63 mm. The filtration process was carried out at an approximate pressure of 0.1 MPa.

Membrane Regeneration Process

Regeneration of the polypropylene membranes was conducted according to the procedure detailed in our previous work [35]. In summary, a 0.02 M NaOH solution was employed. Filtration of the alkaline solution through the membranes continued for a period of 10 min. Subsequently, the membranes were washed with distilled water.

3.5. Permeate Flux

The calculation of the permeate flux during filtration through the membrane was performed in accordance with the following Equation (11):

$$J = \frac{v}{S \times t} \tag{11}$$

where v is the permeate volume (mL), S is the active surface area of the membrane (cm^2), and t is the time of permeate collection (s).

3.6. Analytical and Characterization Methods

3.6.1. High Performance Liquid Chromatography

A Shimadzu high performance liquid chromatograph model SCL-40 (Shim-Pol, Izabelin, Poland), equipped with a photodiode array (PDA) detector 40 (Shim-Pol, Izabelin, Poland), and a chromatographic column (3 µm ARION® C18, 150 × 4.6 mm) (Shim-Pol, Izabelin, Poland), was used. For the analysis, 30 µL of sample solution was injected and

eluted isocratically at a flow rate of 1 mL × min^{-1}, using a mixture of water and acetonitrile (1:1, *v*/*v*) as a mobile phase. The temperature was kept at 30 °C, and the wavelength was set to 254 nm.

3.6.2. Water Analysis

The concentration of bromides, fluorides, chlorides, nitrates (V), and sulphates (VI) was determined on a Thermo Scientific Dionex Aquion (Thermo Fisher Scientific, Warsaw, Poland) ion chromatograph with a conductometric detector. Determinations of sodium and potassium were conducted utilizing a Flame Photometer Model BWB-XP by MS Spectrum (BWB Technologies, Newbury, UK). UV absorption was measured using a Shimadzu UV-VIS 1800 spectrophotometer (Shim-Pol, Izabelin, Poland). pH and conductivity were determined utilizing a Digital Multimeter HQ40D (Hach Lange, Wrocław, Poland) with an IntelliCAL™ PHC 101 electrode (Hach Lange, Wrocław, Poland). The Chemical Oxygen Demand (COD) was estimated with the Bichromate method, and the Total Organic Carbon (TOC) was measured using the Hach IL550 carbon analyzer (Hach Lange, Wrocław, Poland).

4. Conclusions

The present study employs *core–shell* molecularly imprinted polymers for the detection of S-metolachlor in water samples collected from a river and a pond in proximity to cornfields in Poland. The purification of the water samples by membrane filtration, specifically microfiltration and ultrafiltration, did not enhance the sorption capacity of S-metolachlor by CS-MIP. A very important conclusion from this study is that the sorbent can be used for the detection and determination of S-metolachlor concentration from a complex water matrix without prior sample preparation, which significantly facilitates and shortens the analysis time. A method for the desorption of S-metolachlor from a multicomponent solution was also developed, thereby demonstrating that the optimum eluent is a 50% aqueous ethanol solution with a pH of approximately 9. The sorbents were also investigated to ascertain their sorption properties. The kinetics and isotherms of sorption were the focus of the study. The experimental results demonstrated that the kinetics for CS-MIP followed the particle diffusion model, while for CS-NIP, they exhibited a tendency to fit the film diffusion model. The Scatchard model was found to be the most appropriate isotherm model for CS-MIP, and the Dubinin–Radushkevich was found to be the most appropriate model for CS-NIP.

Author Contributions: Conceptualization, D.R.-K., K.S.-K. and J.W.; Methodology, D.R.-K., K.S.-K. and J.W.; Software, K.S.-K.; Validation, D.R.-K. and A.U.; Formal analysis, D.R.-K. and A.U.; Investigation, D.R.-K., K.S.-K., J.W. and A.U.; Resources, K.S.-K.; Data curation, D.R.-K. and A.U.; Writing—original draft, D.R.-K.; Writing—review & editing, K.S.-K., J.W. and A.U.; Visualization, D.R.-K., K.S.-K. and J.W.; Supervision, K.S.-K. and J.W.; Project administration, K.S.-K.; Funding acquisition, K.S.-K. All authors have read and agreed to the published version of the manuscript.

Funding: This research was funded in whole by the National Science Center, Poland, 2021/42/E/ST5/00019 (02NB/0002/22). For the purpose of Open Access, the author has applied a CC-BY public copyright license to any Author Accepted Manuscript (AAM) version that arises from this submission. The research was also supported by Wroclaw University of Science and Technology as part of the Academia Professorum Iuniorum.

Institutional Review Board Statement: Not applicable.

Informed Consent Statement: Not applicable.

Data Availability Statement: Data are contained within the article.

Conflicts of Interest: The authors declare no conflicts of interest.

References

1. Qu, R.Y.; He, B.; Yang, J.; Lin, H.; Yang, W.; Wu, Q.; Li, Q.X.; Yang, G. Where are the new herbicides? *Pest Manag. Sci.* **2021**, *77*, 2620–2625. [CrossRef] [PubMed]
2. Parven, A.; Meftaul, I.M.; Venkateswarlu, K.; Megharaj, M. Herbicides in modern sustainable agriculture: Environmental fate, ecological implications, and human health concerns. *Int. J. Environ. Sci. Technol.* **2025**, *22*, 1181–1202. [CrossRef]
3. Riedo, J.; Wettstein, F.E.; Rosch, A.; Herzog, C.; Banerjee, S.; Buchi, L.; Charles, R.; Wachter, D.; Martin-Laurent, F.; Bucheli, T.D.; et al. Widespread occurrence of pesticides in organically managed agricultural soils-The ghost of a conventional agricultural past? *Environ. Sci. Technol.* **2021**, *55*, 2919–2928. [CrossRef]
4. Statista Research Department. Forecast Agricultural Consumption of Pesticides Worldwide from 2023 to 2027. 2024. Available online: https://www.statista.com/statistics/1401556/global-agricultural-use-of-pesticides-forecast/?srsltid=AfmBOoqqRYVjBhGelkVJXe7sFXCuvfAaQDldPWMxqJj3zi9qXQtLvS-B (accessed on 1 March 2026).
5. Sánchez-Bayo, F.; Van den Brink, P.; Mann, R.M. (Eds.) *Ecological Impacts of Toxic Chemicals*; Bentham Science Publishers: Sharjah, United Arab Emirates, 2011.
6. de Souza, R.C.; Silva, L.M.; Moraes, M.J.; Vieira, L.F.A. Ecotoxicity of nicosulfuron and S-metolachlor-based herbicides on non-target plants. *J. Toxicol. Environ. Health-Part A Curr. Issues* **2025**, *88*, 802–817. [CrossRef]
7. He, L.; Wang, Y.; Liu, R.; Wang, Y.; Wanh, Y.; Li, Y.; Zhou, F.; Qiu, Y.; Liu, Y.; Luo, X.; et al. Co-application of biochar and iron-based materials for remediating agricultural soil polluted with metolachlor and s-metolachlor: Field research evidence. *Chem. Eng. J. Adv.* **2025**, *22*, 100758. [CrossRef]
8. Trigo, C.; Spokas, K.A.; Hall, K.E.; Cox, L.; Koskinen, W.C. Metolachlor Sorption and Degradation in Soil Amended with Fresh and Aged Biochars. *J. Agric. Food Chem.* **2016**, *64*, 3141–3149. [CrossRef]
9. Ccanccapa, A.; Masia, A.; Novarro-Ortega, A.; Pico, Y.; Barcelo, D. Pesticides in the Ebro River basin: Occurrence and risk assessment. *Environ. Pollut.* **2016**, *211*, 414–424. [CrossRef]
10. Qin, Y.; Cao, H.; Zhou, L.; Cheng, C.; Jianf, R.; Zhou, X.; Li, X.; Liu, J. Occurrence and ecological risk of typical pesticides in a river–lake system. *Water Sci. Eng.* **2025**, *18*, 422–430. [CrossRef]
11. Vera-Candioti, J.; Araujo, P.I.; Huerga, I.R.; Rojas, D.E.; Cristos, D.S.; Malmantile, A.D. Pesticides detected in surface and groundwater from agroecosystems in the Pampas region of Argentina: Occurrence and ecological risk assessment. *Environ. Monit. Assess.* **2021**, *193*, 689. [CrossRef] [PubMed]
12. Loos, R.; Gawlik, B.M.; Locoro, G.; Rimaviciute, E.; Contini, S.; Bidoglio, G. EU-wide survey of polar organic persistent pollutants in European river waters. *Environ. Pollut.* **2009**, *157*, 561–568. [CrossRef] [PubMed]
13. Marchand, H.; Barst, B.D.; Boulanger, E.; Vachon, N.; Houde, M.; Liu, L.; Bayen, S.; Head, J.A. Contaminants in the Richelieu River (Quebec, Canada) and toxicity to early life stage river (*Moxostoma carinatum*) and copper redhorse (*Moxostoma hubbsi*). *Integr. Environ. Assess. Manag.* **2025**, *21*, 926–942. [CrossRef]
14. Le Bellec, F.; Velu, A.; Fournier, P.; Le Squin, S.; Michels, T.; Tendero, A.; Bockstaller, C. Helping farmers to reduce herbicide environmental impacts. *Ecol. Indic.* **2015**, *54*, 207–216. [CrossRef]
15. Mottes, C.; Lesueur-Jannoyer, M.; Le Bail, M.; Maleziaux, E. Pesticide transfer models in crop and watershed systems: A review. *Agron. Sustain. Dev.* **2014**, *34*, 229–250. [CrossRef]
16. Ashraf, M.; Ozturk, M.; Ahmad, M.S.A. *Plant Adaptation and Phytoremediation*; Springer: Dordrecht, The Netherlands, 2010. [CrossRef]
17. Chandran, P.; Suresh, S.; Balasubramain, B.; Gangwar, J.; Raj, A.S.; Aarathy, U.L.; Meyyazhahan, A.; Pappuswamy, M.; Joseph, K.S. Biological treatment solutions using bioreactors for environmental contaminants from industrial waste water. *J. Umm Al-Qura Univ. Appl. Sci.* **2025**, *11*, 185–207. [CrossRef]
18. Smolinska-Kempisty, K.; Cowen, T.; Duda, J.; Bryjak, M. Environmentally friendly molecularly imprinted polymers as an insert for SPE type columns in the gentamicin monitoring process. *Talanta* **2025**, *282*, 126966. [CrossRef]
19. Gątarek, P.; Rosiak, A.; Kałużna-Czaplińska, J. Chromatographic Methods for the Determination of Organic Pollution in Urban Water: A Current Mini Review. *Crit. Rev. Anal. Chem.* **2025**, *55*, 840–857. [CrossRef]
20. Li, X.; Shen, X.; Jiang, W.; Xi, Y.; Li, S. Comprehensive review of emerging contaminants: Detection technologies, environmental impact, and management strategies. *Ecotoxicol. Environ. Saf.* **2024**, *278*, 116420. [CrossRef]
21. Li, F.; Yue, S.; Zhao, Z.; Liu, K.; Wang, P.; Zhan, S. Application of molecularly imprinted polymers in the water environmental field: A review on the detection and efficient removal of emerging contaminants. *Mater. Today Sustain.* **2024**, *27*, 100904. [CrossRef]
22. Shekari, M.; Moghari, S.; Dawi, E.A.; Khonakdar, H.A. Molecularly Imprinted Polymers for Diagnosis and Medical Applications: Recent Advances and Progress. *Polym. Adv. Technol.* **2025**, *36*, e70293. [CrossRef]
23. Ayerdurai, V.; Cieplak, M.; Kutner, W. Molecularly imprinted polymer-based electrochemical sensors for food contaminants determination. *Trends Anal. Chem.* **2023**, *158*, 116830. [CrossRef]
24. Rapacz-Kinas, D.; Smolińska-Kempisty, K.; Wolska, J. Core-shell molecularly imprinted polymer for selective recognition and detection of S-metolachlor in aqueous samples. *Sci. Rep.* **2026**, *in press*.

25. Rapacz, D.; Smolińska-Kempisty, K.; Wolska, J. Detection of S-metolachlor herbicide in water samples using new molecularly imprinted polymer for solid-phase extraction. *J. Water Process Eng.* **2025**, *75*, 107980. [CrossRef]
26. Regulation of the Minister of Infrastructure of 25 June 2021 on the Classification of Ecological Status, Ecological Potential and Chemical Status, and the Method of Classification. Warsaw. 2021. Available online: https://isap.sejm.gov.pl/isap.nsf/download.xsp/WDU20210001475/O/D20211475.pdf (accessed on 21 October 2025).
27. Zafar, S.; Khalid, N.; Daud, M.; Mirza, M.L. Kinetic Studies of the Adsorption of Thorium Ions onto Rice Husk from Aqueous Media: Linear and Nonlinear Approach. *Nucleus* **2015**, *52*, 14–19. [CrossRef]
28. Pooresmaeil, M.; Namazi, H. Chapter 14–Application of polysaccharide-based hydrogels for water treatments. In *Hydrogels Based on Natural Polymers*; Elsevier: Amsterdam, The Netherlands, 2019; pp. 411–455. [CrossRef]
29. Moussout, H.; Ahlafi, H.; Aazza, M.; Maghat, H. Critical of linear and nonlinear equations of pseudo-first order and pseudo-second order kinetic models. *Karbala Int. J. Mod. Sci.* **2018**, *4*, 244–254. [CrossRef]
30. Pilśniak-Rabiega, M.; Wolska, J. Removal of silver from chloride solutions using new polymer materials. *Physicochem. Probl. Miner. Process.* **2023**, *59*, 174357. [CrossRef]
31. Rodriguez, N.A.M.; Costa, M.; Di Masi, S.; Zaleski, C.; García-Cruz, A.; Mele, G.; Paradiso, V.M.; Piletsky, S.; Malitesta, C.; De Benedetto, G.E. Adsorption Isotherm Analysis for Hybrid Molecularly Imprinted Polymeric Gold-Decorated Nanoparticles Suitable for Reliable Quantification of Gluconic Acid in Wine. *Nanomaterials* **2025**, *15*, 211. [CrossRef] [PubMed]
32. Wolska, J.; Rapacz, D.; Smolińska-Kempisty, K. Core-shell molecularly imprinted polymers for the monitoring of dimethyl phthalate in the children's toys1. *Talanta* **2025**, *293*, 128075. [CrossRef] [PubMed]
33. Ghaffari, H.R.; Pasalari, H.; Tajvar, A.; Dindarloo, K.; Goudarzi, B.; Alipour, V.; Ghanbarneajd, A. Linear and Nonlinear Two-Parameter Adsorption Isotherm Modeling: A Case-Study. *Int. J. Eng. Sci.* **2017**, *6*, 1–11. Available online: https://www.theijes.com/papers/vol6-issue9/A0609010111.pdf (accessed on 1 March 2026).
34. Akpomie, K.G.; Ofomatah, A.C.; Chukwuemeka-Okorie, H.O.; Ani, J.U.; Agbo, S.C.; Odewole, O.A.; Ojo, F.K.; Alum, O.L.; Conradie, J. Equilibrium isotherm investigation on the sequestration of ciprofloxacin from solution via adsorption onto yam peel powder. *IOP Conf. Ser. Earth Environ. Sci.* **2023**, *1178*, 012020. [CrossRef]
35. Smolinska-Kempisty, K.; Urbanowska, A.; Rapacz-Kinas, D.; Marczuk, A.; Wolska, J. Membrane floodwater treatment using molecularly imprinted polymers to detect micropollutants. *Membranes* **2026**, *in press*.

8. Dyskusja wyników osiągniętych podczas realizacji pracy doktorskiej

W pracy doktorskiej *Molekularnie wdrukowywane polimery jako sensory selektywne wobec S–metolachloru*, wykorzystując polimeryzację w masie zsyntezowano polimery blokowe, które wykazywały odpowiedź na zmianę temperatury (**P2**, **P3**) lub pH (**P4**). Ponadto otrzymano cząstki o strukturze rdzeń–otoczka z warstwą molekularnie wdrukowanego polimeru, wrażliwe na zmianę temperatury (**P5**) lub pH (**P6**, **P7**). Wszystkie sorbenty zostały zsyntezowane zgodnie z założeniami tak zwanej „*zielonej chemii*", jednocześnie wpisując się w zasady „*zielonego odcisku molekularnego*", określonego akronimem „*greenification*". Dodatkowo właściwości samoregenerujące tych materiałów, pozwalają na ich kilkukrotne wykorzystanie, minimalizując ilość generowanych odpadów.

W przypadku blokowych polimerów molekularnie wdrukowanych wykazujących odpowiedź na zmianę temperatury (**P2**, **P3**), wartość sorpcji (w trybie statycznym) S–metolachloru przez MIP była równa 2,4 mg × g^{-1}, a dla układu referencyjnego wynosiła 0,5 mg × g^{-1}, co wskazuje, iż wartość IF (czyli współczynnika wdrukowania) jest bliska 5, potwierdzając obecność specyficznych miejsc wiążących. Badania selektywności wykazały, iż MIP sorbuje S–metolachlor z wieloskładnikowego roztworu bardzo popularnych herbicydów stosowanych w uprawach roślin, około 3 razy lepiej niż atrazynę oraz około 6 razy lepiej niż glifosat i fenoksaprop–P–etylu. Proces sorpcji–desorpcji przy użyciu tego samego materiału na kolumnach typu SPE może być przeprowadzony trzykrotnie, uzyskując powtarzalne wyniki. Jako eluent zastosowano wodę o temperaturze 4°C, co potwierdziło mechanizm „*smart*" PNIPAMu.

W przypadku blokowych polimerów molekularnie wdrukowanych reagujących na zmianę pH (**P4**), wartość sorpcji dla najefektywniejszego MIPu wynosiła 0,75 mg × g^{-1}, a dla jego analogu bez odcisku była ponad czterokrotnie mniejsza. Proces sorpcji przeprowadzony z wieloskładnikowego roztworu herbicydów, dowiódł, iż MIP sorbuje S–metolachlor około trzykrotnie lepiej niż atrazynę, 2,4–D i mezotrion. Najbardziej korzystne wartości sorpcji otrzymano prowadząc proces w pH równym 4,5 i 6,5, co jest powiązane z transformacją sieci kwasu poliakrylowego. Zgodnie z przyjętą konwencją, do desorpcji wykorzystano wodę o pH wynoszącym około 9. Prawdopodobnie wtedy, wszystkie grupy karboksylowe zostały przekształcone w aniony karboksylanowe, co spowodowało rozluźnienie sieci polimeru i ułatwiło proces desorpcji. Po optymalizacji warunków stwierdzono, że przy zachowaniu powtarzalności wyników możliwe jest dwukrotne przeprowadzenie cyklu sorpcji–desorpcji na kolumnach typu SPE na tym samym materiale. Jest to spowodowane tym, iż w trzecim cyklu wartość desorpcji S–metolachloru z MIPu zmniejszyła się z ponad 90% do 65%, co prawdopodobnie mogło wynikać z kolmatacji złoża lub przedostania się drobniejszych części polimeru wraz z eluentem poza kolumnę. Natomiast wartość sorpcji przez NIP wzrosła o około 40% w porównaniu do drugiego procesu, co mogło być efektem nagromadzenia się cząsteczek S-metolachloru w porowatej strukturze polimeru.

W przypadku sorbentów typu rdzeń–otoczka z warstwą molekularnie wdrukowanego polimeru wrażliwego na zmianę temperatury (**P5**), wartość sorpcji dla MIPu była równa 1,06 mg × g^{-1}, a dla NIPu 0,82 mg × g^{-1}. Wartość współczynnika wdrukowania (IF), obliczonego

jako stosunek wartości sorpcji MIPu do NIPu, była o około 70% mniejsza, w stosunku do polimerów blokowych. Co prawdopodobnie jest spowodowane tym, iż cząsteczka PVC stanowiąca rdzeń materiału, również sorbuje cząsteczkę S–metolachloru. Natomiast na całkowitą wartość sorpcji składa się wartość sorpcji herbicydu przez rdzeń oraz przez selektywną warstwę polimeru, stanowiącą otoczkę. Ponieważ warstwa ta jest bardzo cienka, różnica w wartościach sorpcji pomiędzy CS–MIP i CS–NIP jest mniejsza. Proces desorpcji herbicydu wykazał mniejszą skuteczność w porównaniu z polimerami blokowymi, co wynikało prawdopodobnie również z tego, że część cząsteczek S–metolachloru została zaabsorbowana przez cząsteczki rdzenia. Opracowano metodologię desorpcji S–metolachloru, po wcześniejszej sorpcji z wieloskładnikowego roztworu. W ramach tego procesu przeprowadzono dwukrotne oczyszczanie złoża za pomocą 10% roztworu etanolu, co umożliwiło usunięcie większości mikrozanieczyszczeń. Następnie S–metolachlor został zdesorbowany wodą o temperaturze 4°C, z wykorzystaniem mechanizmu opartego na „*inteligentnych*" właściwościach PNIPAMu.

W przypadku materiałów typu rdzeń–otoczka z warstwą molekularnie wdrukowanego polimeru, wykazującego odpowiedź na zmianę pH (**P6**, **P7**), sorpcja S–metolachloru przez MIP osiągnęła wartość 0,364 mg × g^{-1}, a dla NIPu wynosiła 0,201 mg × g^{-1}. Proces desorpcji przeprowadzono przy użyciu 30% roztworu etanolu o pH~9, co pozwoliło usunąć większość mikrozanieczyszczeń. Aby jednak w pełni zregenerować złoże i zdesorbować większość cząsteczek S–metolachloru, konieczne było zastosowanie czterokrotnego cyklu desorpcji etanolem. Pomimo cienkiej warstwy polimeru, sorbent wykazuje dużą selektywność wobec S–metolachloru, sorbując go około dwa razy skuteczniej niż atrazynę i 2,4–D z roztworu wieloskładnikowego.

Wszystkie analizowane sorbenty wykazują dużą selektywność w stosunku do S–metolachloru, co potwierdza obecność swoistych wnęk wiążących na powierzchni matrycy polimerowej. Natomiast zarówno cząstki typu rdzeń–otoczka, jak i polimery blokowe, wykazują pewne wady i zalety. Atutem cząstek typu rdzeń–otoczka jest krótszy, w porównaniu do polimerów blokowych, czas inkubacji MIPu z roztworem S-metolachloru lub eluentu, co wynika z badań kinetyki sorpcji, a zatem proces sorpcji i desorpcji jest szybszy. Ponadto mniejsza ilość reagentów niezbędnych do przeprowadzenia reakcji syntezy sorbentów typu rdzeń–otoczka sprzyja założeniom „*zielonej chemii*". Z kolei do ich przygotowania, niezbędna jest modyfikacja cząstek PVC, obejmująca reakcję dehydrochlorowania i aminowania, oraz oczyszczania produktów po każdym etapie, co wydłuża czas syntezy. Większą pojemność sorpcyjną obserwuje się w przypadku polimerów blokowych, w porównaniu do sorbentów typu rdzeń–otoczka, gdzie warstwa sorpcyjna ograniczona jest do cienkiej warstwy polimeru. Dodatkowo w polimerach blokowych stosunek sorpcji pomiędzy MIPem i NIPem jest większy, co wpływa na większą wartość współczynnika wdrukowania, będącego miarą selektywności i wydajności MIPu. Natomiast przy polimerach blokowych pojawiają się problemy z kolmatacją złoża. Niemniej jednak do elucji zaabsorbowanych cząsteczek herbicydu z polimerów blokowych, można wykorzystać mechanizm „*smart*" PNIPAMu lub PAAc, przeprowadzając desorpcję z wykorzystaniem wyłącznie roztworów wodnych. W przypadku cząstek typu rdzeń–otoczka, z powodu prawdopodobnej sorpcji S–metolachloru również przez

rdzeń sorbentu, niezbędny jest dodatek alkoholu do wodnego eluentu. Bazując na doświadczeniu zdobytym podczas realizacji niniejszej rozprawy doktorskiej, można stwierdzić, iż najlepszym materiałem okazały się polimery blokowe wrażliwe na temperaturę. Przewagę nad pozostałymi sorbentami uzyskały, przede wszystkim ze względu na przyjazny środowisku proces desorpcji cząsteczek herbicydu, wyłącznie wodą o temperaturze 4°C. Ponadto możliwe było wykonanie trzech powtarzalnych cykli sorpcji–desorpcji, a prace laboratoryjne związane z syntezą oraz przeprowadzeniem procesu sorpcji i desorpcji z wykorzystaniem tych sorbentów, należały do najłatwiejszych.

Na podstawie wyników uzyskanych w ramach realizacji niniejszej rozprawy doktorskiej można stwierdzić, że dotychczas występująca w literaturze naukowej luka, dotyczącą polimerów wdrukowanych molekularnie selektywnych wobec S–metolachloru, zsyntetyzowanych zgodnie z koncepcją tak zwanej „*zielonej chemii*", została uzupełniona o nowe pozycje literaturowe. Korzyści płynące z opracowywania i potencjalnego wdrażania „*zielonych*" polimerów wdrukowanych molekularnie, obejmują między innymi: poprawę zdrowia ludzi i zwierząt, ochronę środowiska oraz promowanie zrównoważonego rozwoju.

Otrzymane materiały mogą być wykorzystywane w procesie monitorowania stężenia oraz oznaczania zawartości herbicydu S–metolachloru w wodach powierzchniowych, a także w wodzie pitnej czy wodach pochodzących z oczyszczalni ścieków, w znacznym stopniu ułatwiając oraz skracając czas wstępnego przygotowania próbki oraz późniejszej analizy. Przyszłe zadania badawcze zostaną rozszerzone o opracowanie innowacyjnych sorbentów, selektywnych wobec określonych herbicydów, jako potencjalnych materiałów umożliwiających multifunkcyjne oznaczenia analizowanych związków oraz posiadających sprecyzowane zastosowania praktyczne.

9. Źródła finansowania pracy

Badania zrealizowane w ramach niniejszej pracy były współfinansowane przez poniższe instytucje:

- Narodowe Centrum Nauki w ramach grantu badawczego „Molekularnie wdrukowany materiał sensoryczny do monitorowania stężenia mikrozanieczyszczeń w środowisku wodnym" SONATA BIS 11 nr 2021/42/E/ST5/00019 (02NB/0002/22).
- Ministerstwo Nauki i Szkolnictwa Wyższego w ramach ustawowej subwencji dla Politechniki Wrocławskiej.
- Politechnikę Wrocławską w ramach programu *Academia Professorum Iuniorum.*

10. Życiorys naukowy

EDUKACJA

- VII 2020 Uzyskanie tytułu licencjata chemii

Wydział Chemii Uniwersytetu im. Adama Mickiewicza w Poznaniu.
Specjalność: synteza i analiza chemiczna.
Tytuł pracy: Synteza hybrydowych poli(metakrylanów) o złożonej architekturze na drodze polimeryzacji ATRP
Promotor: dr hab. Adrian Franczyk

- VI 2022 Uzyskanie tytułu magistra chemii

Wydział Chemii Uniwersytetu im. Adama Mickiewicza w Poznaniu.
Specjalność: analityka chemiczna.
Tytuł pracy: Synteza gwiaździstych poli(metakrylanów), zawierających w swojej strukturze jednostki POSS, metodą polimeryzacji ATRP
Promotor: dr hab. Ireneusz Kownacki

- od X 2022 doktorantka Szkoły Doktorskiej Politechniki Wrocławskiej

Wydział Chemiczny Politechniki Wrocławskiej
Dyscyplina: inżynieria chemiczna.
Promotor: dr hab. inż. Joanna Wolska, dr hab. inż. Katarzyna Smolińska-Kempisty

PUBLIKACJE

- D. Rapacz*, K. Smolińska-Kempisty, J. Wolska. Progress in development and the current state of the art depending on the polymerization environment – Short review. Journal of Environmental Chemical Engineering. 2024, vol. 12, nr 2, art. 112159, s. 1-12. (IF=7.2, 100 pkt. MNSiW). https://doi.org/10.1016/j.jece.2024.112159.

- D. Rapacz*, K. Smolińska-Kempisty, J. Wolska. A novel green molecularly imprinted polymers synthesized in an aqueous medium as S-metolachlor sensitive materials. Talanta. 2024, vol. 280, art. 126674, s. 1-9. (IF=6.1, 100 pkt. MNSiW). https://doi.org/10.1016/j.talanta.2024.126674.

- J. Wolska, D. Rapacz, J. Winiarski, K. Smolińska-Kempisty. Analysis of the Sorption Properties of Molecularly Imprinted Polymers as Materials for Potential Monitoring of the Amount of Amoxicillin in an Aqueous Environment, Solvent Extraction and Ion Exchange. 2024, vol. 42, nr 4, s. 319-344. (IF=2.4, 70 pkt. MNSiW). https://doi.org/10.1080/07366299.2024.2382698.

- D. Rapacz*, K. Smolińska-Kempisty, J. Wolska. Preparation and characterization of SPE column with smart green molecularly imprinted polymers materials for selective determination of S-metolachlor herbicide. Scientific Reports. 2025, vol. 15, art. 3153, s. 1-10. (IF=3.9, 140 pkt. MNSiW). https://doi.org/10.1038/s41598-025-87685-2.

- K. Smolińska-Kempisty, A. Urbanowska, D. Rapacz, M. Jakowski, M. Pilśniak-Rabiega, J. Wolska. Novelty application of pressurised membrane processes for the recovery of water after the extinguishing of an electric car fire. Environmental Pollution. 2025, vol. 370. art. 125925, s. 1-9. (IF=7.3, 100 pkt. MNSiW). https://doi.org/10.1016/j.envpol.2025.125925.

- J. Wolska, D. Rapacz, K. Smolińska-Kempisty. Core-shell molecularly imprinted polymers for the monitoring of dimethyl phthalate in the children's toys. Talanta. 2025, vol. 293, art. 128075, s. 1-10. (IF=6.1, 100 pkt. MNSiW). https://doi.org/10.1016/j.talanta.2025.128075.

- D. Rapacz*, K. Smolińska-Kempisty, J. Wolska. Detection of S-metolachlor herbicide in water samples using new molecularly imprinted polymer for solid-phase extraction. Journal of Water Process Engineering. 2025, vol. 75, art. 107980, s. 1-10. (IF=6.7, 100 pkt. MNSiW). https://doi.org/10.1016/j.jwpe.2025.107980.

- D. Rapacz*, K. Smolińska-Kempisty, J. Wolska. Eco friendly core-shell particles coated with molecularly imprinted polymers for S-metolachlor recognition and separation. Analytica Chimica Acta. 2025, vol. 1367, art. 344310, s. 1-10. (IF=6.0, 100 pkt. MNSiW). https://doi.org/10.1016/j.jwpe.2025.107980.

- D. Rapacz-Kinas*, K. Smolińska-Kempisty, J. Wolska. Core-shell molecularly imprinted polymer for selective recognition and detection of S-metolachlor in aqueous samples. Scientific Reports. 2026, vol. 16, art. 14750, s. 1-11. (IF=3.9, 140 pkt. MNSiW). https://doi.org/10.1038/s41598-026-44780-2.

- D. Rapacz-Kinas*, K. Smolińska-Kempisty, A. Urbanowska, J. Wolska. Detection of S–metolachlor in Surface Water Near Cornfields Using pH-Sensitive Green Molecularly Imprinted Polymers. Molecules. 2026, vol. 31, art. 932, s. 1-17. (IF=4.6, 140 pkt. MNSiW). https://doi.org/10.3390/molecules31060932.

- K. Smolińska-Kempisty, A. Urbanowska, D. Rapacz-Kinas, J. Wolska, A. Marczuk. Membrane floodwater treatment using molecularly imprinted polymers to detect micropollutants. Chemical Engineering Research and Design – w recenzji. (IF=3.9, 140 pkt. MNSiW).

- K. Smolińska-Kempisty, D. Rapacz-Kinas, J. Łakomiak. pH-sensitive molecularly imprinted polymers with affinity toward gentamicin obtained in accordance with the idea of green chemistry. Analytica Chimica Acta – w recenzji. (IF=6.0, 100 pkt. MNSiW).

- J. Wolska, K. Smolińska-Kempisty, D. Rapacz-Kinas. Synthesis, Characterization and Application of pH-sensitive Molecularly Imprinted Polymers for Dimethyl Phthalate Monitoring in Real Aqueous Matrices. Journal of Hazardous Materials – wysłana do czasopisma. (IF=11.3, 200 pkt. MNSiW).

*autor korespondencyjny

ZGŁOSZENIA PATENTOWE

- K. Smolińska-Kempisty, D. Rapacz, J. Wolska. „Sposób otrzymywania molekularnie wdrukowywanych polimerów selektywnych wobec metolachloru". Zgłoszenie patentowe nr P.447229. Rok 2023.
- K. Smolińska-Kempisty, D. Rapacz, J. Wolska. „Sposób otrzymywania polimerowych cząsteczek z nadrukiem molekularnym typu rdzeń-powłoka selektywnych wobec S-metolachloru". Zgłoszenie patentowe nr P.449207. Rok 2024.
- D. Rapacz, K. Smolińska-Kempisty, J. Wolska. „Polimery z nadrukiem molekularnym selektywne wobec S-metolachloru, sposób ich otrzymywania oraz sposób wstępnego przygotowania próbki do selektywnego oznaczania S-metolachloru w procesie sorpcji i desorpcji z roztworu mikrozanieczyszczeń". Zgłoszenie patentowe nr: P.451250. Rok 2025.
- D. Rapacz, K. Smolińska-Kempisty, J. Wolska. „Polimerowe cząstki z nadrukiem molekularnym typu rdzeń-powłoka selektywne wobec S-metolachloru, sposób ich otrzymywania oraz sposób wstępnego przygotowania próbki do selektywnego oznaczenia S-metolachloru z próbek wodnych". Zgłoszenie patentowe nr: P 452797. Rok 2025.

KONFERENCJE

- A. Franczyk, J. Szyling, D. Rapacz. Poly(methacrylate)s with POSS groups - synthesis and characterization. 4 International Symposium on Silsesquioxanes-based Functional Materials. Busan, Korea, 4-6.11.2020. Współautor wystąpienia ustnego.
- A. Franczyk, J. Szyling, D. Rapacz. Synthesis of hybrid poly(methacrylate)s with polyhedral oligomeric silsesquioxanes moieties. 10th International Colloids Conference ONLINE, 7-9.12.2020. Współautor wystąpienia ustnego.
- D. Rapacz, A. Franczyk. POSS-MAs and their application in the preparation of hybrid (co)Polymers. International Symposium on Synthesis and Catalysis 2021. Evora, Portugalia, 31.08-3.09.2021. Wystąpienie ustne.
- A. Franczyk, D. Rapacz, J. Walkowiak. POSS-MA- synteza, charakterystyka oraz zastosowanie w procesach polimeryzacji. 63. Zjazd Naukowy Polskiego Towarzystwa Chemicznego w Łodzi. Łódź, Polska, 13-17.09.2021. Poster.
- D. Rapacz, A. Franczyk, I. Kownacki. Synteza poli(metakrylanów) gwiaździstych zawierających POSS w swej strukturze na drodze polimeryzacji ATRP. V Poznańskie Sympozjum Młodych Naukowców w Poznaniu. Poznań, Polska, 10.06.2022. Wystąpienie ustne.
- D. Rapacz, K. Smolińska-Kempisty, J. Wolska. Molecularly imprinted polymers toward metolachlor. NANOTECH POLAND CONFERENCE. Poznań, Polska, 14-16.06.2023. Poster.

- D. Rapacz, K. Smolińska-Kempisty, J. Wolska. Materiały zdolne do wykrywania S-metolachloru. Międzynarodowa konferencja naukowa: 47. Międzynarodowe Seminarium Naukowo-techniczne "Chemistry for Agriculture". Karpacz, Polska, 26-29.11.2023. Wystąpienie ustne.
- D. Rapacz, K. Smolińska-Kempisty, J. Wolska. Polimery z nadrukiem molekularnym jako selektywne sorbenty zdolne do wychwytu cząsteczek S-metolachloru. II edycja Konferencji Naukowej Chemia we Wrocławiu WrocChem 2024. Wrocław, Polska, 11.06.2024. Wystąpienie ustne.
- D. Rapacz, K. Smolińska-Kempisty, J. Wolska. Molecularly imprinted polymers sensitive to S-metolachlor. The 12th International Conference on Molecular Imprinting. Werona, Włochy, 19-21.06.2024. Poster.
- D. Rapacz, K. Smolińska-Kempisty, J. Wolska. Separation of S-metolachlor from water based on interactions of molecularly imprinted polymers with herbicide groups. 7th Conference of Electrochemical and Membrane Separations Science and Technology. Wrocław, Polska, 18-22.05.2025. Poster.
- J. Wolska, K. Smolińska-Kempisty, D. Rapacz, A. Urbanowska, M. Pilśniak-Rabiega, M. Jakowski. Pressurised membrane processes for the recovery of water after the extinguishing of an electric car fire. 8th International Symposium on Membrane Technologies and Applications. Izmir, Turcja, 12-14.11.2025. Poster.
- D. Rapacz-Kinas, K. Smolińska-Kempisty, A. Urbanowska, J. Wolska. „Zielone" sorbenty typu rdzeń-otoczka z warstwą polimeru wdrukowanego molekularnie do monitorowania stężenia S-metolachloru w próbkach wody. Konferencja Naukowo-Techniczna „Woda, Ścieki, Odpady – Infrastruktura i Technologia". Trzebnica, Polska, 20-22.05.2026. Poster.
- J. Wolska, K. Smolińska-Kempisty, D. Rapacz-Kinas, M. Pilśniak-Rabiega, A. Urbanowska, M. Mroczek. Ciśnieniowe procesy membranowe do odzyskiwania wody po gaszeniu pożaru samochodu elektrycznego. Konferencja Naukowo-Techniczna „Woda, Ścieki, Odpady – Infrastruktura i Technologia". Trzebnica, Polska, 20-22.05.2026. Poster.
- K. Smolińska-Kempisty, A. Urbanowska, D. Rapacz-Kinas, M. Mroczek, J. Wolska. Detekcja mikrozanieczyszczeń z wykorzystaniem molekularnie wdrukowywanych polimerów. Konferencja Naukowo-Techniczna „Woda, Ścieki, Odpady – Infrastruktura i Technologia". Trzebnica, Polska, 20-22.05.2026. Poster.
- D. Rapacz-Kinas, K. Smolińska-Kempisty, J. Wolska. pH-sensitive MIPs selective towards S-metolachlor. The 13th International Conference on Molecular Imprinting - MIP2026. Wiedeń, Austria, 12-15.07.2026. Poster.

STAŻE NAUKOWE

- 09.2018–06.2021 wolontariat naukowy w grupie badawczej prof. Jędrzeja Walkowiaka w Wielkopolskim Centrum Zaawansowanych Technologii w Poznaniu.
- 2–13.04.2024 staż naukowy w grupie badawczej prof. Coriny Madreiter-Sokolowski na Medical Univeristy of Graz (Austria).
- 6-17.10.2025 staż naukowy w grupie badawczej prof. Sergey'a Piletsky na Univeristy of Leicester (Wielka Brytania).
- 1-6.12.2025 staż naukowy w grupie badawczej prof. Coriny Madreiter-Sokolowski na Medical Univeristy of Graz (Austria).

WSPÓŁPRACA NAUKOWA

- Od 01.2024 międzynarodowa współpraca naukowa realizowana z Medical Univeristy of Graz (Austria) z zespołem badawczym prof. Coriny Madreiter-Sokolowski.
- Od 09.2024 współpraca naukowa realizowana z Wydziałem Inżynierii Środowiska Politechniki Wrocławskiej z dr hab. inż. Agnieszką Urbanowską.
- Od 02.2025 międzynarodowa współpraca naukowa realizowana z University of South Bohemia (Czechy) z zespołem badawczym prof. Vitezslava Stranak.
- Od 02.2025 współpraca z Politechniką Warszawską z grupą prof. Mateusza Śmietany.
- Od 05.2025 współpraca naukowa z Politechniką Krakowską z dr Joanną Kuc.
- Od 10.2025 międzynarodowa współpraca naukowa realizowana z University of Leicester z prof. Eleną Piletską.
- Od 02.2026 współpraca naukowa realizowana z Wydziałem Elektroniki, Fotoniki i Mikrosystemów Politechniki Wrocławskiej z dr hab. inż. Damianem Wojcieszakiem.

DOŚWIADCZENIE

- 07.2020–05.2022 – „Dwufunkcyjne silseskwioksany $RR'_7Si_8O_{12}$ – precyzyjnie zaprojektowane bloki budulcowe do syntezy zaawansowanych materiałów hybrydowych", grant LIDER/6/0017/L-9/17/NCBR/2018, finansowany przez NCBiR – wykonawca.
- 12.2020–11.2021 – „Synteza hybrydowych polimerów gwiaździstych zawierających w swej strukturze POSS z wykorzystaniem procesu ATRP", grant ID-UB: 009/34/UAM/0016, finansowany przez MNSiW w ramach II edycji konkursu Study@reserach w programie Inicjatywa Doskonałości – Uczelnia Badawcza – kierownik.
- 07.2022 – 09.2022 – Analityk laboratoryjny w Browarze Namysłów Grupa Żywiec S.A.

- Od 10.2022 – „Molekularnie wdrukowany materiał sensoryczny do monitorowania stężenia mikrozanieczyszczeń w środowisku wodnym", grant Sonata Bis11, 2021/42/E/ST5/00019 (02NB/0002/22), finansowany przez NCN – główny wykonawca.
- Od 01.2024 – "Establishing an immobilization method for compound screens based on fluorescence microscopy in nematodes", grant NAWA, BPN/BAT/2023/1/00029 – wykonawca.
- Od 07.2025 – „Powódź 2024 a jakość wód – kompleksowa ocena skażeń i efektywność procesów oczyszczania", grant wewnętrzny otrzymany w ramach I edycji programu „Wsparcie zespołów badawczych 2025", finansowany przez PWr – wykonawca.
- Od 11.2025 – „Molekularnie wdrukowywane membrany w procesie oczyszczania wody z krótkołańcuchowych PFAS", grant OPUS 28 2024/55/B/ST5/00384, finansowany przez NCN – wykonawca.

STYPENDIA I NAGRODY

- 10.2024-09.2025 Stypendium o zwiększonej wysokości dla doktorantów Szkoły Doktorskiej finansowane przez Politechnikę Wrocławską.
- 04.2025; 08.2025; 04.2026 Nagroda programu PRIMUS dla doktorantów.
- 05.2025; 05.2026 Stypendium naukowe z własnego funduszu na stypendia Politechniki Wrocławskiej.
- 05.2025 Nagroda programu SEXTUS dla doktorantów.
- 11.2025 Nagroda Rektora Politechniki Wrocławskiej za wybitne osiągnięcie naukowe w roku akademickim 2024/2025.
- 11.2025 Laureatka Studenckiego Programu Stypendialnego Prezydenta Wrocławia dla doktorantów w kategorii Stypendium im. Mariana Suskiego w zakresie nauk inżynieryjno-technicznych.
- 10.2025-09.2026 Stypendium o zwiększonej wysokości dla doktorantów Szkoły Doktorskiej finansowane przez Politechnikę Wrocławską.

SZKOLENIA

- Szkolenie chromatograficzne „Design of Experiments (DoE), Analytical Quality by Design (AQbD) oraz oprogramowania LabSolutions Method Development" organizowane przez firmę SHIM-POL A.M. Borzymowski w dniu 8.05.2023, Wrocław.
- IX Akademia Chemii Analitycznej organizowana przez firmę SHIM-POL A.M. Borzymowski w dniach 25-28.05.2025, Jachranka.

- Food Shim-Pol Day „Najnowsze rozwiązania w analizie żywności” szkolenie organizowane przez firmę SHIM-POL A.M. Borzymowski w dniu 11.06.2025, Wrocław.
- Shim-Pol Day Users & Friends szkolenie organizowane przez firmę SHIM-POL A.M. Borzymowski w dniu 15.04.2026, Wrocław.

ZAJĘCIA DYDAKTYCZNE

- Instrumental drug analysis – laboratorium.
- Modification of recovered bio–components – laboratorium.
- Bio–components characterization – laboratorium.
- Fabrication of smart polymers– laboratorium.
- Polimery w biotechnologii – laboratorium.
- Materiały funkcjonalne – laboratorium.
- Kontrola jakości surowców i produktów – laboratorium.
- Chemia techniczna organiczna – laboratorium.

DZIAŁALNOŚĆ ORGANIZACYJNA

- Program Erasmus+ Blended Intensive Program „Circularity of Polymers”, Wrocław, 19.02-23.02.2024.
- Warsztaty dla przedszkolaków z Kiełczowa, Wrocław, 26.03.2024.
- Komitet organizacyjny konferencji 7th Conference of Electrochemical and Membrane Separations Science and Technology, Wrocław, 18-22.05.2025.

11. Literatura

[1] I. C. Vasilachi, D. M. Asiminicesei, D. I. Fertu, and M. Gavrilescu. Occurrence and fate of emerging pollutants in water environment and options for their removal. *Water,* 2021, (13). doi: 10.3390/w13020181.

[2] A. Otalora, T. A. Lerma, Y. Arrieta-Urango, M. Palencia. Emerging organic pollutants in aqueous environments: Detection, monitoring, and removal techniques. *Journal of Science with Technological Applications,* 2021, (10). doi: 10.34294/j.jsta.21.10.68.

[3] A. Wołowicz, H. M. S. Munir. Emerging organic micropollutants as serious environmental problem: A comprehensive review. *Science of the Total Environment,* 2025, (958). doi: 10.1016/j.scitotenv.2024.177948.

[4] N. Bolong, A. F. Ismail, M. R. Salim, T. Matsuura. A review of the effects of emerging contaminants in wastewater and options for their removal. *Desalination,* 2009, (239). doi: 10.1016/j.desal.2008.03.020.

[5] M. Gromiec, A. Sadurski, M. Zalewski, P. Rowiński. Zagrożenia związane z jakością wody. *Nauka,* 2014, (1).

[6] F. Alfat, M. Z. Hashmi, U. Farooq, Z. U. Rehman, M. U. Hmeed, R. Batool, S. Pongpiachan. Chapter 21 - Nanotechnology to treat the environmental micropollutants. *Environmental Micropollutants,* 2022. doi: 10.1016/B978-0-323-90555-8.00017-9.

[7] N. K. Khanzada, M. U. Farid, J. A. Kharraz, J. Choi, C. Y. Tang, L. D. Nghiem, A. Jang, A. K. An. Removal of organic micropollutants using advanced membrane-based water and wastewater treatment: A review. *Journal of Membrane Science,* 2020, (598). doi: 10.1016/j.memsci.2019.117672.

[8] K. Smolinska-Kempisty, T. Cowen, J. Duda, M. Bryjak. Environmentally friendly molecularly imprinted polymers as an insert for SPE type columns in the gentamicin monitoring process. *Talanta,* 2025, (282). doi: 10.1016/j.talanta.2024.126966.

[9] A. Borreca, S. Vuilleumier, G. Imfeld. Combined effects of micropollutants and their degradation on prokaryotic communities at the sediment–water interface. *Scientific Reports,* 2024, (14). doi: 10.1038/s41598-024-67308-y.

[10] J. R. Dean. *Extraction Methods for Environmental Analysis*. John Wiley & Sons, Chichester, 1999.

[11] M. A. A. Abdelhamid, M. R. Ki, H. J. Yoon, S. P. Pack. Microfluidic Sensors for Micropollutant Detection in Environmental Matrices: Recent Advances and Prospects. *Biosensors,* 2025, (15). doi: 10.3390/bios15080474.

[12] Y. Shao, J. Duan, M. Wang, J. Cao, Y. She, Z. Cao, G. Li, F. Jin, J. Wang, A. M. A. El-Aty. Application of Molecularly Imprinted Electrochemical Biomimetic Sensors for

Detecting Small Molecule Food Contaminants. *Polymers,* 2023, (15). doi: 10.3390/polym15010187.

[13] M. Arabi, A. Ostovan, J. Li, X. Wang, Z. Zhang, J. Choo, L. Chen. Molecular Imprinting: Green Perspectives and Strategies. *Advanced Materials,* 2021, (33). doi: 10.1002/adma.202100543.

[14] J. Namieśnik, P. Szefer. Preparing Samples for Analysis – the Key to Analytical Success. *Ecological Chemistry and Engineering*, 2008 (15).

[15] V. David, T. Galaon, E. Bacalum. Sample Enrichment by Solid-Phase Extraction for Reaching Parts per Quadrillion Levels in Environmental Analysis. *Chromatographia,* 2019, (82). doi: 10.1007/s10337-019-03696-y.

[16] N. Fontanals, R. M. Marcé, F. Borrull. New hydrophilic materials for solid-phase extraction. *Trends in Analytical Chemistry,* 2005, (24). doi: 10.1016/j.trac.2005.01.012.

[17] L. Chen, H. Wang, Q. Zeng, Y. Xu, L. Sun. H. Xu, L. Ding. On-line Coupling of Solid-Phase Extraction to Liquid Chromatography—A Review. *Journal of Chromatographic Science,* 2009, (47). doi: 10.1093/chromsci/47.8.614.

[18] S. Piovesana, A. Laganà, A. L. Capriotti. Current advances in carbonaceous materials for analytical applications in liquid phase. *Trends in Analytical Chemistry,* 2023, (168). doi: 10.1016/j.trac.2023.117297.

[19] M.-C. Hennion. Graphitized carbons for solid-phase extraction. Journal of Chromatography A, 2000, (885). doi: 10.1016/s0021-9673(00)00085-6.

[20] J. C. Nadal, F. Borrull, R. M. Marcé, N. Fontanals. Novel in-house mixed-mode ion-exchange materials for sorptive phase extraction techniques. *Advances in Sample Preparation*, 2022, (1). doi: 10.1016/j.sampre.2022.100008.

[21] J. S. Fritz. Factors affecting selectivity in ion chromatography. *Journal of Chromatography A*, 2005, (1085). doi: 10.1016/j.chroma.2004.12.087.

[22] M. E. I. Badawy, M. A. M. El-Nouby, P. K. Kimani, L. W. Lim, E. I. Rabea. A review of the modern principles and applications of solid-phase extraction techniques in chromatographic analysis. *Analytical Sciences,* 2022, (38). doi: 10.1007/s44211-022-00190-8.

[23] N. P. Kalogiouri, A. Kabir, K. G. Furton, V. F. Samanidou. A tutorial on the synthesis and applications of molecularly imprinted polymers in analytical chemistry. *Journal of Chromatography Open,* 2025, (8). doi: 10.1016/j.jcoa.2025.100244.

[24] O. I. Parisi, F. Francomano, M. Dattilo, F. Patitucci, S. Prete, F. Amone, F. Puoci. The Evolution of Molecular Recognition: From Antibodies to Molecularly Imprinted Polymers (MIPs) as Artificial Counterpart. *Journal of Functional Biomaterials,* 2022, (13). doi: 10.3390/jfb13010012.

[25] B. Ö. Acet, T. İnanan, K. Salieva, B. Borkoev, M. Odabaşı, Ö. Acet. Molecular imprinted polymers: important advances in biochemistry, biomedical and biotechnology. *Polymer Bulletin,* 2024, (81). doi: 10.1007/s00289-024-05238-5.

[26] M. Marć. MIP synthesis, characteristics and analytical application. Elsevier, 2019.

[27] S. Bhogal, K. Kaur, A. K. Malik, C. Sonne, S. S. Lee, K. H. Kim. Core-shell structured molecularly imprinted materials for sensing applications. *Trends in Analytical Chemistry,* 2020, (133). doi: 10.1016/j.trac.2020.116043.

[28] M. Marć, A. Martín-Esteban. Assessment of the greenness of molecularly imprinted polymers used in sample preparation. *Advances in Sample Preparation,* 2025, (14). doi: 10.1016/j.sampre.2025.100167.

[29] W. Guo, J. Xu, Z. Tang, W. Li, D. Zhang. Green development of molecularly imprinted polymers and the application in CO2 adsorption and separation: A review. *Separation and Purification Technology,* 2025, (362). doi: 10.1016/j.seppur.2025.131784.

[30] A. Fattah-alhosseini, R. Chaharmahali, S. Alizad, M. Kaseem, B. Dikici. A review of smart polymeric materials: Recent developments and prospects for medicine applications. *Hybrid Advances,* 2024, (5). doi: 10.1016/j.hybadv.2024.100178.

[31] M. R. Aguilar, J. San Román. Chapter 1 - Introduction to Smart Polymers and Their Applications in *Smart Polymers and their Applications (Second Edition)*. Woodhead Publishing, 2019.

[32] A. Balcerak-Woźniak, M. Dzwonkowska-Zarzycka, J. Kabatc-Borcz. A Comprehensive Review of Stimuli-Responsive Smart Polymer Materials—Recent Advances and Future Perspectives. *Materials,* 2024, (17). doi: 10.3390/ma17174255.

[33] S. M. M. Morsi, M. E. Abd El-Aziz, H. A. Mohamed. Smart polymers as molecular imprinted polymers for recognition of target molecules. *International Journal of Polymeric Materials and Polymeric Biomaterials,* 2023, (72). doi: 10.1080/00914037.2022.2042287.

[34] Y. Li, J. Luo, G. Xie, D. Zhu, C. Zhao, X. Zhang, M. Liu, Y. Wu, Y. Guo, W. Tu. Recent Progress on Regulating the LCST of PNIPAM-Based Thermochromic Materials. *ACS Applied Polymer Materials,* 2025, (7). doi: 10.1021/acsapm.4c03406.

[35] X. Lang, A. D. Patrick, B. Hammouda, M. J. A. Hore. Chain Terminal Group Leads to Distinct Thermoresponsive Behaviors of Linear PNIPAM and Polymer Analogs. *Polymer,* 2018, (145). doi: 10.1016/j.polymer.2018.04.068.

[36] L. J. Abbott, A. K. Tucker, M. J. Stevens. Single Chain structure of a poly(N - isopropylacrylamide) surfactant in water. *Journal of Physical Chemistry B*, 2015, (119). doi: 10.1021/jp511398q.

[37] N. Zafar, A. Mahmood, S. Ilyas, H. Ijaz, R. M. Sarfraz, W. A. Mahdi, M. M. Salem-Bekhit, M. A. Ibrahim, Y. Benguerba, B. Ernst. Novel Natrosol/Pectin-co-poly (acrylate) based pH-responsive polymeric carrier system for controlled delivery of Tapentadol Hydrochloride. *Saudi Pharmaceutical Journal,* 2023, (31). doi: 10.1016/j.jsps.2023.06.004.

[38] W. H. W. Ishak, O. Y. Jia, I. Ahmad. pH-responsive gamma-irradiated poly(acrylic acid)-cellulose-nanocrystal-reinforced hydrogels. *Polymers,* 2020, (12). doi: 10.3390/POLYM12091932.

[39] T. Swift, L. Swanson, M. Geoghegan, S. Rimmer. The pH-responsive behaviour of poly(acrylic acid) in aqueous solution is dependent on molar mass. *Soft Matter,* 2016, (12). doi: 10.1039/c5sm02693h.

[40] S. Orbay, O. Kocaturk, R. Sanyal, A. Sanyal. Molecularly Imprinted Polymer-Coated Inorganic Nanoparticles: Fabrication and Biomedical Applications. *Micromachines,* 2022, (13). doi: 10.3390/mi13091464.

[41] R. A. Ramli, W. A. Laftah, S. Hashim. Core-shell polymers: A review. *RCS Advances,* 2013, (36). doi: 10.1039/c3ra41296b.

[42] M. Niu, C. Pham-Huy, H. He. Core-shell nanoparticles coated with molecularly imprinted polymers: a review. *Microchimica Acta,* 2016, (183). doi: 10.1007/s00604-016-1930-4.

[43] P. J. O'connell, C. T. Harms, J. R. F. Allen. Metolachlor, S-metolachlor and their role within sustainable weed-management. *Crop Protection,* 1998, (17). doi: 10.1016/S0261-2194(98)80011-2.

[44] N. Iqbal, A. Khaliq, Z. A. Cheema. Weed control through allelopathic crop water extracts and S-metolachlor in cotton. *Information Processing in Agriculture,* 2020, (7). doi: 10.1016/j.inpa.2019.03.006.

[45] J. M. Marín-Benito, E. Herrero-Hernández, J. M. Ordax, M. J. Sánchez-Martín, M. S. Rodríguez-Cruz. The role of two organic amendments to modify the environmental fate of S-metolachlor in agricultural soils. *Environmental Research,* 2021, (195). doi: 10.1016/j.envres.2021.110871.

[46] C. Trigo, K. A. Spokas, K. E. Hall, L. Cox, W. C. Koskinen. Metolachlor Sorption and Degradation in Soil Amended with Fresh and Aged Biochars. *Journal of Agricultural and Food Chemistry,* 2016, (64). doi: 10.1021/acs.jafc.6b00246.

[47] S-Metolachlor 960 Hebricide. Safety Data Sheet according to WHS Regulations. *Corteva Agriscience Canada Company,* 2020.

[48] Why choose Dual Magnum brand herbicides over generic metolachlor? *Syngenta.* Dostępne online (10.03.2026): https://assets.syngenta-us.com

[49] H. Liu, W. Ye, X. Zhan, W. Liu. A comparative study of rac- and S-metolachlor toxicity to Daphnia magna. *Ecotoxicology and Environmental Safety,* 2006, (63). doi: 10.1016/j.ecoenv.2005.02.002.

[50] Pesticides - Fact Sheet for Metolachlor. *United States Environmental Protection Agency.* Prevention, Pesticides, And Toxic Substances (7508W). EPA-738-F-95-007, 1995.